Fémek elektromos polarizáció nélkül végbemenő adszorpciója és néhány alkalmazása

A doktori értekezésben idézett dolgozataim

S z a b ó   S á n d o r

MTA Központi Kémiai Kutató Intézete

B u d a p e s t

1 9 9 3

1. Underpotential deposition of metals on foreign metal substrates. S. Szabó, International Rev. in Phys. Chem., 10 (1991) 207.
2. Process for the preparation of platinum catalysts modified by adsorbed metals. S. Szabó, F. Nagy and D. Móger, Acta Chim. Acad. Sci. Hung., 93 (1977) 33.
3. Investigations of silver, bismuth and copper adsorption via the ionization of hydrogen adsorbed on platinized platinum in perchloric acid media. S. Szabó and F. Nagy, J. Electroanal. Chem., 70 (1976) 357.
4. Investigations of copper adsorption in hydrochloric acid media, via the ionization of hydrogen adsorbed on platinized platinum. S. Szabó and F. Nagy, J. Electroanal. Chem., 84 (1977) 93.
5. Investigations of bismuth adsorption via the ionization of hydrogen adsorbed on platinized platinum in hydrochloric acid solutions. S. Szabó and F. Nagy, J. Electroanal. Chem., 87 (1978) 261.
6. The effect of media on the adsorption of bismuth on platinum. S. Szabó and F. Nagy, J.Electroanal. Chem.,88 (1978) 259.
7. Deposition of palladium on platinum in hydrochloric acid media. S. Szabó and F. Nagy, Israel J. Chem., 18 (1979) 162.
8. Investigations of gold adsorption on platinized platinum in hydrochloric acid media. S. Szabó and F. Nagy, J. Electroanal. Chem., 85 (1977) 339.
9. Investigation of ruthenium deposition onto a platinized platinum electrode in sulfuric acid media. S. Szabó and I. Bakos, J. Electroanal. Chem., 230 (1987) 233.
10. Investigation of ruthenium deposition onto a platinum electrode in hydrochloric acid media. S. Szabó and I. Bakos, J. Electroanal. Chem., 271 (1989) 269.

11. Investigations of copper, silver and bismuth deposition on palladium in perchloric acid media. S. Szabó, J. Electroanal. Chem., 77 (1977) 193.

12. Investigation of lead adsorption via ionization of hydrogen adsorbed on platinized platinum. S. Szabó and F. Nagy, J. Electroanal. Chem., 160 (1984) 299.

13. Investigation of tin adsorption on a platinized platinum electrode in hydrochloric acid media. S. Szabó, J. Electroanal. Chem., 172 (1984) 359.

14. Study of electrochemical gold adsorption on polycrystalline platinum surfaces. I. Bakos and S. Szabó, J. Electroanal. Chem., 344 (1993) 303.

15. Isszledoványije adszorpcii renyija na platyinirovannom platinovom elektrode v rasztvore hlornoj kiszlotü. Ifandi M., Szabó S., Nagy F., Elektrohimija, 18 (1982) 1205.

16. TPD studies of hydrogen sorption on platinum powder catalysts modified by adsorbed gold. S. Szabó, D. Móger, M. Hegedűs and F. Nagy, React.Kinet.Catal. Lett.,6 (1977) 89.

17. Study of the underpotential deposition of copper onto polycrystalline palladium surfaces. S. Szabó, I. Bakos, F. Nagy and T. Mallát, J. Electroanal. Chem., 263 (1989) 137.

18. Modification of supported metal catalysts by adsorbed metals. F. Nagy and S. Szabó, React.Kinet.Catal.Lett,35(1987)133.

19. On the multiple states of gold deposited onto polycrystalline platinum substrates. I. Bakos and S. Szabó, J. Electroanal. Chem., közlésre beküldve.

20. Platinán végbemenő palládiumleválás vizsgálata sósavas közegben. Szabó Sándor és Nagy Ferenc, Magy. Kém. Folyóirat, 86 (1980) 371.

21. Adszorbeált fémekkel módositott katalizátorok előállitása. Szabó Sándor és Nagy Ferenc, Magyar Kémikusok Lapja, 36 (1981) 410.

22. Titration of hydrogen chemisorbed on supported platinum catalysts by ferric chloride solution. S. Szabó and F. Nagy, Appl. Catal., 16 (1985) 209.

23. Verfahren zum Hartlöten von Kupfer an Kupfer oder an Stahllegierungen, Szabó Sándor, Szentgyörgyi Alfonz, Szabó Péter és Nagy Ferenc, Német szabadalom, DE 32 47 830 C 2.

24. Eljárás réznek rézhez vagy rozsdamentes acélhoz, illetve rozsdamentes acéloknak egymáshoz történő keményforrasztására, Szabó Sándor, Szentgyörgyi Alfonz, Szabó Péter és Nagy Ferenc, Magyar szabadalom, 188 730.

25. Procede de brasage de cuivre sur du cuivre ou sur des alliages d'acier, Szabó Sándor, Szentgyörgyi Alfonz, Szabó Péter és Nagy Ferenc, Francia szabadalom, 2 518 440-Bl.

26. Réz-acél vagy bronz-acél kötőelem és eljárás annak előállitására, Szabó Sándor, Kovács Gizella, szabó Péter és Kwaysser Endre, Magyar szabadalom, 188 340.

INTERNATIONAL REVIEWS IN PHYSICAL CHEMISTRY, 1991, VOL. 10, NO. 2, 207–248

Underpotential deposition of metals on foreign metal substrates

by S. SZABÓ
Central Research Institute of Chemistry, Hungarian Academy of Sciences, H-1525 Budapest, P.O. Box 17, Hungary

The underpotential deposition of metals on foreign metal substrates has been reviewed, but this term is used in a wider sense in this monograph. All the redox processes resulting in adsorbed metal atoms on foreign metal substrates are included in this term. Based on the source of electrons taking part in the underpotential deposition, the classification of the processes leading to adsorbed metal atoms is also given.

1. Introduction

The anomalous behaviour of small amounts of metals electrodeposited on foreign metal substrates has been known for a very long time [1, 2]. The anomaly is the apparent violation of Nernst's law, that is, a part of the metals electrodeposited on foreign metal surfaces is oxidized at a much more positive potential than the reversible Nernst potential in the same electrolyte. Later, the potential difference between the oxidation potential of submonolayer amounts of metals deposited on 'inert' foreign metal substrates and the reversible Nernst potential of the depositing metal in the same electrolyte was called underpotential shift and the process itself underpotential deposition (UPD). (It must be taken into consideration that this phenomenon has also been termed metal adsorption [3], adatom deposition [4], chemisorption of metals [5], electrosorption of metals or metal ions [6, 7], specific adsorption or adsorption of cations [8, 9], formation of monolayer metal films [10], ...)

The adsorption of metals on foreign metal substrates has been studied also in gaseous phase in ultra-high vacuum [11]. Investigations in this field started only in the mid-1930s. The two fields developed separately, without any interrelation between the two areas. A few papers have been published recently in which electrochemical and surface chemical methods were applied simultaneously [12, 13].

This strong separation of the two fields can be explained by the different experimental techniques rendering difficult communication between the two fields.

There are other reasons for this strong isolation. In the course of underpotential deposition, besides metal adsorption a charge-transfer process must also take place. Therefore underpotential deposition is sometimes called electrochemical metal adsorption to distinguish this process from vapour-phase metal adsorption [14].

In contrast to metal adsorption from the gas phase, electrosorption of metals on foreign metal substrates depends on the potential of the substrate metal. In addition, adsorption takes place under the influence of the double layer, which renders adsorption even more complicated.

Because of the charge-transfer processes, underpotential deposition is regarded mostly as an electrochemical phenomenon in electrochemistry, sometimes ignoring the non-electrochemical aspects of metal adsorption or the possibility of such redox processes resulting also in adsorbed metal layers on foreign metal surfaces without electrochemical manipulation.

0144-235X/91 $3.00 © 1991 Taylor & Francis Ltd

For the above reasons, in this article the term underpotential deposition (UPD) will be used in a wider sense. All the redox processes resulting in adsorbed metal atoms on foreign metal surfaces are included in this term.

Based on the source of electrons taking part in the deposition of adsorbed metal atoms on foreign metal surfaces, the redox processes resulting in adsorbed metal layers can be classified. The classification is also included in this article.

2. General description of the phenomenon

Underpotential deposition (UPD) of metals is an electroreduction of metallic ions on foreign metal substrates (S) in the so-called underpotential range (ΔU), that is, in a potential region positive to the Nernst potential (E_N) of the depositing M^{z+}/M couple [10, 15–18]:

$$\Delta U = E_{ads} - E_N \geqslant 0. \tag{1}$$

The reason for the underpotential deposition is the excess binding energy of an adsorbed metal atom on a foreign metal surface ($S\text{–}M_{ads}$) relative to the binding energy of a deposited metal atom on a surface of its own kind ($M\text{–}M_{ads}$):

$$S\text{–}M_{ads} \geqslant M\text{–}M_{ads}. \tag{2}$$

The binding energy is independent of the equilibrium at the metal–electrolyte interface, and consequently of the electrode potential at which the deposition took place [19, 20].

Therefore, in practice, all deposited metals oxidized at a more positive potential (E_{ads}) than the Nernst potential of the depositing ion are taken for an underpotentially deposited metal irrespective of whether electroreduction (or reduction by any reducing agent) was carried out in underpotential or in overpotential region.

UPD (ΔU), which is sometimes called underpotential shift [19], extends from a few millivolts to over several hundred millivolts, depending on the strength of adsorbate substrate interactions, namely on the system studied.

The ΔU values depend on the crystal faces on which metal adsorption takes place and thus the underpotential deposition of metals on foreign metal surfaces has a multiple-state character [4, 16, 21].

Sometimes irreversible adsorption [22, 23] and even alloy formation can be observed [24, 25].

Underpotential deposition can easily be observed as waves on constant current charging curves [5, 22, 26] or as current peaks on potentiodynamic curves [4, 15]. The values of the underpotential (ΔU) are usually measured at the waves and peaks of polarization curves [15].

3. The thermodynamics of underpotential deposition

In the course of underpotential deposition of metals on foreign metal surfaces (S) the ions of the depositing metal (M^{z+}) penetrate into the double layer and come in direct contact with the substrate metal (S) [26, 27, 28]. During this process adsorbed water molecules are removed from the surface of the substrate metal and the solvation shell of the depositing ions will be partly or completely destroyed [27]. Depending on the chemical nature of the interaction between adsorbent (S) and adsorbate (M^{z+}) a purely physical bond or a much stronger chemical bond is formed. If a chemical bond (chemisorption) is formed (which can only be considered as underpotential deposition) then partial charge transfer of λ electrons will take place from the substrate metal to the depositing ions [26–28] (figure 1).

Underpotential deposition can be described by the following electrochemical reaction [26–28]:

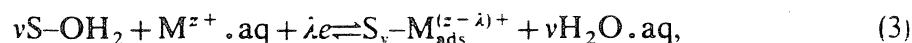

$$\nu S\text{–}OH_2 + M^{z+}.aq + \lambda e \rightleftharpoons S_\nu\text{–}M_{ads}^{(z-\lambda)+} + \nu H_2O.aq, \quad (3)$$

λ is the partial charge transfer coefficient, introduced by Lorenz and Salié [29]. λ takes into account the fact that the transfer of charge goes on in non-integral elementary steps during an electrosorption reaction. The charge transfer coefficient is defined by the difference between the actual charge of the deposited metal atom (z_{ads}) and the ionic charge of the adsorbing ions (z):

$$\lambda = z - z_{ads}. \quad (4)$$

The partial charge on adsorbed metal atoms is usually small and cannot be determined experimentally [26–29].

In a few papers [18, 30, 31] the partial charge transfer coefficient is substituted for electrosorption valency (γ). When γ is used in place of λ then the change of potential of zero charge and double layer structure due to underpotential deposition is ignored.

From the concept of partial charge transfer it follows that the adsorbing metal ions penetrate into the double layer and they are held at a certain potential (potential of adsorption φ_{ads}) which is smaller than the potential of the substrate (φ_S). Therefore the adsorbed species are affected by only a fraction of the total potential drop across the compact double layer (Helmholtz layer):

$$\varphi_{ads} \leqslant \varphi_S. \quad (5)$$

The position of the adsorbed ions in the Helmholtz layer is described by a geometric factor (g) [16, 27, 28, 32, 33]:

$$g = (\varphi_{ads} - \varphi_e)/(\varphi_S - \varphi_e), \quad (6)$$

where φ_e is the potential of the adsorbing ions in the supporting electrolyte. In the case of underpotential deposition without supporting electrolyte it must be taken into account that $\varphi_h - \varphi_e \neq 0$, (where φ_h is the potential in the Helmholtz layer) and φ_e has to be substituted for φ_h in equation (6) [27, 28, 32, 33].

3.1. *The potential dependence of electrosorption equilibrium*

3.1.1. *Quasi-Nernstian formalism*

If ionic charge on the adsorbed metal atoms is low ($z_{ads} \approx 0$), indicating the absence of coadsorption phenomena, then the sorption behaviour of M^{z+} can be described by a quasi-Nernst equation [10, 17, 32]:

$$E = E_o + \frac{RT}{zF} \ln \frac{a_{M^{z+}}}{a(\Gamma)}, \quad (7)$$

where the activity of the M_{ads} adsorbate ($a(\Gamma)$) represents the system specific type of isotherm as a function of Γ only [17].

3.1.2. *Electrosorption valency* (γ)

The potential dependence of electrosorption equilibrium and the charge flow of electrosorption processes during the electrosorption reaction can be described by

electrosorption valency (γ) [27, 28, 32–34]. In the case of excess supporting electrolyte (when $\varphi_h = \varphi_e$) the electrosorption valency is defined by equation (8) [27, 28, 32–34]:

$$\gamma F = -\left(\frac{\partial q_S}{\partial \Gamma}\right)_E = \left(\frac{\partial \mu_M}{\partial E}\right)_{\Gamma_{ads}}, \tag{8}$$

where μ_M is the chemical potential of M^{z+} in the supporting electrolyte, E is the electrode potential, q_S is the substrate charge and Γ_{ads} is the surface concentration of the adsorbed metal. Equation (8) can be used at either ideally polarizable or at reversible electrodes remembering that in the absence of excess supporting electrolyte μ_M must be replaced by the chemical potential of the depositing ions in the Helmholtz layer (μ_{Mh}) and E must be substituted by the potential drop across compact double layer ($\Delta\varphi$) [27].

Another restriction, is that in this form equation (8) cannot be applied to mixed electrosorption systems [34–36]. The thermodynamic treatment of the problem yielded an equation similar to equation (8) but with a 'mixed electrosorption valency' [34, 36]. In the case of a second electrosorbed substance, X, the γ_{mix} is the sum of the two single valencies

$$\gamma_{mix} = \gamma + \rho\gamma_X, \tag{9}$$

where ρ is the coupling factor ($\rho = \partial\Gamma_{X,ads}/\partial\Gamma_{Mads})_{E,\mu X}$) which is positive in co-adsorption and negative in competitive electrosorption [36].

Electrosorption valency is equivalent to the Nernst valency and controls potential dependence and charge flow during underpotential deposition in the same way as z does in the case of electrodeposition of metals [27, 34].

3.1.2.1. *Interpretation of electrosorption valency*

In contrast to the Nernst or Faraday valency, electrosorption valency can be a fractional number dependent on different variables. Comprehensive treatment of electrosorption reactions resulted in relations in which electrosorption valency is correlated with non-measurable microscopic features of the system [27, 28, 32–34].

Electrosorption valency at the potential of zero charge (E_{PZC}) is given by equation (10) [27, 28, 32]

$$\gamma_{PZC} = gz - \lambda(1-g) + k_M - \nu k_w, \tag{10}$$

where k_M and k_w are dipole terms of adsorbed metal (k_M) and desorbed water (k_w) which take into account that part of the electrical energy which is due to oriented dipoles with dipole moment m_i [27, 28]:

$$k_i = \pm\frac{m_i}{e_o l_i} \tag{11}$$

where m_i/e_o is the dipole length and

$$l_i = \frac{\varphi_S - \varphi_E}{dE/dx}, \tag{12}$$

provided the use of excess supporting electrolyte. ν is the number of solvent molecules displaced by one adsorbed atom.

For metal adatoms $\nu = 0$ if it is assumed that the water molecules displaced by adsorbed atoms will adsorb again on adatoms in the same way as on the substrate [16].

In the case of underpotential deposition of metals k_M is also zero, hence the electrosorption valency at the potential of zero charge is [28]

$$\gamma_{PZC} \approx gz - \lambda(1-g). \tag{13}$$

At potentials distinct from the potential of zero charge the electrosorption valency can only be calculated if its dependence on the potential is taken into consideration. According to thermodynamic analysis the potential dependence is brought about by the change in the double layer capacity (C_D) due to increasing surface concentration of adsorbed material (Γ_{ads}) [27, 28, 32, 33]:

$$\gamma = \gamma_{PZC} - \frac{1}{F}\int_{E_{PZC}}^{E} \left(\frac{\partial C_D}{\partial \Gamma}\right)_E dE, \tag{14}$$

where $C_D = (\partial q_S/\partial E)_{\Gamma_{ads}}$ when excess supporting electrolyte is used. Electrosorption valencies for cationic systems in aqueous solutions at small coverages hardly depend on potential ($d\gamma/dE \approx 0$) and thus $\gamma \approx \gamma_{PZC}$ [28].

Although occasionally electrosorption valencies of cationic systems depend strongly on coverages (UPD of Cu^{2+} ions on Pt [26]) there are systems where such dependence cannot be observed (UPD of H^+ ions on Pt [27]).

The effect of temperature on electrosorption valency seems to be negligible because g and λ are expected to be temperature independent [28].

3.1.2.2. *Determination of electrosorption valency*

(*a*) Determination from charge flow

If the surface concentration of adsorbed metal can be measured then on the basis of equation (8) the electrosorption valency can be calculated. As follows from this equation, the substrate metal charge, q_S, must be measured or calculated at constant E [27, 28].

(*b*) Determination from potential dependence

If activity coefficients are constant, μ_M in equation (8) can be substituted by the concentration of the depositing ions c_M. At constant coverage of the deposited metal atoms the derivative $(\partial \ln c_M/\partial E)_{\Gamma_{ads}}$ yields γ [27, 28].

(*c*) Determination from kinetic measurements

Electrosorption valency can be determined from the sum of electrochemical transfer coefficients $\alpha + \beta$ [27, 28]:

$$(\alpha + \beta)z = \gamma. \tag{15}$$

3.1.3. *Submonolayer equilibrium potential*

When the underpotential deposition of metals takes place with partial charge transfer then equation (7) cannot be used to describe the equilibrium between the depositing ions (M^{z+}) and adsorbed species (M_{ads}) because differences may occur between the value of electrosorption valency (γ) and the charge ($z+$) on the metal ions in the electrolyte and thus monolayer activity does not exhibit a simple exponential dependence on the electrode potential.

The description of equilibrium properties in this case is based on the concept of 'submonolayer equilibrium potential' (E_{ML}) which is developed on the basis of equal electrochemical potentials of the adsorbed species in solution and on the substrate surface, due to the charge transfer equilibrium of reaction (3) [18, 37, 38].

The submonolayer equilibrium potential (E_{ML}) is defined as follows [18, 38]:

$$E_{ML} = E^{\circ}_{ML} + \frac{RT}{\gamma F} \ln \left(\frac{a_{M^{z+}}}{a_{ML}} \right), \tag{16}$$

where $a_{M^{z+}}$ is the activity of the depositing metal ion in the supporting electrolyte and a_{ML} is the activity of the adsorbed metal atoms at a coverage between 0 and 1. a_{ML} depends on the adsorption isotherm that can be applied to describe the activity of the adsorbed species and on the multiple energy states if these exist [18, 38]. E°_{ML} is the standard submonolayer potential and is connected with the standard free energy of the formation of a submonolayer [38]:

$$\Delta G^{\circ}_{ML} = \gamma F E^{\circ}_{ML}, \tag{17}$$

E°_{ML} and consequently ΔG°_{ML} depends on the adsorption isotherm that can be used to describe the activity of the adsorbed species in the same way as a_{ML} does.

By definition of the submonolayer equilibrium potential a more correct definition can be given for the underpotential (shift) by substituting E_{ads} for E_{ML} in equation (1) ($\Delta U = E_{ML} - E_N$) [18, 38].

The underpotential (ΔU) in an explicit form is

$$\Delta U = (E^{\circ}_{ML} - E^{\circ}) + \frac{RT}{F} \left(\frac{1}{\gamma} - \frac{1}{z} \right) \ln a_{M^{z+}} - \frac{RT}{\gamma F} \ln a_{ML}, \tag{18}$$

where

$$E^{\circ}_{ML} - E^{\circ} = \Delta U^{\circ} = \frac{\Delta G^{\circ}}{zF} - \frac{\Delta G^{\circ}_{ML}}{\gamma F}, \tag{19}$$

where E° is the standard equilibrium potential for the bulk M/M^{z+} couple and ΔG° its standard free-energy change [18, 38].

3.2. *Underpotential coverage isotherms*

Based on the concept of submonolayer equilibrium potential, underpotential-coverage (θ) isotherms can be derived relying upon equations (18) and (19). In the course of derivation, however, the dependence of monolayer free energy on coverage (θ) and the existence of multiple energy states in the monolayer range have to be taken into account [18, 38]. (Coverage (θ) means the coverage of adsorbed metal (M_{ads}) on substrate S if otherwise not stated.)

3.2.1. *No interaction case*

The hypothetical absence of interaction between the adsorbed species and the absence of their interaction with the substrate leads to a Langmuir-type adsorption. The Langmuir adsorption isotherm can generally be applied to electrosorption reactions when the coverage is below 0·2 [38].

If Langmuir-type adsorption exists, the adsorption isotherms of metals adsorbed on foreign metal surfaces for single energy state, can be derived from equation (18) since

$$a_{ML} = \frac{\theta}{1 - \theta}. \tag{20}$$

By substitution of equation (20) into equation (18), the new equation can be used in potentiodynamic experiments if the desorption of UPD species is reversible. At $\theta = 0{\cdot}5$

and at unit activity of the depositing ions in the supporting electrolyte the standard free energy (ΔG°_{ML}) of formation of adsorbed metal monolayer can be determined.

Under Langmuir conditions, the half-width of a monolayer stripping peak of a univalent adsorbed metal is about 0·09 V. Broadening of the stripping peak can very often be observed. This has been explained by the large lattice mis-match between the substrate and adsorbate and a 'dissociative' Langmuir isotherm has been suggested [39] to explain such results.

3.2.2. *Particle–substrate interactions*

The idealized model of the Langmuir adsorption isotherm can very often not be applied to characterize underpotential deposition since most substrate surfaces are energetically heterogeneous and thus the monolayer free energy depends on the coverage. Another important factor is the change in work function of the substrate as a consequence of the formation of an adsorbed metal monolayer [38].

If it is assumed that the monolayer free energy decreases linearly with coverage (the Temkin concept) [38]:

$$\Delta G^{\circ}_{ML} = \Delta G^{\theta \to 0}_{ML} + fRT\theta, \qquad (21)$$

where $\Delta G^{\theta \to 0}$ is the free energy change of adsorption at the beginning of underpotential deposition. The underpotential (ΔU) can then be calculated in the case of particle–substrate interactions by substituting equation (21) into equation (18) taking into account equation (19) and thus

$$\Delta U = \left(\frac{\Delta G^{\circ}}{zF} - \frac{\Delta G^{\theta \to 0}_{ML}}{\gamma F}\right) + \frac{RT}{F}\left(\frac{1}{\gamma} - \frac{1}{z}\right) \ln a_{M^{z+}} - \frac{RT}{\gamma F}\left[\ln\left(\frac{\theta}{1-\theta}\right) + f\theta\right], \qquad (22)$$

$\Delta G^{\theta \to 0}_{ML}$ can be obtained from the intercept of the ΔU against $f\theta + \ln[\theta/(1-\theta)]$ diagram. The value of the electrosorption valency must be determined in a separate experiment.

Usually very large Temkin parameters can be measured for adsorbed metal species. The high Temkin parameters cannot be explained wholly by particle–particle interaction.

Work function differences measured at the metal/gas interface verified that the Temkin parameter (f) is predominantly determined by particle substrate interactions during underpotential deposition [18]. The correlation between underpotential shifts and work-function differences indicates also the existence of particle–substrate interactions in UPD processes [15, 19].

3.2.3. *Particle–particle interactions*

In addition to particle–substrate interactions the contribution of lateral interaction energy to the variation of monolayer free energy can also be expected even without partially charged species in UPD layers [18]. In addition, the presence of partially discharged species in the adsorbed metal layer gives rise to repulsive forces [40]. An UPD layer composed of partially discharged ions has a tendency to attract oppositely charged ions [6, 7] so that the repulsive forces will be screened or even converted to attractive forces. This can be identified by its $\theta^{3/2}$ dependence [40].

The standard free energy of formation of a monolayer for these interactions is [18, 38]

$$\Delta G^{\circ}_{ML} = \Delta G^{\theta \to 0}_{ML} + fRT\theta + gRT\theta^{3/2}. \qquad (23)$$

where g is the interaction parameter defined in reference [40]. (In equation (23) g may be considered also to be a Frumkin parameter.) Thus the expression for underpotential in the presence of particle–substrate and particle–particle interactions is [38]

$$\Delta U=\left(\frac{\Delta G^{\circ}}{zF}-\frac{\Delta G_{\mathrm{ML}}^{\theta\to 0}}{\gamma F}\right)+\frac{RT}{F}\left(\frac{1}{\gamma}-\frac{1}{z}\right)\ln a_{\mathrm{M}^{z+}}-\frac{RT}{\gamma F}\left[\ln\left(\frac{\theta}{1-\theta}\right)+f\theta+g\theta^{3/2}\right], \quad (24)$$

where

$$\frac{\Delta G^{\circ}}{zF}-\frac{\Delta G_{\mathrm{ML}}^{\theta\to 0}}{\gamma F}=\Delta U^{\theta\to 0}. \quad (25)$$

When electrosorption valency (γ) is hardly lower than the ionic charge ($z+$) of the depositing ions, that is $\gamma\approx z$, which is usually the case, then equation (24) can be simplified [18]:

$$\Delta U=\Delta U^{\theta\to 0}-\frac{RT}{\gamma F}\left[\ln\left(\frac{\theta}{1-\theta}\right)+f\theta+g\theta^{3/2}\right], \quad (26)$$

and then the dependence of ΔU on the activity of depositing ions in the supporting electrolyte vanishes [18].

3.2.4. *General isotherm*

The adsorption isotherms defined above have a Langmuir basis, which implies the additivity of particle–particle and particle–substrate interactions. These isotherms can be applied to describe adsorption processes of underpotential deposition if the adsorbed monolayer constitutes of single energy state [18]. When metal monolayers formed by underpotential deposition are composed of multiple energy states and the various states do not interact with each other then each energy state can be described by an adsorption isotherm based on the Langmuir concept [18].

Assuming additivity of interactions, we may write the general isotherm for the jth state as follows [18]:

$$\Delta U=\Delta U_j^{\theta\to\theta_{j-1}}+\frac{RT}{F}\left(\frac{1}{\gamma}-\frac{1}{z}\right)\ln a_{\mathrm{M}^{z+}}-\frac{RT}{\gamma F}\left[\ln\left(\frac{\theta-\theta_{j-1}}{\theta_j-\theta}\right)+f_j(\theta-\theta_{j-1})+g_j(\theta-\theta_{j-1})^{3/2}\right], \quad (27)$$

where θ_{j-1} is the initial and θ_j is final coverage of the jth energy state. Equation (27) can be considered to be a general isotherm. When $\theta_{j-1}=0$ and $\theta_j=1$ then equation (27) becomes the general isotherm of an adsorbed monolayer with a single energy state.

3.2.5. *Interaction effects in electrodeposited monolayers*

The simplified model of $\theta^{3/2}$ dependence of particle–particle interactions (section 3.2.3) does not properly describe the interaction effects in monolayers formed by underpotential deposition. A more correct treatment can be given to the phenomenon based on the application of the concept of adsorption pseudo-capacitance [21, 30, 40].

This section will examine how partially charged adsorbed atoms should behave in a two-dimensional lattice in relation to the deviation of γ from z. Two effects arise in consequence of $\gamma<z$. Even in the hypothetical absence of coulombic repulsive effects, an important effect of $\gamma<z$ on the shape of the adsorption isotherm can be predicted

because a broader range of potential is required to achieve full coverage. In addition to this effect, the Coulombic interactions between the partially charged atoms will cause an additional change of energy of adsorption and widening of capacitance (C) against potential (E) profile [30, 40].

3.2.5.1. *Definition of adsorption pseudocapacitance*

The kinetic equation for the net current i passing per cm^2 of S in reaction (3) can be written as [21]:

$$i = Q\frac{d\theta}{dt} \equiv Q\frac{d\theta}{dE}\frac{dE}{dt} = C_p\frac{dE}{dt} = C_p s, \tag{28}$$

where θ is the coverage of deposited metal (M_{ads}) on substrate (S) and Q is the charge required for generation of the monolayer of M_{ads} on substrate (S). C_p, usually called the 'adsorption pseudocapacitance', is to be distinguished from the double-layer capacitance, C_{dl}. Normally $C_p \gg C_{dl}$. $dE/dt = s =$ constant is the so-called sweep rate in a single or repetitive sweeps.

In terms of the kinetic equations, the equilibrium conditions for reaction (3), in the absence of lateral interactions, taking into account the electrosorption valency [21, 40] is

$$k_3(1-\theta)c_{M^{z+}} \exp[\alpha\gamma FE/RT] = k_{-3}\theta \exp[-(1-\alpha)\gamma FE/RT], \tag{29}$$

The electrosorption equilibrium derived from equation (29) is

$$\theta/(1-\theta) = K_3 c_{M^{z+}} \exp(\gamma FE/RT), \tag{30}$$

where $K_3 = k_3/k_{-3}$. In earlier papers it was usually assumed that for surface heterogeneity and/or interaction effects K_3 has the form $K_3^0 \exp(-g\theta)$. It follows from this assumption that there is a linear variation of lateral interaction energy in the monolayer with coverage characterized by a parameter g. However, results measured by temperature programmed desorption in gas/solid experiments [41] and by electrochemical methods [42] show that K_3 is usually neither independent of coverage nor a continuous function of it. K_3 often has a series of discrete values over distinguishable small ranges of θ as the coverage is changed from 0 to 1. This constitutes the phenomenon of 'multiple state' adsorption in monolayers [21].

The adsorption pseudocapacitance ($C_p = Q\, d\theta/dE$) for process (3) can be obtained by differentiation of equation (30) with respect to E. Here Q is the charge required for formation of a monolayer of M_{ads} on substrate (S) but only when $\gamma = z$. Instead of Q, the actual charge $(\gamma/z)Q$ is used in the formation of a monolayer, which has to be substituted into equations when $\gamma < z$ [30, 40].

The adsorption pseudocapacitance is given by [21, 30, 40]:

$$\begin{aligned}\frac{\gamma}{z}Q\frac{d\theta}{dE} &= C_p = Q\frac{\gamma^2 F}{zRT}\theta(1-\theta)\\ &= Q\frac{\gamma^2 F}{zRT}\frac{K_3 c_{M^{z+}} \exp(\gamma FE/RT)}{[1 + K_3 c_{M^{z+}} \exp(\gamma FE/RT)]^2}\end{aligned} \tag{31}$$

in terms of θ or E.

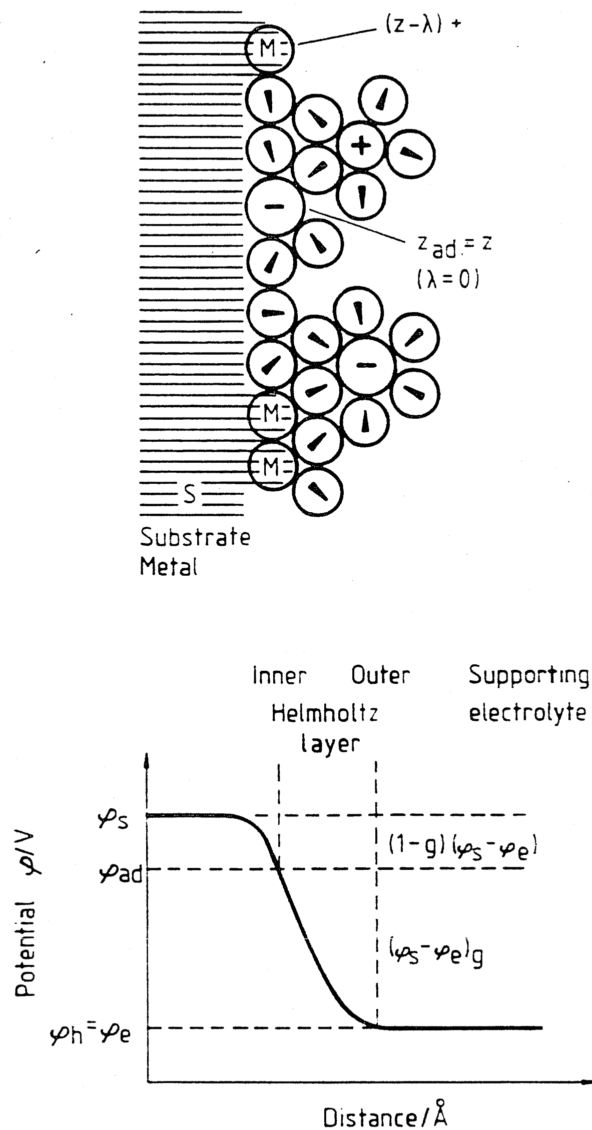

Figure 1. Schematic double layer model with non-adsorbed ions in the outer Helmholtz layer, adsorbed water molecules and adsorbed ions in the inner layer, when excess supporting electrolyte is used [28].

3.2.5.2. *Capacitance behaviour without lateral interactions*

First the effect of $\gamma < z$ on the form of the C_p against E profile will be evaluated separately by consideration of the anticipated repulsive effects which can arise due to the presence of partially charged species in adsorbed metal layers formed by underpotential deposition.

As can be seen from equation (31), the electrosorption valency enters into the C_p-E relation in two ways. Once as a scaling factor in the pre-exponential factor and then in the exponent. It follows from this that the magnitude of the value of C_p at any potential will be attenuated by the fraction γ^2 and the shape of C_p against E profiles will depend on γ as can be seen from figure 2 [30, 40].

The effect of electrosorption valency in broadening and lowering the C_p against E profiles (figure 2) may be eliminated by an interesting method, which allows the anticipated repulsion to be separately demonstrated.

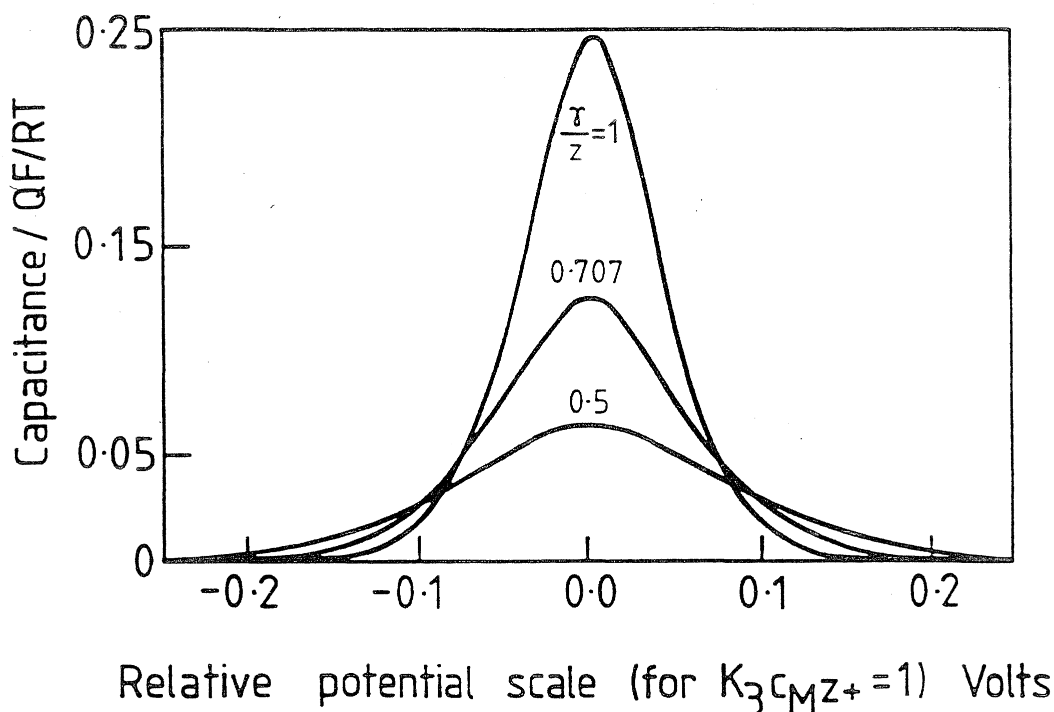

Figure 2. Pseudocapacitance (C) against potential profiles for a one e, single-state UPD process for three values of the electrosorption valency [30].

From equation (31) it can be seen that the decreasing effect of $\gamma < z$ on C_p against E profile will disappear if a reduced capacitance, $C_p/(\gamma^2/z^2)$ is plotted as $f(E)$. The broadening effect will also disappear if the reduced capacitance is plotted against a scaled potential, $(\gamma/z)E$. The new plot will have the same form as the C_p against E profile for any value of electrosorption valency and will show a Langmuir behaviour [43]. When the lateral interaction effects are taken into account then the increase of the half-widths of $C_p/(\gamma^2/z^2)$ against $(\gamma/z)E$ profiles takes place in a characteristic way as it does in the general case [30, 44].

3.2.5.3. *Lateral interaction effects*

The behaviour of adsorbed species deposited by underpotential deposition is usually reversible and takes place over a characteristic range of potential, very often in multiple states below monolayer coverage, as has been mentioned earlier. This behaviour can be explained by the fact that the adsorbed atoms are deposited in an array or sequential series of arrays rather than as nucleated islands [30]. When partially discharged species are present in the adsorbed layers Coulombic repulsive forces will be expected to operate between adsorbed atoms, thus minimizing the free energy of formation of a 2D lattice array. In this case the adsorption isotherm must contain a term resulting from the long-range 2D free energy of lateral interactions

When the adsorbed metal atoms bear an effective charge $(1 - \gamma/z)e$, because $\gamma < z$, the 2D repulsive forces bring about a change of energy of adsorption proportional to $\theta^{3/2}$ if an image surface dipole of $\pm(1 - \gamma/z)el$ arises over a charge-separation distance l

[19, 40], as has already been mentioned (see section 3.2.3). The lateral interaction energy U is given in the nearest-neighbour approximation [40] as follows:

$$U \approx \frac{n}{2}\frac{\mu^2}{\mathscr{R}^3}\theta^{3/2} = \frac{n}{2}\frac{(1-\gamma/z)^2 e^2 l^2}{\mathscr{R}^3}\theta^{3/2}, \tag{32}$$

where n is the 2D coordination number of the surface lattice array and $\mathscr{R}$ is the nearest-neighbour distance at $\theta = 1$. In this case μ is the surface dipole moment $(1-\gamma/z)el$.

Substituting equation (32) into equation (30) gives

$$\frac{\theta}{1-\theta} = K_3 \exp\left[-\frac{n}{2}\frac{(1-\gamma/z)^2 e^2 l^2}{\mathscr{R}^3}\frac{\theta^{3/2}}{RT}\right] c_{M^{z+}} \exp\left(\frac{\gamma FE}{RT}\right). \tag{33}$$

Comparing equation (33) with a Frumkin-type isotherm leads to a definition of the (Frumkin) interaction parameter g [40]:

$$g = \frac{n}{2}\frac{\mu^2}{\mathscr{R}^3 RT} = \frac{n}{2}\frac{(1-\gamma/z)^2 e^2 l^2}{\mathscr{R}^3 RT} = (1-\gamma/z)^2 \frac{r}{RT}. \tag{34}$$

If the partially charged adsorbed metal atoms are regarded simply as adsorbed ions, the interaction potential arises from simple charge repulsion only and would vary as $(n-2)(1-\gamma/z)^2 e^2 \theta^{1/2}/\mathscr{R}$ [45] and the g parameter is defined by

$$g' = \frac{n}{2}\frac{(1-\gamma/z)^2 e^2}{\mathscr{R}RT}. \tag{35}$$

Differentiating equation (33) with respect to E the result is multiplied by $(\gamma/z)Q$ and the required pseudocapacitance will be obtained [40]:

$$C_p = \frac{\gamma}{z}Q\frac{d\theta}{dE} = \frac{\gamma^2 QF}{zRT}\frac{\theta(1-\theta)}{1+\frac{3}{2}g\theta^{3/2}(1-\theta)}. \tag{36}$$

In the absence of lateral interaction effects ($g=0$), equation (36) will be simplified and will have the form of equation (31).

In the case of equation (36) an explicit expression cannot be written for C_p as $f(E)$, but numerical evaluation can be made easily, using C_p as $f(\theta)$ from equation (36) together with $\theta = f(E)$ from equation (33) for various values of γ, because the actual magnitude of γ can be determined from separate experiments [40].

If the reduced adsorption capacitance values $(C_p/(\gamma^2/z^2))$ calculated by equation (36) are plotted against scaled potentials $((\gamma/z)E)$, then the lateral interactions in electrodeposited monolayers can be demonstrated for different values of $\gamma < z$. The g factor can be evaluated from the resulting half-widths and interpreted in terms of an adion or surface dipole model of the lateral interactions. The plot of the scaled half-width as $f(g)$ for lateral repulsive interactions between partially charged adsorbed atoms in a random 2D array is almost linear in g for $g > 0$ [40].

A more realistic approach to lateral interactions is based on the calculation of electrostatic free energy of interaction (G_e) separately for partial charges and for surface dipoles originating from partial charges and their images [30]. The form of $f(\theta)$ in this case will depend on whether the adsorbed atoms are assumed to interact as simple partial charges, $(1-\gamma/z)e$, or surface dipoles with a surface dipole moment $m = (1-\gamma/z)e \times 2d$ where d is the effective contact distance of adsorbed atoms from the surface of the substrate (S) [30].

The electrostatic free energy of interaction for partial charges:

$$G_e = \frac{n}{2}\frac{(z-\gamma)^2 e^2}{\varepsilon r}, \tag{37}$$

and for surface dipoles:

$$G_e = \frac{n}{2}\frac{(z-\gamma)^2 e^2 4d^2}{\varepsilon r^3}, \tag{38}$$

where r is the interparticle separation at a coverage θ and ε is the dielectric constant of the interphase.

Taking into consideration that $\mathcal{R}$ is given by $r=\mathcal{R}/\theta^{1/2}$ in relation to θ and r if the substrate surface is a (111), (100) or (110) crystal plane, equations (37) and (38) in terms of θ become

$$G_e = \frac{n}{2}\frac{(z-\gamma)^2 e^2}{\varepsilon \mathcal{R}}\theta^{1/2}. \tag{39}$$

or

$$G_e = \frac{n}{2}\frac{(z-\gamma)^2 e^2 4d^2}{\varepsilon \mathcal{R}^3}\theta^{3/2} \tag{40}$$

respectively [30].

The corresponding adsorption isotherms for the above two cases are

$$\frac{\theta}{1-\theta} = K_3 c_{M^{z+}} \exp\left[-\frac{n}{2}\frac{(z-\gamma)^2 e^2}{2\varepsilon \mathcal{R} kT}\theta^{-1/2}\right]\exp\left(\frac{\gamma FE}{RT}\right), \tag{41}$$

$$\frac{\theta}{1-\theta} = K_3 c_{M^{z+}} \exp\left[-\frac{n}{2}\frac{(z-\gamma)^2 e^2 6d^2}{\varepsilon \mathcal{R}^3 kT}\theta^{1/2}\right]\exp\left(\frac{\gamma FE}{RT}\right). \tag{42}$$

It should be noted that the G_e terms have to be differentiated with respect to the particle number density in order to obtain the chemical potentials of the ad-phase and hence the adsorption isotherms [30].

Earlier papers on image effects indicate that these effects persist even at short distances from metal surfaces but the image potential is modified by a screening factor when d becomes comparable with atomic dimensions. Hence the lateral interactions calculated in terms of repulsion amongst surface dipoles arising from the partial charges and their images provides the preferred basis for the adsorption isotherm of the adsorbed metal atoms deposited by underpotential deposition on foreign metal substrates as it is given by equation (42) rather than equation (41) [30].

In order to obtain the adsorption pseudocapacitance equation (42) has to be differentiated [30]:

$$C_p = \frac{\gamma^2 QF}{zRT}\frac{\theta(1-\theta)}{1+\frac{1}{2}g^*\theta^{1/2}(1-\theta)}, \tag{43}$$

where g^* is the interaction parameter and when $g^*=0$ then equation (43) will assume the form of equation (31).

Equation (43) is similar to equation (36), thus its application in the evaluation of lateral interactions is also the same. For evaluation of the interaction effects in terms of reduced pseudocapacitance ($C_p(\gamma^2 z^2)$) calculated by equation (43) at different values

of g^*, the results must be plotted against scaled potential $((\gamma/z)E)$. Because of the dependence of C_p on θ as well as on $\theta^{1/2}$ terms the shape of the resulting $C_p/(\gamma^2/z^2)$ functions will be asymmetric [30]. The difference between the curves calculated by equations (36) and (43) at different hypothetical g values are the loci of reduced pseudocapacitance maxima. With the use of equation (36) for calculations the loci of the pseudocapacitance maxima are almost independent of the magnitude of g whilst the loci of maxima of the curves obtained by equation (43) are shifted gradually towards a positive range of scaled potentials, with increasing values of g^*.

The half-widths are almost linear in g^* as they are obtained with curves calculated by equation (36).

3.2.5.4. *Conclusions on interaction effects*

The first effects of $\gamma < z$ are the broadening and lowering of the C_p versus E profiles without dependence on some arbitrary parameters (figure 2) and these effects should be manifested in experimental capacitance curves. Experimental C_p against E curves are well resolved into several distinguishable peaks which could not arise if γ were appreciably less than 1 because the broadening and lowering would obscure the distinguishable states of adsorbed metal atoms by overlap [30].

The fact that most experimental results of underpotential deposition show clear resolution into multiple states over a narrow potential range requires that γ be close to z [4, 16, 17, 19, 46]. Another explanation of the experimental observations could be the screening effect by ions of opposite charges and solvent dipoles staying amongst the ad-species in the monolayer [30]. The screening effect, however, must diminish as $\theta \rightarrow 1$ due to exclusion of the screening dipoles or ions from the monolayer, but resolution of multiple states of adsorption in a monolayer is not usually noticeably smaller at high coverages. This indicates that screening effects do not seem to be a major factor in the behaviour of monolayers formed by underpotential deposition [30].

3.3. *The thin-layer technique in the thermodynamics of UPD*

The twin-electrode thin layer cell [10, 16, 47–49] consists of four electrodes: the working or indicator electrode, the generator electrode and the usual reference and counter electrodes. The generator and indicator electrodes are situated parallel to each other about 50 μm apart and they have independent potential regulation.

The generator electrode must be a reversible electrode for the same metal as that to be deposited at the indicator (working) electrode. The metal ion activity in the cell is given by the potential of the generator electrode according to Nernst's law. The potential of the generator electrode is usually fixed at a certain point, therefore any changes in concentration within the thin layer due to metal ion deposition or dissolution are compensated by the generator.

The advantage of this technique is that the charge and mass fluxes at the indicator electrode can be measured. The charge flux is given by the current density at the indicator electrode, whereas the mass flux to the indicator electrode corresponds to the current density at the generator electrode.

Under the conditions of constant temperature, pressure and electrolyte composition the thermodynamics of the adsorbate on the indicator electrode in the underpotential range $E \geqslant E_N$ is described by q (the charge on the indicator electrode) and Γ (the surface concentration of adsorbed metal on the indicator electrode) as functions of the indicator (E) and generator (E_N) potentials. At constant generator

electrode potential, the chemical potential of the depositing ions in the thin layer of the supporting electrolyte is also constant.

Upon variation of the potential of metal deposition from an initial equilibrium (E_i) at the initial time (t_i) to a new equilibrium (E_f) at the final time (t_f) in the time interval $t_i \leqslant t \leqslant t_f$, the integral of the current at the generator electrode (i_g) will be equal to the mass flux deposited onto the indicator electrode [48, 49], and thus,

$$-(zFA)^{-1} \int_{t_i}^{t_f} i_g \, dt = \Gamma(M_{ads_f}, E_f) - \Gamma(M_{ads_i}, E_i), \tag{44}$$

where $\Gamma(M_{ads_i}, E_i)$ is the initial surface concentration and $\Gamma(M_{ads_f}, E_f)$ is the final surface concentration of the metal deposited onto the indicator electrode at constant solution composition and activity of the depositing ions. A is the electrode surface area and the sign is positive for reduction current.

The charge used for metal deposition (or oxidation) can be calculated by the integral of the current at the indicator electrode (i) [48, 49]:

$$A^{-1} \int_{t_i}^{t_f} i \, dt = q(E_f, \Gamma_f) - q(E_i, \Gamma_i), \tag{45}$$

where $q(E_i, \Gamma_i)$ is the charge on the electrode at the beginning of polarization and $q(E_f, \Gamma_f)$ is the charge on the electrode at the end of deposition also at constant solution composition and activity of the depositing ions.

At a sufficiently positive potential $E_i > E_{ML}$ the coverage of adsorbed metal on the indicator electrode vanishes

$$\lim_{E \to \infty} \Gamma(M_{ads}, E) = 0, \tag{46}$$

and thus it is possible to determine the absolute values of Γ by the appropriate choice of E_i (where $\Gamma(M_{ads_i}, E_i) = 0$).

When $E_i > E_{ML}$ then the charge on the indicator electrode is at zero coverage and at E_i initial potential is $q(E_i, \Gamma = 0)$.

At a sufficiently negative generator electrode potential (E_g) (where there are no depositing ions in the thin layer) the charge used for double layer charging in the potential interval of underpotential deposition can easily be determined [48, 49]:

$$\lim_{E_g \to -\infty} A^{-1} \int_{t_i}^{t_f} i \, dt = q(E_f, \Gamma = 0) - q(E_i, \Gamma = 0) \equiv A^{-1} \int_{t_i}^{t_f} i_b \, dt, \tag{47}$$

where $q(E_i, \Gamma = 0)$ is the charge on the indicator electrode at the beginning of polarization and $q(E_f, \Gamma = 0)$ is the charge at the end in the supporting electrolyte free of the depositing ions. i_b is the double layer charging current.

Combination of equations (45) and (47) yields the charge (Δq) due to (underpotential) deposition of metal ions onto the indicator electrode [48]

$$A^{-1} \int_{t_i}^{t_f} (i - i_b) \, dt = q(E_f, \Gamma_f) - q(E_f, \Gamma = 0) \equiv \Delta q. \tag{48}$$

From equations (44) and (46) the amount of adsorbed material on the indicator electrode can be calculated and from equation (48) the amount of charge used for underpotential deposition may be derived. By partial differentiation of Δq with respect to Γ the electrosorption valency is obtained [48, 49].

The thin layer technique yields thermodynamic data such as adsorption isotherms with high accuracy. Kinetic data cannot be obtained by this method because the system must always be in a quasi-equilibrium state or in the steady state so as to make possible the mathematical treatment of the experimental results [10, 16].

The flow-through thin-layer technique also provides independent q and Γ data at a very high accuracy, thus allowing a direct determination of electrosorption valency [50].

4. The kinetics of underpotential deposition

The formation of adsorbed metal monolayers on foreign metal substrates (S) is a complex process composed of several phenomena. The very first of these is the transport of the depositing ions from the bulk of the (supporting) electrolyte to the substrate surface. The second is the charge transfer (reaction (3)) and then the adsorption of the discharged metal atom on one or more adsorption sites of the substrate metal surface. (There are authors, however, who assume that adsorption precedes charge transfer [51]. In the course of monolayer formation from a multivalent ion this can be the reaction sequence.)

After discharge and adsorption the 2D nucleation and growth phenomena must be taken into consideration in the process of monolayer formation. Before the appearance of bulk deposition the surface diffusion of the deposited metal atoms may play a role in the formation of an UPD layer.

Naturally, any of these phenomena can be the rate-determining step in the course of underpotential deposition. It must be taken into account that the formation of adsorbed metal monolayers on foreign metal substrates is usually carried out in very diluted solutions of the ions to be deposited, so that the mass transport has a profound effect on the kinetics of underpotential deposition. It follows that the most suitable methods for studying the kinetics of underpotential deposition at low solution concentration of the depositing ions involve rotating electrodes [18, 31, 38, 51–53].

Kinetics of underpotential deposition have also been studied at stationary electrodes [10, 16, 17, 26].

In some cases potentiostatic or galvanostatic pulse measurements were used for studying the kinetics of underpotential deposition of metals [10, 26, 54–56].

In the course of underpotential deposition the change of surface concentration of adsorbed species ($d\Gamma$) is connected with the change of the charge on substrate metal (dq_S), therefore the rate of metal adsorption on foreign metal substrates ($v = d\Gamma/dt$) results in an adsorption current density ($i = dq_S/dt$) [27]. In the case of use of excess supporting electrolyte and at constant substrate potential the current density of underpotential deposition is [27]

$$i = \left(\frac{\partial q_S}{\partial t}\right)_E = \left(\frac{\partial q_S}{\partial \Gamma}\right)_E \left(\frac{\partial \Gamma}{\partial t}\right)_E = -\gamma F v, \tag{49}$$

taking into consideration equation (8).

With the help of a similar equation the rate of desorption of adsorbed metal atoms can be described [26].

The rate equation depends on the adsorption isotherm chosen to describe the activity of adsorbed metal atoms.

4.1. *Study of the kinetics of underpotential deposition with rotating electrodes*

As has been mentioned earlier, for the low concentration of the depositing ions ($\leqslant 10^{-4}$ M) in the supporting electrolyte the rotating electrodes are excellent tools to study the kinetics of underpotential deposition. A widely used variety of the rotating electrodes is the rotating ring-disc electrode (RRDE) which is an exceptionally powerful tool for the study of the kinetics of UPD [18, 51, 52, 57]. Construction of RRDE: the disc electrode is made of substrate metal and the ring electrode is preferably made from the same metal deposited on the disc [18, 57].

Before its use in the experiments the RRDE electrode must be pretreated in a strictly reproducible manner to achieve appropriate reproducibility. The pre-treatment is mechanical polishing and then electrochemical stabilization of the surface [18]. This is accomplished by plating the ring with at least ten layers of the metal deposited on the disc electrode [18].

It is very important that in the course of the experiments the depositing ions must undergo convective-diffusion-controlled reduction at the ring electrode. This is achieved by using a sufficiently negative ring potential [18].

The ring electrode response allows quantitative study of the kinetics of underpotential deposition whilst the disc electrode data facilitate the determination of the dynamic electrosorption valency [52]. In the absence of simultaneous adsorption and partial charge transfer the disc current is a measure of the double layer charging component accompanying a shift in the PZC (potential of zero charge) of the substrate metal. The disc current data can be used to evaluate the double layer capacitance as a function of coverage at various potentials of metal deposition and various metal ion concentrations [52].

4.1.1. *Ring-electrode behaviour*

Two cases of coupling of mass transport with surface phenomena will be considered: fast heterogeneous equilibrium on the disc surface, and slow surface processes.

4.1.1.1. *Diffusion control with coupled heterogeneous equilibrium*

In this case the rate of underpotential deposition is controlled by the diffusion of depositing ions from the bulk of supporting electrolyte and equilibrium is established rapidly between the species adsorbed on the disc electrode and the depositing ions at the disc surface.

The rate of underpotential deposition obtained from the ring response can be calculated from the difference between the instantaneous and fully unshielded ring currents (ΔI_R^t), the ring collection efficiency (N) and the instantaneous coverage (θ_t) of the deposited metal atoms. The rate of underpotential deposition (I_a^t) is given by [52]

$$I_a^t = \frac{\Delta I_R^t}{N} = 0{\cdot}6204 zFAD^{2/3}\nu^{-1/6}\omega^{1/2}(C^b - C_t^s), \qquad (50)$$

where C^b and C^s are bulk and surface concentrations respectively and the other symbols have their usual significance.

The instantaneous surface concentration of the depositing ions (C_t^s) can be calculated from equation (16). On the assumption that $\gamma = z$ and the monolayer free

energy decreases linearly with coverage (equation (21)), equation (50) can be converted to

$$I_a^t = 0{\cdot}6204zFAD^{2/3}\nu^{-1/6}\omega^{1/2}\left\{C^b - \left(\frac{\theta_t}{I-\theta_t}\right)\exp\left[f\theta_t + \frac{zF}{RT}(E_{ML}^a - E_{ML}^o)\right]\right\}, \quad (51)$$

where E_{ML}^a is the potential applied in potentiostatic case and θ_t is instantaneous coverage [52].

Instantaneous coverage (θ_t) can be calculated from

$$\theta_t = \frac{1}{\Gamma_s}\int_0^t J_a^t \, dt, \quad (52)$$

where

$$J_a^t = 0{\cdot}6204D^{2/3}\nu^{-1/6}\omega^{1/2}(C^b - C_t^s), \quad (53)$$

and Γ_s is maximum surface concentration at unit coverage [52].

4.1.1.2. *Mass transport coupled to slow surface processes*

When the rate of surface processes are not fast enough compared to convective-diffusion conditions, mixed control will exist. Initially the adsorption rate is high but as coverage increases the activity of the electrode decreases leading to a decrease in the forward rate of underpotential deposition and an increase in stripping (backward) rate. It follows that the potentiostatic transient response of this process is initially mass transport controlled, followed by mixed control and finally results in surface reaction control as the system approaches equilibrium [52].

Adsorption coupled to charge transfer (and/or surface diffusion) will be considered. The absence or presence of control by surface diffusion may be deduced from the magnitude of kinetic parameters [52].

For the UPD process given by equation (3), the flux of depositing ions (M^{z+}) is given by [52]

$$J = k_f' a_{ML}^u C^s - k_b' a_{ML}^c, \quad (54)$$

$$J = D(C^b - C^s)/\delta, \quad (55)$$

where $\delta = 1{\cdot}612D^{1/3}\nu^{1/6}\omega^{-1/2}$. a_{ML}^u is the activity of the uncovered portion of the substrate metal and a_{ML}^c is the activity of the covered portion. $a_{ML}^c \cdot a_{ML}^u = a_{ML}$ is the activity of the deposit.

Due to the coupled charge transfer the rate constants in equation (54) (k_f' and k_b') are potential dependent. Monolayer activities of covered and uncovered portions of the substrate metal can be calculated using the adsorption isotherm obtained from equations (16) and (21). After substituting the results of the calculation of rate constants and monolayer activities in equation (54) the flux of underpotentially deposited species at the disc surface is

$$J = k_f(1-\theta)C^s \exp\left(-\frac{\alpha zF}{RT}E_{ML}^a\right)\exp(-\beta f\theta)$$
$$- k_b\theta \exp\left[(1-\alpha)\frac{zF}{RT}E_{ML}^a\right]\exp[(1-\beta)f\theta]. \quad (56)$$

where β is the adsorption coefficient and the other symbols have their usual significance.

Surface concentration of the depositing species (C^s) under mixed mass transport and potential-dependent adsorption is obtained by the combination of equations (55) and (56). The rate (I_a^t) of underpotential deposition obtained from the ring shielding response is found by eliminating C^s from equation (50) using the result of combination of equations (55) and (56), and thus the UPD rate under mixed control is given by [18, 52]:

$$I_a^t = zFAD\left\{k_f C^b(1-\theta_t)\exp(-\beta f\theta_t)\exp\left(-\frac{\alpha zF}{RT}E_{ML}^a\right) - k_b\theta_t\exp\left[(1-\alpha)\frac{zF}{RT}E_{ML}^a\right]\exp[(1-\beta)f\theta_t]\right\} \times\left[D+1{\cdot}612D^{1/3}\nu^{1/6}\omega^{-1/2}k_f(1-\theta_t)\exp(-\beta f\theta_t)\exp\left(-\frac{\alpha zF}{RT}E_{ML}^a\right)\right]^{-1}. \quad (57)$$

Several limiting cases of equation (57) corresponding to mass transport control with rapid heterogeneous equilibrium and surface reaction control have been discussed in reference [52].

The rate of underpotential deposition can also be expressed in terms of exchange current density [52]:

$$I_a = I_a^o\left\{\frac{1-\theta_t}{1-\theta_e}\frac{C^s}{C^b}\exp[\beta f(\theta_e-\theta_t)] - \frac{\theta_t}{\theta_e}\exp[-(1-\beta)f(\theta_e-\theta_t)]\right\}, \quad (58)$$

where θ_e is the equilibrium coverage.

Two types of overpotentials may exist for an UPD reaction (equation (16)) under potentiostatic conditions. One is due to the departure of surface concentration from the bulk value (η_c); the other results from the difference in monolayer activity from its final value at equilibrium (η_a). Total overpotential (η_{ads}) is the sum of these ($\eta_{ads} = \eta_c + \eta_a$) [18, 52]:

$$\eta_{ads} = \frac{RT}{\gamma F}\ln\frac{C^s}{C^b} + \frac{RT}{\gamma F}\left[\ln\frac{\theta(1-\theta_e)}{\theta_e(1-\theta)} + f(\theta-\theta_e)\right]. \quad (59)$$

The instantaneous overpotential can be calculated from the ring current data and it is a measure of the extent of departure from equilibrium conditions at any instant during the transient response [52].

4.1.2. *Disc electrode behaviour*

The disc electrode current transient allows the determination of the dynamic electrosorption valency (γ_d), which involves a coupling of charge-separation and charge-transfer components [18, 52]. The dynamic electrosorption valency is defined by [18, 31, 52]:

$$\gamma_d = \frac{1}{F}\left(\frac{\partial q}{\partial \Gamma}\right)_E = \frac{(\partial q/\partial t)_E}{F(\partial \Gamma/\partial t)_E} \quad (60)$$

where $\partial q/\partial t$ is given by the instantaneous disc current transient and $\partial\Gamma/\partial t$ is the instantaneous ring current accompanying the underpotential deposition at the disc.

γ_d is a measure of the total instantaneous charge that flows during underpotential deposition, due to charge separation and charge leakage processes per mole of deposited metal atoms [18, 52].

The dynamic electrosorption valency at constant applied potential ($\gamma_{d,E}$) [18] is

$$\gamma_{d,E}F = \gamma_{cs,E}F + \gamma_{ct,E}F = \left(\frac{\partial q_S}{\partial \Gamma}\right)_{E_a} + \left(\frac{\partial q_c}{\partial \Gamma}\right)_{E_a}, \tag{61}$$

The charge separation term of dynamic electrosorption valency (γ_{cs}) is a measure of the change in charge on the metal due to two effects:

(*a*) a shift in potential of zero charge caused by work function change accompanying underpotential deposition of metals (γ_{cs}^{ma}), and
(*b*) changes in specific adsorption of anions (γ_{cs}^{aa}) [18].

The charge separation component of dynamic electrosorption valency (γ_{cs}^{ma}) will always result in deviations of dynamic electrosorption valency ($\gamma_{d,E}$) from z (even if anion adsorption does not contribute to the deviation).

The charge-transfer component (γ_{ct}) of dynamic electrosorption valency is also determined by two effects:

(*a*) the Faradic charge-transfer reaction resulting in adsorbed metal monolayer (reaction (3)) (γ_{ct}^{ma}), and
(*b*) chemisorption reactions involving the discharge and adsorption of anions of the solvent, which take place at the same potential where underpotential deposition of metals (γ_{ct}^{aa}) occurs, for instance hydrogen adsorption and oxide formation [18].

Taking into consideration that the charge on the substrate metal (q_S) is a function of the rational potential ($E_R = E_{PZC} - E_a$) and the solution composition (μ) thus,

$$dq_S = \left(\frac{\partial q_S}{\partial E}\right)_\mu dE_{PZC} - \left(\frac{\partial q_S}{\partial E}\right)_\mu dE_a + \left(\frac{\partial q_S}{\partial \mu}\right)_E d\mu. \tag{62}$$

At constant applied potential (E_a) and solution composition (μ)

$$\left(\frac{\partial q_S}{\partial \Gamma}\right)_{E_a,\mu} = \left(\frac{\partial q_S}{\partial E}\right)_\mu \left(\frac{\partial E_{PZC}}{\partial \Gamma}\right)_{E_a} = C_{\mu_s}\left(\frac{\partial E_{PZC}}{\partial \Gamma}\right)_{E_a} = \gamma_{cs,E}^{ma}F. \tag{63}$$

where C_{μ_s} has the dimensions of electrode capacitance at constant coverage [52].

The potentials of zero charge for metals are linearly related to the work function, and the underpotential shift is approximately equal to the difference between the work functions of the substrate and the adsorbate, therefore $\Delta E_{PZC} \approx \Delta U$ [18, 52]. Taking into account equation (22), assuming that $\gamma = z$ and substituting the result into equation (63), we have

$$\gamma_{cs,E}^{ma}F = C_{\mu_s}\frac{RT}{zF\Gamma_s}\left(\frac{\theta}{1-\theta} + f\theta\right). \tag{64}$$

γ_{ct}^{ma} will be equal to z in most cases. The non-Faradic mechanism, when $\gamma_{ct}^{ma} \neq z$, has already been discussed.

If anion adsorption and chemisorption effects are not separable *a priori*, γ_{cs}^{aa} and γ_{ct}^{aa} will also contribute to $\gamma_{d,E}$ [18, 52].

4.2. *Potentiodynamic study of underpotential deposition using rotating ring-disc electrode technique*

Cyclic voltammetry is the most frequently used method in studying underpotential deposition of metals on foreign metal substrates. The number of UPD peaks on cyclic voltammograms and the width of peaks were considered in interpreting the thermodynamical and adsorption character of underpotential deposition. However, the current at an electrode does not define mass flux to the substrate metal. For this reason, if the cyclic voltammetric method is not combined with a simultaneous method of monitoring the flux of depositing ions at the substrate metal, interpretation of the cyclic voltammetric data becomes ambiguous for two reasons [53].

Firstly, as can be seen from section 4.1.2, underpotential deposition modifies the double layer structure [53].

Secondly, underpotential equilibrium may not be rapidly established and simultaneous chemisorption processes may interfere with UPD. On the other hand, different phenomena, such as diffusion, charge transfer or adsorption, can be the rate-determining step of UPD. The rate laws of these phenomena will also influence the shape of cyclic voltammograms. The different potential dependence of the rate determining steps must be taken into consideration in the analysis of potentiodynamic responses [53].

4.2.1. *Ring electrode response*

Models including mass transfer, charge transfer and adsorption kinetics will be analysed below.

4.2.1.1. *Potential scan control with rapid heterogeneous equilibrium*

In this case the rate of underpotential deposition (j_a^E) at any instantaneous potential (E) will be controlled by the potential scan rate $(\mathrm{d}E/\mathrm{d}t)=s$

$$j_a^E=\Gamma_s\left(\frac{\mathrm{d}\theta_E}{\mathrm{d}t}\right)=\Gamma_s\left(\frac{\mathrm{d}\theta_E}{\mathrm{d}E}\right)\left(\frac{\mathrm{d}E}{\mathrm{d}t}\right)=\Gamma_s s\frac{\mathrm{d}\theta_E}{\mathrm{d}E}, \tag{65}$$

where θ_E is the coverage at potential E.

The changes in solution composition at the interface are assumed to be negligible in this model [53].

The ring current response is given by

$$I_R^s=I_R-zFANj_a^E, \tag{66}$$

where I_R is the fully unshielded ring current and I_R^s is the shielded ring current response.

Calculating $\mathrm{d}\theta_E/\mathrm{d}E$ from the combination of equations (16) and (21) and substituting the result into equation (66) yields the ring current [53]:

$$I_R^s=I_R-\frac{zFANs}{RT}\frac{\theta_E(1-\theta_E)}{1+f\theta_E(1-\theta_E)}. \tag{67}$$

4.2.1.2. *Mixed control of surface processes and mass transport*

The concentration of depositing metal ions in supporting electrolyte is usually low and so the rate of underpotential deposition can be under mixed control of mass transport and/or surface processes (adsorption and charge transfer). The potentiodynamic ring current is obtained by the same method as described in section 4.1.1.2 [52, 53].

A detailed description of the derivation of the equation of potentiodynamic ring current can be found in references [52] and [53]. Therefore only two limiting cases will be outlined here.

(*a*) Rapid heterogeneous equilibrium with mass transport control.

In this case the potentiodynamic ring current is given by

$$I_R - I_R^s = (NzFAD/\delta)(C^b - C^s), \tag{68}$$

where

$$C^s = \frac{\theta_E}{1-\theta_E}\exp\left[f\theta_E - \frac{zF}{RT}(E^o_{ML} - E^i_{ML} - st)\right], \tag{69}$$

where $E^o_{ML} - E^i_{ML}$ is an overpotential of underpotential deposition at the initial potential E^i_{ML} [53].

Under these conditions, surface concentration (C^s) may be much lower than bulk concentration (C^b). Equilibrium between the electrode surface covered with adsorbed metal atoms and ions at the substrate surface can be rapidly established. This process results in a convective-diffusion controlled flux at the disc electrode. As coverage increases, C^s will also increase, and finally, at $\theta = 1$, C^s will be equal to C^b.

(*b*) Slow heterogeneous equilibrium with negligible concentration polarization.

Under these circumstances the potentiodynamic ring current is given by [53]

$$I_R - I_R^s = NzFA\left\{k_f C^b \exp\left[-\frac{\alpha zF}{RT}(E^{a,i}_{ML} + st)\right](1-\theta_E)\exp(-\beta f\theta_E) - k_b\theta_E \exp\left[(1-\alpha)\frac{zF}{RT}(E^{a,i}_{ML} + st)\right]\exp[(1-\beta)f\theta_E]\right\} \tag{70}$$

where $E^{a,i}_{ML}$ is the initial absolute potential.

The limiting case may be achieved at very positive applied potentials when the charge transfer in reaction (3) is slow with respect to transport processes [53].

4.2.2. *Disc electrode response*

The potentiodynamic disc electrode response yields also the value of dynamic electrosorption valency but at constant solution composition ($\gamma_{d,\mu}$), and this is again composed of charge separation (γ_{cs}) and charge transfer (γ_{ct}) contributions [18, 53]

$$\gamma_{d,\mu}F = \left(\frac{\partial q}{\partial \Gamma}\right)_\mu = \gamma_{cs,\mu}F + \gamma_{ct,\mu}F. \tag{71}$$

Underpotential deposition results in a negative shift in the potential of zero charge. Usually, the potential is also scanned negatively when investigation of UPD takes place by cyclic voltammetry. Because of the shift of PZC, charging current will arise and the direction of this current will be opposite to that due to the potential scan.

From equation (62) at constant solution composition [18]:

$$\gamma_{cs,\mu}F = \left(\frac{\partial q_S}{\partial \Gamma}\right)_\mu = C_{\mu,s}\left(\frac{\partial E_R}{\partial \Gamma}\right)_\mu. \tag{72}$$

The non-Faradic charge separation current (i_{cs}) will be [18]

$$i_{cs} = \gamma_{cs,\mu} F \frac{d\Gamma}{dt} = C_{\mu,s} \frac{dE_{PZC}}{dt} - C_{\mu,s} \frac{dE_a}{dt}. \quad (73)$$

From equation (73) it follows that there will be no charging current when the scan rate (dE_a/dt) is equal to the rate of shift of potential of zero charge (dE_{PZC}/dt).

The charge-transfer contribution to electrosorption valency is [18, 53]:

$$\gamma_{ct,\mu} F = \gamma_{ct,\mu}^{ma} F + \gamma_{ct,\mu}^{aa} F = \left(\frac{\partial q_{ma}}{\partial \Gamma}\right)_\mu + \left(\frac{\partial q^a}{\partial \Gamma^-}\right)_\mu \left(\frac{\partial \Gamma^-}{\partial \Gamma}\right)_\mu. \quad (74)$$

The $\gamma_{ct,}^{ma}$ contribution to the charge-transfer portion ($\gamma_{ct,\mu}$) of dynamic electrosorption valency is due to the charge transfer (reaction (3)) of underpotential deposition. The simultaneous chemisorption reactions are taken into account by $\gamma_{ct,\mu}^{aa}$. The extent of interaction of the chemisorption processes with underpotential deposition is measured by the coupling factor ($\partial\Gamma^-/\partial\Gamma$). When it is equal to zero, the simultaneous chemisorption reactions do not interact with the underpotential deposition [18, 53].

4.3. *Conclusions drawn from the study of kinetics with rotating electrodes*

The rate of underpotential deposition can be under mixed control by mass transport and adsorption with coupled charge transfer. The charge transfer coefficient is similar to that observed for bulk deposition. From the dependence of exchange current density and double layer capacitance on applied potential the formation of a randomly adsorbed structure at low coverage and a more ordered structure at higher coverages can be concluded.

The potentiodynamic peak structure not only depends on the thermodynamics of underpotential deposition but also on the kinetics of metal adsorption on foreign metal surfaces.

The formalism proposed for the dynamic electrosorption valency (γ_d) shows that even in the absence of simultaneous chemisorption reactions the value of dynamic electrosorption valency will differ from Faradic reaction valency owing to the shift in the potential of zero charge caused by underpotential deposition.

Experimental details are given in references [18, 52, 53].

4.4. *Kinetics of underpotential deposition with several adsorbed states*

According to the general phenomenological theory of chemisorption reactions [29, 58], a consecutive mechanism can be written in this case in three steps

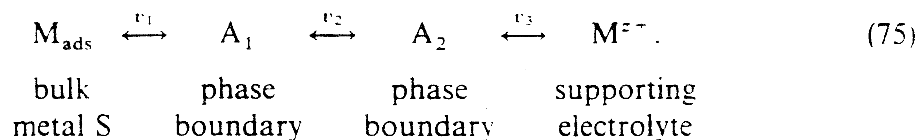

The adsorbed intermediates carry the macroscopic charges, zl_1 in A_1 boundary and $z(l_1 + l_2)$ in A_2 boundary, including double layer contributions. v_1, v_2 and v_3 are reaction rates [58].

4.4.1. *Charge and mass balances*

The charge balance of reaction (75) is given by [58]

$$j=\sum_{i=1}^{3}\lambda_i zFv_i+\frac{d\sigma}{dt}, \tag{76}$$

where j is the total current, λ is the partial charge transfer coefficient and σ is the (double layer) charge on the electrode [58].

Variation of (double layer) charge

$$d\sigma=\left(\frac{\partial\sigma}{\partial E}\right)dE+\sum\left(\frac{\partial\sigma}{\partial\Gamma_i}\right)d\Gamma_i+\left(\frac{\partial\sigma}{\partial c_{\mathrm{Mads}}}\right)dc_{\mathrm{Mads}},\quad x=0, \tag{77}$$

where $(\partial\sigma/\partial E)$ is equal to the high-frequency double layer capacity (C_∞).

In the derivation of the combination of equations (76) and (77), the mass balances from equation (76) are [58]

$$d\Gamma_1/dt=v_1-v_2, \tag{78 a}$$

$$d\Gamma_2/dt=v_2-v_3. \tag{78 b}$$

The l coefficients which contain the double-layer parameters $(\partial\sigma/\partial\Gamma_i)$ are

$$l_1=\lambda_1+(\partial\sigma/\partial\Gamma_1)_E/zF, \tag{79 a}$$

$$l_2=\lambda_2+[(\partial\sigma/\partial\Gamma_2)_E-(\partial\sigma/\partial\Gamma_1)_E]/zF, \tag{79 b}$$

$$l_3=\lambda_3-(\partial\sigma/\partial\Gamma_2)_E/zF, \tag{79 c}$$

and $\sum l_i=1$ [29, 58].

The l coefficient is the same quantity as electrosorption valency [27, 58]. Variation of the double layer structure with underpotential deposition, namely the shift of PZC and co-adsorption phenomena, is taken into consideration in equations (79), and thus the l coefficient is practically the same as dynamic electrosorption valency [58].

Determination of the l coefficient is based on the comparison of mass transport and charge transport in underpotential deposition.

4.4.2. *Charge and mass relations for the potentiostatic step method at rotating ring-disc electrodes or in thin-layer cells*

In this case it is assumed that at the beginning of the potentiostatic experiments, the potential is in a potential range where Γ_1, Γ_2 and c_{Mads} are practically zero and at $t=0$ the potential is stepped to E in the underpotential range. The disc (working) electrode current (i_D) and the ring (generator) electrode current (i_R) are derived from equations (76–78):

$$\frac{i_D}{A_D}=j=zFv_1-zF(l_2+l_3)\frac{d\Gamma_1}{dt}-zFl_3\frac{d\Gamma_2}{dt}+\frac{\partial\sigma}{\partial c_{\mathrm{Mads}}}\frac{dc_{\mathrm{Mads}}(x=0)}{dt}, \tag{80}$$

$$\frac{i_R}{zFA_DN}=-v_1+\frac{d\Gamma_1}{dt}+\frac{d\Gamma_2}{dt}, \tag{81}$$

where A_D is the area of the disc and the other symbols have their usual significance [58].

Integration of the disc and ring currents yields the charge relation

$$Q_D=\int j\,dt=-zFm_{\mathrm{Mads}}-zF(l_2+l_3)\Gamma_1-zF\,l_3\Gamma_2+\Delta Q \tag{82}$$

and mass relation

$$Q_R = \int \frac{i_R}{A_D N} \, dt = zFm_{M_{ads}} + zF(\Gamma_1 + \Gamma_2), \tag{83}$$

where the portion of the completely discharged material (M_{ads}) which is accumulated in the substrate S and diffuses into the bulk of S

$$m_{M_{ads}} = -\int v_1 \, dt \tag{84}$$

and the changing of the double-layer charge caused by metal deposition

$$\Delta Q(c_{M_{ads}}; E) \equiv \int_0^{c_{M_{ads}}} \frac{\partial \sigma}{\partial c_{M_{ads}}} \, dc_{M_{ads}}, \quad x = 0. \tag{85}$$

It is assumed for the integration that the l_k coefficients are almost independent of adsorption densities [29]. (Equations (80)–(83) can be applied for adsorption as well as desorption experiments. In the latter case the signs of the right-hand sides of equations (81) and (82) are changed [58].)

From equations (77) and (78) the time-dependent current quotient

$$\frac{-i_D N}{i_R} = \frac{l_3 \dfrac{d\Gamma_2}{dt} + (l_2 + l_3)\dfrac{d\Gamma_1}{dt} - v_1 - \dfrac{\partial \sigma}{\partial c_{M_{ads}}} \dfrac{dc_{M_{ads}}}{dt}}{\dfrac{d\Gamma_2}{dt} + \dfrac{d\Gamma_1}{dt} - v_1} \tag{86}$$

and the charge quotient

$$\frac{-Q_D}{Q_R} = \frac{l_3 \Gamma_2 + (l_2 + l_3)\Gamma_1 + m_{M_{ads}} + \Delta Q}{\Gamma_2 + \Gamma_1 + m_{M_{ads}}}. \tag{87}$$

If a single intermediate state is formed during underpotential deposition and the amount of $m_{M_{ads}}$ and Q are negligible, the l coefficient is

$$\frac{-Q_D}{Q_R} = \frac{-i_D(t) N}{i_R(t)} = l_3. \tag{88}$$

If the charge:mass quotient (equations (86) and (87)) is found to be independent of potential then it can be concluded that only one term dominates in the denominator and numerator. The corresponding l coefficient results from one step and can be evaluated by equation (88). If experimental Q_D:Q_R values depend on potential then the l coefficients must be determined by a full analysis of the potential dependent adsorption isotherms [29, 58].

4.5. *Study of kinetics of underpotential deposition with pulse methods*

The great advantage of pulse measurements in the investigation of underpotential deposition is the possibility to study the kinetics of metal-ion adsorption [10]. Both galvanostatic and potentiostatic pulse measurements were used to obtain kinetic data.

The kinetics of underpotential deposition of copper on a polycrystalline platinum electrode were determined with galvanostatic pulse measurements of the dependence on copper ion activity, copper coverage and substrate potential [26]. It has been found that the rate-determining process is the charge transfer (reaction (3)) when $\theta < 1$.

(Similar results were observed in the case of gold substrate [10].) The electrochemical transfer coefficients were also determined and their sum yields electrosorption valency (γ). Based on equation (49), adsorption and desorption current density is given by

$$i_{ads} = -\gamma F k_{ads} c_{M^{z+}} \exp\left(-\frac{\beta_c f\theta}{RT}\right) \exp\left(-\frac{\beta_e(\theta) zFE}{RT}\right), \tag{89}$$

$$i_{des} = \gamma F k_{des} \exp\left(\frac{\alpha_c f\theta}{RT}\right) \exp\left(\frac{\alpha_e(\theta) zFE}{RT}\right), \tag{90}$$

where subscripts c and e denote chemical and electrochemical and the other symbols have their usual significance [26].

Many papers have been devoted to applying galvanostatic or potentiostatic pulse techniques to the problem of deciding between the two different models describing the formation and desorption of adsorbed metal layers. Practically single-crystal surfaces and very often Ag substrates made electrolytically by the Budevski capillary method were used in the experiments [59].

At first the experimental results of underpotential deposition were interpreted in terms of a homogeneous sorption model taking into account the multi-state character of adsorbed monolayers [21]. In this model M^{z+} transfer from the electrolyte to the substrate surface and the surface diffusion of M_{ads} are regarded to be rate-determining steps. In the case of single-crystal substrates surface structure is considered to be composed of distinct homogeneous microregions separated by an array of line discontinuities (grain or subgrain boundaries or monoatomic steps). Metal-ion transfer takes place within the homogeneous regions and at discontinuities. Local differences in the surface concentration of M_{ads} give rise to a 2D mass transport described by a linear surface diffusion model [10, 17, 54, 56, 60].

The adsorption model describes the structure of the adsorbed metal layer at small coverages because the adsorption can proceed by random deposition until approximately half the sites are filled and the adatoms are still quite widely separated. Further increase in coverage necessitates bringing adjacent atoms into very close proximity and this requires the development of nuclei to overcome the electrostatic repulsion between separate adsorbed atoms [61]. This concept involves 2D nucleation and growth steps corresponding to a first-order phase transition process. On the basis of theoretical considerations a discontinuity of the adsorption isotherms at the critical nucleation potential can be expected. The existence of non-monotonous current-time transients under potentiostatic pulse polarization conditions is another evidence of the 2D nucleation and growth model [17, 55, 62–65].

Another important result of these investigations is that in all cases, even for deposition at very high overpotentials, the initiation of bulk deposition by 3D nucleation does not occur until the underpotential monolayer has been formed. The underpotential deposition appears to be an essential precursor to bulk deposition [61]. Ignoring underpotential deposition in theoretical treatments and experimental studies of electrocrystallization on foreign substrates resulted in inadequate models of this phenomenon [17].

5. The study of underpotential deposition by optical methods

The adsorbed metal atoms producing various features seen on linear sweep voltammograms also give rise to the corresponding optical effects [55, 66]. The most common optical methods of investigation of the properties of adsorbed metal atoms on

metal substrates are ellipsometry, modulation spectroscopy and differential reflectance spectroscopy [16].

In the case of modulation spectroscopy and differential reflectance spectroscopy the relative reflectivity changes $\Delta R/R$ are measured [16, 63, 64, 66–68]. $\Delta R/R$ is defined by

$$\frac{\Delta R}{R}=\frac{R_d-R}{R}, \tag{91}$$

where R_d is the reflectance of the surface covered with adsorbed metal of mean thickness d and R is the reflectance of the substrate free of adsorbed metal.

Differential reflectance spectroscopy combined with cyclic voltammetry is widely used in electrochemistry to study adsorbate properties [16, 55, 66–68]. The $\Delta R/R$ against E curve at constant photon energy resembles the corresponding i–E profile expressing a close relationship between relative reflectivity and covarage. In general, the measurements are carried out at different wavelengths with fixed angles of incidence. In all cases the optical properties of adsorbed metal layers were observed to be different from those of bulk deposits. The measured changes are so large that optical effects from the solution side of the double layer can be neglected. There remain only two effects to be considered, the electroreflectance effect from the metal substrate and the optical contribution from the deposited adsorbed metal layer. Thus the relative change in reflectivity can be written as [55]

$$\frac{\Delta R}{R}=\frac{1}{R}\left(\frac{\partial R}{\partial q}\right)_\theta \Delta q+\frac{1}{R}\left(\frac{\partial R}{\partial \theta}\right)_q \Delta\theta, \tag{92}$$

where q is the surface charge density on the substrate and θ is the coverage of the adsorbed metal. The magnitude of electroreflectance coefficient $(\partial R/\partial q)_\theta$ can be estimated from the slope of $\Delta R/R$–q curve. Generally, this slope is comparatively small and it can be shown that the contribution of electroreflectance to $\Delta R/R$ is negligible. If the deposited atoms are assumed to have a 20% ionic character, then Δq will be about $40\,\mu C\,cm^{-2}$ for a monolayer. In this case $(1/R)(\partial R/\partial q)_\theta \Delta q$ is equal to $+1{\cdot}2\times10^{-3}$ whereas the $\Delta R/E$ values measured under these circumstances are about -2×10^{-2}, therefore neither the sign nor the reflectivity changes are consistent with the effect of electroreflectance [55].

Another important factor which can influence the nature of the reflectance/charge plots is the effective thickness ($\bar{d}$) of the deposited layer because $\Delta R/R$ is proportional to $\bar{d}$ [55]:

$$\bar{d}=\frac{1}{A}\sum_i^n d_i\,\delta A_i, \tag{93}$$

where d_i is the local thickness of the deposit and δA_i is the area of an island of the film on the substrate metal of area A. $\bar{d}$ is proportional to the surface coverage of adsorbed metal atoms and hence to q. This model assumes that the values of optical constants of the investigated system remain independent of the coverage which imply no interactions in the ad-layer.

If the electroreflectance effects are ignored, it can be seen that changes in the gradient of a reflectance–charge plot can be due to either the variations of electrosorption valency or changes in optical properties of the deposited metal layer [55]. From the change in the measured reflectance data for metal layers deposited by underpotential deposition on foreign metal surfaces it can be concluded that metal

atoms adsorbed at relatively high ΔU are partially discharged whereas the adsorbed metal layers formed at lower ΔU are metal-like monolayers [17].

Later, this method was extended to the investigation of cation adsorption on oxide layers [67, 68].

Details of the fundamentals and experimental techniques of optical reflectance methods have already been extensively discussed in excellent reviews and they are not reviewed here [16, 69].

6. The influence of adsorbed substances on underpotential deposition

It has been recognized long ago that adsorbed substances can have a strong influence on the underpotential deposition of metals [6, 7, 16, 19]. It was observed that underpotential deposition of metals was accompanied by an increase in anion adsorption in spite of great excess of supporting electrolyte [6, 7] and the difference between electrosorption valency and Faraday valency can be attributed to simultaneous adsorption of metal ions and anions [7].

Another example of anion effect on underpotential deposition is demonstrated by cyclic voltammograms measure in the presence of different anions and organic species [16, 19, 70]. It was found that the effect of anions increased with the increase of specific adsorption in the sequence [16, 19, 70]

$$ClO_4^- < F^- < SO_4^{2-} < Cl^- < Br^- < SCN^- < I^-.$$

According to experimental observations, the adsorption of anions and organic substances may cause a decrease in underpotential shift (ΔU) [16, 70], presumably due to reduction in bond strength between the adsorbed metal atom and substrate surface. The complex-forming effect of anions, however, must also be taken into consideration in the explanation of this phenomenon, since the underpotential shift depends also on the activity of the depositing ions (see equation (18)).

Differentiating equation (18) with respect to metal ion activity in the supporting electrolyte yields [70]:

$$\left[\frac{\mathrm{d}(\Delta U)}{\mathrm{d}\ln a_{M^{z+}}}\right]_{a_{ML}} = \frac{RT}{F}\left(\frac{1}{\gamma} - \frac{1}{z}\right). \tag{94}$$

Using equation (94), we may calculate the electrosorption valency of adsorbed metal atoms in different solutions from the dependence of underpotential shift on metal-ion activity. On the assumption that the activity coefficient of the depositing metal ions in the supporting electrolyte is equal to 1 and with the use of the calculated values of electrosorption valency, the quasi-standard potentials and free-energy differences of underpotential deposition can be calculated [70].

A more detailed discussion of the electrosorption valency in the course of co-adsorption and competitive adsorption is given in reference [36].

The kinetic effects of condensed-phase formation have been discussed in theory for two mechanisms, those of instantaneous and progressive nucleation [71, 72]. The dependence of characteristics of cyclic voltammograms on sweep rate for the two mechanisms of condensed-phase formation provide experimental data to distinguish between the two mechanisms in solutions of different composition [70, 72].

A detailed analysis of the kinetics of underpotential deposition of lead on a silver single crystal in the presence of perchlorate, acetate and citrate has been made. It was found that, in solutions of concentration below 10^{-2} M in the depositing ions the

process is diffusion controlled, but at higher concentrations nucleation phenomena take over control and the kinetics is affected by anions in line with their adsorbability [70].

During a potentiostatic pulse, the current response in the underpotential region indicates a course obeying the equation derived for underpotential deposition controlled by 2D growth with overlap of growing centres formed by instantaneous nucleation [70]. At the beginning of deposition by the potentiostatic pulse, the rate-determining step of lead deposition is the charge transfer with the formation of a low-density superstructure and later the growth of the compact layer becomes dominant [70].

7. Effect of metal adsorption on hydrogen adsorption

In the case of substrate metals (S) which adsorb hydrogen well, such as Pt, metal adsorption inhibits the hydrogen adsorption because underpotential deposition of metals takes place on the same adsorption sites where hydrogen atoms can adsorb. The number of hydrogen adsorption sites occupied by one adsorbed metal atom (S_r, site requirement) has very often been determined [4, 22, 73, 74, 75]:

$$S_r = \frac{N^S - N^S_{surf}}{N_{M_{ads}}} = \frac{Q^o_H - Q_H}{Q_{M_{ads}}/z}, \tag{95}$$

where N^S is the total number of surface substrate atoms, N^S_{surf} is the number of surface substrate atoms free of adsorbed metal atoms and $N_{M_{ads}}$ is the number of adsorbed metal atoms. These numbers can be obtained experimentally from the quantity of charge required for the oxidation of hydrogen adsorbed on substrate surface free of adsorbed metal atoms (Q^o_H) and on substrate covered with adsorbed metal atoms (Q_H) and that required for the oxidation of adsorbed metal atoms ($Q_{M_{ads}}$) and z is the number of positive charges of the metal ions formed in the course of oxidation of M_{ads}.

The observed values of the hydrogen adsorption sites occupied by one adsorbed metal atom (Sr) on Pt, Ir and Rh are summarized in references [74, 75]. They are very often close to the valency of the given adsorbed metal atom and hardly depend on the kind of substrate metal.

In a few cases, however, there is no agreement about the number of hydrogen adsorption sites covered with one adsorbed metal atom [76]. The greatest discrepancy among the site requirement data can be found in the results of Bi adsorption on Pt. According to the first measurements: $S_r = 2$[22, 73, 77–79]. Later, it was shown that Bi adsorption in $HClO_4$ supporting electrolyte is a more complicated process because some part of the adsorbed Bi does not desorb at anodic polarization. This part was called irreversibly adsorbed Bi and its $S_r = 3$ [22], while under the same circumstances at larger Bi coverages $S_r = 2$ also [73]. (Without regard to these results the phenomenon was re-investigated as cation adsorption on oxide layers [68].)

Some minor discrepancy can be observed among the site requirement data of copper adsorbed on Pt. The results in hydrochloric acid supporting electrolyte are $S_r = 1{\cdot}2$ [80, 81] while in H_2SO_4 solution S_r is only 1 [75]. The discrepancy in the results can be explained by anion adsorption taking place in hydrochloric acid solutions [6].

An unexpected result of investigation of Pd adsorption on Pt is the slight inhibition of hydrogen adsorption on Pt [82]. This observation can also be used for calculation of the number of hydrogen adsorption sites occupied by one adsorbed Pd atom.

Considering that adsorbed Pd atoms also adsorb hydrogen, site requirement can be calculated by the following relation [82]:

$$S_r = 1 + \frac{2\,\Delta Q_H}{Q_{Pd}}, \tag{96}$$

where $\Delta Q_H = Q_H^o - Q_H^r$. Calculated from the experimental data $S_r = 1{\cdot}5$ [82]. The site requirement as a function of coverage was also investigated. The surface requirement decreases with increasing coverage but the significant changes observed for Bi and Au adsorption are lacking here [22, 73, 82, 83].

The number of hydrogen-adsorption sites occupied by one ruthenium atom adsorbed on platinized Pt could also be calculated [84]:

$$S_r = \frac{z}{0{\cdot}85}\left(1 - \frac{Q_H^r}{Q_H^o}\right), \tag{97}$$

where Q_H^r is the charge required for the oxidation of the hydrogen adsorbed on Pt surface covered with adsorbed Ru. The S_r value of a Ru atom adsorbed on Pt is about 1·8 [84].

In the case of UPD studied on single crystal surfaces, two limiting cases of superlattice structure formation must be considered. When $r_{M_{ads}}/r_S \leqslant 1$ (1 : 1 adsorption) and when $r_{M_{ads}}/r_S > 1$ (1 : *n* multi-site adsorption), where $r_{M_{ads}}$ and r_S denote the radii of the adsorbate and substrate respectively [17]. In the case of 1 : 1 adsorption epitaxial superlattice structures can be formed whereas multi-site adsorption blocking *n* adsorption sites leads to more complex ordered structures of different density and symmetry [17].

8. Classification of underpotential deposition of metal ions on foreign metal surfaces

The underpotential deposition of metals on foreign metal substrates is metal deposition in the so-called underpotential range (ΔU). In practice, however, all of the deposited metal oxidized in the underpotential range is called adsorbed metal, that is underpotentially deposited metal regardless of the potential of the deposition.

Naturally, the mechanism and the final result of the reactions of underpotential deposition may depend on the circumstances of the deposition, therefore some classification of the reactions that may result in adsorbed metal atoms on foreign metal surfaces would be advisable. The electrochemical literature is still lacking such a classification but, as has been mentioned in the introduction, the different redox processes resulting in adsorbed metal atoms oxidized in the underpotential range can be classified by the source of electrons consumed in reaction (3).

The different redox processes resulting in adsorbed metal atoms which can be oxidized at a more positive potential than the Nernst potential under the same circumstances will be classified and discussed according to the above concept.

8.1. *Underpotential deposition by electric polarization*

In the electrochemical investigations of underpotential deposition the source of electrons in reaction (3) is a system of electrochemical polarization used in electrochemistry. In practice, polarization of the substrate metal in aqueous solutions can be carried out between the potential of hydrogen and oxygen evolution. In the interpretation of the results, however, the value of the Nernst potential of the depositing

ions has to be taken into consideration to decide the region of underpotential deposition.

If the Nernst potential of the depositing ions is more negative than the potential of the hydrogen electrode in the same supporting electrolyte (for example Pb, Sn, Tl, etc.) then the whole range positive to hydrogen potential is the underpotential range. In the case of investigation of underpotential deposition of noble metals (Cu, Au, Ag, etc.), however, the underpotential range is sometimes quite narrow. Occasionally, it is ignored in the discussion of the results.

8.1.1. *Metal adsorption in the underpotential region*

If the potential of metal deposition (E_d) is more negative than the Nernst potential the depositing ions ($E_d \geqslant E_N$) then metal deposition is actually underpotential deposition, which can be described by reaction (3), although even in this case side reactions may take place. In the most reliable papers dealing with underpotential deposition, the undervoltage–overvoltage transition is rigorously taken into consideration in the interpretation of the results.

8.1.2. *Metal adsorption in the overpotential region*

If the potential of metal deposition (E_d) is more negative than the Nernst potential of the metal ions to be deposited ($E_d < E_N$), underpotential deposition can also be carried out, but in addition to metal adsorption bulk deposition may also take place [4, 85] (figure 3). Formation of a large amount of bulk deposit is avoided by application of depositing ions in low concentration (10^{-3}–10^{-7} M) in the supporting electrolyte. In spite of the low concentration of depositing ions, bulk deposition starts before completion of the first monolayer [4].

The adsorbed metal layer formed at overpotential, under open circuit conditions and in the presence of metal ions, was rearranged which resulted in increased coverage of the adsorbed metal [4, 86]. The rate of rearrangement depended on the concentration of the depositing ions, that is it took place via local cell mechanism [4]. The generally accepted mechanisms for electrocrystallization could be excluded [4]. In the case of less noble metals investigated with the same method, bulk deposition was not observed [87–89].

Similar phenomena have been observed in the case of lead adsorption on silver single-crystal surfaces [90–93]. Structural transformation processes in the course of underpotential deposition of lead occur as a result of incorporation of lead adatoms mainly in the crystal lattice of the terraces on the adsorbent surface at low coverages whilst the rate of structural transformation at high coverages increases with step density [90–93].

The most widely used method in the investigation of underpotential deposition is cyclic voltammetry [16, 19, 21, 46, 68, 78]. If the Nernst potential of the ion investigated is between the limits of potential cycling then underpotential deposition takes place both in the underpotential and overpotential region and thus bulk deposition can be expected [93–97] (figure 4). Depending on sweep rate and concentration of the depositing ions, however, bulk deposition cannot occur [93, 94], but in the interpretation of the results the possibility of bulk deposition must be taken into account since bulk deposition (formation of the second or third layer) on an atomic scale might occur [4, 86].

By application of any electrochemical polarization system in the formation or investigation of adsorbed metal layers the value of the Nernst potential of the ions

invesgitated must be taken into account in the planning of experiments and in the interpretation of the results.

8.2. *Underpotential deposition by reduction*

Naturally, the source of electrons in reaction (3) is not necessarily a system of electrochemical polarization. It can also be some reducing agent. In this case formation of an adsorbed metal layer on foreign metal substrates, or in other terms, underpotential deposition, may occur without electrochemical polarization, merely by chemical reduction. The processes of spontaneous formation of an adsorbed metal layer and the final results of underpotential deposition by reduction can only be investigated by electrochemical methods.

Underpotential deposition by reduction is an almost entirely ignored field of electrochemistry though its results could have been applied in many fields of chemistry of chemical technology, such as catalyst modification and corrosion.

8.2.1. *Metal adsorption via ionization of pre-adsorbed hydrogen*

In the case of substrate metals which can adsorb hydrogen well, such as Pt and Pd, adsorbed metal layers can be formed on the same substrate via ionization of pre-adsorbed hydrogen. Metal adsorption by this method takes a somewhat different course from that of underpotential deposition by electrochemical polarization. The substrate metal should be saturated with hydrogen first then adsorbing ions are introduced into the supporting electrolyte. Under open circuit conditions, underpotential deposition takes place with simultaneous ionization of the pre-adsorbed hydrogen and increase in the potential of the substrate metal in the positive direction:

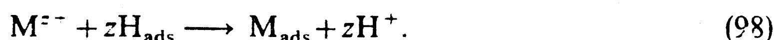

$$M^{z+} + zH_{ads} \longrightarrow M_{ads} + zH^{+}. \tag{98}$$

Experimental results have led to the conclusion that underpotential deposition via ionization of pre-adsorbed hydrogen results in an adsorbed metal layer having the same character as obtained by electrochemical methods [73, 81–83].

By application of constant current charging curves the site requirement data can also be determined. The site requirement data for adsorbed metal atoms deposited via ionization of preadsorbed hydrogen were the same as in the case of metal atoms deposited by electrochemical polarization [73, 81–83].

If metal adsorption via ionization of preadsorbed hydrogen results in an adsorbed metal layer of the same character as obtained by electrochemical polarization, the same potential dependence of electrosorption equilibrium must exist (chapter 2.1).

By application of the above concept a new method has been developed for the measurement of electrosorption valency of the metal layers formed via ionization of pre-adsorbed hydrogen [81]. Measurement is based on the assumption that an adsorbed metal layer built up from partially discharged species under appropriate conditions can be reduced to a zero-valent layer.

The charge required for the oxidation of an adsorbed metal layer

$$\mathrm{d}\,q_S = \gamma F\,\mathrm{d}\Gamma, \tag{99}$$

and the charge required for the oxidation of the same adsorbed layer prepared on the same surface after reduction

$$\mathrm{d}\,q_{S_R} = zF\,\mathrm{d}\Gamma. \tag{100}$$

The ratio of equations (99) and (100) yields electrosorption valency as q_S and q_{S_R} can be determined from charging curves. The experimentally determined γ for copper adsorption was the same as published in the literature [81].

8.2.1.1. *Noble metal adsorption via ionization of pre-adsorbed hydrogen*

As has been mentioned earlier, if underpotential deposition occurs at a potential negative to Nernst potential of the depositing ions then in addition to metal adsorption bulk deposition can also be expected. Experimental results of noble metal adsorption via ionization of pre-adsorbed hydrogen have verified this prediction because underpotential deposition of Cu, Ag, Bi, Au, Pd on platinized Pt substrate took place in two steps [73, 82, 83]. The first step, mostly bulk deposition with simultaneous ionization of adsorbed hydrogen:

$$M^{z+} + ze \longrightarrow M_{bulk}, \qquad (101)$$

$$H_{ads} \longrightarrow H^+ + e. \qquad (102)$$

When the above step was completed, then under open circuit circumstances and only in the presence of the depositing ions the bulk metal crystals were ionized and the adsorbed metal layer was formed:

$$M_{bulk} \longrightarrow M^{z+} + ze, \qquad (103)$$

$$M^{z+} + ze \longrightarrow M_{ads}. \qquad (104)$$

Sometimes the mechanism of spontaneous adsorption is even more complex because side reactions may also occur.

This mechanism of rearrangement is the same local cell mechanism as observed at underpotential deposition in the overpotential range [4].

In addition to thermodynamic reasons, kinetic conditions which necessarily lead to bulk deposition will be defined [82]. If the potential of a substrate metal is scanned to a more negative potential than the Nernst potential of a M^{z+}/M system, then the following processes occur [82]:

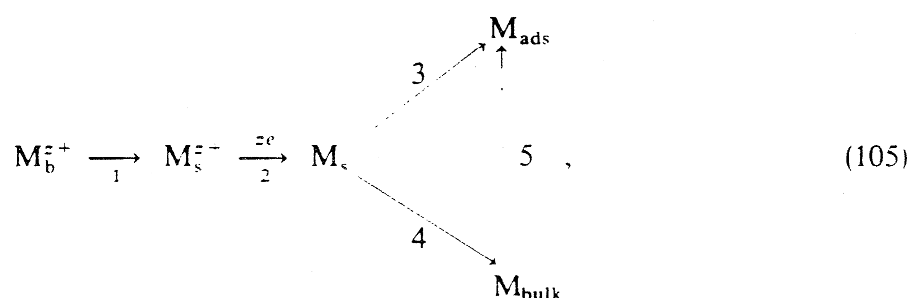

where process **1** is metal-ion diffusion to the surface, process **2** is charge transfer, process **3** is metal adsorption and process **4** is bulk deposition. With the assumption that the rate-determining step may be either diffusion or adsorption and bulk deposition

$$r_1 = r_3 + r_4. \qquad (106)$$

The rate of adsorption is a function of the coverage, consequently, bulk deposition should begin if $r_1 \geqslant r_3$. Because of the slow pore diffusion the effective number of adsorption sites during the first step (reactions (101) and (102)) is very small if

platinized Pt is used and thus, the ratio of r_3 and r_4 is strongly dependent on surface roughness [4, 82, 98].

When non-equilibrium conditions come to an end (the end of reactions (101) and (102)) the potential of the substrate metal has already been in the underpotential range and in the presence of the depositing ions reactions (103) and (104) started, resulting in the rearrangement (process 5 in reaction (105)) of the system [73, 82, 83].

This mechanism, however, proved to be invalid in Ru adsorption via ionization of hydrogen adsorbed on platinized platinum [84]. The different character of Ru could be explained by the assumption that the rate of charge transfer (process 2 in reaction (105)) is low and for this reason a ruthenium ion has enough time to diffuse into the depth of pores of Pt black, consequently, instead of bulk deposition an adsorbed layer is mainly formed [84].

If underpotential shift (ΔU) is very small (gold adsorption on Pt [83]) then metal adsorption via ionization of preadsorbed hydrogen is a more suitable method than electrochemical procedures for the preparation of adsorbed metal layers.

8.2.1.2. *Common metal adsorption via ionization of preadsorbed hydrogen*

The Nernst potential of the common metals is more negative than the hydrogen potential and thus bulk deposition cannot be expected during their adsorption via ionization of preadsorbed hydrogen. If side reactions do not occur then

$$M^{z+} + ze \longrightarrow M_{ads}, \qquad (107)$$

$$H_{ads} \longrightarrow H^{+} + e, \qquad (108)$$

is the mechanism of the spontaneously formed adsorbed metal layer while the potential of the substrate metal rises in a positive direction during metal adsorption [99, 100].

Other characteristics of underpotential deposition of common metals by this method is similar to those of noble metals.

8.2.2. *Catalytic disproportionation*

In the course of investigation of tin and rhenium adsorption on platinized Pt, it has been observed that an adsorbed metal monolayer could be formed spontaneously without any external source of electrons used for metal adsorption [100–102] (figure 5). The phenomenon has been called catalytic disproportionation [100, 102]:

$$z_2 M^{z_1+} \rightleftharpoons (z_2 - z_1) M_{ads} + z_1 M^{z_2+}, \qquad (109)$$

where the sequence of ionic charges is $z_2 > z_1 > 0$.

Characteristics of adsorbed metal monolayers formed by catalytic disproportionation proved to be similar to those formed by other methods [100].

8.2.2.1. *Thermodynamic reasons of disproportionation*

Naturally, catalytic disproportionation occurs only in the case of ions with several states of oxidation. For example there are M^{z_1+} and M^{z_2+} ions in water solution and they do not disproportionate. It follows that the sequence of their standard redox potentials is

$$E^{\circ}_{M^{z_1+}/M_{bulk}} < E^{\circ}_{M^{z_2+}/M_{bulk}} < E^{\circ}_{M^{z_2+}/M^{z_1+}}. \qquad (110)$$

In the presence of an adsorbing metal surface, new equilibria appear. The equilibrium constant of catalytic disproportionation (K_d) is given by (111) provided that the activity of M_{ads} is nearly one:

$$K_d = \frac{[M^{z_2+}]^{z_1}}{[M^{z_1+}]^{z_2}}. \qquad (111)$$

The thermodynamic condition of equilibrium in a solution in which disproportionation takes place is that the potential of all redox systems are equal to each other. Applying this concept we may calculate the ion activities of equilibrium by equation (16) assuming that ionic charge is equal to electrosorption valency and the ion activities can be substituted for concentrations. Substitution of the results into equation (111) yield

$$\ln K_d = \frac{F}{RT} z_1 z_2 (E^{\circ}_{ML_{M^{z_1+}}/M_{ads}} - E^{\circ}_{ML_{M^{z_2+}}/M_{ads}}). \qquad (112)$$

The thermodynamic condition of disproportionation is: $K_d > 1$. This condition is fulfilled only if the following sequence of standard electrosorption potentials is valid [100]:

$$E^{\circ}_{ML_{M^{z_1-}}/M_{ads}} > E^{\circ}_{ML_{M^{z_2+}}/M_{ads}} > E^{\circ}_{M^{z_2+}/M^{z_1+}}. \qquad (113)$$

If the above conditions are fulfilled, catalytic disproportionation may take place. This is an entirely spontaneous process and results in an adsorbed metal monolayer on a suitable substrate metal surface without any outer source of electrons [100]. The source of electrons in the processes of underpotential deposition in this case is the disproportionation.

8.2.3. *Metal adsorption by polarization with gaseous hydrogen*

Instead of polarization with an electrochemical polarization system a substrate metal can be polarized with gaseous hydrogen if the ionization of hydrogen

$$H_2 \longrightarrow 2H^+ + 2e, \qquad (114)$$

can take place on the substrate metal surface. The potential of the substrate metal depends on the partial pressure of hydrogen. For practical reasons, however, the variation of potential of the substrate metal can only be between −0·06 V and 0·1 V (measured against a hydrogen electrode in the same supporting electrolyte), consequently, the underpotential deposition of common metals can only be carried out by this method because their Nernst potentials are more negative than these potentials. If noble metals are deposited by polarization with hydrogen gas then bulk and adsorbed deposits hardly can be separated.

It is well known that reaction (114) is a catalytic process; this method can therefore be applied if the substrate is one of the metals (Pt, Pd, etc.) used for catalytic hydrogenation.

This method can be used for the modification of metal catalysts with adsorbed metals [103, 104]. The catalysts of catalytic hydrogenation in water solutions are very often modified by addition of different metal ions into the reactor [105, 106].

8.2.4. *The cementation of metals*

If it is true that underpotential deposition is an essential precursor to bulk deposition [61] then the cementation can be interpreted as metal deposition via

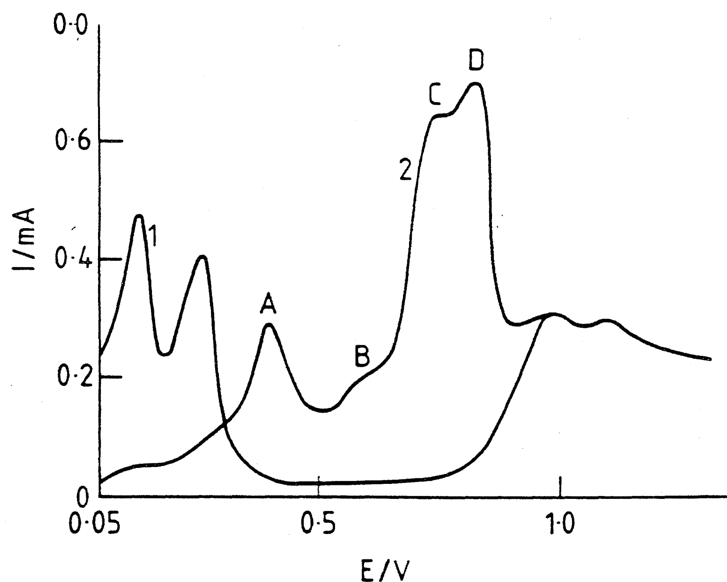

Figure 3. Potential sweep of a Pt electrode in 0·5 M H_2SO_4 solution (1). Potential sweep of the same Pt electrode held at 0·05 V for 14 min in 0·5 M H_2SO_4 containing $CuSO_4$ at the concentration of 3×10^{-6} M (2). Dissolution of bulk deposit (A) and adsorbed species (B, C and D). Sweep rate 5 V s^{-1} (figure 4).

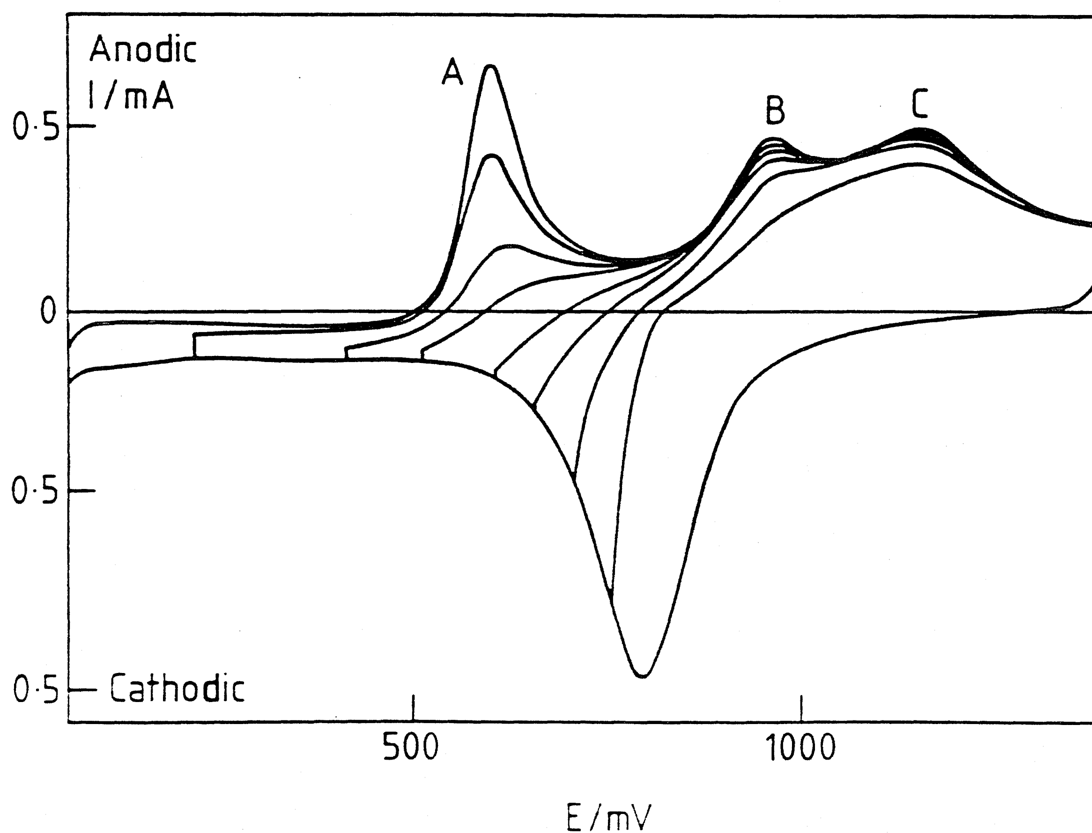

Figure 4. Voltammetry curves of a stationary Pt electrode in the presence of 10^{-4} M Ag^{+} in 1 M $HClO_4$ solution. Sweep rate 20 mV s^{-1}. Dissolution of the bulk deposit (A) and adsorbed species (B and C).

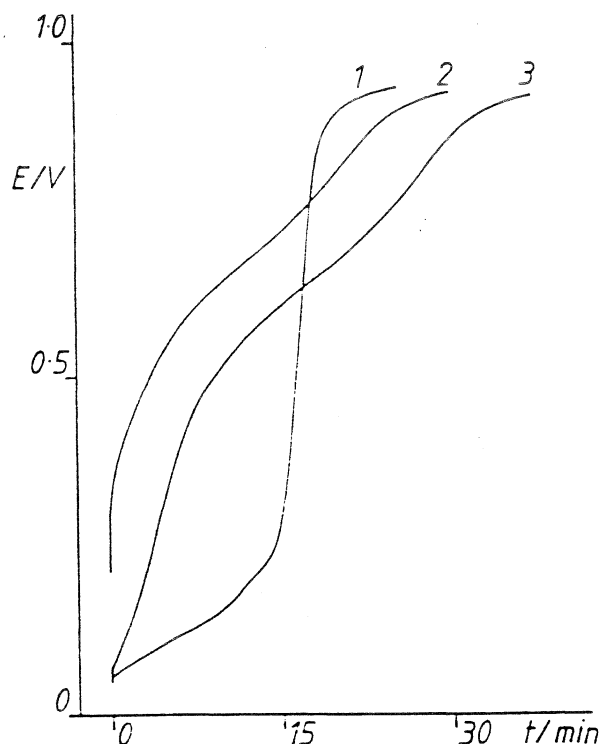

Figure 5. Underpotential deposition of tin by catalytic disproportionation. Charging curve of the platinized Pt electrode in 1 M HCl solution (1). Charging curve in 1 M HCl of the same electrode covered with UPD tin without saturation with hydrogen (2), and as in (2) but after saturation with hydrogen (3). $I = 0{\cdot}25$ mA, concentration of Sn^{2+} is 2×10^{-3} M [100].

ionization of the substrate metal and the very first step of this process must be underpotential deposition. Since the cementation takes place in the overpotential region, therefore bulk deposits appear on the surface after metal adsorption.

If the Nernst potentials of the substrate metal and depositing ions are close to each other then a slow formation of bulk deposit can be expected.

The role of adatoms had been recognized in an early state of investigation of the cementation [107].

8.2.5. *Metal adsorption by polarization with any reducing agent*

Of course, any organic or inorganic reducing agent can be the source of electrons in underpotential deposition of metals on foreign metal surfaces. There are two fields of metal deposition in which adatoms play some role and should be mentioned here. One is contact plating [108] and the other is a process termed as electroless metal deposition [108–110].

9. The physical nature of underpotential deposition

A generally accepted model of the adatom–substrate bond is that the charge transferred from the adatom to the substrate is proportional to the difference in their electronegativities. The chemical bond thus gains a polarity in the electron distribution and this results in an energy gain of the bond [16, 19]. On the other hand, there is a linear correlation between Pauling's electronegativity (x_M) of a metal atom and the work function (Φ) of the same metal [111, 112]. The empirical formula is

$$x_M = 0{\cdot}5\Phi - \text{constant} \qquad (115)$$

with a constant of value 0·29 for sp metals and 0·55 for transition metals [112].

From the fact that the difference in the electronegativities is linearly related to the work functions, the underpotential shift (ΔU) is plotted against the difference in work functions between bulk substrate and bulk deposited metal [16, 19]:

$$\Delta U = \alpha \Delta \Phi, \quad \alpha = 0{\cdot}5\ \mathrm{V\,eV^{-1}}. \tag{116}$$

This empirical correlation shows an astonishingly little scatter when working with polycrystalline substrates (figure 6). The extremely good linear relation between underpotential shift and work function differences suggests that the covalent part of the adatom–substrate bond does not differ appreciably from the bond strength between the adatom and the surface of the same metal [16].

The good linear correlation between monolayer and substrate exists as long as no specific interaction between substrate and adsorbate can be found. The points really scattered in figure 6 are those for systems Ag^{+}/Au, Hg^{2+}/Au and Au^{3+}/Pt. For silver and mercury extensive alloying and therefore covalency in bonds may be expected [15]. No explanation, however, can be given for the Au^{3+}/Pt system where the underpotential shift is very small [83] or for some pairs which show no underpotential effect [19]. When the underpotential effect is missing the differences in work function are relatively small.

A better approach would be to use the underpotential value for the deposition of the first atom obtained by adding the half-width of the desorption peak to the value for the peak [15]. It has been demonstrated using an energy cycle that for an adsorbed metal ion the difference in bodn strengths for two different substrate metals is given by their work-function difference [15].

Values of underpotential shift for the deposition of the first atoms of metals plotted as a function of difference in work functions for the bulk metals [113] results in a straight line which appears to conform well to the model [15].

It has also been reported that equation (116) seems to hold fairly well for underpotential deposition of various metals on 110 gold surface using $\Delta\Phi$ data of the polycrystalline materials [114]. Since it is believed that the 110-face contributes mostly to a polycrystalline surface this result can be understood.

Evaluation of applicability of equation (116) raises the question as to whether $\Delta\Phi$ has to be considered as an absolute value of work function differences. According to experimental observations the work function of the substrate must be higher than that of the adsorbate metal. This seems to be a necessary condition for monolayer formation [16].

The difference in $\Delta\Phi$ can be considered to be a measure of the ionicity of the adatom–substrate bond, furthermore, there is a definite correlation between Pauling's electronegativity of an atom and the work function of the solid [19]. According to Pauling, the polarity of a chemical bond increases with increasing difference in electronegativities of the atoms involved in the bond [28, 115].

Since γ_{PZC}/z is a measure of bond formation between substrate and adsorbate, plotting absolute difference of the electronegativities, $|\Delta x| = |x_S - x_{M_{ads}}|$ of the substrate (x_S) and of the adsorbate (x_M), against γ_{PZC}/z values for mononuclear ions resulted in a reasonable correlation for cations as well as anions (similar correlations can be obtained for non-aqueous solvents) [28, 116]. When $|\Delta x < 0{\cdot}51$, the γ_{PZC}/z ratio is nearly 1 but decreases with increasing Δx [28].

When γ_{PZC}/z is nearly one the bond formed between substrate and adsorbate is a covalent bond ($\lambda \approx -z$), but at $\gamma_{PZC}/z \ll 1$ a mainly electrostatic adsorption without

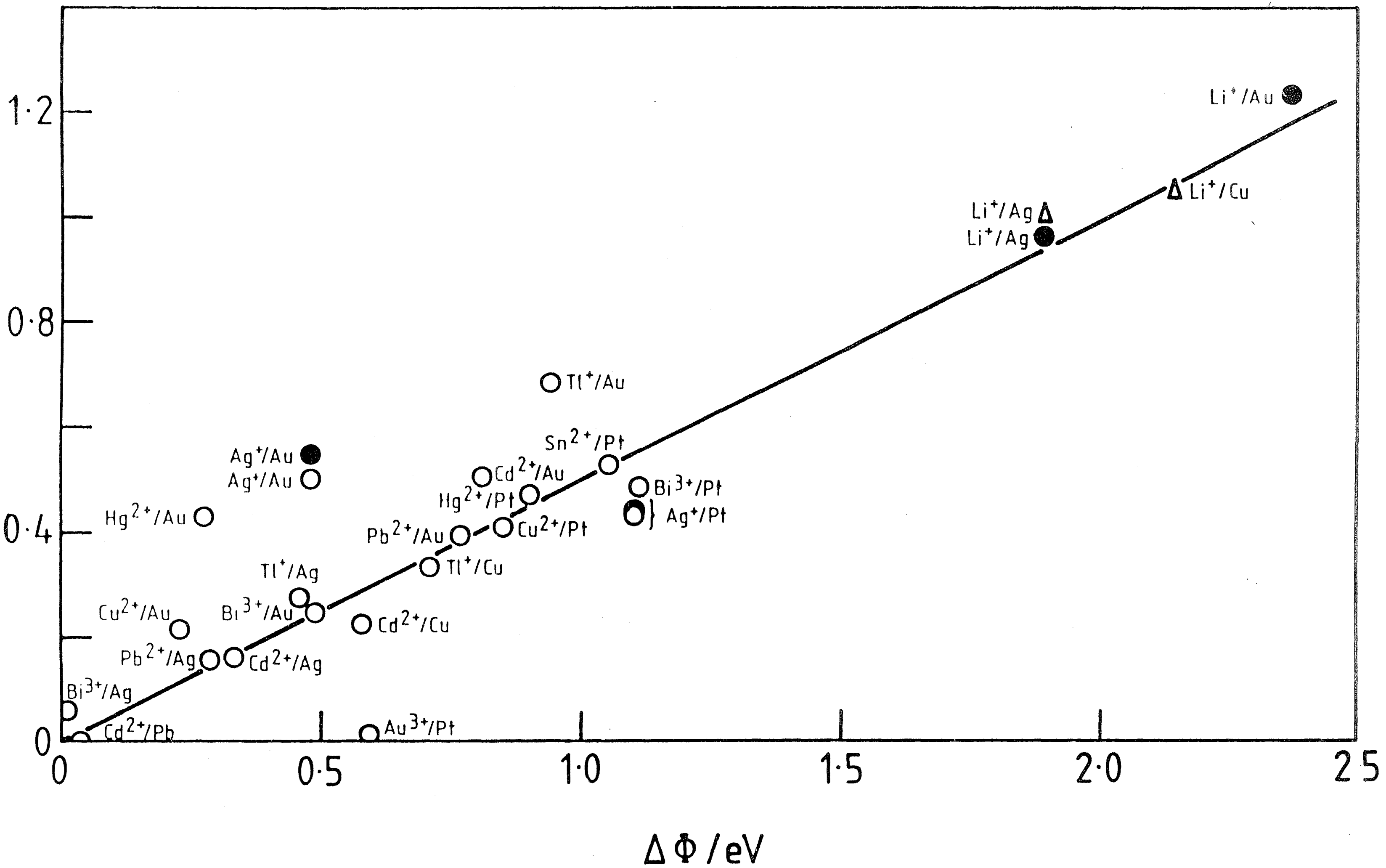

Figure 6. Underpotential shift ΔU between bulk and monolayer stripping peak as a function of $\Delta\Phi$, the difference in work functions of bulk substrate and bulk adsorbed material. (○) aqueous solution, (●) acetonitrile and (△) propylene carbonate [19].

charge transfer ($\lambda \approx 0$) takes place [27, 28]. The formation of polarized bonds with a partial charge transfer is important in the range, $0{\cdot}3 < |\Delta x| < 1{\cdot}0$.

According to Pauling the covalent bond formation and, consequently, the charge transfer can be evaluated from the difference of electronegativities using the following empirical relation [28, 115]:

$$-\lambda/z = \exp\,[-a(\Delta x)^2]. \tag{117}$$

This formula describes the charge transfer in diatomic molecules in the gas phase, but it will not be valid with the same constant a in aqueous solutions. Because of its large dielectric constant, the water supports the ionization, therefore a higher constant a can be expected for aqueous media [28].

The geometric factor g increases with increasing charge transfer and in the range, $|x| < 0{\cdot}3$, where underpotential deposition generally takes place, the assumption for g is [28]

$$g = g_{\min} - b(\lambda/z), \tag{118}$$

where $b = 0{\cdot}84 = 1 - g_{\min}$, since λ/z is generally negative.

The combination of equation (118) with equations (13) and (117) yields [28]

$$\gamma_{PZC}/z = g_{\min} + 2b\exp\,[-a(\Delta x)^2] - b\exp\,[-2a(\Delta x)^2]. \tag{119}$$

This equation describes the correlation between absolute difference of electronegativities and electrosorption valency, fits the experimental data well and can give a rough idea of the real distribution of charge. Of course, differences in the hydration of ions, in bond length, in crystallographic orientation and in the band structure of the substrate may be reasons for deviations of experimental data from the assumed model [28]. On the other hand, the qualitative agreement is reasonable, and this justifies the qualitative application of the model [28].

Acknowledgments

The author wishes to express his thanks to Professor F. Nagy for stimulating discussions and to Professor F. Márta for his encouragement of this monograph. The financial support of the Hungarian Research Fund (No. OTKA: 1004) is gratefully acknowledged.

References

[1] HEVESY, G. V., 1912, *Phys. Z.*, **13**, 715.
[2] HAISSINSKY, M., 1933, *J. chim. Phys.*, **30**, 27.
[3] TAYLOR, A. H., KIRKLAND, S., and BRUMMER, S. B., 1971, *Trans. Faraday Soc.*, **67**, 809.
[4] FURUYA, N., and MOTOO, S., 1976, *J. electroanal. Chem.*, **72**, 165.
[5] BREITER, M. W., 1969, *Trans. Faraday Soc.*, **65**, 2197.
[6] HORÁNYI, G., and VÉRTES, G., 1973, *J. electroanal. Chem.*, **45**, 295.
[7] HORÁNYI, G., 1974, *J. electroanal. Chem.*, **55**, 45.
[8] BOWLES, B. J., 1965, *Electrochim. Acta*, **10**, 717.
[9] MIKUNI, F., and TAKAMURA, T., 1970, *Denki Kagaku*, **38**, 113.
[10] LORENZ, W. J., HERMANN, H. D., WÜTHRICH, N., and HILBERT, F., 1974, *J. electrochem. Soc.*, **121**, 1167.
[11] SOMORJAI, G. A., 1981, *Chemistry in Two Dimensions* (London: Cornell University Press).
[12] SCHARDT, B. C., STICKNEY, J. L., STERN, D. A., WIECKOWSKI, A., ZAPIEN, D. C., and HUBBARD, A. T., 1987, *Langmuir*, **3**, 239.
[13] NISHIMURA, K., MACHIDA, K., and ENYO, M., 1988, *J. electroanal. Chem.*, **257**, 21.
[14] ROMEO, F. M., TUCCERI, R. I., and POSADAS, D., 1988, *Surf. Sci.*, **203**, 186.
[15] TRASATTI, S., 1975, *Z. phys. Chem. N.F.*, **98**, 75.

[16] KOLB, D. M., 1978, *Advances in Electrochemistry and Electrochemical Engineering*, Vol. 11, edited by H. Gerischer and C. W. Tobias (New York: John Wiley), p. 25.
[17] JÜTTNER, K., and LORENZ, W. J., 1980, *Z. phys. Chem. N.F.*, **122**, 163.
[18] SWATHIRAJAN, S., and BRUCKENSTEIN, S., 1983, *Electrochim. Acta*, **28**, 865.
[19] KOLB, D. M., PRZASNYSKI, M., and GERISCHER, H., 1974, *J. electroanal. Chem.*, **54**, 25.
[20] STUCKI, S., 1977, *J. electroanal. Chem.*, **80**, 375.

[21] CONWAY, B. E., and ANGERSTEIN-KOZLOWSKA, H., 1981, *Accts chem. Res.*, **14**, 49.
[22] SZABÓ, S., and NAGY, F., 1978, J. electroanal. Chem., **88**, 259.
[23] RODES, A., FELIU, J. M., and CLAVILIER, J., 1988, *J. electroanal. Chem.*, **256**, 455.
[24] GOSSNER, K., and MIZERA, E., 1981, *J. electroanal. Chem.*, **125**, 359.
[25] SALVAREZZA, R. C., VASQUEZ MOLL, D. V., GIORDANO, M. C., and ARVIA, A. J., 1986, *J. electroanal. Chem.*, **223**, 301.
[26] SCHULTZE, J. W., 1970, *Ber. Bunsenges. phys. Chem.*, **74**, 705.
[27] SCHULTZE, J. W., and VETTER, K. J., 1973, *J. electroanal. Chem.*, **44**, 63.
[28] SCHULTZE, J. W., and KOPPITZ, 1976, *Electrochim. Acta*, **21**, 327.
[29] LORENZ, W., and SALIE, G., 1977, *J. electroanal. Chem.*, **80**, 1.
[30] CONWAY, B. E., and MARSHALL, S., 1983, *Electrochim. Acta*, **28**, 1003.
[31] ADZIC, R. R., and MINEVSKI, LJ. V., 1987, *Electrochim. Acta*, **32**, 125.
[32] VETTER, K. J., and SCHULTZE, J. W., 1972, *Ber. Bunsenges. phys. Chem.*, **76**, 920.
[33] VETTER, K. J., and SCHULTZE, J. W., 1972, *Ber. Bunsenges. phys. Chem.*, **76**, 927.
[34] VETTER, K. J., and SCHULTZE, J. W., 1974, *J. electroanal. Chem.*, **53**, 67.
[35] FRUMKIN, A. N., DAMASKIN, B., and PETRII, O., 1974, *J. electroanal. Chem.*, **53**, 57.
[36] SCHULTZE, J. W., and VETTER, K. J., 1974, *Electrochim. Acta*, **19**, 913.
[37] FLETCHER, S., 1981, *J. electroanal. Chem.*, **118**, 419.
[38] SWATHIRAJAN, S., MIZOTA, H., and BRUCKENSTEIN, S., 1982, *J. phys. Chem.*, **86**, 2480.
[39] ENGELSMANN, K., LORENZ, W. J., and SCHMIDT, E., 1980, *J. electroanal. Chem.*, **114**, 1.
[40] CONWAY, B. E., and ANGERSTEIN-KOZLOWSKA, H., 1980, *J. electroanal. Chem.*, **113**, 63.
[41] TSUCHIYA, S., AMENOMIYA, Y., and CVETANOVIĆ, R. J., 1970, *J. Catal.*, **19**, 245.
[42] ANGERSTEIN-KOZLOWSKA, H., CONWAY, B. E., and SHARP, W. B. A., 1973, *J. electroanal. Chem.*, **43**, 9.
[43] CONWAY, B. E., and GILEADI, E., 1962, *Trans. Faraday Soc.*, **58**, 2493.
[44] CONWAY, B. E., GILEADI, E., and DZIECIUCH, M., 1963, *Electrochim. Acta*, **8**, 143.
[45] BARRADAS, R. G., and CONWAY, B. E., 1961, *Electrochim. Acta*, **5**, 319.
[46] CHIERCHIE, T., and MAYER, C., 1988, *Electrochim. Acta*, **33**, 341.
[47] SCHMIDT, E., and SIEGENHALER, H., 1969, *Helv. Chim. Acta*, **52**, 2245.
[48] SCHMIDT, E., and WÜTHRICH, N., 1970, *J. electroanal. Chem.*, **28**, 349.
[49] BORT, H., JÜTTNER, K., LORENZ, W. J., and SCHMIDT, E., 1978, *J. electroanal. Chem.*, **90**, 413.
[50] SIEGENTHALER, H., and SCHMIDT, E., 1977, *J. electroanal. Chem.*, **80**, 129.
[51] RIEDHAMMER, T. M., MELNICKI, L. S., and BRUCKENSTEIN, S., 1978, *Z. phys. Chem. N.F.*, **111**, 177.
[52] SWATHIRAJAN, S., and BRUCKENSTEIN, S., 1982, *J. electrochem. Soc.*, **129**, 1202.
[53] SWATHIRAJAN, S., and BRUCKENSTEIN, S., 1983, *J. electroanal. Chem.*, **146**, 137.
[54] HERMANN, H. D., WÜRTHRICH, N., LORENZ, W. J., and SCHMIDT, E., 1976, *J. electroanal. Chem.*, **68**, 273, 289.
[55] BEWICK, A., and THOMAS, B., 1975, *J. electroanal. Chem.*, **65**, 911.
[56] ENGELSMANN, K., LORENZ, W. J., and SCHMIDT, E., 1980, *J. electroanal. Chem.*, **114**, 11.
[57] BRUCKENSTEIN, S., and MILLER, B., 1977, *Accts chem. Res.*, **10**, 54.
[58] SALIE, G., 1988, *J. electroanal. Chem.*, **245**, 1.
[59] BUDEVSKI, E., and BOSTANOV, V., 1964, *Electrochim. Acta*, **9**, 477.
[60] JÜTTNER, K., and SIEGENTHALER, H., 1978, *Electrochim. Acta*, **23**, 971.
[61] BEWICH, A., JOVICEVIC, J., and THOMAS, B., 1977, *Faraday Symp. Chem. Soc.*, **12**, 24.
[62] BEWICK, A., and THOMAS, B., 1976, *J. electroanal. Chem.*, **70**, 239.
[63] BEWICK, A., and THOMAS, B., 1977, *J. electroanal. Chem.*, **84**, 127.
[64] BEWICK, A., and THOMAS, B., 1977, *J. electroanal. Chem.*, **85**, 329.
[65] SCHULTZE, J. W., and DICKERTMANN, D., 1978, *Ber. Bunsenges. phys. Chem.*, **82**, 528.
[66] ADZIC, R., YEAGER, E., and CAHAN, B. D., 1974, *J. electrochem. Soc.*, **121**, 476.
[67] ADZIC, R. R., and MARKOVIC, N. M., 1979, *J. electroanal. Chem.*, **102**, 263.
[68] ADZIC, R. R., and MARKOVIC, N. M., 1985, *Electrochim. Acta*, **30**, 1473.

[69] McIntyre, J. D. E., 1973. *Advances in Electrochemistry and Electrochemical Engineering*, Vol. 9, edited by R. H. Miller (New York: Wiley-Interscience), p. 61.
[70] Jovicevic, J. N., Jovic, V. D.. and Despic, A. R., 1984, *Electrochim. Acta*, **29**, 1625; 1985, **30**, 1455.
[71] Bosco, E., and Rangarajan. S. K.. 1981. *J. chem. Soc. Faraday Trans. I*, **77**, 483.
[72] Bosco, E., and Rangarajan. S. K.. 1981. *J. electroanal. Chem.*, **129**, 25.
[73] Szabó, S., and Nagy, F.. 1976. *J. electroanal. Chem.*, **70**, 357.
[74] Furuya, N., and Motoo. S.. 1979. *J. electroanal. Chem.*, **98**, 189.
[75] Furuya, N., and Motoo. S.. 1980. *J. electroanal. Chem.*, **107**, 159.
[76] Adzic, R. R., 1984, *Advances in Electrochemistry and Electrochemical Engineering*, Vol. 13, edited by H. Gerischer and C. W. Tobias (New York: Wiley), p. 159.
[77] Bowles, B. J., 1970, *Electrochim. Acta*, **15**, 737.
[78] Cadle, S. H., and Bruckenstein, S., 1972. *Analyt. Chem.*, **44**, 1993.
[79] Sazbó, S., and Nagy, F., 1978. *J. electroanal. Chem.*, **87**, 261.
[80] Bowles, B. J., 1970, *Electrochim. Acta*, **15**, 589.
[81] Szabó, S., and Nagy, F., 1977. *J. electroanal. Chem.*, **84**, 93.
[82] Szabó, S., and Nagy, F.. 1979. *Israel J. Chem.*, **18**, 162.
[83] Szabó, S., and Nagy, F.. 1977. *J. electroanal. Chem.*, **85**, 339.
[84] Szabó, S., Bakos, I., and Nagy. F., 1989, *J. electroanal. Chem.*, **271**, 269.
[85] Scortichini, C. L., and Reilley. C. N., 1983, *J. Catal.*, **79**, 138.
[86] Margheritis, D., Salvarezza. R. C., Giordano, M. C., and Arvia, A. J., 1987. *J. electroanal. Chem.*, **229**, 327.
[87] Furuya, N., and Motoo. S.. 1977. *J. electroanal. Chem.*, **78**, 243.
[88] Furuya, N., and Motoo, S.. 1979. *J. electroanal. Chem.*, **98**, 195.
[89] Furuya, N., and Motoo. S.. 1979. *J. electroanal. Chem.*, **99**, 19.
[90] Vitanov, T., Popov, A., Staikov. G., Budevski, E., Lorenz, W. J., and Schmidt, E.. 1986, *Electrochim. Acta*, **31**, 981.
[91] Popov, A., Dimitrov, N.. Velev. O.. Vitanov, T., Budevski, E.. Schmidt, E.. and Siegenthaler, H., 1989. *Electrochim. Acta*, **34**, 265.
[92] Popov, A., Dimitrov, N., Kashchiev, D., Vitanov, T., and Budevski. E.. 1989, *Electrochim. Acta*, **34**, 269.
[93] Barradas, R. G., Fletcher, S.. and Szabó, S., 1978, *Can. J. Chem.*, **56**, 2029.
[94] Clavilier, J., Feliu, J. M., and Aldaz, A., 1988, *J. electroanal. Chem.*, **243**, 419.
[95] Parajon Costa, B., Palotta. C. D., De Tacconi, N. R., and Arvia. A. J.. 1983. *J. electroanal. Chem.*, **145**, 189.
[96] Rand, D. A. J., and Voods. R.. 1973. *J. electroanal. Chem.*, **44**, 83.
[97] Adzic, R. R., Spasojevic. M. D.. and Despic. A. R., 1978, *J. electroanal. Chem.*, **92**, 31.
[98] Sticki, S.. 1977. *J. electroanal. Chem.*, **80**, 375.
[99] Szabó. S.. and Nagy, F.. 1984. *J. electroanal. Chem.*, **160**, 299.
[100] Szabó, S., 1984. *J. electroanal. Chem.*, **172**, 359.
[101] Szabó, S., unpublished result.
[102] Nagy. F.. and Szabó. S.. 1987. *React. Kinet. Catal. Lett.*, **35**, 133.
[103] Mallát, T., Szabó, S., and Petró, J.. 1985. *Acta Chim. Hung.*, **119**, 127.
[104] Mallát, T., Szabó, S., and Petró. J., 1987. *Appl. Catal.*, **29**, 117.
[105] Sokolskii, D. V., 1966, *Catalysis of Liquid Phase Hydrogenation* (Alma-Ata: Nauka) (in Russian).
[106] Sokolskii, D. V., and Zakumbaeva, G. D., 1973. *Adsorption and Catalysis by Metals of VIII Group in Solutions* (Alma-Ata: Nauka) (in Russian).
[107] Despic. A. R., Drazic. D. M.. and Sepa, D.. 1966. *Electrochim. Acta*, **11**, 507.
[108] Graham, A. K., 1971, *Electroplating Engineering Handbook*, third edition (London: Van Nostrand Reinhold Company).
[109] Flis. J.. and Duquette. D. J.. 1984. *J. electrochem. Soc.*, **131**, 34.
[110] Flis. J.. and Duquette. D. J.. 1984. *J. electrochem. Soc.*, **131**, 254.
[111] Gordy. W.. and Thomas. W. J. O.. 1956. *J. chem. Phys.*, **24**, 439.
[112] Trasatti. S., 1971. *J. electroanal. Chem.*, **33**, 351.
[113] Trasatti. S.. 1972. *J. chem. Soc. Faraday I*. **68**, 229.
[114] Schultze, J. W.. and Dickertmann. D.. 1976. *Surf. Sci.*, **54**, 489.
[115] Pauling, L.. 1960. *The Nature of the Chemical Bond*. 3rd edn (Ithaca: Cornell University Press).
[116] Koppitz. F. D.. and Schultze. J. W.. 1976. *Electrochim. Acta*, **21**, 337.

2.

Acta Chimica Academiae Scientiarum Hungaricae. Tomus 93 (1), pp. 33—42 (1977)

PROCESS FOR THE PREPARATION OF PLATINUM CATALYSTS MODIFIED BY ADSORBED METALS

S. SZABÓ, F. NAGY and D. MÓGER

(Central Research Institute for Chemistry, Hungarian Academy of Sciences, Budapest)

Received May 31, 1976

A method has been developed for the preparation of platinum catalysts modified by adsorbed metals, suitable for the purposes of gas phase heterogeneous catalytic investigations.

Similarly, a method has been elaborated, for investigating the effect of adsorption of atmospheric oxygen and of heat treatment on air-dry, modified catalyst.

The methods have been illustrated on the example of Pt catalysts covered by copper: it has been established that neither oxygen adsorption nor heat treatment up to 100 °C does change the properties of a Pt catalyst covered with adsorbed copper. In the case of a platinum catalyst covered with gold, the original properties are retained up to 350 °C.

It is well known that various metals are adsorbed on platinum at potentials more positive than their reversible Nernst potential [1—22]. The metal adsorbed changes the adsorptive and catalytic properties of platinum [21—27].

Metal adsorption proceeding on the platinum surface can be precisely measured by electrochemical methods and, under suitable experimental conditions, a coverage of the desired degree can be attained. This permits to change reproducibly the adsorptive and catalytic properties by metal adsorption to the desired extent.

According to our knowledge, this possibility has been utilized so far only in the field of electrocatalysis, because the similarity of electrochemical and electrocatalytic methods simplifies the experimental conditions [21—27]. Since in gas phase heterogeneous catalysis the kinetic investigations cannot be performed in an electrochemical cell with metal adsorption, the 'damage-free' transfer of the catalyst into the reactor should be ensured. The adsorbed metal may be reoxidized in the presence of water by atmospheric oxygen according to the following equation:

$$Me_{ads} + \frac{n}{4} O_2 + \frac{n}{2} H_2O \rightleftharpoons Me^{n+} + n\,OH^- \qquad (1)$$

Therefore, the damage-free transfer of the catalyst can be ensured only with the exclusion of either oxygen or water. As the maintenance of oxygen-free conditions during the transfer of the catalyst into the catalytic reactor is difficult, the exclusion of water was chosen. An electrochemical cell has

been designed for this purpose in which not only the formation of the adsorbed metal layer. but the washing and drying of the catalyst can be carried out under oxygen-free conditions.

The catalyst came into contact with oxygen only in an air-dry state (free of adhering water). It has been experimentally checked whether the properties of the adsorbed metal are not permanently changed by oxygen adsorption during this process. Moreover, it has been investigated to what temperatures the catalyst prepared in this way can be heated without changing the original properties of the adsorbed metal.

I. Cell for catalyst preparation

As can be seen in Fig. 1, the cell differs only in its main electrode space from the three-vessel cells well known in electrochemical methodics. The space of the main electrode is closed at the bottom by a sealed-in glass filter (F).

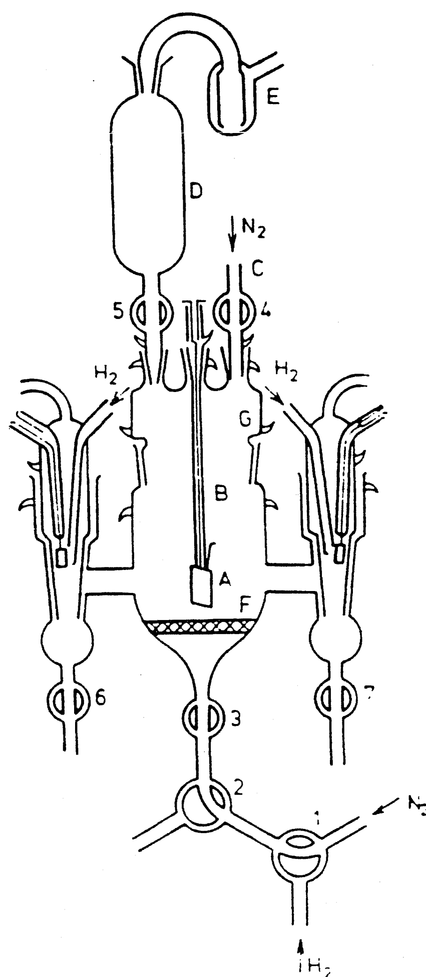

Fig. 1. Cell used for the preparation of the modified catalyst

and at the top by a ground stopper (G). The upper gas inlet cock (C), the main electrode (A. B) and the de-oxygenating vessel (D). together with the bubbling vessel (E) closing the latter, are connected with the main electrode space through ground joints sealed to stopper 'G'. (Ground joints are held together by clamping springs coated with cadmium.)

The liquid drain (2) and the gas inlet Y-cock (1) are joined through cock (3) to the bottom of the main electrode space.

After the closing of cocks 4, 6 and 7, the apparatus operates as a cell divided into three electrode spaces, as used in electrochemical methodics, with the difference that the flushing gas is introduced through glass filter 'F' into the main electrode space, and departs through de-oxigenating vessel 'D' into the atmosphere.

Only cocks 1. 2, 3, 4, 6 and 7 need lubrication during operation, the other cocks and ground joints do not.

1. *Exchange of solutions under oxygen-free conditions*

The exchange of solutions is performed in the following way: through cocks 1. 2 and 3. oxygen-free N_2 is bubbled into the main electrode space, while the new solution is poured into de-oxygenating vessel 'D' and the opening of cock 5 is adjusted so as to prevent the flow of liquid into the cell. After de-oxygenation for an adequate period, cock 5 is closed, the draining Y-cock is set to outflow, and the flushing gas is introduced through upper branch 'C', through the opening of cock 4, from the top into the cell. The solution can be removed in this way from the cell. Next, cock 2 is reset, and the flushing gas is introduced again through glass filter 'F' to the electrode, while cock 4 is closed and cock 5 is adjusted so that the new solution, which has been previously de-oxygenated in vessel 'D', flows slowly, under passing of flushing gas, into the space of the main electrode.

The exchange of solutions under oxygen-free conditions makes the cell suitable, in addition to preparative procedures, also for the electrochemical and electrocatalytic investigation of catalysts modified by adsorbed metals.

2. *Drying under oxygen-free conditions*

As mentioned in the introduction, in the presence of water, atmospheric oxygen destroys the adsorbed metal layer according to Eq. (1). Therefore, after the formation of the adsorbed metal layer and the washing of the catalyst with triply distilled (oxygen-free) water, drying can also be performed under oxygen-free conditions. For this purpose, after draining of the washing liquid through the main electrode space, dry, oxygen-free N_2 is passed until adhering water is also removed. Drying can be accelerated by the heating of the apparatus

with an infrared lamp. However, when a drying lamp is used, care must be excercised that the catalyst should not be exposed to thermal effects, which change the structure of the adsorbed metal layer.

After the termination of drying, the catalyst modified with adsorbed metal can be removed from the cell in an air-dry state and transferred into the catalytic reactor.

3. *Design of the electrodes*

Electrodes of two kinds were used in the cell. If further operations (heat treatment, chemical reaction) were to be carried out with the catalyst modified by adsorbed metal, the electrode shown in Fig. 1 was chosen. In this case, the electrode is a platinum plate of 99.99% purity and ~2 cm^2 apparent surface ('A'), suspended on a Pt wire ('B'), bent to a hook, and sealed into a glass tube. During the various operations, the Pt electrode was handled only with teflon pincers.

For electrochemical investigations (10—12), the platinum plate, similarly of ~2 cm^2 apparent surface and 99.99% purity, has been fixed by point-welding on the platinum wire sealed into glass.

The electrodes were washed with aqua regia until the appearance of the crystal texture and platinized in the way described in our earlier communication [10]. The hook electrode proper ('B') was not subjected to pretreatment other than washing with aqua regia.

The reference and auxiliary electrodes were also made of platinized platinum, according to a design employed in electrochemical practice.

II. Effect of oxygen adsorption on the adsorbed metal

Since the catalyst is transferred in air into the catalytic reactor, we have investigated whether or not oxygen adsorption during this process affects the properties of the adsorbed metal. For this purpose, the following series of experiments were carried out.

a) The charging curve of the platinized platinum catalyst in 1 *M* HCl was recorded (Fig. 2, curve 1). After this, an adsorbed copper layer was formed in the way described earlier [11], and the charging curve of this catalyst, covered with copper, was also recorded (Fig. 2, curve 2).

b) After recording of the charging curve, an adsorbed copper layer was again produced on the surface and the electrode washed and dried as described above.

c) The air-dry catalyst was taken out of the cell and kept for about 5 min in air, then placed back into the cell.

d) Next, dry H_2 gas was passed for 5 min through the main electrode space to reduce the oxygen adsorbed on the catalyst and to prevent thereby the oxidation of the adsorbed metal according to Eq. (1). After stopping of the hydrogen stream, 1 *M* HCl was again introduced under oxygen-free conditions and the charging curve of the catalyst pretreated in this way was recorded (Fig. 2, curve 3).

A comparison of curves 2 and 3 shows that, on applying the above process, the properties of the copper layer adsorbed on the platinized platinum catalyst do not change on contact with the atmosphere.

Similar experiments with platinized platinum catalysts covered by other metals (Au, Bi, Pd) gave the same results. However, in the case of platinum covered by adsorbed gold [28] and adsorbed palladium [29], adsorbed oxygen does not cause structural changes even in the presence of adhering water indeed or even perchloric acid, which considerably simplifies and extends the applicability of such catalysts.

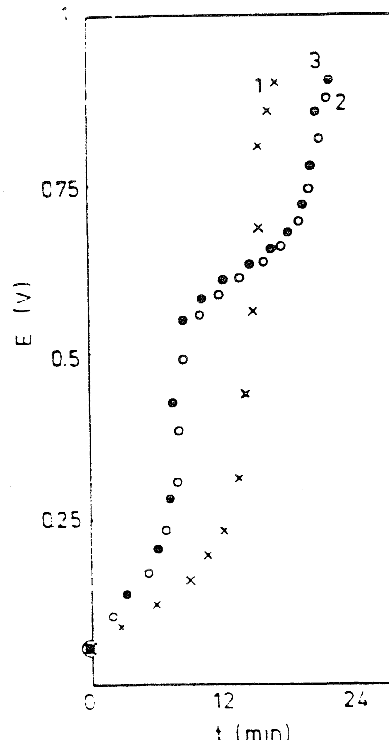

Fig. 2. 1. Charging curve in 1 *M* HCl; 2. charging curve of the catalyst covered by copper 3. charging curve of the catalyst covered by copper after contact with atmospheric oxygen

III. Effect of thermal treatment on the modified catalysts

From the viewpoint of the applicability of catalysts modified with adsorbed metals, it is very important to know the highest temperature up to which they preserve their original structure. For the study of this problem,

operations described in part II have been complemented, after section c), by heat treatment performed under hydrogen.

Naturally, before the investigation of the modified catalysts, the platinized platinum plate proper has been subjected to thermal treatment under the same conditions as those used with the catalyst covered by adsorbed metal. During thermal treatment, the roughness factor of the catalyst decreased by about an order of magnitude and did not change any more after heat treatment of 15 min. In the further operations, a platinized platinum plate pretreated in this way was used.

For the heat treatment of air-dry catalysts covered by the metal, section c) of the previous paragraph was complemented by the following operations, presented specifically for copper covered catalysts.

c/1. The catalyst was placed into a reactor, air was removed with dry N_2, then dry H_2 gas was passed through the vessel.

c/2. The reactor was placed onto a thermostat of the desired temperature (accuracy ± 1 °C) and kept there for 20 min.

c/3. After thermostating, hydrogen was flushed with N_2 gas from the reactor, which was then allowed to cool. The heat-treated catalyst of room temperature was put back into the cell and its charging curve was recorded as described in section d) of the preceding paragraph.

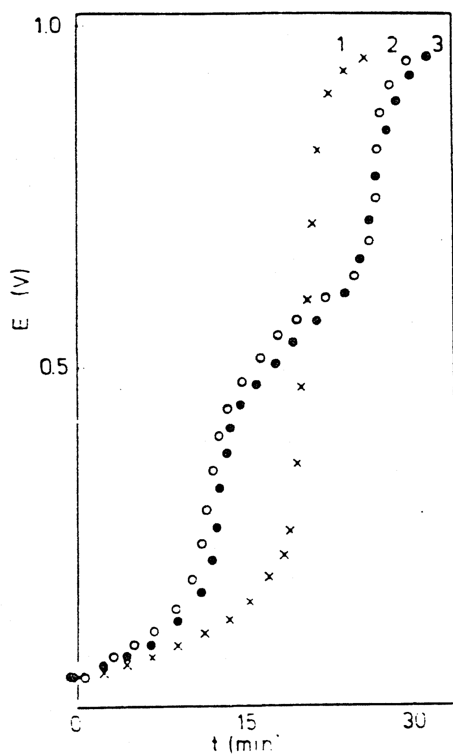

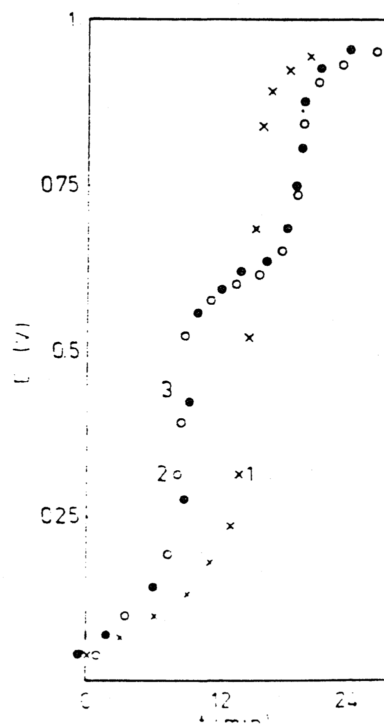

Fig. 3. 1. Charging curve in 1 *M* HCl; 2. charging curve of the catalyst covered by copper; 3. charging curve of the catalyst covered by copper after heat treatment at 100 °C

Fig. 4. 1. Charging curve in 1 *M* HCl; 2. charging curve of the catalyst covered by copper; 3. charging curve of the catalyst covered by copper after heat treatment at 150 °C

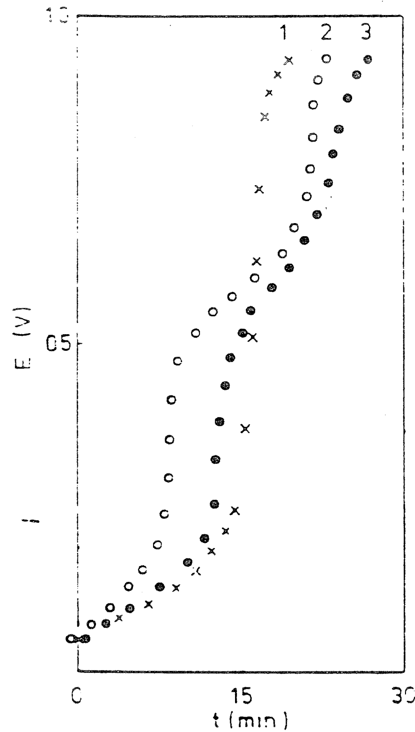

Fig. 5. 1. Charging curve in 1 *M* HCl; 2. charging curve of the catalyst covered by copper; 3. charging curve of the catalyst covered by copper after heat treatment at 200 °C

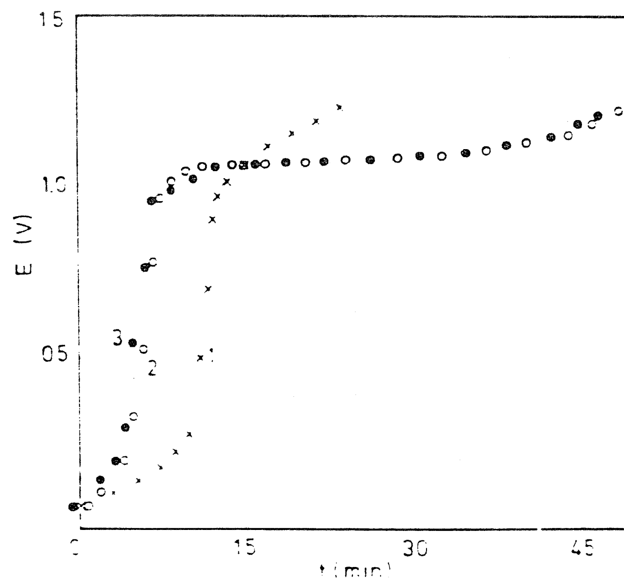

Fig. 6. 1. Charging curve in 0.2 *M* HCl; 2. charging curve of the catalyst covered by gold; 3. charging curve of the catalyst covered by gold after heat treatment at 350 °C

In the case of the copper-covered catalyst, heat treatment was performed at 100, 150 and 200 °C. As shown by Fig. 3, heat-treatment at 100 °C does not change the structure of the adsorbed metal since the charging curves of the treated and untreated catalysts coincide. However, on heat treatment at 150 °C (Fig. 4), and particularly at 200 °C (Fig. 5), there is a considerable

difference between the two charging curves, indicating alloy formation with the adsorbed metal layer. This is supported also by the observation that on cutting off the current after recording the charging curve, the potential of the catalyst returns to the range corresponding to the copper section. After washing and exchange of the solution under oxygen-free conditions, the charging curve was recorded again. At the potential corresponding to the copper section, a small wave actually appears on the charging curve, which may be due only to the oxidation of copper alloyed into the surface; no such wave has been observed in other measurements [11].

The heat treatment of the Pt catalyst covered with adsorbed gold deposited from a hydrochloric acid medium has also been performed [28]. As shown also by the comparison of Figs 6 and 7, up to 350 °C, gold does not form an alloy with the platinum base metal.

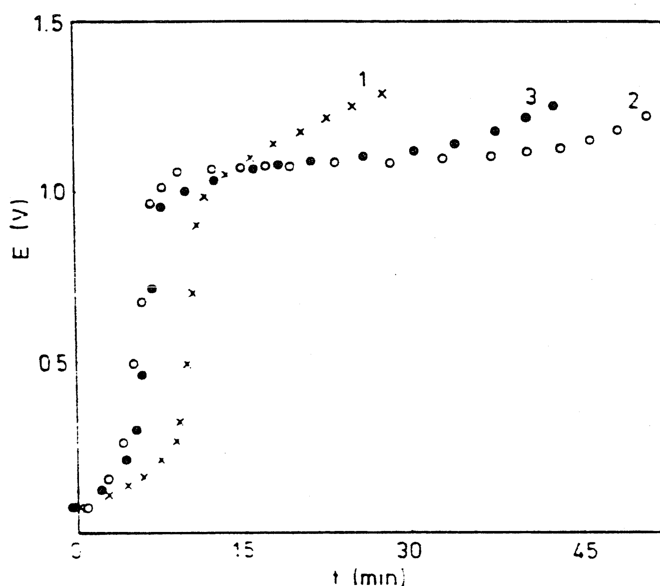

Fig. 7. 1. Charging curve in 0.2 *M* HCl; 2. charging curve of the catalyst covered by gold; 3. charging curve of the catalyst covered by gold after heat treatment at 400 °C

IV. Preparation of supported platinum catalysts modified by adsorbed metal

Since the adsorbed metal layer can be produced also by the ionization of hydrogen adsorbed on platinum [7], [10—12], [16—18], in principle, supported catalysts modified by adsorbed metals can also be prepared.

We started our work on the basis of data published in the literature [7], [16—18], however, it soon became evident that the available results are insufficient for the interpretation of the experimental phenomena. Using a type AP-56 Pt catalyst on Al_2O_3 support (USSR) in perchloric acid medium as model substance, we have found that its colour becomes a darker grey

after metal deposition (Ag, Cu, Bi). The conclusions of this study are reported in a previous publication [10, 12]: the adsorption process involves two steps. In the first step, a metal crystal is deposited on each platinum site. If, for some reason, this metal crystal cannot be transformed onto adsorbed metal in the next step, the colour of the catalyst will be changed by the finely dispersed metal, as has indeed been found in perchloric acid.

If in the case of a supported catalyst no conditions are found under which the metal coating is transformed into adsorbed coating, an alloy catalyst can be obtained by the heat treatment of the catalyst at the appropriate temperature in hydrogen atmosphere. This means that platinum deposited previously on the carrier is alloyed with an amount of the alloying substance equivalent to its original hydrogen capacity.

Metal deposition in hydrochloric acid medium does not change the colour of the AP-56 catalyst, thus in this case adsorbed metal has actually been formed. However, in the case of copper, the loss in charge due to redox system Cu^{2+}/Cu^{+} must also be taken into consideration in estimating the coverage; this loss is presumably strongly dependent on the pore structure of the catalyst [11].

The preparation itself can also be carried out in the cell shown in Fig. 1. However, when a perchloric acid medium is used, chloride ions leached from the supported catalyst must also be taken into account. In other words, in the preparation of supported catalysts involves the same considerations as that of pure metals.

REFERENCES

[1] Breiter, M. W.: J. Electrochem. Soc., **114**, 1125 (1967)
[2] Breiter, M. W.: Trans. Faraday Soc., **65**, 2179 (1969)
[3] Yoshida, T., Matsuda, I., Takeshita, T., Yoshioka, O.: Denki Kagaku, **40**, 853 (1972)
[4] Mikuni, F., Takamura, T.: Denki Kagaku, **38**, 113 (1970)
[5] Bowles, B. J.: Electrochim. Acta, **15**, 589 (1970)
[6] Bowles, B. J.: Electrochim. Acta **15**, 737 (1970)
[7] Cadle, S. H., Bruckenstein, S.: Anal. Chem., **43**, 1858 (1971)
[8] Cadle, S. H., Bruckenstein, S.: Anal. Chem., **44**, 1993 (1972)
[9] Furuya, N., Motoo, S.: Denki Kagaku, **41**, 307 (1973)
[10] Szabó, S., Nagy, F.: Magy. Kém. Folyóirat, **81**, 239 (1975)
[11] Szabó, S., Nagy, F.: Magy. Kém. Folyóirat, **81**, 365 (1975)
[12] Szabó, S., Nagy, F.: J. Electroanal. Chem. (In press)
[13] Schultze, W.: Ber. Bunsenges. Phys. Chem., **74**, 705 (1970)
[14] Tindall, G. W., Bruckenstein, S.: Electrochim. Acta, **16**, 245 (1971)
[15] Mikuni, F., Takamura, T.: Denki Kagaku, **39**, 579 (1971)
[16] Miller, J., Tóth, G.: Magy. Kém. Folyóirat, **78**, 265 (1971)
[17] Tóth, G.: Magy. Kém. Folyóirat, **70**, 361 (1964)
[18] Miller, J., Tóth, G.: Isotopenpraxis, **3**, 19 (1967)
[19] Kolb, D. M., Przasnyski, M., Gerisher, H.: J. Electroanal. Chem., **54**, 25 (1974)
[20] Lorenz, W. J., Hermann, H. D., Wüthrich, N., Hilbert, F.: J. Electrochem. Soc., **121**, 1167 (1974)
[21] Taylor, A. H., Kirkland, S., Brummer, S. B.: Trans. Faraday Soc., **67**, 809 (1971)
[22] Taylor, A. H., Kirkland, S., Brummer, S. B.: Trans. Faraday Soc., **67**, 819 (1971)
[23] Watanabe, M., Motoo, S.: J. Electroanal. Chem., **60**, 259 (1975)
[24] Watanabe, M., Motoo, S.: J. Electroanal. Chem., **60**, 267 (1975)

[25] WATANABE. M.. MOTOO. S.: J. Electroanal. Chem.. **60**. 275 (1975)
[26] ADZIC. R. R.. SIMIC. D. N.. DRAZIC. D. M.. DESPIC. A. R.: J. Electroanal. Chem.. **61**. 117 (1975)
[27] ADZIC. R. R.. SIMIC. D. N.. DRAZIC. D. M.. DESPIC. A. R.: J. Electroanal. Chem.. **65**, 587 (1975)
[28] SZABÓ. S.. NAGY. F.: Magy. Kém. Folyóirat (In press).
[29] SZABÓ. S.: unpublished results

Sándor SZABÓ
Ferenc NAGY
Dezső MÓGER
H-1025 Budapest, Pusztaszeri út 59—67.

J. Electroanal. Chem., 70 (1976) 357—364

© Elsevier Sequoia S.A., Lausanne — Printed in The Netherlands

3.

INVESTIGATIONS OF SILVER, BISMUTH AND COPPER ADSORPTION VIA THE IONIZATION OF HYDROGEN ADSORBED ON PLATINIZED PLATINUM IN PERCHLORIC ACID SOLUTIONS

S. SZABÓ and F. NAGY

Central Research Institute for Chemistry, Hungarian Academy of Sciences, H-1025/17 Budapest (Hungary)

(Received 21st July 1975; in revised form 20th October 1975)

ABSTRACT

Silver, bismuth and copper deposition via the ionization of hydrogen adsorbed on platinized platinum results in an adsorbed layer of the same character as obtained by electrochemical methods. The formation of the adsorbed layer, however, is preceded by bulk deposition. Then, with the ionization of the bulk metal the formation of the adsorbed layer is begun, by the formation of the most strongly adsorbed species.

INTRODUCTION

Many publications have discussed the adsorption or electrosorption of metal atoms on metal surfaces in various media at potentials positive with respect to the reversible Nernst potential [1—8]. The various investigations have shown metal adsorption on metals to be a general phenomenon [6].

In the case of silver, bismuth and copper adsorption on platinum, in addition to the determination of undervoltage values, the connection between metal adsorption and hydrogen adsorption has been investigated. Metal adsorption has been found to inhibit hydrogen adsorption. The number of hydrogen adsorption sites occupied by one adsorbed metal atom has also been determined [8—13].

Besides the investigation of adsorbed metal layers formed through electrochemical methods, spontaneous metal deposition via the ionization of adsorbed hydrogen has been investigated to a lesser degree [13,14]. In this way, in open-circuit experiments, adsorbed metal layers can be formed on metals that adsorb hydrogen well. The understanding of the formation and the character of adsorbed metal layers formed via the ionization of adsorbed hydrogen is particularly important in the case of finely dispersed metals, e.g. in the case of various catalysts.

The purpose of our studies has been to investigate the metal deposition via the ionization of hydrogen adsorbed on platinized platinum and to understand the character of the resulting metal deposits. In this case, the discharge

or adsorption process takes a somewhat different course from that of the deposition by current. The base metal should be saturated with hydrogen first, then metal ions are introduced into the solution and metal deposition takes place, with the simultaneous ionization of adsorbed hydrogen. If the potential of the platinum at the introduction of the metal ions is more negative than the reversible Nernst potential of the metal to be adsorbed, bulk deposition is possible, in addition to the formation of an adsorbed layer.

The character of the metal layer was examined by means of constant-current charging curves. This method allowed the determination of the undervoltage values of the metal layers and the calculation of the number of hydrogen adsorption sites occupied by one adsorbed metal atom, from the following relation:

$$S = (Q_H^0 - Q_H^x)/(Q_M/z) \quad (1)$$

where Q_H^0 and Q_H^x are the charges required for the oxidation of hydrogen adsorbed on platinum before and after metal adsorption, respectively; Q_M is the charge required for the oxidation of the adsorbed metal and z is the number of positive charges of the ions formed in the oxidation of the adsorbed metal [4].

EXPERIMENTAL

The apparatus differed from the usual three-compartment electrochemical cells only in that it allowed solutions to be changed in the main compartment with the exclusion of air. For this purpose, an upper vessel was connected to the main compartment through a stopcock. Purified nitrogen gas, rinsing the main compartment, flowed also through this vessel. When the electrolyte was to be changed, the solution was poured first into this upper vessel and it was admitted to the main compartment only after deoxygenation for a sufficient period. Ionic connection between the compartments was maintained by greaseless ground joints moistened with the base solution.

The solutions were made with triply distilled water, prepared in the following way. $KMnO_4$ was added to distilled water and boiled in a beaker for about 15 min to destroy organic contaminants. The dilute $KMnO_4$ solution was then distilled and the resulting doubly distilled water was then distilled again in order to remove traces of $KMnO_4$. This resulted in the elimination of most of the organic contaminants. Water obtained by this method, however, is not completely free from organic materials [17].

$AgClO_4 \cdot H_2O$ and $Cu(ClO_4)_2 \cdot 6H_2O$ (made by Fluka) were employed to introduce silver and copper ions into the system; bismuth ions were obtained by dissolving Bi_2O_3, in order to avoid difficulties arising from the adsorption of other anions [6,15,16]. In all cases deoxygenation (and traces of hydrogen) was effected by continuous bubbling of purified nitrogen gas through the cell.

Platinized platinum electrodes were prepared by washing the platinum elec-

trode (geometrical surface $\sim 2\ cm^2$) in aqua regia, rinsing in distilled water and polarising cathodically for 10 min with 15 mA cm^{-2}, then for 3.5 h with 3 mA cm^{-2} in a solution of 3 g of $PtCl_4$ in 20 ml concentrated HCl, diluted to 120 ml. The surface of the electrode decreases in use, but this caused no problem, since the charging curve of the electrode in the pure, hydrogen-free base solution was determined before each experiment (curves 1 on the Figures).

A hydrogen electrode in a solution of the same pH was used as a reference electrode.

The experiments were made in the following sequence. The platinized platinum electrode was activated by anodic polarization in 0.1 *M* $HClO_4$ in a separate cell, then it was placed into the cell containing the base solution and was saturated with hydrogen.

After determining the charging curve in the base solution, the electrode was again saturated with hydrogen, then the trace of hydrogen was removed from the solution by the continuous nitrogen stream. When the electrode potential with respect to the reference electrode reached ~ 0.04 V, the metal perchlorate solution (previously poured in the upper vessel) was introduced into the main compartment. (0.1 g of copper perchlorate or 0.05 g of silver perchlorate or 0.05 g of bismuth oxide was used, giving $\sim 4 \times 10^{-3}$ *M* metal ions in the main compartment.) After reaching the equilibrium, the solution containing metal ions was removed. The cell then was repeatedly rinsed with deoxygenated triply distilled water and filled with deoxygenated base solution. The electrode was again saturated with hydrogen and after removing traces of hydrogen the charging curve was determined. The charging curves shown on the Figures were obtained in this way.

In some cases a charging curve was determined in the presence of the metal ions, after reaching the equilibrium. The respective charging curves are also shown on the Figures.

RESULTS AND DISCUSSION

(1) Deposition of silver

A platinized platinum electrode was saturated with hydrogen in 0.1 *M* $HClO_4$ solution, then silver ions were added. The electrode potential rose to ~ 0.73 V. The charging curve of the electrode prepared thus in the solution containing silver ions is curve 2 in Fig. 1. The comparison of curve 1 and curve 2 shows that the amount of the deposited silver is equivalent to that of the adsorbed hydrogen, since the curves coincide.

The experiment was then repeated and the charging curve of silver-covered electrode after reaching the equilibrium was determined in the 0.1 *M* $HClO_4$ base solution (curve 3 in Fig. 1). The curve shows that the hydrogen capacity of the platinum electrode decreased considerably but did not vanish completely. This agrees with the result to be expected on the basis of the references, indicating the formation of an adsorbed silver layer on the surface.

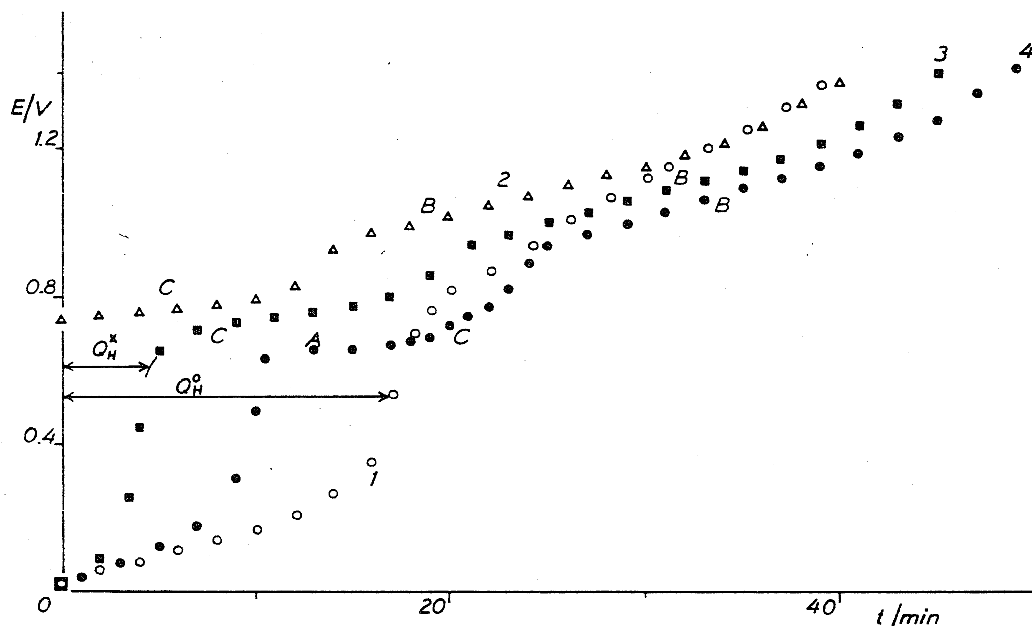

Fig. 1. I = 0.2 mA. (1) Charging curve in 0.1 M $HClO_4$ solution. (2) Charging curve of the silver-covered electrode in the solution containing silver ions, and (3) in the base solution. (4) Charging curve of the electrode in base solution after completion of metal deposition but before reaching the equilibrium.

The comparison of the silver region of curve 2 and curve 3 shows that saturation by hydrogen did not alter the oxidation degree of the adsorbed layer, consequently the surface is covered by completely discharged silver atoms.

From curves 1 and 3, by the above-mentioned formula (1), it is possible to determine the number of hydrogen adsorption sites occupied by one silver atom. Since the amount of the deposited silver is equivalent to that of the adsorbed hydrogen, $Q_H^0 = Q_M$,

$$S = (18 - 4.5)/18 = 0.75 \qquad (2)$$

The result corresponds to that to be expected on the basis of refs. 11 and 13, indicating the formation of an adsorbed silver layer on the surface. Thus the B and C regions of the curves show the oxidation of adsorbed silver.

Following these investigations, it was examined whether the bulk silver, visibly appearing for a period before reaching the equilibrium, is transformed into adsorbed silver in the absence of silver ions. For this purpose the solution containing silver ions was removed from the cell after completion of bulk deposition and curve 4 was determined. If the electrode was kept in the base solution for a longer time before saturation with hydrogen, the same curve (4) was obtained. It indicates that the transformation may not occur without participation of silver ions.

Besides visual observation, the presence of bulk silver is indicated by the appearance of the A region of the curve and the increase of the hydrogen region with respect to the previous experiment.

The experiments made in 0.1 M $HClO_4$ were repeated in M $HClO_4$, too. No

difference was found; the site demand (S) of the adsorbed silver and the charging curves were exactly the same as those determined in the 0.1 M $HClO_4$ base solution.

The underpotential values for silver oxidized at 1.1 V (region B, Fig. 1) correspond with those in the references. In the case of the undervoltage values for region C of the curves, the small difference (~0.08 V) between region C of curve 3 and region A of curve 4 makes the differentiation between the bulk and the adsorbed forms difficult. This probably accounts for the lack of precise agreement with the values in the references in this case.

The mechanism of the formation of the adsorbed silver layer. According to the experimental results, the first step of the formation of the adsorbed silver layer is the bulk deposition of silver with simultaneous ionization of adsorbed hydrogen.

$$\begin{aligned} Ag^+ + e &\rightarrow Ag \\ H_a &\rightarrow H^+ + e \end{aligned} \qquad (3)$$

The first step is followed by the formation of the adsorbed layer with simultaneous ionization of the equivalent amount of bulk silver clinging to the surface.

$$\begin{aligned} Ag &\rightarrow Ag^+ + e \\ Ag^+ + e &\rightarrow Ag_{ads} \end{aligned} \qquad (4)$$

The existence of step (4) is indicated by the fact that bulk silver is not transformed into adsorbed silver in the absence of Ag^+ ions. Consequently, if the bulk silver deposited in the first step (3) forms such a dense coating on the surface as to block transport between the platinum surface and the solution, then the bulk silver can be transformed into an adsorbed layer only slowly, because of the low diffusion rate of the silver ions. This can account for the slower formation of the adsorbed silver layer on a freshly platinized electrode. In such cases the first (3) and second (4) steps were better separated than those demonstrated in Fig. 1.

According to Fig. 1, an adsorbed species, ionized at 1.1 V is the first to be formed (region B) and the completion of this process is followed by the formation of the other species ionized at ~0.75 V (region C). Curve 4 in Fig. 1 represents the moment when the formation of region B has been completed and region C is beginning to develop. This is indicated by the small wave on the curve at 0.7 V.

(2) The deposition of bismuth

With the deposition of bismuth via the ionization of hydrogen adsorbed on a platinized platinum electrode in M $HClO_4$ solution, the potential of the elec-

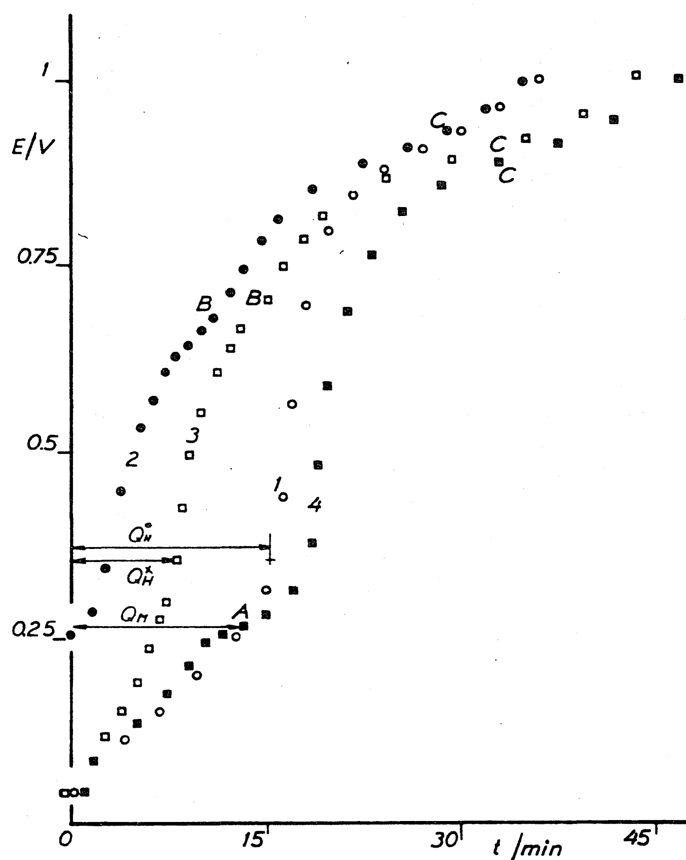

Fig. 2. I = 0.2 mA. (1) Charging curve in M $HClO_4$ solution. Bismuth deposition had already taken place on the electrode. (2) Charging curve of the bismuth-covered electrode in the solution containing bismuth ions, and (3) in the base solution. (4) Charging curve of the electrode in base solution if the deposition process was frozen at 0.21 V.

trode rose to ~0.25 V. The charging curve of the electrode after reaching the equilibrium is curve 2 in Fig. 2. According to curve 2, the amount of the bismuth is equivalent to that of the ionized hydrogen (curves 1 and 2 coincide). The charging curve of the electrode in M $HClO_4$ solution after the same pretreatment is curve 3, showing that the hydrogen capacity of the surface decreased considerably. This indicates the formation of an adsorbed layer in this case, too.

From curves 1 and 2 it is also possible to determine the number of hydrogen adsorption sites occupied by one adsorbed metal atom, but the fact should be taken into consideration that the electrode potential during the deposition of bismuth rose only to ~0.25 V. From Fig. 2:

$$S = (16 - 8)/(12/3) = 2 \qquad (5)$$

The result is in excellent agreement with those in refs. 8 and 10.

If the deposition process was frozen before reaching the equilibrium (at ~0.21 V), curve 4 was obtained in the base solution. The comparison of curve 4 and curve 3 clearly shows that the formation of adsorbed layer begins with bulk deposition (region A on the curve) in this case, too. The experimental

results show that bulk bismuth is transformed into adsorbed bismuth only in the presence of bismuth ions.

Bulk deposition is indicated also by the fact that the hydrogen capacity of the platinum changed very little. The obvious explanation for this is that the bulk metal clings to the surface only at some points, chiefly at peaks of the platinum black.

The undervoltage values determined from region B and region C, and the initial potential of the oxidation of adsorbed bismuth (~0.4 V) agree with the results of other authors' experiments [5,8,10]. It must be noted, however, that region C represents the oxidation of not only the adsorbed bismuth but of that dissolved in the base metal [8,18]. In our experience, if once bismuth deposition had taken place on an electrode then the original charging curve could not be reproduced. Instead of the original charging curve, in our work, this curve was taken as a reference, since only this state could be reproduced by anodic polarization.

The mechanism of the formation of the adsorbed bismuth layer. Figure 2 shows clearly that the formation of the adsorbed bismuth layer begins with bulk deposition in this case, too; that is, the formation of the adsorbed layer follows the same two-step mechanism as in the case of silver deposition.

According to Fig. 2, bulk deposition is followed by the formation of the species adsorbed at highest potential, similarly to silver deposition.

(3) The deposition of copper

0.1 *M* and *M* $HClO_4$ solutions were used as base solutions. The results obtained in the two solutions were in good agreement.

After the bulk deposition the electrode potential rose to ~0.25 V which is in good agreement with the potential of the copper electrode in the same solution. With the completion of the potential rise, a visible copper coating was formed on the electrode. The charging curve of the electrode in the base solution is curve 2 in Fig. 3, showing no copper adsorption: the hydrogen region of the curve remained unchanged and there are no regions due to oxidation of adsorbed copper [2,3,9]. In longer period, however, bulk deposition is followed by the formation of the adsorbed layer, if copper ions are present.

The hydrogen capacity of the surface decreases as bulk copper (region A in the curves) turns into adsorbed copper (region B). The charging curve of the electrode in this case is curve 4. The transition state between the two extremes is represented by curve 3.

The site demand could not be determined from the charging curves in this case, since the copper region and the hydrogen region are not clearly separated. The undervoltage value determined from the curves (~0.7 V) is in accordance with the results of other authors' experiments [1—4,6,15].

The mechanism of the formation of the adsorbed copper layer. In the absence

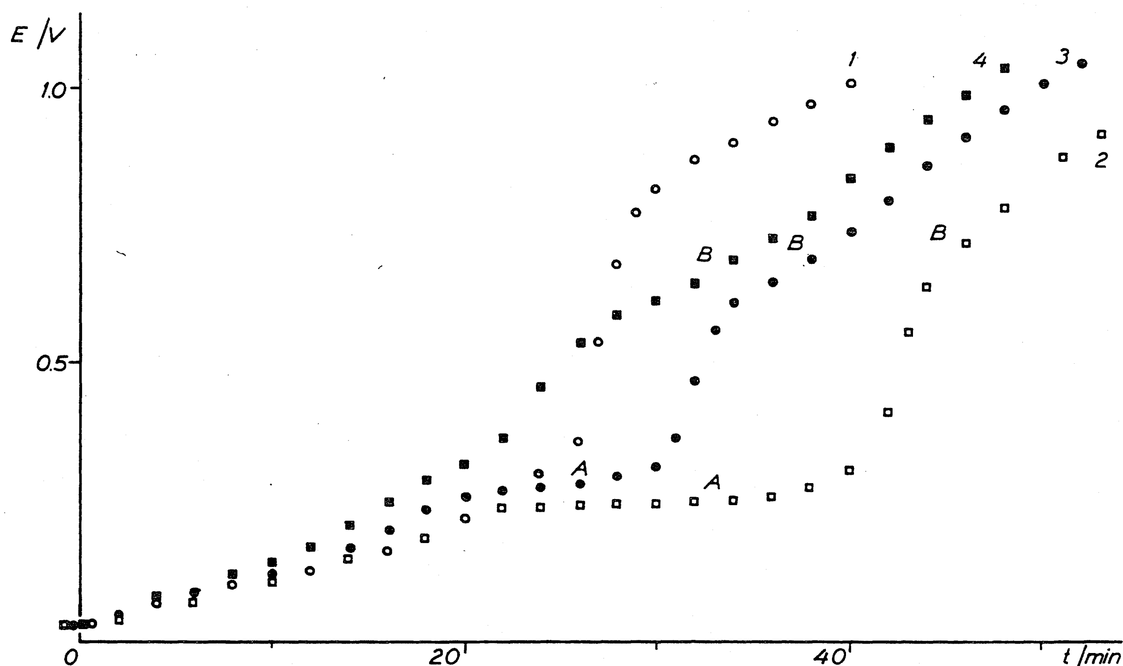

Fig. 3. $I = 0.5$ mA. (1) Charging curve in M $HClO_4$ solution. (2) Charging curve of the electrode in base solution after completion of bulk deposition. (3) Charging curve of the electrode covered by bulk and adsorbed copper, and (4) after reaching the equilibrium.

of copper ions the bulk deposit is not transformed into adsorbed copper, indicating that the mechanism of the formation of the adsorbed layer is the same as in the case of silver and bismuth.

According to Fig. 3, the formation of the adsorbed layer begins with the formation of the most strongly adsorbed species, similarly to the other cases.

REFERENCES

1 M.W. Breiter, J. Electrochem. Soc., 114 (1967) 1125.
2 M.W. Breiter, Trans. Faraday Soc., 65 (1969) 2197.
3 J.W. Schultze, Ber. Bunsenges. Phys. Chem., 74 (1970) 705.
4 T. Yoshida, I. Matsuda, T. Takeshita and O. Yoshioka, Denki Kagaku, 40 (1972) 853.
5 F. Mikuni and T. Takamura, Denki Kagaku, 38 (1970) 113.
6 D.M. Kolb, M. Przasnyski and H. Gerischer, J. Electroanal. Chem., 54 (1974) 25.
7 G.W. Tindall and S. Bruckenstein, Electrochim. Acta, 16 (1971) 245.
8 S.H. Cadle and S. Bruckenstein, Anal. Chem., 44 (1972) 1993.
9 B.J. Bowles, Electrochim. Acta, 15 (1970) 589.
10 B.J. Bowles, Electrochim. Acta, 15 (1970) 737.
11 A.H. Taylor, S. Kirkland and S.B. Brummer, Trans. Faraday Soc., 67 (1971) 819.
12 N. Furuya and S. Motoo, Denki Kagaku, 41 (1973) 307.
13 S.H. Cadle and S. Bruckenstein, Anal. Chem., 43 (1971) 1858.
14 J. Miller und G. Tóth, Isotopenpraxis, 3 (1967) 19.
15 G. Horányi and G. Vértes, J. Electroanal. Chem., 45 (1973) 295.
16 G. Horányi, J. Electroanal. Chem., 55 (1974) 45.
17 B.E. Conway, H. Angerstein-Kozlowska, W.B.A. Sharp and E.E. Criddle, Anal. Chem., 45 (1973) 1331.
18 F. Mikuni and T. Takamura, Denki Kagaku, 39 (1971) 579.

J. Electroanal. Chem., 84 (1977) 93—98
© Elsevier Sequoia S.A., Lausanne — Printed in The Netherlands

INVESTIGATIONS OF COPPER ADSORPTION IN HYDROCHLORIC ACID MEDIA, VIA THE IONIZATION OF HYDROGEN ADSORBED ON PLATINIZED PLATINUM

S. SZABO and F. NAGY

Central Research Institute for Chemistry, Hungarian Academy of Sciences, H-1525/17 Budapest (Hungary)

(Received 14th April 1976; in revised form 16th November 1976)

ABSTRACT

Copper deposition in hydrochloric acid media, via the ionization of hydrogen adsorbed on platinized platinum, results in an adsorbed metal layer similar to that formed potentiostatically. However, the adsorbed hydrogen is replaced by adsorbed copper only to a certain extent, owing to the formation of Cu^+ ions. This discrepancy depends on the chloride ion activity and the structure of the platinum black.

Owing to the complex-forming effect [1] and specific adsorption of chloride ions [2] (which is increased by copper adsorption [3]) the results of adsorption of copper on platinum obtained in perchloric acid solution [4] cannot be extended to hydrochloric acid media. For these reasons, the copper adsorption, via the ionization of hydrogen adsorbed on platinized platinum has been investigated in hydrochloric acid. The present paper is devoted to this subject.

EXPERIMENTAL

The method and apparatus were exactly the same as described in our previous paper [4]. As a copper salt, $CuCl_2 \cdot 2\,H_2O$ was employed, in a concentration of 4×10^{-4} *M*.

The reference electrode was Pt/H_2 in the same solution.

RESULTS

Dependence of the amount of adsorbed copper upon hydrochloric acid concentration

After the determination of the charging curve in 0.1 *M* HCl, the platinized platinum electrode was resaturated with hydrogen. The solution was then dehydrogenated and the copper salt introduced. The potential rose to ~0.66 V. After completion of the potential rise, the charging curve was determined in the copper solution (curve 2, Fig. 1). The experiment was then repeated so that the copper solution was removed from the cell after reaching equilibrium. The cell was rinsed with deoxygenated distilled water and filled with deoxygenated sup-

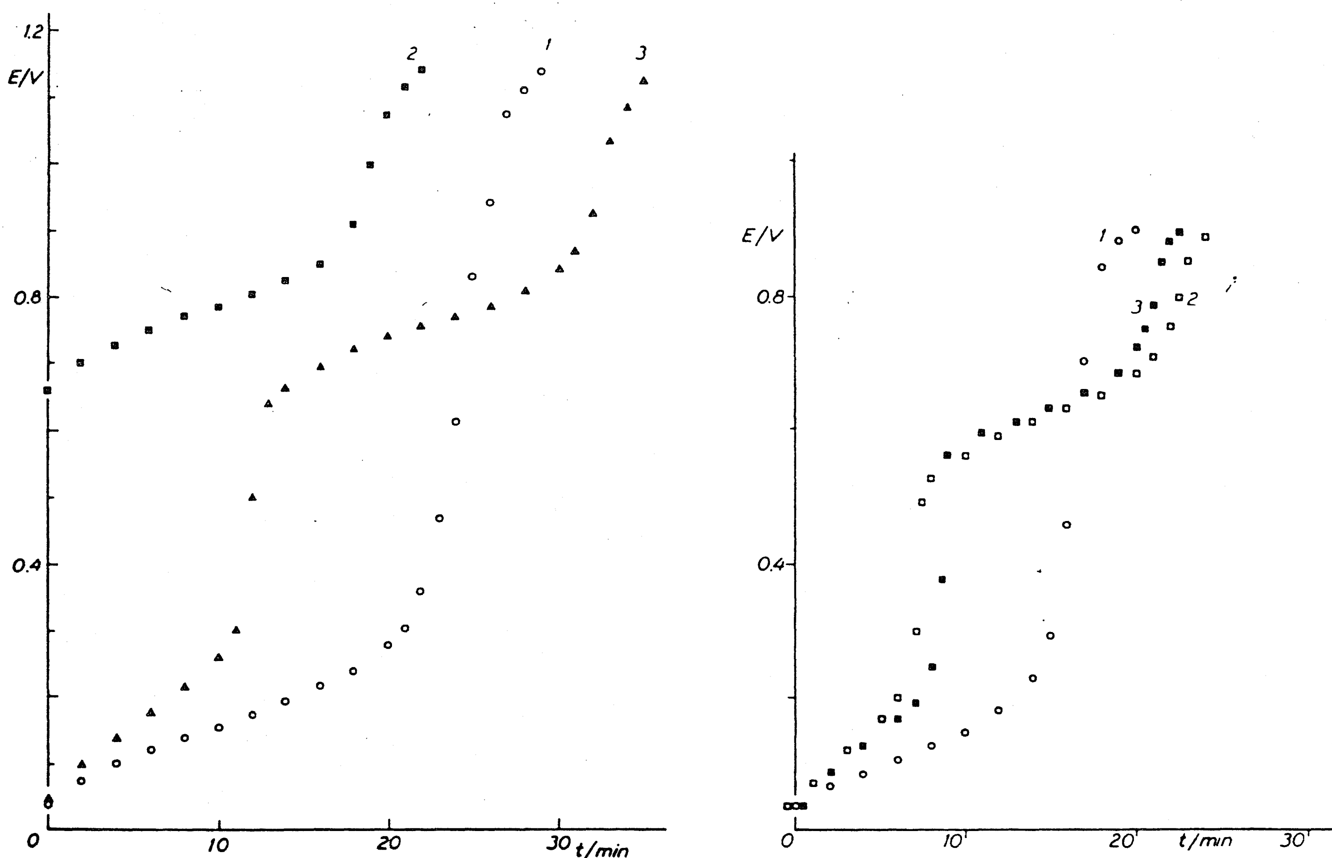

Fig. 1. I = 1.0 mA. (1) Charging curve in 0.1 M HCl; (2) charging curve of the copper-covered electrode in the copper solution, and (3) in the supporting electrolyte.

Fig. 2. I = 0.25 mA. (1) Charging curve in 1.0 M HCl; (2) charging curve of the electrode oversaturated with copper; (3) charging curve of the electrode after reaching equilibrium coverage.

porting electrolyte. The charging curve of the copper-covered electrode, after saturation with hydrogen, is curve 3 in Fig. 1.

The experiment was also performed in 1.0 M HCl. The result is illustrated by curve 3 in Fig. 2.

As the curves indicate, the results are in agreement with the published charging curves of copper-covered platinum [5]. It can also be concluded from the curves that the adsorbed hydrogen is replaced by adsorbed copper to a certain extent. Since copper ions form various complexes with chloride ions and the complexes containing Cu^+ ions are also stable [1], the discrepancy can be accounted for by the formation of Cu^+ complexes.

Comparison of results obtained in different hydrochloric acid concentrations shows that greater discrepancies are observed at the higher HCl concentrations. Experiments indicate that the ratio Q_M/Q_H^0 is a function of only the HCl concentration (Q_H^0 is the charge required for the oxidation of hydrogen adsorbed on blank platinum surface, and Q_M is that for the oxidation of adsorbed copper).

Finally, it must be noted that deposition and ionization of bulk copper could be observed during the metal adsorption at $c_{HCl} \leq 0.4$ M. This can be explained by the fact that owing to the increasing chloride activity, the Nernst potential of the copper/copper chloride system becomes more negative than the potential of the platinum at the beginning of the deposition process.

Site demand of one adsorbed copper atom

With the help of the relation published in our previous paper [4] the number of hydrogen adsorption sites (S) occupied by a copper atom can be determined. Substituting the data of Fig. 1 into the equation, we obtain

$$S = (24 - 13)/(18/2) \approx 1.2 \tag{1}$$

This result is in agreement with those in the literature [5] which, together with the undervoltage values, demonstrate the formation of an adsorbed metal layer.

Dissolution process

The reason for the stability of the ratio Q_M/Q_H^0 at constant HCl concentration was investigated next. For this purpose, the adsorption processes were interrupted before reaching equilibrium by removing the copper solution at a potential between 0.4 and 0.5 V. The charging curve was then determined in the supporting electrolyte. In 1.0 M HCl curve 2 in Fig. 2 was obtained. The curves show that at the beginning of the adsorption the coverage becomes higher than the equilibrium coverage, and the final value is reached via the dissolution of excess copper.

The dissolution process could also be demonstrated in dilute (0.2 M) HCl, but only after the second formation of the adsorbed layer. This was because the coverage formed in the first instance was very close to the equilibrium value.

Since the dissolution was observed only in the presence of Cu^{2+} ions, it is clear that it could only be caused by the oxidation of a part of the adsorbed copper to Cu^+ by Cu^{2+} ions. Thus, the overall equilibrium is the result of the following two reactions:

$$Cu_{ads} \rightleftharpoons Cu^+ + e \tag{2}$$

$$Cu^{2+} + e \rightleftharpoons Cu^+ \tag{3}$$

It is evident that the part of the adsorbed copper which is adsorbed at a more negative potential than that of the Cu^{2+}/Cu^+ redox system will be dissolved from the surface.

According to ref. 1, the redox system thus formed has a rather high positive potential, which is moved towards more positive values by increasing chloride ion activity. Since in HCl solution the Cu^+ ions are present as $CuCl_4^{3-}$ ions, it can be readily appreciated that the potential of the equilibrium (2) is moved in a negative direction by an increase in HCl concentration. These two opposite effects account for the fact that the copper coverage depends very strongly upon the HCl concentration.

Mechanism of the formation of the adsorbed layer

In such HCl concentrations where bulk deposition plays no part, the first step is the formation of adsorbed metal and Cu^+ ions, whilst the adsorbed hydrogen is ionized:

$$Cu^{2+} + 2\,e \rightarrow Cu_{ads} \tag{4}$$

$$Cu^{2+} + e \rightarrow Cu^{+} \tag{5}$$

$$H_a \rightarrow H^{+} + e \tag{6}$$

As we have seen, the adsorbed copper is partly ionized, too, thus the (4), (5) and (6) simultaneous reactions are followed by the equilibria (2) and (3).

In dilute HCl, where deposition and ionization of bulk copper also take place during the formation of the adsorbed layer, the above mechanism should be extended to include this process. Since the ionization produces both Cu^{+} and Cu^{2+} ions, this means that we may define three more reactions:

$$Cu^{2+} + 2\,e \rightarrow Cu_{bulk} \tag{7}$$

$$Cu_{bulk} \rightarrow Cu^{2+} + 2\,e \tag{8}$$

$$Cu_{bulk} \rightarrow Cu^{+} + e \tag{9}$$

though probably the bulk copper is transformed mainly to Cu^{+} ions [6].

The resulting electrons are used up only in the processes (4) and (5), of course.

Effect of the structure of platinum black on the deposition mechanism

When a copper deposition took place in 0.2 *M* HCl on a platinized platinum electrode whose platinizing solution differed in composition from that described in our previous paper [4], barely more than 40% of the adsorbed hydrogen was replaced by copper, in contrast with the 85—90% observed in other experiments. It follows from this that the ratios of the rates of processes (4)—(9) depend also upon the transport processes in the pores of the platinum black.

Determination of electrosorption valency of the adsorbed copper layer

The electrosorption of copper ions on platinum is regarded as a partial charge transfer reaction, i.e. the copper ion penetrates into the double layer but is not completely discharged. This is based on the observation that the electrosorption process is accompanied by a charge transfer which has a lower charge than that required for a complete discharge. This is reflected in the quantity called the electrosorption valency (γ) by Schultze and Vetter [7—9].

Under potentiostatic conditions, in the presence of a large excess of supporting electrolyte, the use of the following equation is proposed for the determination of the electrosorption valency [8]:

$$dq_m = -\gamma F\, d\Gamma_{ad} \tag{10}$$

This equation requires the combination of coulometric measurements for the determination of q_m and analytical measurements for the determination of Γ_{ad}.

The measurement of the Γ_{ad}, however, can be avoided in the following way.

Let us suppose that an adsorbed metal layer is formed under potentiostatic conditions and then reoxidized. The charge required for the oxidation, on the basis of eqn. (10), must be equal to $-q_m$. If the partially discharged atoms of the adsorbed metal layer are reduced before the oxidation, then the charge required for oxidation ($-q_{mF}$) is equal to

$$-dq_{mF} = -zF\, d\Gamma_{ad} \tag{11}$$

where z is the Faraday or Nernst valency. Considering the negative sign of q_m, the quotient of eqns. (10) and (11) is:

$$dq_m/dq_{mF} = \gamma/z \qquad (12)$$

It must, however, be underlined that the calculation of γ via eqn. (12) is based upon the assumption that not only does the reduction take place, but also there is no loss of the adsorbed metal atoms during the required experimental manipulation.

On the basis of eqn. (12), γ was determined in the following way. The platinum electrode was polarized at 0.5 V in 0.2 M HCl and 4×10^{-3} M $CuCl_2$ for 60 min, and then the charging curve of this electrode was determined in the supporting electrolyte (curve 1, Fig. 3). The experiment was then repeated so that the electrode was saturated with hydrogen before the determination of the charging curve (curve 2, Fig. 3). The copper region of curve 1 was taken as q_m and that of curve 2 as q_{mF}. Thus γ was calculated to be 1.7. For all experiments in which γ was measured the result was found to lie reproducibly in the range 1.7—1.8, which is in agreement with the results of published experiments [7,10], although the double layer capacity was not taken into account.

In the calculation of electrosorption valency the data of Fig. 1 can also be used. Since there is no difference between the copper regions of curves 2 and 3, γ = 2. Secondary processes, however, might change the adsorbed layer in this case. For this reason the experiment was repeated in 0.2 M HCl with the difference that the adsorption processes were interrupted between 0.4 and 0.5 V by

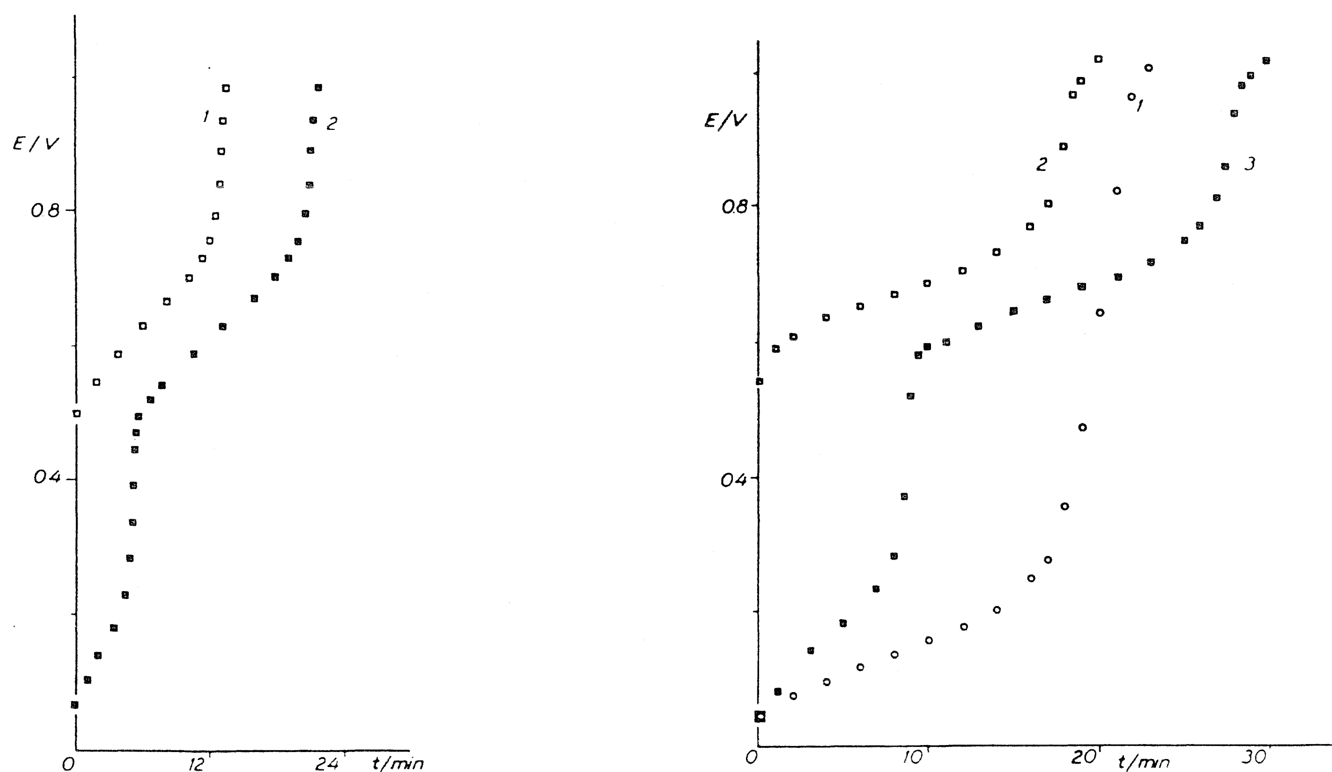

Fig. 3. I = 0.25 mA. (1) Charging curve of the electrode covered with copper at 0.5 V; (2) charging curve of the copper-covered electrode, after saturation with hydrogen in the supporting electrolyte.

Fig. 4. I = 0.25 mA. (1) Charging curve in 0.2 M HCl; (2) charging curve of the copper-covered electrode in supporting electrolyte; (3) charging curve of the copper-covered electrode in supporting electrolyte after saturation with hydrogen.

removing the copper solution. The result is illustrated in Fig. 4. The value of γ was 1.9. Generally, the results of repeated experiments were very near to $\gamma = 2$, meaning that the adsorbed copper atoms could not be further reduced. The same result was obtained in a 1.0 *M* HCl solution.

It follows from the previous experimental results that secondary processes have to be taken into consideration when an electrode covered with adsorbed metal is used for some other experimental purpose.

REFERENCES

1 F. Hine and K. Yamakawa, Electrochim. Acta, 13 (1968) 2119.
2 G. Horanyi, J. Solt and F. Nagy, J. Electroanal. Chem., 31 (1971) 95.
3 G. Horanyi and G. Vertes, J. Electroanal. Chem., 45 (1973) 295.
4 S. Szabo and F. Nagy, J. Electroanal. Chem., 70 (1976) 357.
5 B.J. Bowles, Electrochim. Acta, 15 (1970) 589.
6 L. Kiss, J. Farkas and A. Korosi, Magy. Kem. Folyoirat, 76 (1970) 569.
7 J.W. Schultze, Ber. Bunsenges. Phys. Chem., 74 (1970) 705.
8 J.W. Schultze and K.J. Vetter, J. Electroanal. Chem., 44 (1973) 63.
9 K.J. Vetter and J.W. Schultze, J. Electroanal. Chem., 53 (1974) 67.
10 G. Horanyi, J. Electroanal. Chem., 55 (1974) 45.

J. Electroanal. Chem., 87 (1978) 261—265
© Elsevier Sequoia S.A., Lausanne — Printed in The Netherlands

5.

INVESTIGATIONS OF BISMUTH ADSORPTION VIA THE IONIZATION OF HYDROGEN ADSORBED ON PLATINIZED PLATINUM IN HYDROCHLORIC ACID SOLUTIONS

S. SZABO and F. NAGY

Central Research Institute for Chemistry, Hungarian Academy of Sciences, H-1525/17 Budapest (Hungary)

(Received 16th September 1976; in revised form 22nd March 1977)

ABSTRACT

The formation of an adsorbed bismuth layer via the ionization of hydrogen adsorbed on platinized platinum in HCl media is described. Not only bulk bismuth but also adsorbed BiO can act as intermediates. The electrosorption valency (γ) of a potentiostatically-formed adsorbed bismuth layer is calculated to be 2.85.

Previous studies have described the adsorption of bismuth on platinum in various media, but with somewhat different results [1—4]. In particular, it is clear that results obtained in perchloric acid solutions may not be extended to hydrochloric acid solutions; specific adsorption and complex formation effects associated with the chloride ion preclude this possibility. For these reasons, we have studied the adsorption of Bi on Pt in 1.0 *M* in detail, as part of a general scheme dealing with metal adsorption [4].

EXPERIMENTAL

The apparatus and general method have been described previously [4]. Because of the hydrolysis of bismuth salts, however, the cell was always rinsed in situ with deoxygenated 1.0 *M* HCl supporting electrolyte rather than distilled water.

Bi^{3+} solutions were prepared by dissolving Bi_2O_3 in HCl. Their bulk concentration during deposition was 1.6×10^{-3} *M*.

All electrode potentials are referred to that of the hydrogen electrode in the same solution.

RESULTS AND DISCUSSION

Deposition of bismuth

After the determination of the charging curve of the Pt electrode in 1.0 *M* HCl (curve 1 in Fig. 1), its surface was saturated with hydrogen and Bi^{3+} ions were introduced at 0.04 V. The introduction of the Bi^{3+} ions caused the poten-

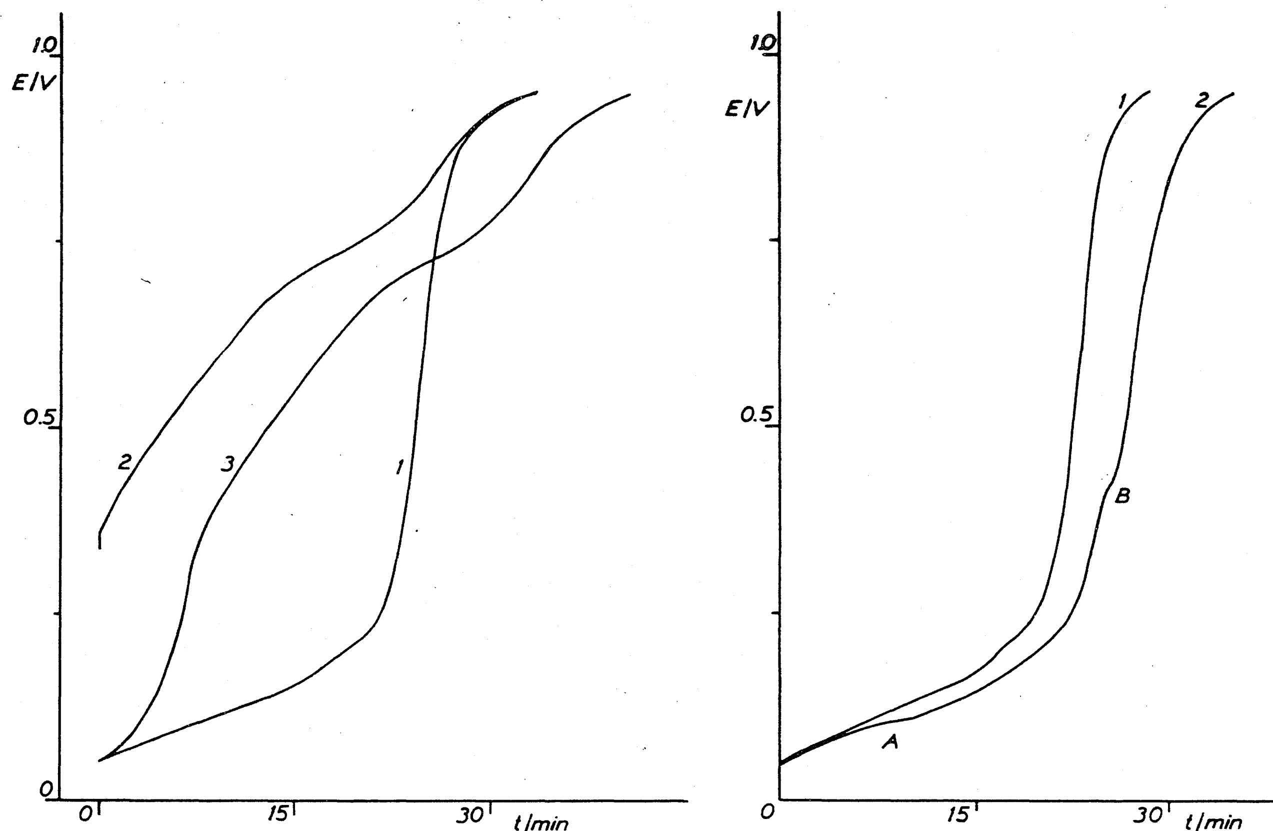

Fig. 1. I = 0.25 mA. (a) Charging curve of the Pt electrode in 1.0 M HCl, (2) Charging curve of the electrode covered with Bi_{ads} in solution containing the depositing Bi^{3+} ions, and (3) in 1.0 M HCl supporting electrolyte.

Fig. 2. I = 0.5 mA.(1) Charging curve of the Pt electrode in 1.0 M HCl, (2) Charging curve of the electrode in 1.0 M HCl when the processes of the formation of adsorbed monolayer were interrupted at 0.1 V.

tial to shift to +0.35 V. After reaching equilibrium, the charging curve of the Pt electrode was then re-determined (curve 2 in Fig. 1). The convergence of curves 1 and 2 clearly indicates that the adsorbed hydrogen has been replaced by bismuth without any net loss of charge.

The experiment was then repeated in the same way, but following the formation of the adsorbed Bi layer (Bi_{ads}) the Bi^{3+}-containing solution was removed from the cell, which was then rinsed and filled with deoxygenated 1.0 M HCl. Subsequent saturation with hydrogen allowed the charging curve of the electrode to be recorded, and this is shown as curve 3 in Fig. 1.

Site demand of one adsorbed bismuth atom

The number of hydrogen adsorption sites occupied by one adsorbed bismuth atom may be readily determined [4]. Denoting the site demand by S, we obtain from the data of Fig. 1 $S \approx 2$ since $Q_M = Q_H$.

This result is in good agreement with published data [2—4]. Beside the obvious undervoltage values, this result also indicates the formation of adsorbed metal layer of the same character as that prepared by electrochemical methods [2].

Mechanism of the formation of the adsorbed bismuth layer

When the bismuth adsorption processes were interrupted at 0.1 V by the removal of the solution containing Bi^{3+} ions, the charging curve in Fig. 2 was obtained in pure 1.0 *M* HCl. It can be seen from the curve that almost as much hydrogen was adsorbed on the platinum as without Bi deposition, so that no Bi_{ads} was formed in this case. The only observable difference is the appearance of two small waves at ~0.1 V and ~0.4 V.

Because the standard potential of the $Bi + 4Cl^- \rightleftharpoons BiCl_4^- + 3\,e$ equilibrium is +0.168 V we conclude that region A simple corresponds to the oxidation of bulk bismuth.

The explanation of the appearance of region B may be found in Bowles' paper [2]. According to his investigations, the formation of adsorbed BiO can be observed in 0.1 *M* HCl solution at 0.4 V. In spite of the use of 1.0 *M* HCl supporting electrolyte in the present work, the very similar oxidation potentials suggest that region B may also be attributed to the oxidation of adsorbed BiO, because no adsorbed Bi species oxidized at this potential [2].

When the processes of formation of Bi_{ads} at 0.115 V were interrupted, curve 2 in Fig. 3 could be obtained in pure 1.0 *M* HCl. The wave at ~0.4 V is better defined in this instance, no bulk form is present (no wave at 0.1 V), and the formation of the adsorbed species can be seen to have begun.

Since the adsorbed hydrogen is replaced by Bi_{ads} without any net loss of charge, and the different adsorbed species are ionized at more positive potentials than that adsorbed BiO also ionized and Bi_{ads} formed as a consequence.

From the experimental results it may be concluded that up to ~0.1 V, the ionization of adsorbed hydrogen is accompanied by the bulk deposition of Bi and the formation of BiO_{ads}:

$$H_a \rightarrow H^+ + e \qquad (1)$$

$$Bi^{3+} + 3\,e \rightarrow Bi_{bulk} \qquad (2)$$

$$BiO^+ + e \rightarrow BiO_{ads} \qquad (3)$$

Above ~0.1 V, the formation of adsorbed BiO accelerates, the Bi_{bulk} is ionized and the formation of Bi_{ads} begins.(The ionization of the adsorbed hydrogen continues, of course.)

$$Bi_{bulk} \rightarrow Bi^{3+} + 3\,e \qquad (4)$$

$$Bi^{3+} + 3\,e \rightarrow Bi_{ads} \qquad (5)$$

The final step in the formation of Bi_{ads} is the ionization of the remaining hydrogen and also of BiO_{ads}:

$$BiO_{ads} \rightarrow BiO^+ + e \qquad (6)$$

The electrons produced in (1), (4) and (6) are consumed in process (5), either directly or via the interventation of processes (2) and (3). Bi_{ads} results.

From the above considerations we conclude that in the formation of Bi_{ads}, not only Bi_{bulk} but also BiO_{ads} can be intermediates

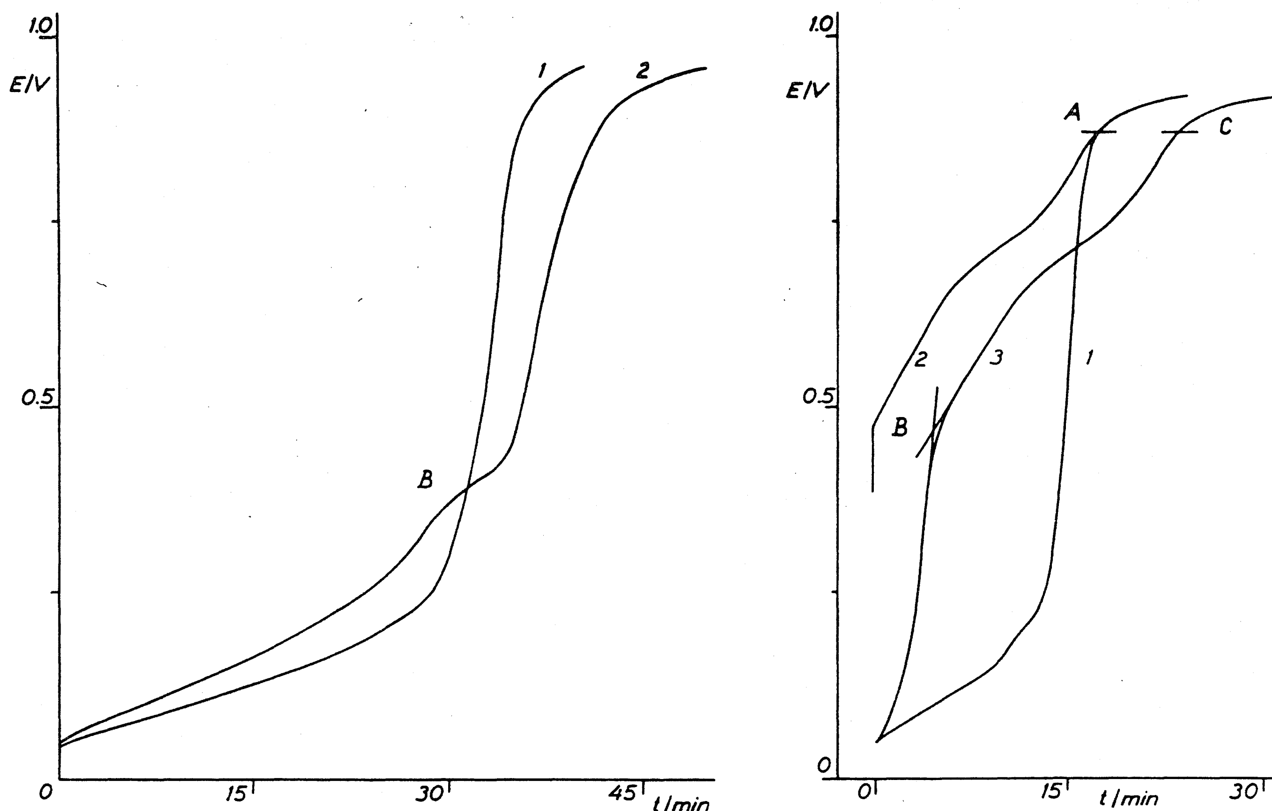

Fig. 3. I = 0.3 mA. (1) Charging curve of the Pt electrode in 1.0 M HCl, (2) Charging curve of the electrode in 1.0 M HCl when the processes of the formation of adsorbed monolayer were interrupted at 0.115 V.

Fig. 4. I = 0.25 mA. (1) Charging curve of the Pt electrode in 1.0 M HCl, (2) Charging curve of the electrode covered with Bi_{ads} in 1.0 M HCl, (3) Charging curve of the electrode covered with Bi_{ads} in 1.0 M HCl after saturation with hydrogen.

Determination of the electrosorption valency of the adsorbed bismuth layer

With the help of the relationships deduced in our previous paper [5], the electrosorption valency (γ) or formal charge transfer coefficient [6,7] of the adsorbed bismuth layer was also determined.

The charging curve of the Pt electrode was first determined in 1.0 M HCl (curve 1 in Fig. 4), then Bi^{3+} ions were introduced and the electrode polarized for 60 min at 0.4 V. After this treatment the solution was replaced by deoxygenated 1.0 M HCl and the charging curve re-determined (curve 2 in Fig. 4). The experiment was then repeated after the electrode had been saturated with hydrogen (curve 3 in Fig. 4).

Since the bismuth region of curve 2 (the region up to A) can be taken as q_m and the bismuth region of curve 3 (region BC) as q_{m_F}, the value of γ can be determined since [5]:

$$dq_m/dq_{m_F} = \gamma/z \qquad (7)$$

The result is than that γ = 2.85. This value is in close agreement with the data published recenly by Schultze and Koppitz [8].

REFERENCE

1 F. Mikuni and T. Takamura, Denki Kagaku, 39 (1971) 579.
2 B.J. Bowles, Electrohim. Acta, 15 (1970) 737.
3 S.H. Cadle and S. Bruckenstein, Anal. Chem., 44 (1972) 1993.
4 S. Szabo and F. Nagy, J. Electroanal. Chem., 70 (1976) 357.
5 S. Szabo and F. Nagy, J. Electroanal. Chem., 84 (1977) 93.
6 J.W. Schultze and K.J. Vetter, J. Electroanal. Chem., 44 (1973) 63.
7 A. Frumkin, B. Damaskin and O. Petrii, J. Electroanal. Chem., 53 (1974) 57.
8 J.W. Schultze and F.D. Koppitz, Electrochim. Acta, 21 (1976) 327.

J. Electroanal. Chem., 88 (1978) 259–264

© Elsevier Sequoia S.A., Lausanne – Printed in The Netherlands

6.

THE EFFECT OF MEDIA ON THE ADSORPTION OF BISMUTH ON PLATINUM

S. SZABO and F. NAGY

Central Research Institute for Chemistry, Hungarian Academy of Sciences, H-1525/17 Budapest (Hungary)

(Received 27th September 1976; in revised form 16th May 1977)

ABSTRACT

It has been shown that the distortion of the charging curve of a Pt electrode after Bi adsorption in $HClO_4$ solution is caused by irreversible adsorbed Bi which desorbs in HCl. At low coverages, adsorbed Bi atoms occupy three former hydrogen adsorption sites. The electrosorption valency in $HClO_4$ of an adsorbed Bi layer formed in HCl is $\gamma \approx 2.3$. The existence of a BiCl surface radical is assumed.

A number of papers have considered bismuth adsorption on platinum [1–5]. It has been observed that once bismuth adsorption has taken place on a platinum electrode in $HClO_4$ media, then the charging curve characteristic of the bismuth-free surface can no longer be reproduced [2–4]. No such observation has been reported in the case of HCl media [1,5]. This indicates that the medium plays a more significant role in bismuth adsorption on platinum than hitherto supposed.

The aim of the present work was to investigate this problem. For this purpose adsorbed metal layers were formed on platinized platinum electrodes in HCl media, and their properties subsequently examined both in HCl and $HClO_4$ acid media.

EXPERIMENTAL

The cell and the method were the same as those used to investigate the adsorption of other metals on platinum [4]. 1.0 *M* HCl and 1.0 *M* $HClO_4$ were used as supporting electrolytes. Bi^{3+} solutions were prepared by dissolving Bi_2O_3 in HCl. Their bulk concentration during the formation of the adsorbed monolayer was 1.6×10^{-3} *M*.

All electrode potentials are referred to that of the hydrogen electrode in the same solution.

When examining the properties of a Pt electrode in $HClO_4$, which had previously been covered with Bi in HCl, the following operations were carried out. After the formation of the adsorbed Bi layer, the cell was rinsed twice with deoxygenated 1.0 *M* HCl in order to avoid interference caused by the hydrolysis of bismuth salts. Following this, the cell was rinsed four times with deoxygenated triply-distilled water, and filled with deoxygenated 1.0 *M* $HClO_4$. The

charging curve of the electrode was then determined. After the determination of the charging curve, the solution was tested for chloride ions with $AgNO_3$ solution, and the charging curve was accepted as valid if the result was negative.

RESULTS AND DISCUSSION

Effect of media on bismuth desorption

To demonstrate the effect of media on the bismuth desorption, an adsorbed Bi layer was formed on a Pt electrode by polarization in the presence of Bi^{3+} ions at 0.3 V for 60 min in HCl. After this pretreatment the charging curve was determined, in one case in pure 1.0 *M* HCl (curve 1 in Fig. 1), and in the other case in pure 1.0 *M* $HClO_4$ (curve 3 in Fig. 1).

In both cases, the bismuth desorption was followed by the determination of the charging curve of the electrode in 1.0 *M* $HClO_4$. Since the two experiments were made on the same electrode in succession, curves 2 and 4 should be the same. The difference demonstrates the distortion mentioned in refs. 2—4.

The next question was whether the charging curve of the Pt electrode covered with Bi in 1.0 *M* HCl was changed if the electrode was saturated with hydrogen in pure 1.0 *M* $HClO_4$, and the charging curve determined in 1.0 *M* HCl afterwards.

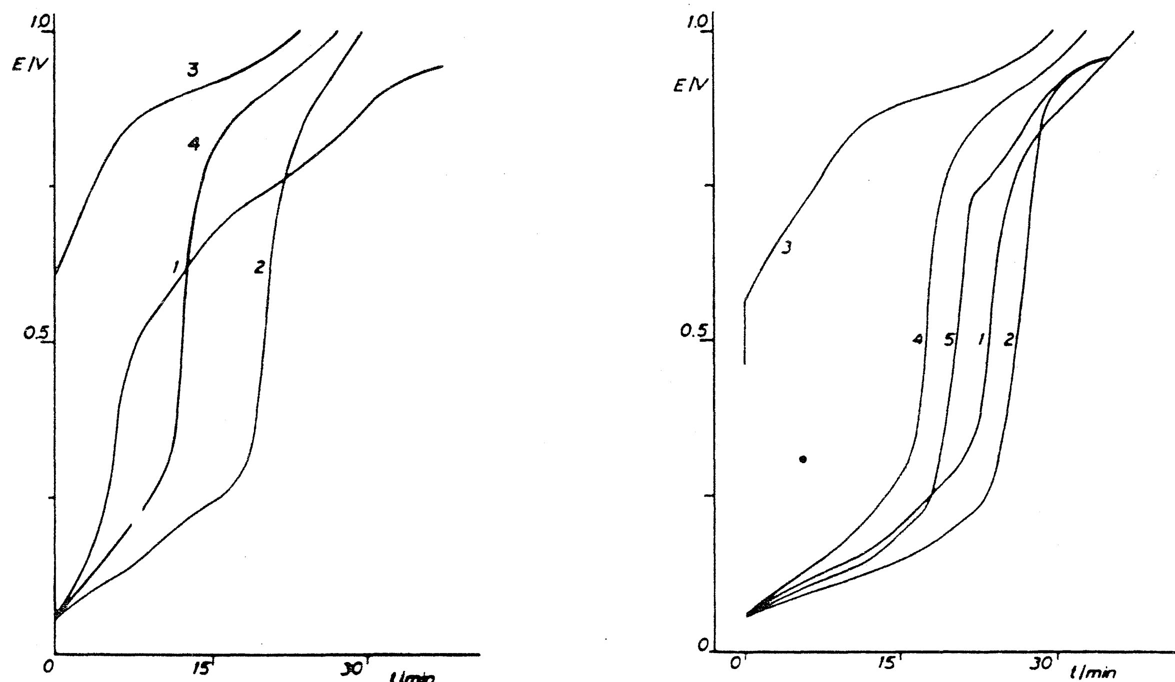

Fig. 1. I = 0.25 mA. (1) Charging curve in 1.0 *M* HCl of the Pt electrode covered with Bi. (2) Charging curve in 1.0 *M* $HClO_4$, after the Bi desorption in 1.0 *M* HCl (curve 1). (3) Charging curve in 1.0 *M* $HClO_4$ of the Pt electrode covered with adsorbed Bi in 1.0 *M* HCl. (4) Charging curve in 1.0 *M* $HClO_4$, after the Bi desorption in 1.0 *M* $HClO_4$ (curve 3).

Fig. 2. I = 0.25 mA. (1) Charging curve of the Pt electrode in 1.0 *M* $HClO_4$, and (2) in 1.0 *M* HCl. (3) Charging curve in 1.0 *M* $HClO_4$ of the Pt electrode covered with adsorbed Bi in 1.0 *M* HCl (desorption of the reversibly adsorbed Bi). (4) Charging curve of the electrode in 1.0 *M* $HClO_4$, after the determination of curve 3. (5) Charging curve in 1.0 *M* HCl, after the determination of curve 4 (desorption of the irreversibly adsorbed Bi).

It turned out that the changes causing the distortion in $HClO_4$ media disappeared in HCl even if they had taken place in Cl^--free conditions. This enables the determination of the amount of Bi causing the distortion of the charging curve in $HClO_4$ solutions.

Determination of the amount of bismuth causing the distortion of the charging curve

The determination was made by means of the experiments illustrated in Fig. 2. The charging curve of the Pt electrode was determined first in 1.0 *M* $HClO_4$ (curve 1), then 1.0 *M* HCl (curve 2) and afterwards adsorbed Bi layer was formed in 1.0 *M* HCl via the ionization of adsorbed hydrogen [5].

After these manipulations the cell was washed free of chloride ions and the charging curve of the bismuth covered electrode was determined in pure 1.0 *M* $HClO_4$ (curve 3). Then the solution was replaced with $HClO_4$ and the charging curve determined again (curve 4).

The determination of curve 4 was followed by polarization to a potential more negative than 0.5 V, in order to reduce adsorbed oxygen. The cell was then filled with deoxygenated 1.0 *M* HCl and the charging curve was determined again (curve 5).

The amount of Bi causing the distortion of the charging curve is given by the difference of curve 2 and 5, because after the determination of curve 5 the original charging curve could be reproduced both in pure 1.0 *M* HCl and in 1.0 *M* $HClO_4$. Therefore no adsorbed Bi remained on the surface.

It can also be seen from curves 2 and 5 that the site demand of adsorbed Bi at such low coverages is not 2 but almost 3, since the two curves converge.

Site demand at low coverage

The result of the above experiments led us to a separate experiment in order to determine the site demand of the adsorbed Bi atoms at low coverage. For this purpose the potential of the Pt electrode was set to 0.2 V in 1.0 *M* HCl, then Bi^{3+} ions were introduced. This caused a potential shift to 0.71 V, and hence only the quantity of Bi corresponding to the 0.2–0.71 V potential region was adsorbed. The charging curve after Bi adsorption in pure 1.0 *M* HCl is curve 2 in Fig. 3.

It follows from the Figure that at this coverage the site demand is ~ 3, since the two curves converge after Bi desorption.

It was found that a further decrease in coverage did not alter the site demand.

On the reasons for the distortion of the charging curve

The distortion of the charging curve could be caused by the rapid adsorption of bismuth, or else by the adsorption of Bi^{3+} ions on oxidized platinum surface, according to refs. 2 and 3.

The investigations with constant-current charging curves have shown that the first assumption is quite improbable.

The hypothesis of the adsorption of Bi^{3+} ions was tested in the following way.

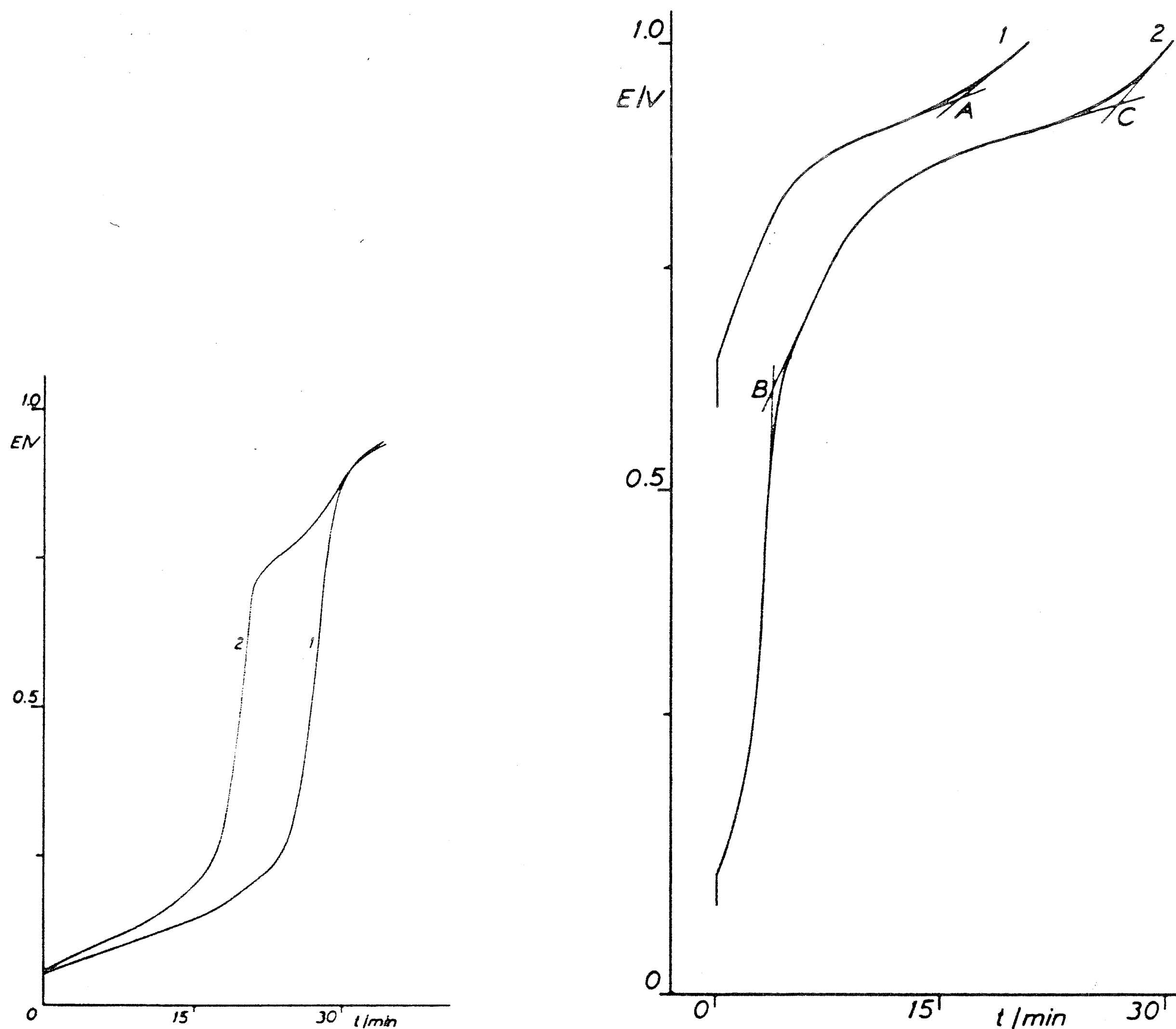

Fig. 3. I = 0.25 mA. (1) Charging curve of the Pt electrode in 1.0 M HCl. (2) Charging curve in 1.0 M HCl of the electrode covered with the quantity of Bi corresponding to 0.2—0.71 V potential region.

Fig. 4. I = 0.2 mA. Charging curve in 1.0 M $HClO_4$ of the Pt electrode covered with Bi in HCl at 0.3 V without saturation with hydrogen (curve 1) and after saturation with hydrogen (curve 2).

After determining the charging curve of a Pt electrode in 1.0 M $HClO_4$ the potential of the electrode was set to 1.2 V and Bi^{3+} ions were introduced into the solution. The potential of the electrode was kept at 1.2 V for 120 min, then the charging curve was re-determined in pure 1.0 M $HClO_4$. The difference between the charging curves showed that the amount of bismuth adsorbed at 1.2 V was negligible compared to that remaining on the surface after Bi desorption in $HClO_4$.

On the basis of these results it seems very probable that a fraction of the Bi^{3+} ions formed in the oxidation of adsorbed Bi atoms cannot desorb in $HClO_4$, and the peak or wave appearing at ~ 0.8 V is caused by the oxidation and reduction of this irreversibly adsorbed bismuth. In HCl, since the Bi^{3+} ions formed during the desorption are dissolved as complex ions, the effect does not occur.

Electrosorption valency of the adsorbed Bi layer formed in HCl and determined in $HClO_4$

The basic considerations in these experiments were the same as in our previous paper [6]. The Pt electrode was polarized in 1.0 *M* HCl in the presence of Bi^{3+} ions at 0.3 V for 60 min and the charging curve was determined in 1.0 *M* $HClO_4$ afterwards (curve 1 in Fig. 4). The experiment was then repeated so that the electrode was saturated with hydrogen before the determination of the charging curve (curve 2 in Fig. 4).

The region to A on curve 1 was taken as q_m and region BC on curve 2 as q_{m_F}, the value of γ being given by [6]:

$$dq_m/dq_{m_F} = \gamma/z \tag{1}$$

The result is that $\gamma = 2.3$.

The potentiostatic measurements were repeated in such way that the adsorbed Bi layer was formed via the ionization of hydrogen adsorbed on platinum [5] (Fig. 5). Since the charging curves determined in 1.0 *M* HCl at the beginning of the measurements were identical (curve 1), the region to A on curve 4 in Fig. 5 was taken as q_m and region BC on curve 2 as q_{m_F}. The value of γ from the data of the Figure was $\gamma = 2.4$.

Curve 3 in Fig. 5 illustrates the distortion caused by irreversibly adsorbed bismuth. It was desorbed prior to any experiments by anodic polarization in HCl, in order to provide the same initial conditions in each case.

γ measured by this method differs considerably from that measured in 1.0 *M*

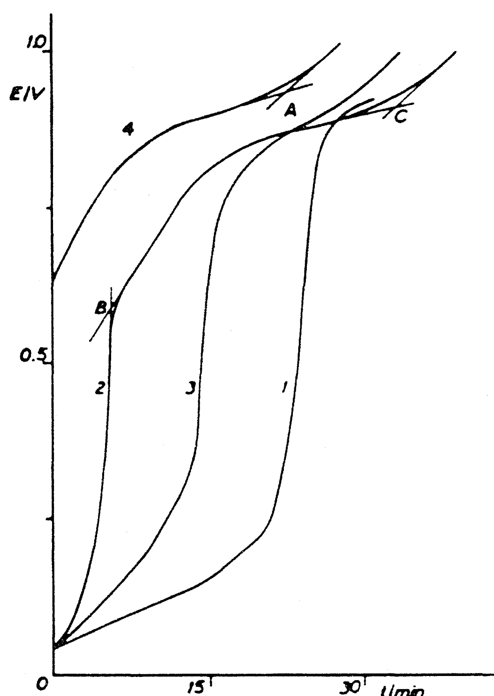

Fig. 5. I = 0.25 mA. (1) Charging curve of the Pt electrode in 1.0 *M* HCl. (2) Charging curve in 1.0 *M* $HClO_4$ of the electrode covered with adsorbed Bi in 1.0 *M* HCl, after saturation with hydrogen. (3) Charging curve in pure 1.0 *M* $HClO_4$, after curve 2. (4) Charging curve in 1.0 *M* $HClO_4$ of the electrode covered with adsorbed Bi in 1.0 *M* HCl, without saturation with hydrogen.

HCl [5], and if this difference is really caused by further reduction of the adsorbed species then the result can be interpreted in the following way.

Interpretation of the results

If the double layer capacity and the oxygen adsorption is also taken into account, then the electrosorption valency in $HClO_4$ is approximately 2, which is equal to the site demand of one adsorbed Bi atom [1,5]. This is not likely to be purely accidental. The same is true in the case of low coverages, the site demand of one adsorbed Bi atom being equal to valence of Bi.

In our opinion, the results can be explained as follows. At low coverages the adsorbed Bi atom gains three electrons and forms bonds with three former hydrogen adsorption sites, resulting in a site demand of $S = 3$.

At higher coverages, however, only two electrons are gained and a BiCl radical is formed on the surface which is indicated by $S \approx 2$.

If the reduction of the BiCl radical can take place in Cl^--free circumstances, then a big difference in electrosorption valency should be observed by our method in different media.

This hypothesis is contradicted by the fact that the site demand in $HClO_4$ is also $S \approx 2$ [4], where the formation of BiCl radical is not possible. This contradiction may be resolved only by assuming that after the reduction in $HClO_4$ of the BiCl radical, the resulting adsorbed Bi atom is also linked to only two former hydrogen adsorption sites.

REFERENCES

1 B.J. Bowles, Electrochim. Acta, 15 (1970) 737.
2 F. Mikuni and T. Takamura, Denki Kagaku, 39 (1971) 579.
3 S.H. Cadle and S. Bruckenstein, Anal. Chem., 44 (1972) 1993.
4 S. Szabo and F. Nagy, J. Electroanal. Chem., 70 (1976) 357.
5 S. Szabo and F. Nagy, J. Electroanal. Chem., 84 (1977) 93.
6 S. Szabo and F. Nagy, J. Electroanal. Chem., 85 (1977) 339.

7.

Deposition of Palladium on Platinum in Hydrochloric Acid Media

S. SZABÓ AND F. NAGY
Central Research Institute for Chemistry, Hungarian Academy of Sciences, P.O. Box 17, H-1525 Budapest, Hungary

(*Received 22 December 1978*)

Abstract. Palladium adsorbed on platinum has been shown to decrease the amount of adsorbed hydrogen because the site requirement of Pd_{ads} is about 1.5 times higher than that of adsorbed hydrogen. Metal adsorption via the ionization of adsorbed hydrogen occurs in two steps: the first leading to bulk deposition. This is followed by bulk ionization and repeated reduction, producing the adsorbed metal layer. The electrosorption valency of the adsorbed Pd layer thus formed is about 1.8. The Pd_{ads} does not desorb in Cl^--free media.

The adsorption of platinum metal on one another has not been extensively studied,[1] although, in addition to its theoretical importance, this process is relevant to the modificatio of various platinum metals. Earlier investigations have revealed that Pd does adsorb on platinum, however, no attempt has been made to clarify the details and processes of metal deposition and adsorption.

This work was aimed at elucidating Pd deposition and adsorption on Pt, as well as at studying the properties of platinum covered with palladium. Another objective was to investigate Pd adsorption occurring via the ionization of hydrogen adsorbed on Pt. Therefore, HCl solutions had to be used despite the specific adsorption and complexing properties of Cl^- ions. In the non-equilibrium experiments, the expected bulk deposit can only be converted to the adsorbed metal at suitable Pd^{2+} concentrations,[2,3] which can only be ensured in HCl solutions.

In the present investigation the principal techniques employed were cyclic voltametry and the determination of charging curves at constant current.

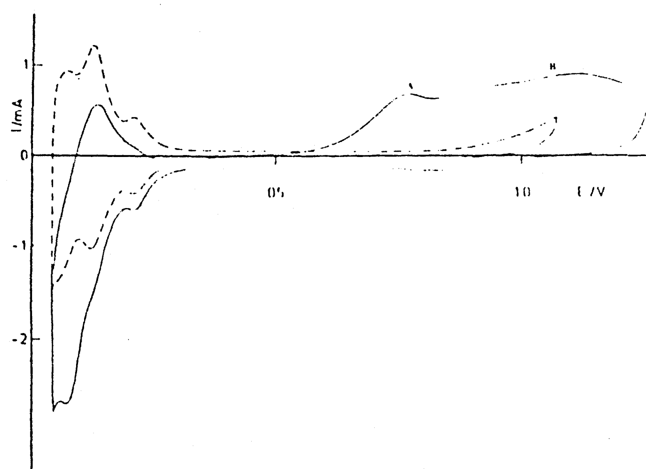

Fig. 1. Cyclic voltamogram of a smooth Pt electrode in the presence of 5×10^{-4} M $PdCl_2$. Sweep rate 0.05 V/s; the dashed line is the voltamogram of the electrode in 1 M HCl.

EXPERIMENTAL

The cell and method used were the same as described in the preceding paper.[1] The solution in the cell could be replaced with the exclusion of the air, which permitted study of the properties of the Pd-covered Pt electrode in the absence of adsorbing ions.

The solutions were prepared from MERCK and ARISTAR reagents with triply distilled water. Oxygen was removed by flushing with purified nitrogen gas. The electrodes were platinized as described earlier.[3] A few experiments were also carried out with a smooth Pt sheet, washing the surface with *aqua regia* till the appearance of the crystal structure.

The sources of constant potential and current were a PAR 170 and a Radelkis instrument, respectively. The potentials were measured against a hydrogen electrode immersed into a solution of the same pH.

When studying the sorption of palladium via the ionization of hydrogen adsorbed on the platinum, the adsorbed metal layer was produced at a $PdCl_2$ concentration of 1.3×10^{-3} M.

RESULTS AND DISCUSSION

Pd Deposition at Underpotentials

A continuous linear sweep of the potential between 1.3 and 0.04 V yielded the steady-state curve shown in Fig. 1. The sweep rate was 0.05 V/s and the solution contained 5×10^{-4} M $PdCl_2$ in 1 M HCl. The experiment was carried out on a stationary, smooth Pt electrode without stirring of the solution.

Comparison of the curve recorded in the pure supporting solution with the one obtained in the presence of Pd^{2+} ions reveals several separate processes. Hydrogen adsorption and desorption, as well as the ionization of deposited Pd can clearly be distinguished. Unlike the case of silver deposition, Pd adsorption, nucleation and the growth of Pd crystals cannot be sharply differentiated on the curve.[4]

Ionization of deposited Pd resulted in a well-defined peak and in a broad region. Without doubt, region B is due to the ionization of adsorbed Pd. Although Fig. 1 seems to indicate that region B is the superposition of two different peaks, this cannot be unambiguously ascertained owing to the lack of support from other experiments. Judging from results obtained with lower sweep rate and higher Pd concentrations (Fig. 2), peak A can only correspond to the ionization of bulk Pd. This is contradicted by the fact that the peak potential is more positive than can be expected from the standard potential (0.623 V) of the reaction $PdCl_4^{2-} + 2e \rightleftharpoons Pd + 4Cl^-$. The explanation for this may be that (i) ionization involves a certain overvoltage, and (ii) the Pd deposited on the first monolayer is also ionized at more positive potentials than the Nernst value, i.e. there is a transitional phase between the bulk and adsorbed phases.

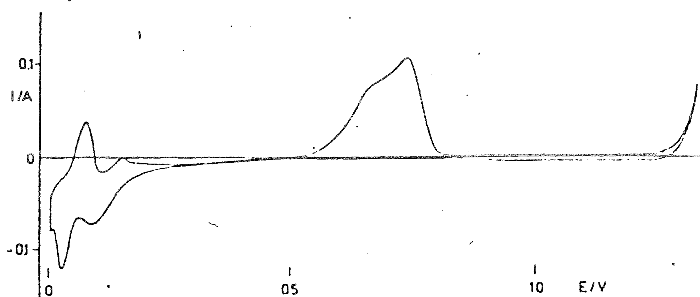

Fig. 2. Cyclic voltamogram of a smooth Pt electrode in the presence of 1.2×10^{-2} M $PdCl_2$. Sweep rate 0.1 V/s.

Pd Deposition at Overpotentials

The experiment described in the preceding section was repeated in the presence of 1.2×10^{-2} M $PdCl_2$ between 1.34 and 0.0 V at a potential sweep rate of 0.1 V/s. The result is shown in Fig. 2, revealing that the amount of adsorbed Pd is negligible relative to the bulk phase. The potential peak corresponding to the $\alpha-\beta$ transition characteristic of the Pd/H system is clearly apparent at about 0.05 V upon adsorption and at about 0.06 V upon desorption of hydrogen.

The most surprising consequence of the change in concentration is that the dissolution of the bulk deposit resulted not in one but in two overlapping peaks, similar to silver deposition.[4] This confirms the view that the reason for the appearance of two peaks should be sought in the nature of the Pt surface.[4] The presence of two, and not more, peaks lends support to the conclusion that adsorption on Pt occurs on the 111 and 100 crystal faces, producing two peaks[5] unless other processes pose an obstacle.[6]

Another surprising feature is the absence of a peak due to crystal nucleation and growth, to be expected at about 0.5 V when changing the potential in the negative direction. As this process corresponds to a well-defined peak in the case of silver under similar conditions,[4] the low rate of diffusion cannot be the reason for its absence.

It is important that the cycles between 1.34 and 0.3 V do not lead to appreciable metal deposition under the conditions used, although this would have been thermodynamically possible.

The above results show that metal deposition occurs primarily in the potential range of 0.3–0.0 V, where the process $H^+ + e \rightarrow H_a$ also takes place. Consequently, adsorbed H atoms are also involved in the reduction, which can thus be separated into two processes:

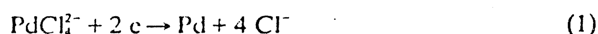

$$PdCl_4^{2-} + 2\,e \rightarrow Pd + 4\,Cl^- \qquad (1)$$

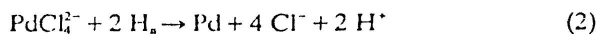

$$PdCl_4^{2-} + 2\,H_a \rightarrow Pd + 4\,Cl^- + 2\,H^+ \qquad (2)$$

According to the above considerations, process (2) should be faster than process (1).

Pd Adsorption via the Ionization of Hydrogen Adsorbed on Platinized Platinum

After the determination of the charging curve in 0.2 M HCl solution (Fig. 3, curve 1), the Pt electrode was resaturated with hydrogen and $PdCl_4^{2-}$ ions were added to the solution at a potential of 0.04 V. As a consequence, the potential of the electrode rose to about 0.7 V, and its charging curve was curve 2 in Fig. 3. The convergence of curves 1 and 2 shows that Pd has deposited on the surface in an amount equivalent to the adsorbed hydrogen.

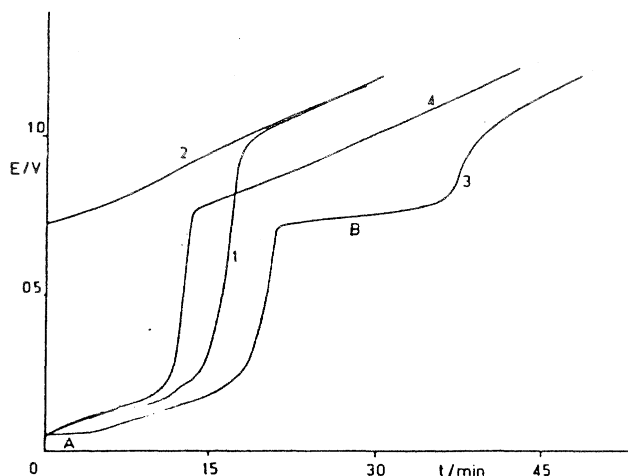

Fig. 3. (I = 0.5 mA) 1 — Charging curve of Pt electrode in 0.2 M HCl; 2 — Charging curve of a Pd-covered electrode after metal deposition; 3 — Charging curve of the electrode covered with Pd_{bulk} in 0.2 M HCl; 4 — Charging curve of the electrode covered with Pd_{ads} in 0.2 M HCl.

The experiment was subsequently repeated, interrupting metal deposition at about 0.65 V by removing the $PdCl_4^{2-}$ solution from the cell, washing three times with deoxygenated distilled water and refilling with deoxygenated supporting solution. After saturation with hydrogen, charging curve 3 in Fig. 3 was obtained. When washing and refilling took place after the metal deposition equilibrium had been reached, charging curve 4 was recorded.

The comparison of curves 3 and 4 clearly indicates that after metal deposition, further processes occur in the potential range of 0.65–0.70 V. In order to understand the nature of these processes, it is necessary to clarify the origin of sections A and B on curve 3. Since the potential of section A (about 0.06 V) is characteristic of hydrogen desorption from metallic Pd, bulk palladium must have deposited on the surface. Consequently, section B must be due to the ionization of bulk palladium. The occurrence of bulk deposition is proved also by the fact that up to section B the hydrogen and double-layer sections of curves 1 and 3 differ only in section A.

It follows from the above that curve 4 is the charging curve of Pt covered with adsorbed Pd. This is also supported by the appearance of a section attributable to Pd ionizing at a more positive potential, which replaces section A. The formation of an adsorbed metal layer proves that the amount of hydrogen adsorbed on the Pt electrode has also changed, as manifested by the differeng hydrogen sections of curves 1 and 4.

Mechanism of Formation of the Adsorbed Layer

The experimental results described in the preceding paragraph permit us to conclude that the first step in the formation of an adsorbed metal layer is:

$$PdCl_4^{2-} + 2\,e \rightarrow Pd_{bulk} + 4\,Cl^- \qquad (3)$$

$$H_a \rightarrow H^+ + e \qquad (4)$$

However, in the presence of $PdCl_4^{2-}$ ions, bulk deposition is followed by the spontaneous formation of an adsorbed palladium layer with simultaneous ionization of Pd_{bulk}.

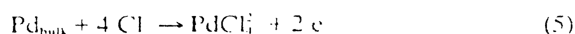

$$Pd_{bulk} + 4\,Cl^- \rightarrow PdCl_4^{2-} + 2\,e \qquad (5)$$

$$PdCl_4^{2-} + 2\,e \rightarrow Pd_{ads} + 4\,Cl^- \quad (6)$$

Our experience indicates that, under non-equilibrium conditions bulk deposition should always be reckoned with if it is thermodynamically possible.[5,7] Since opinions vary on this point,[2,3,7] we now wish to define the kinetic conditions that necessarily lead to bulk deposition.

If the potential of a Pt electrode is scanned to a more negative potential than the Nernst potential of a Me/Me^{n+} system, then the following processes occur:

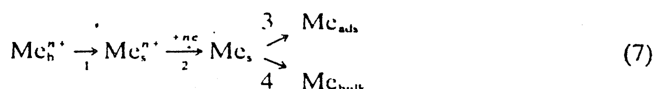

$$Me_b^{n+} \xrightarrow{1} Me_s^{n+} \xrightarrow[2]{+ne} Me_s \begin{array}{l} \xrightarrow{3} Me_{ads} \\ \xrightarrow{4} Me_{bulk} \end{array} \quad (7)$$

where process 1 is metal ion diffusion to the surface, process 2 is charge transfer, process 3 is metal adsorption and process 4 is bulk deposition. Assuming that the charge transfer has the highest reaction rate, the rate-determining step may be either diffusion, or adsorption and bulk deposition, i.e.

$$r_1 = r_3 + r_4 \quad (8)$$

According to the experimental observations, adsorption has always preceded bulk deposition (2), therefore, initially $r_3 > r_4$. However, the rate of adsorption is a function of the coverage, consequently, bulk deposition should begin if $r_1 \geqq r_3$. Of course the r_3 and r_4 ratio depends strongly on the surface roughness.[2,3]

Site Requirement of an Adsorbed Pd Atom

Figure 3 shows that Pd adsorption decreases the amount of hydrogen adsorbed on Pt. This can be used for calculating the surface area required by an adsorbed Pd atom. For this purpose, the following notations are introduced:

S: number of hydrogen adsorption sites occupied by an adsorbed Pd atom;

Q_H^o: charge required for oxidation of the hydrogen adsorbed on Pt;

Q_H: charge required for oxidation of the hydrogen adsorbed on the electrode after Pd adsorption;

$Q_{H_{Pd}}$: charge required for oxidation of the hydrogen adsorbed on adsorbed Pd atoms, assuming that $H_a/Pd_{ads} \approx 1$;

Q_{Pd}: charge required for oxidation of Pd_{ads};

$Q_{H_{Pt}}$: charge required for oxidation of the hydrogen adsorbed on the free Pt surface.

Evidently, after Pd adsorption

$$Q_H = Q_{H_{Pd}} + Q_{H_{Pt}} \quad (9)$$

Since

$$Q_{H_{Pd}} = 0.5\,Q_{Pd} \quad (10)$$

and

$$Q_{H_{Pt}} = Q_H^o - 0.5\,Q_{Pd}S \quad (11)$$

one obtains from Eqs. (10) and (11) that

$$S = 1 + \frac{2\Delta Q_H}{Q_{Pd}} \quad (12)$$

where $\Delta Q_H = Q_H^o - Q_H$.

From the data in Fig. 3, $S = 1.5$.

Since the site requirement for the adsorption of other metals depends on the coverage,[7,8] this point was also examined. The site requirement is plotted against the coverage in Fig. 4, taking the coverage produced by the ionization of Q_H^o as unity. Apparently, the surface requirement decreases with increasing coverage, but the significant changes observed for Au and Bi adsorption[7,8] are lacking here.

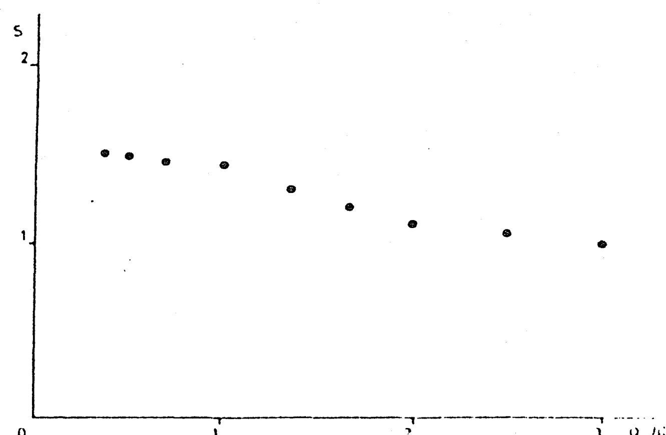

Fig. 4. Site requirement as a function of the coverage.

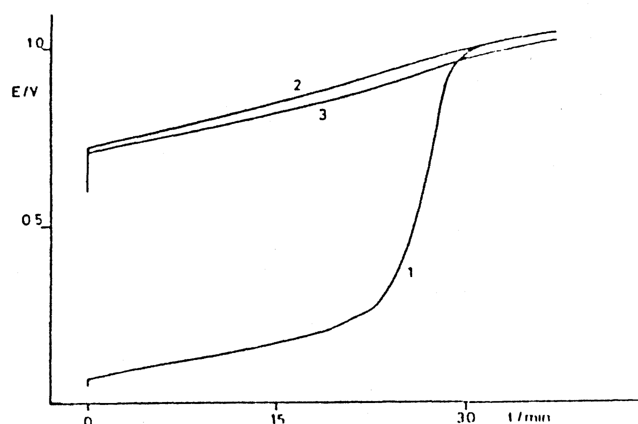

Fig. 5. (I = 0.075 mA) 1 — Charging curve of a Pt electrode in 0.2 M HCl; 2 — Charging curve of the electrode covered with Pd_{ads} in the supporting electrolyte; 3 — Charging curve of the electrode covered with Pd_{ads} in the supporting electrolyte after saturation with hydrogen.

Electrosorption Valency of the Adsorbed Palladium Layer

The electrosorption valency of the adsorbed Pd layer has been determined using the relationship derived in a previous paper.[9] For this purpose, the charging curve of the Pt electrode was first recorded in 0.2 M HCl (Fig. 5, curve 1); then an adsorbed Pd layer was produced via the ionization of the adsorbed hydrogen. The charging curve was again recorded to measure q_m, the charge required for the oxidation of the adsorbed Pd layer (Fig. 5, curve 2). The experiment was then repeated saturating the Pd-covered electrode with hydrogen before measuring q_{m_r}, the charge required for the oxidation of the reduced adsorbed Pd layer (Fig. 5, curve 3); for clarity, the hydrogen section is omitted.

The value of γ can be calculated from Eq. (9):

$$dq_m/dq_{m_r} = \gamma/z. \quad (13)$$

The average result of several measurements gave $\gamma = 1.8$.

Effect of Oxygen Adsorption on Platinum Covered with Adsorbed Palladium

In catalytic and electrocatalytic studies of the catalysts modified by adsorbed metals, it is very important to

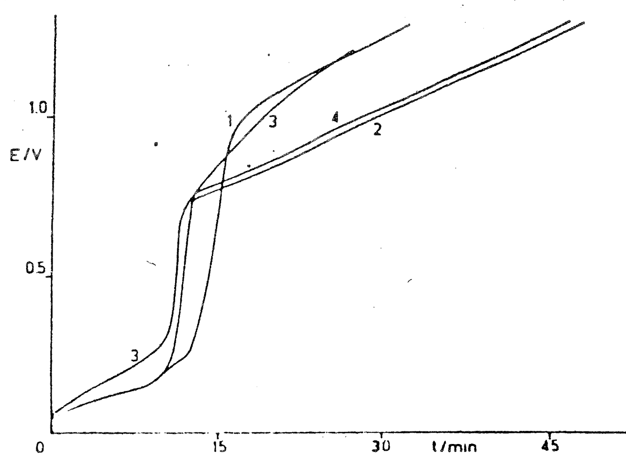

Fig. 6. (I = 0.5 mA) 1 — Charging curve of a Pt electrode in 0.2 M HCl; 2 — Charging curve of the electrode covered with Pd_{ads} in the supporting electrolyte; 3 — Charging curve of the electrode covered with Pd_{ads} in 0.2 M $HClO_4$; 4 — Charging curve in 0.2 M HCl recorded after the preceding curve.

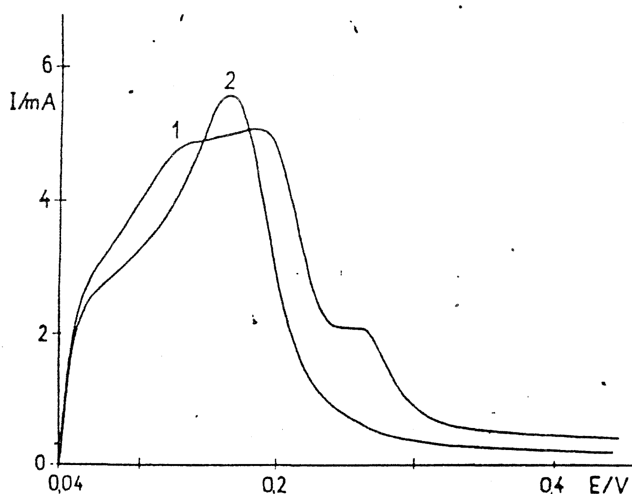

Fig. 7. 1 — Linear voltamogram of a Pt electrode in 0.2 M HCl; 2 — Linear voltamogram of the electrode covered with Pd_{ads} in 0.2 M HCl. Sweep rate 2.7×10^{-3} V/s.

know how oxygen adsorption affects the properties of the catalyst.

According to the figures of this paper, platinum covered with adsorbed Pd is stable in aqueous chloride solutions only up to about 0.72 V. We have studied its stability in the absence of chloride ions similar to the case of Au-covered Pt.[7] The results are shown in Fig. 6. The charging curve of the Pt electrode was first recorded in 0.2 M HCl. After producing an adsorbed Pd Layer, the charging curve was recorded again (Fig. 6, curve 2). After repeated formation of a Pd layer, the charging curve was determined in 0.2 M $HClO_4$ (Fig. 6, curve 3). After this experiment, the electrode was polarized cathodically to about 0.5 V to reduce adsorbed oxygen, then the charging curve was again recorded in 0.2 M HCl (Fig. 6, curve 4).

A comparison of curves 2 and 4 reveals no changes in the properties of the Pt electrode covered with Pd_{ads}, thus it can be used both outside the cell and in electrocatalytic experiments with anodic activation.

Effect of Pd Adsorption on Hydrogen Adsorption

The charging curves recorded at constant current have shown that Pd adsorption decreases the amount of hydrogen adsorbed on the platinum, but the type of hydrogen involved cannot be determined from these data. To elucidate this point, the linear voltamogram of a Pt electrode was first recorded in 0.2 M HCl at a potential sweep rate of 2.7×10^{-3} V/s, then an adsorbed Pd layer was produced and the linear voltamogram determined again (Fig. 7). A comparison of curves 1 and 2 reveals profound changes caused by Pd adsorption in the adsorption of hydrogen, especially in that of the strongly adsorbed form. This is obviously due to the different bonding energy of hydrogen adsorbed on adsorbed palladium.

The adsorbed Pd layer was produced via metal adsorption through the ionization of adsorbed hydrogen, therefore, $Q_{Pd} \approx 0.7$, owing to the relatively large site requirement of Pd_{ads}.

REFERENCES

1. D. A. J. Rand and R. Woods, *J. Electroanal. Chem.*, 44, 83 (1973).
2. N. Furuya and S. Motoo, *J. Electroanal. Chem.*, 72, 165 (1976).
3. S. Szabó and F. Nagy, *J. Electroanal. Chem.*, 70, 357 (1976).
4. R. G. Barradas, S. Fletcher and S. Szabó, *Can. J. Chem.*, 56, 2029 (1978).
5. A. T. Hubbard, R. M. Ishikawa and J. Katekaru, *J. Electroanal. Chem.*, 86, 271 (1978).
6. M. Nakamura and H. Kita, *J. Electroanal. Chem.*, 68, 49 (1976).
7. S. Szabó and F. Nagy, *J. Electroanal. Chem.*, 85, 339 (1977).
8. S. Szabó and F. Nagy, *J. Electroanal. Chem.*, 88, 259 (1978).
9. S. Szabó and F. Nagy, *J. Electroanal. Chem.*, 84, 93 (1977).

J. Electroanal. Chem., 85 (1977) 339—343
© Elsevier Sequoia S.A., Lausanne — Printed in The Netherlands

INVESTIGATIONS OF GOLD ADSORPTION ON PLATINIZED PLATINUM IN HYDROCHLORIC ACID MEDIA

S. SZABO and F. NAGY

Central Research Institute for Chemistry, Hungarian Academy of Sciences, H-1525/17 Budapest (Hungary)

(Received 29th May 1976; in revised form 25th January 1977)

ABSTRACT

Au adsorption via the ionization of adsorbed hydrogen takes place in two steps. The first step is the formation of Au_{bulk}, then the Au_{ads} is formed via the ionization of Au_{bulk}. One adsorbed Au atom occupies 1.25 hydrogen adsorption sites, whilst at low coverages this value rises to 2.5. The Pt covered with Au_{ads} shows a catalytic effect on the oxidation of Cl^- ions. The Au_{ads} does not desorb in Cl^--free media.

In studies of metal adsorption on metals, gold has hitherto played chiefly the role of the base metal [1—3]. The adsorption of gold on other metals has not yet been investigated, apart from an attempt by Cadle and Bruckenstein [4]. Their work offered two basic observations: gold was adsorbed on platinum with no undervoltage and it inhibited hydrogen adsorption.

The aim of the present paper was to develop a more detailed understanding of the properties of a platinum electrode covered with gold.

EXPERIMENTAL

The same method and cell was used as in our previous paper [5]. The main compartment of the cell was continuously flushed with purified N_2. The change of the cell solutions took place with the exclusion of air [5].

All of the charging curves were determined in Au-free supporting electrolyte. The starting point of the curves and the Au deposition was 0.04 V.

The supporting electrolyte was 0.2 *M* HCl, and the concentration of $AuCl_4^-$ ions was 10^{-3} *M*. They were introduced in the form of the $HAuCl_4 \cdot 4\,H_2O$ salt.

The reference electrode was Pt/H_2 in the same solution.

RESULTS

Preparation of platinum surfaces covered with adsorbed gold

Because of the lack of a suitable undervoltage value, our attempts to prepare platinum surfaces covered solely with adsorbed gold by potentiostatic methods were not successful. The bulk (Au_{bulk}) and the adsorbed (Au_{ads}) forms were therefore formed simultaneously and could not be distinguished on the charging curves.

Gold adsorption via the ionization of adsorbed hydrogen (H_a), however, proved a suitable method for the preparation of a Pt surface covered exclusively with Au_{ads}. The procedure was the same as in previous investigations of the adsorption of other metals [5]. The Pt electrode was first saturated with hydrogen, and then under open circuit circumstances gold ions were introduced into the main compartment of the cell. This was followed by the spontaneous formation of a visible Au coating with the simultaneous rise of the potential toward the positive direction. In a few hours, the Au coating further spontaneously transformed into Au_{ads} in the presence of $AuCl_4^-$ ions. The result is illustrated in Fig. 1.

It follows from this Figure that Au_{bulk} did not bring about a change in the amount of H_a because curves 1 and 2 were superposed on the hydrogen and double layer region.

The charging curve of the electrode covered with Au_{ads} (curve 3 in Fig. 1) demonstrates that the amount of H_a was decreased by some other adsorbing species, that is, the surface was really covered with adsorbed gold atoms.

It follows from the experiments that a specific coverage can only be prepared after calculating the charge required for the deposition of gold necessary for the given coverage. After charging the electrode to the calculated extent, then one has to wait at open circuit for the exchange of Au_{bulk} into Au_{ads}.

Site demand of one adsorbed gold atom

Substituting the data of Fig. 1 into the relation published earlier [5], the number of hydrogen adsorption sites (S) occupied by one adsorbed Au atom can be

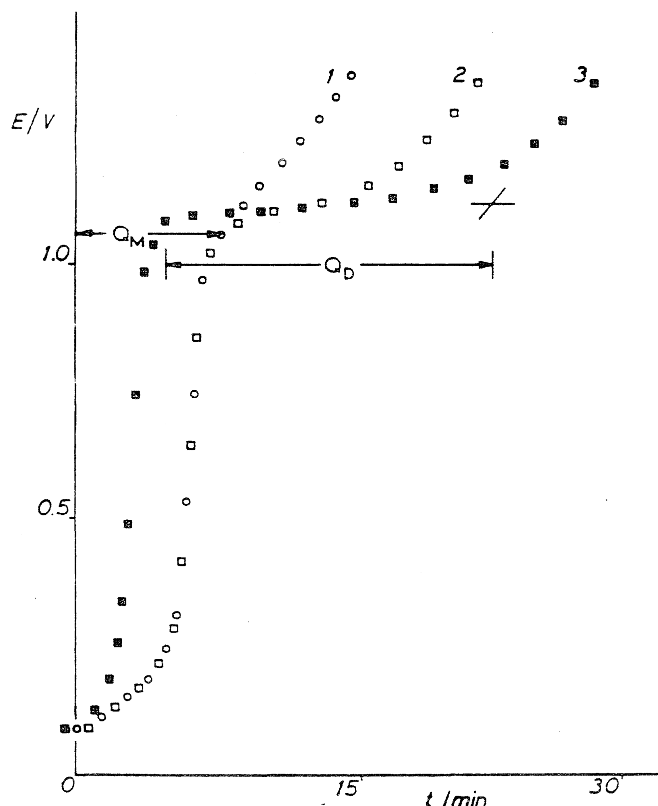

Fig. 1. I = 0.4 mA. (1) Charging curve of the Pt electrode in 0.2 M HCl. Charging curve of the electrode covered with (2) Au_{bulk} and (3) Au_{ads}.

calculated. Since the potential rose to 1.06 V during metal adsorption, Q_M was taken as the value of gold-free charging curve at 1.06 V. Hence

$$S = (6 - 3)/(7.5/3) \approx 1.2 \tag{1}$$

Having taken into account the results of all of our experiments, the average S was determined to be approximately 1.25.

To ascertain the site demand at low coverage the Pt electrode was polarized cathodically to only 0.5 V before the $AuCl_4^-$ ions were introduced. The potential subsequently rose to 1.06 V, and hence only the quantity of Au corresponding to the 0.5—1.06 V potential region was deposited. According to Fig. 2, this small quantity of Au_{ads} brought about a significant change in the hydrogen adsorption. The value of S from Fig. 2. is given by

$$S = (12 - 7)/(6/3) \approx 2.5 \tag{2}$$

Therefore, the site demand of the adsorbed gold atoms depends upon the coverage.

Mechanism of the formation of adsorbed layer

From the results of the experiments illustrated in Fig. 1, it can be concluded that the first step is:

$$\begin{aligned} &AuCl_4^- + 3e \rightarrow Au_{bulk} + 4\,Cl^- \\ &\quad H_a \rightarrow H^+ + e \end{aligned} \tag{3}$$

In the presence of the $AuCl_4^-$ ions, however, the bulk deposition is followed by the spontaneous formation of the adsorbed gold layer, whilst the gold crystals

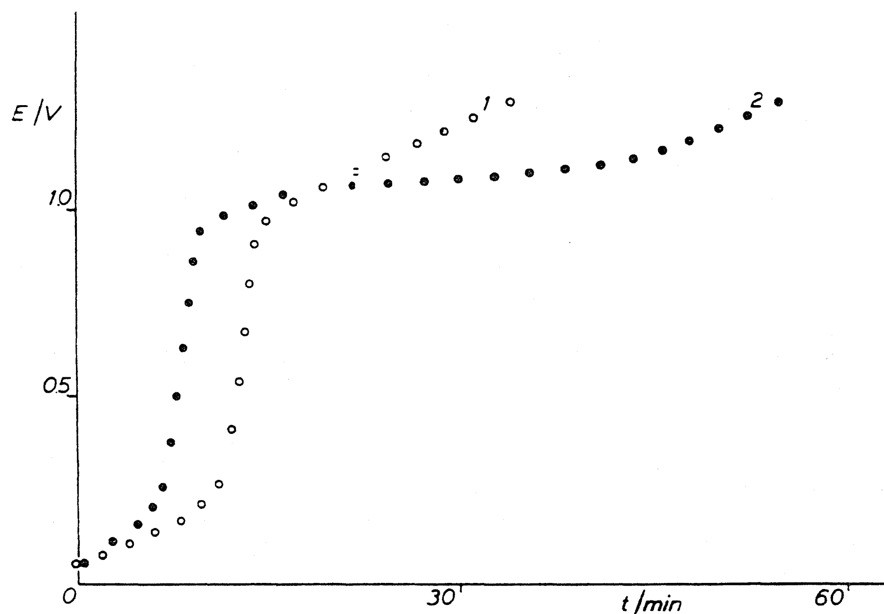

Fig. 2. I = 0.25 mA. (1) Charging curve of the Pt electrode in 0.2 M HCl. (2) Charging curve of the electrode covered with the quantity of Au_{ads} corresponding to the 0.5—1.06 V potential region.

ionized:

$$\begin{aligned} Au_{bulk} + 4\,Cl^- &\rightarrow AuCl_4^- + 3\,e \\ AuCl_4^- + 3\,e &\rightarrow Au_{ads} + 4\,Cl^- \end{aligned} \qquad (4)$$

Anomaly in the charging curve of platinum covered with adsorbed gold

As we have seen during the formation of the adsorbed gold layer a charge of $Q_M = 7.5 \cdot 60 \cdot I$ C was replaced by Au_{ads}, but a charge of $Q_D = 17.5 \cdot 60 \cdot I$ C was required for the oxidation of adsorbed gold atoms (Fig. 1). Since $Q_D/Q_M \approx 2.3$, consequently, beside the oxidation of Au_{ads} some other oxidation process is taking place with about the same rate.

The Pt electrode covered with Au_{ads}, however, shows no anomaly in Cl^--free media (curve 3 in Fig. 3), therefore, some catalytic oxidation of Cl^- ions must be responsible for the observed experimental discrepancy. On the basis of the standard electrode potentials it can be assumed that the $Cl^- + 2\,OH^- \rightarrow ClO^- + H_2O + 2\,e$ reaction takes place because its $E_0 = 0.9$ V.

Effect of oxygen adsorption on platinum covered with adsorbed gold

For the investigation of the stability of Pt electrodes covered with adsorbed gold, the following experiment was carried out. A Pt electrode was covered with Au_{ads} and the charging curve was determined in 0.2 M HCl (curve 2 in Fig. 3). Then the preparation of the gold-covered electrode was repeated in the same way, but the charging curve was determined in 0.2 M $HClO_4$ solution (curve 3 in Fig. 3). (The electrode was polarized to ~1.22 V.)

After this experiment the electrode was polarized cathodically to ~0.5 V, in order to reduce the adsorbed oxygen. Then we went back to the 0.2 M HCl and determined the charging curve again (curve 4 in Fig. 3).

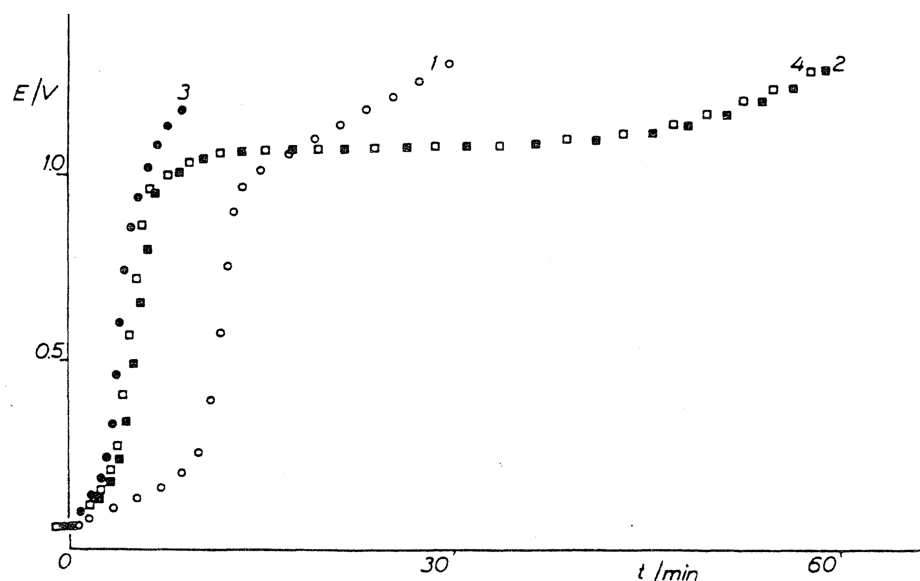

Fig. 3. I = 0.4 mA. (1) Charging curve of the Pt electrode in 0.2 M HCl. Charging curve of the electrode covered with Au_{ads} in (2) 0.2 M HCl, (3) 0.2 M $HClO_4$, and (4) after the polarization in 0.2 M $HClO_4$, charging curve in 0.2 M HCl.

It follows from the Figure that oxygen adsorption did not change the properties of the Pt electrode covered with Au_{ads}, and therefore it can be used outside the cell or can be activated anodically in electrocatalytic experiments. This result is in agreement with the results of published experiments [6].

REFERENCES

1 W.J. Lorenz, H.D. Hermann, N. Wuthrich and F. Hilbert, J. Electrochem. Soc., 121 (1974) 1167.
2 D.M. Kolb, M. Przasnyski and H. Gerischer, J. Electroanal. Chem., 54 (1974) 25.
3 D.A.J. Rand and R. Woods, J. Electroanal. Chem., 44 (1973) 83.
4 S.H. Cadle and S. Bruckenstein, Anal. Chem., 43 (1971) 1858.
5 S. Szabo and F. Nagy, J. Electroanal. Chem., 70 (1976) 357.
6 D.A.J. Rand and R. Woods, J. Electroanal. Chem., 35 (1972) 209.

9.

J. Electroanal. Chem., 230 (1987) 233–240
Elsevier Sequoia S.A., Lausanne – Printed in The Netherlands

INVESTIGATION OF RUTHENIUM DEPOSITION ONTO A PLATINIZED PLATINUM ELECTRODE IN SULFURIC ACID MEDIA

S. SZABÓ and I. BAKOS

Central Research Institute for Chemistry, Hungarian Academy of Sciences, H-1525 Budapest, P.O. Box 17 (Hungary)

(Received 22nd July 1986; in revised form 15th January 1987)

ABSTRACT

Ruthenium deposition onto platinized Pt electrode in 0.5 M H_2SO_4 solution is investigated. The $I-V$ profiles of the Pt electrode covered with Ru depend on the potential of Ru deposition. This phenomenon is explained by the increasing degree of oxidation of the Ru layers deposited at higher potentials. Oxidation of Ru deposited at low potentials begins with comparatively slow processes. A mechanism for Ru deposition via ionization of hydrogen adsorbed on platinized Pt electrode is proposed.

INTRODUCTION

In the past, several papers have been devoted to the investigation of underpotential deposition of noble metals onto noble metal substrates [1–4], but until now no paper has been published on the underpotential deposition of Ru onto a Pt surface. Several papers deal with the electrochemical and electrocatalytic properties of ruthenized Pt electrodes [5–8]. These electrodes can be regarded, however, as Ru electrodes since the electrodeposited Ru layer is thick enough to cover the Pt surface completely.

The only exception is an observation of Watanabe and Motoo [5], who used a Pt electrode covered with Ru adatoms as a Ru/Pt electrocatalyst but failed to study the adsorption of ruthenium onto the Pt surface. Their attempt to calculate ruthenium coverage based on OH^- adsorption is questionable in the light of later results [6–8].

The purpose of our paper is to give an account of the work carried out to describe the spontaneous formation of a ruthenium layer on the surface of a platinized Pt electrode covered with preadsorbed hydrogen. The characteristics of the platinized Pt electrode covered with electrodeposited Ru are also dealt with.

0022-0728/87/$03.50 © 1987 Elsevier Sequoia S.A.

EXPERIMENTAL

All experiments were carried out in the same three-compartment cell described earlier [9]. A characteristic feature of our cell is that cell solutions can be replaced with the exclusion of air. It allows the study of the properties of a Pt electrode covered with deposited metal in the absence of depositing ions.

The 0.5 M H_2SO_4 supporting electrolyte was prepared from Merck reagents with triply distilled water as described earlier [9].

Purified nitrogen was bubbled through the cell to deoxygenate the solutions.

1 g $RuCl_3 \cdot 1\text{–}3\ H_2O$ (Ventron GmbH) was dissolved in 100 cm^3 1 M HCl and this solution was used as a source of Ru ions. The concentration at the beginning of Ru deposition was 0.5–1 mM which, however, never dropped below 0.4 mM in the course of experiments.

It must be taken into consideration, however, in the discussion of the results that the average valence state of ruthenium in this compound is near +4 [10,11].

The polycrystalline platinum electrode was platinized as described previously [9]. Its apparent surface area was ca. 2 cm^2 and the roughness factor was ca. 250.

All potentials are referred to the hydrogen electrode immersed into the same supporting electrolyte in the main compartment of the cell.

RESULTS AND DISCUSSION

Ruthenium deposition via ionization of hydrogen adsorbed on platinized platinum

First the cyclic voltammogram of the Pt electrode was determined in supporting electrolyte (curve 1 in Fig. 1) then the electrode was saturated with hydrogen by

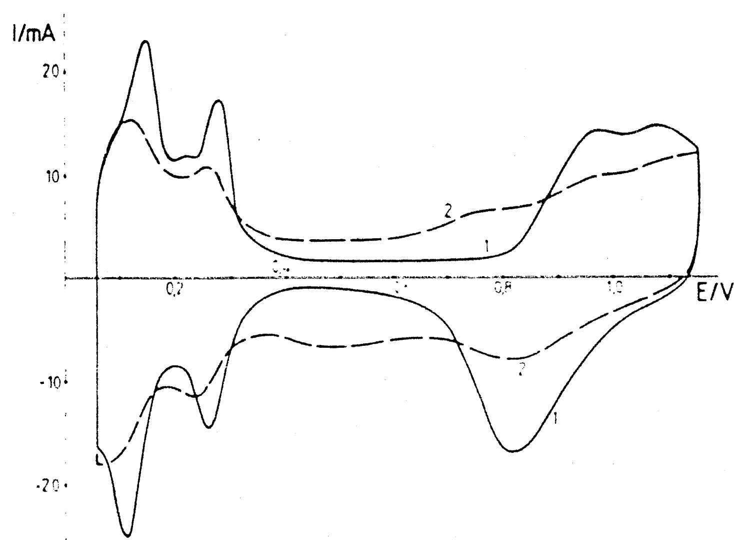

Fig. 1. (1) Voltammogram of Pt electrode in 0.5 M H_2SO_4 solution; (2) voltammogram of Pt electrode covered with ruthenium deposited via the ionization of preadsorbed hydrogen in 0.5 M H_2SO_4 free of ruthenium ions. Sweep rate: 37 mV/s.

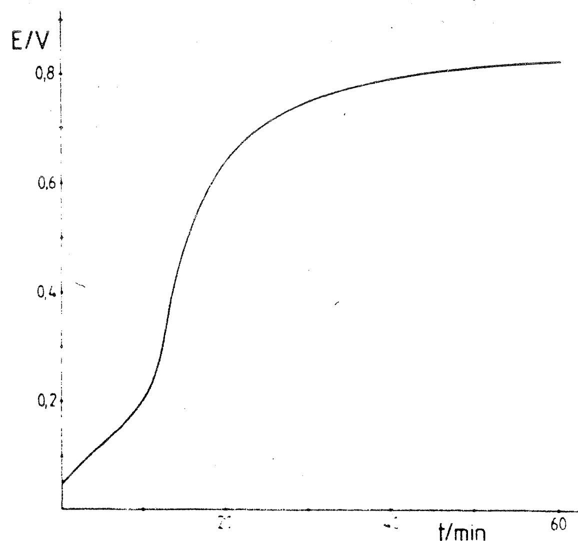

Fig. 2. Variation of electrode potential during the deposition of ruthenium via ionization of hydrogen adsorbed on platinized platinum under open-circuit conditions.

strong cathodic polarization. When, under open-circuit circumstances, the potential reached 0.05 V owing to hydrogen desorption, 0.5 cm^3 of Ru solution was introduced into the main compartment of the cell. It caused a potential shift in the positive direction (Fig. 2). (The amount of charge corresponding to this potential shift from 0.05 to 0.85 V is denoted by $Q°$.)

When equilibrium set in after 60–90 min at about 0.85 V, the cell was rinsed with a deoxygenated supporting electrolyte and then the cyclic voltammogram of the Pt electrode covered with Ru was determined in ruthenium-ion-free supporting electrolyte (curve 2 in Fig. 1).

On the basis of Fig. 1 it may be stated that the deposited Ru inhibits hydrogen adsorption slightly, the double-layer region broadens and the oxygen (OH^-) adsorption character of the Pt is strongly changed. Such a strong effect of metal deposition on the adsorption characteristics of platinized Pt can be explained only by surface processes. It follows from the above, that the deposited Ru must be in the adsorbed state.

A study of the dissolution of ruthenium deposited onto platinized platinum

In the investigation of the electrochemical properties of a ruthenized Pt electrode irreversible oxidation and dissolution of the Ru coating must be taken into consideration [7,8]. In our experience, dissolution of the Ru deposited onto platinized Pt could be detected after 10–15 cycles between potential limits of 0.05 and 1.15 V.

If the upper potential limit of the cyclic voltammetric measurement is high enough, continuous dissolution of the deposited Ru can be observed and finally the initial Pt surface is restored (Fig. 3). In the experiment illustrated in Fig. 3 the Pt electrode was first kept at 0.05 V in the presence of 50 m*M* $RuCl_3 \cdot 1–3\ H_2O$ until a charge of 5 $Q°$ was used for Ru deposition; then the cell was rinsed and refilled

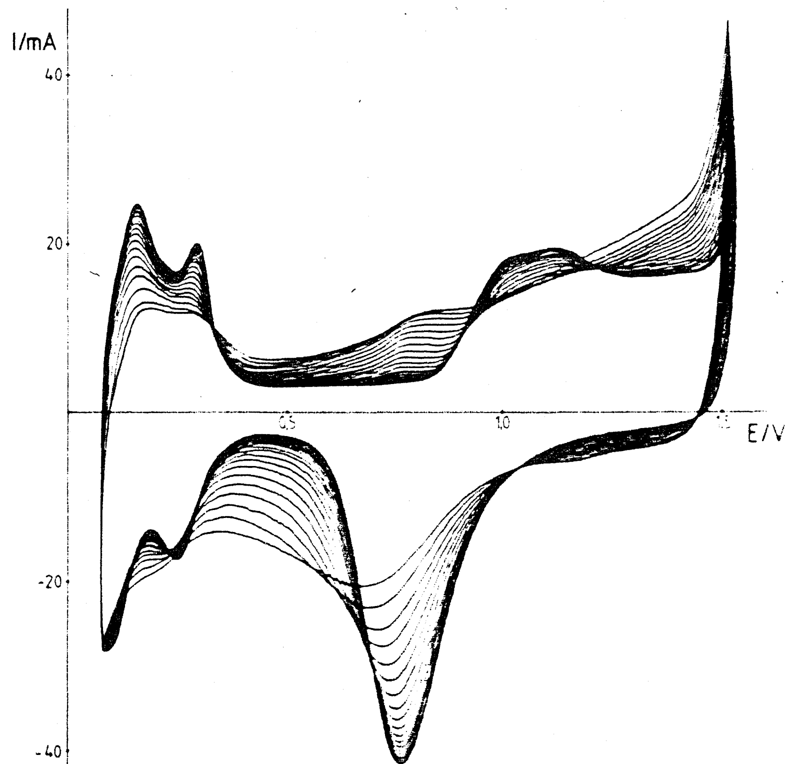

Fig. 3. Dissolution of ruthenium from the Pt surface in 0.5 *M* H_2SO_4 during continuous cycling between potential limits of 0.05 and 1.5 V. Sweep rate: 48 mV/s.

with deoxygenated 0.5 *M* H_2SO_4. After this procedure a cyclic voltammetric measurement was carried out between 0.05 and 1.5 V, the results of which are given in Fig. 3.

Ruthenium deposition at 0.05 V

After determination of the cyclic voltammogram of the Pt electrode (curve 1 in Fig. 4) its potential was scanned to 0.05 V. At this potential 1 ml ruthenium solution was introduced into the main compartment of the cell and ruthenium deposition was continued until a quantity of electricity of 1 Q° was consumed. After this procedure the cell was rinsed and refilled with deoxygenated ruthenium-ion-free supporting electrolyte and then the cyclic voltammogram of the electrode covered with Ru was determined (curve 2 in Fig. 4).

This experiment was repeated, but now the electrode was maintained at 0.05 V until a charge of 4 Q° (curve 3 in Fig. 4) or of 10 Q° (curve 4 in Fig. 4) was consumed for ruthenium deposition.

It should be noted that when a charge of 10 Q° was used for ruthenium deposition, a visible Ru coating was formed on the electrode. In spite of the substantial amount of Ru on the Pt, the two peaks of hydrogen desorption characteristic of Pt were still visible and the amount of hydrogen adsorbed was practically independent of the amount of Ru deposited. From this phenomenon the

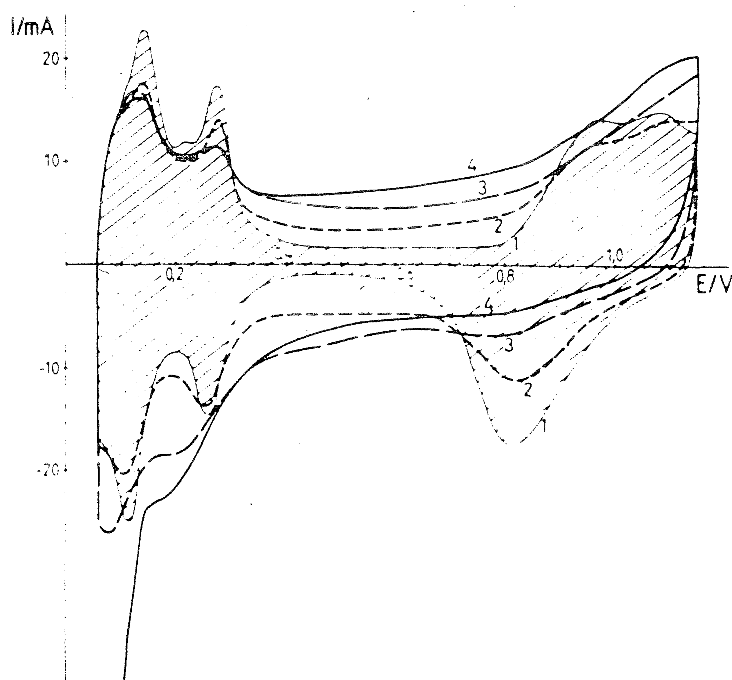

Fig. 4. (1) Voltammogram of Pt electrode in 0.5 *M* H_2SO_4 solution; voltammogram of Pt electrode covered with an amount of Ru $Q°$ (2), 4 $Q°$ (3) and 10 $Q°$ (4) in 0.5 *M* H_2SO_4 supporting electrolyte. Sweep rate: 37 mV/s.

conclusion might be drawn that no adsorbed Ru layer was formed, but merely that a Ru coating was deposited in the form of three-dimensional nuclei in the outer layer of the platinum black substrate.

On the other hand, the oxygen desorption peak typical for Pt gradually disappeared as if Ru adsorption had taken place.

This contradiction might be explained if it is assumed that the presence of Ru nuclei on the Pt surface changed the oxygen adsorption character of the Pt surface free of Ru. An alternative explanation might be that the Ru crystals deposited onto the 100 and 110 crystal faces of polycrystalline Pt in a similar manner as silver and palladium [9,12], covering the Pt surface almost completely, are not uniform in their thermodynamic character, and consequently, hydrogen adsorption on the Ru surface may result in two peaks.

Ruthenium deposition at different potentials

The same amount of Ru was deposited onto a platinized Pt electrode at potentials of 0.00, 0.05, 0.20 and 0.60 V. The potentiostatically deposited Ru coatings were examined in a ruthenium-ion-free supporting electrolyte (Fig. 5).

On the basis of the experimental data it can be stated that the valence state of the Ru coatings deposited between the potential limits of 0 and 0.2 V are almost identical, since the *I–V* profiles are independent of the deposition potential. However, the *I–V* profiles of the electrode covered with Ru above this potential limit are gradually changed. New oxidation reduction peaks appear at ~ 0.75 V in

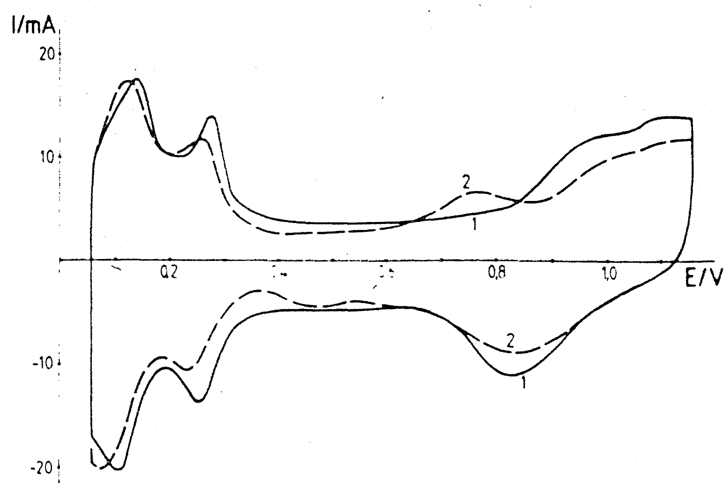

Fig. 5. (1) Voltammogram of Pt electrode covered with an amount of Ru deposited at 0.05 V $Q°$; (2) voltammogram of Pt electrode saturated with Ru at 0.6 V. Sweep rate: 37 mV/s

the oxidation branch and ~ 0.5 V in the reduction branch of the cyclic voltammogram (curve 2 in Fig. 5). With the help of the cyclic voltammogram of a Ru electrode covered with RuO_2 as a result of heat treatment, it could be verified that the peaks are probably due to the formation and reduction of RuO_2 [13].

Short anodization at ~ 1.35 V of a platinized Pt electrode covered with Ru at 0.05 V results in a cyclic voltammogram as if the Ru had been deposited at 0.6 V.

On the basis of the above results, it is clear that the oxidation state of the Ru layers deposited above ~ 0.2 V is gradually increased and the oxidation–reduction process taking place at ~ 0.75 V (and ~ 0.5 V in the negative direction) is preceded by comparatively slow oxidation processes. Products of these slow reactions are oxidized further (and faster) at ~ 0.75 V.

Finally, it must be emphasized that a Ru layer deposited at 0.6 V under these circumstances could not be reduced to the oxidation state characterized by a Ru coating deposited at 0.05 V. This observation verified the above idea about the relatively slow initial oxidation of Ru deposited on platinized Pt at low potentials.

On the mechanism of ruthenium deposition via ionization of hydrogen adsorbed on platinized platinum

On the basis of the above results it may be concluded that the very first stage of the mechanism is Ru deposition with simultaneous ionization of adsorbed hydrogen, consequently shifting the potential in the positive direction. According to our earlier results [3–5], at the beginning (below the Nernst potential) of the spontaneous formation of an adsorbed metal layer, mostly bulk deposition ought to have occurred in the outer layer of the Pt black because the rate-determining step at this stage is diffusion of Ru ions from the bulk of the supporting electrolyte. However, no sharp separation of bulk and underpotential deposition could be experienced

here; therefore, both of them have to be taken into account in the first step of the mechanism:

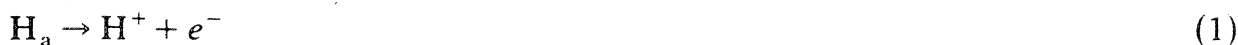

$$H_a \rightarrow H^+ + e^- \quad (1)$$

$$Ru^{n+} + n\,e^- \rightarrow Ru_{bulk} \quad (2)$$

$$Ru^{n+} + n\,e^- \rightarrow Ru_{ads} \quad (3)$$

Comparison of curve 2 in Fig. 1 with curve 2 in Fig. 4 shows that the spontaneous increase of the potential results in some rearrangement [14], and reoxidation of Ru deposited at smaller potentials

$$Ru_{bulk} \rightarrow Ru^{a+} + a\,e^- \quad (4)$$

$$Ru_{ads} \rightarrow Ru^{b}_{ads} + b\,e^- \quad (5)$$

Depending on the actual potential of the electrode, the valency of the ruthenium ions formed by these reactions may be in the range 1–4 because the final value of the spontaneous potential rise (Fig. 2) is in the potential range of RuO_2 formation [8].

Naturally, electrons produced by reactions (4) and (5) are also consumed in additional ruthenium ion deposition, which leads to increased coverage:

$$Ru^{n+} + x\,e^- \rightarrow Ru^{(n-x)+}_{ads} \quad (6)$$

Naturally, in this case also the charge number of the deposited ruthenium ions depends on the electrode potential and might be in the range 1–3.

Considering the standard potentials of different redox processes of ruthenium [8] and the valence state of the ruthenium salt [11] used in the experiments, it is highly improbable that any ruthenium species with a charge higher than 4 takes part in the formation of the adsorbed Ru layer, because catalytic disproportionation was not observed in this case [15].

Taking into account the standard potentials of Ru_2O_3 ($E^\circ = 0.738$ V) and RuO_2 ($E^\circ = 0.937$ V) formation [8], it can be expected that their formation might overlap; therefore, they could be mixed on the Pt surface. It follows that the oxidation peak at ~0.75 V and the reduction peak at ~0.5 V in Fig. 1 can very likely be attributed to the oxidation and reduction of adsorbed Ru(III) and Ru(IV) species. It seems to us that this idea is supported by the concept of the relatively slow initial oxidation of Ru. This process is very likely the formation of Ru(II) species which are oxidized further and faster at ~0.75 V.

REFERENCES

1 S.H. Cadle and S. Bruckenstein, Anal. Chem., 43 (1971) 1858.
2 D.A.J. Rand and R. Woods, J. Electroanal. Chem., 44 (1973) 83.
3 S. Szabó and F. Nagy, J. Electroanal. Chem., 85 (1977) 339.
4 S. Szabó and F. Nagy, Isr. J. Chem., 18 (1979) 162.
5 M. Watanabe and S. Motoo, J. Electroanal. Chem., 60 (1975) 267.
6 S. Hadži-Jordanov, H. Angerstein-Kozlowska, M. Vuković and B.E. Conway, J. Phys. Chem., 81 (1977) 2271.

7 S. Hadži-Jordanov, H. Angerstein-Kozlowska, M. Vuković and B.E. Conway, J. Electrochem. Soc., 125 (1978) 1471.
8 R.O. Lezna, N.R. DeTacconi and A.J. Arvia, J. Electroanal. Chem., 151 (1983) 193.
9 S. Szabó and F. Nagy, J. Electroanal. Chem., 70 (1976) 357.
10 J.A. Rard, Chem. Rev., 85 (1985) 1.
11 E.A. Seddon and K.R. Seddon, The Chemistry of Ruthenium, Elsevier, Amsterdam, 1984, p. 159.
12 R.G. Barradas, S. Fletcher and S. Szabó, Can. J. Chem., 56 (1978) 2029.
13 D. Michell, D.A.J. Rand and R. Woods, J. Electroanal. Chem., 89 (1987) 11.
14 N. Furuya and S. Motoó, J. Electroanal. Chem., 72 (1976) 165.
15 S. Szabó, J. Electroanal. Chem., 172 (1984) 359.

J. Electroanal. Chem., 271 (1989) 269–277
Elsevier Sequoia S.A., Lausanne – Printed in The Netherlands

Investigation of ruthenium deposition onto a platinum electrode in hydrochloric acid media

S. Szabó, I. Bakos and F. Nagy

Central Research Institute for Chemistry, Hungarian Academy of Sciences, H-1525 Budapest, P.O. Box 17 (Hungary)

(Received 20 February 1989; in revised form 16 May 1989)

ABSTRACT

Ruthenium deposition onto the Pt surface has been investigated in 0.5 M HCl and it was shown that the Ru coverage formed via ionization of pre-adsorbed hydrogen does not depend on the Cl^- ion activity. It is strongly dependent, however, if the deposition is carried out at a rather positive potential. The ratio of hydrogen adsorbed on Ru and Pt surfaces of the same area ($H_a^{Ru}/H_a^{Pt} = 0.15$) and the site requirement of an adsorbed Ru atom ($S = 1.8$) have been determined. A mechanism for Ru deposition via ionization of hydrogen adsorbed on platinized Pt is proposed and it is suggested that the $Ru^{n+} + n\,e^- \rightarrow Ru$ process is slow compared to transport processes and adsorption.

INTRODUCTION

In a recent publication we described studies of Ru deposition onto a platinized Pt electrode in 0.5 M H_2SO_4 solution. It was shown that the degree of oxidation of the depositing Ru depends on the potential of its deposition, i.e. the $I-V$ profiles of the Pt electrode covered with Ru were dependent on the potential of Ru deposition. A mechanism for Ru deposition via ionization of hydrogen adsorbed on the platinized Pt electrode was proposed [1].

Because of the various states of oxidation of Ru, the electrochemical characteristics of its deposition onto Pt are much more complex than those of other noble metals [2–4]. Considering the advantage of the complex-forming effect of Cl^- ions, Ru deposition onto the Pt surface has been studied in hydrochloric acid media to obtain more data on the process and to gain a closer insight into the formation and properties of a platinum electrode covered with ruthenium.

0022-0728/89/$03.50 © 1989 Elsevier Sequoia S.A.

EXPERIMENTAL

The cell and method used were the same as those described in our earlier papers [1,5]. The 0.5 M HCl supporting electrolyte was prepared from Merck p.a. grade concentrated HCl with triply distilled water.

Continuous bubbling of purified nitrogen through the main compartment of our cell deoxygenated and agitated the solutions. The gas bubbling also removed the traces of hydrogen dissolved in the supporting electrolyte during the saturation of the working electrode with hydrogen.

One gram of $RuCl_3 \cdot 1\text{–}3\ H_2O$ (Ventron GmbH) was dissolved in 100 cm^3 of 0.5 M HCl and 0.5 ml of this solution was introduced into the main compartment of the cell. It resulted in a Ru ion concentration of 5×10^{-4} M.

All potentials are referred to the hydrogen electrode immersed into the same supporting electrolyte.

RESULTS AND DISCUSSION

Ruthenium deposition via ionization of hydrogen adsorbed on platinized platinum

The cyclic voltammogram of our platinized Pt electrode in ruthenium ion-free 0.5 M HCl is curve 1 in Fig. 1. After this measurement the electrode was saturated with hydrogen (to ~0.01 V) by strong cathodic polarization (~10 mA), and under open-circuit conditions when the potential (in consequence of hydrogen desorption) reached 0.05 V, 0.5 cm^3 of the Ru solution was introduced into the main compartment of the cell.

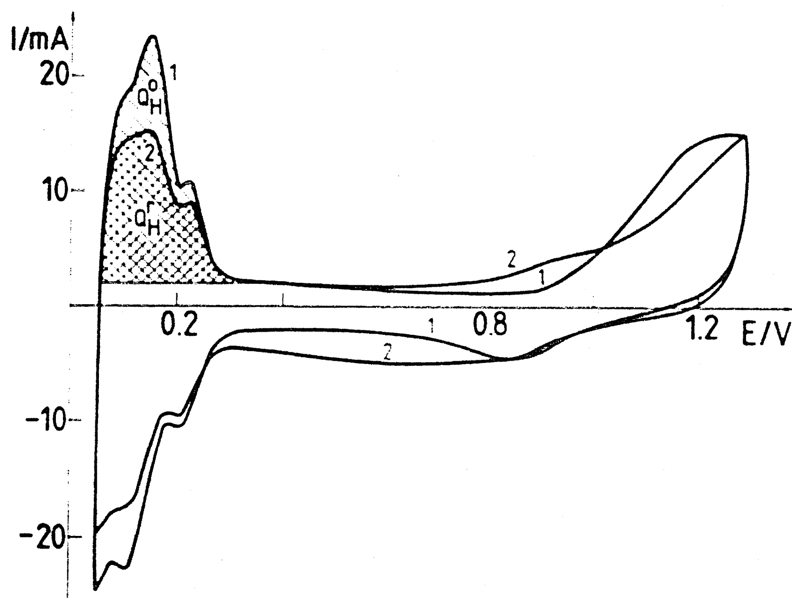

Fig. 1. (1) Voltammogram of Pt electrode in 0.5 M HCl; (2) voltammogram of Pt electrode covered with Ru in 0.5 M HCl free of Ru ions. Sweep rate: 40 mV/s.

Due to the reaction of adsorbed hydrogen with Ru ions, after 90 min the potential rose to about 0.85 V and the cell was rinsed with deoxygenated 0.5 M HCl and then the cyclic voltammogram of the Pt electrode covered with Ru was determined in ruthenium ion-free 0.5 M HCl (curve 2 in Fig. 1). (Curve 2 in Fig. 1 is the first full cycle scanning from 0.85 V toward the lower (0.05 V) potential limit.)

On the basis of Fig. 1, it may be stated that hydrogen adsorption is inhibited by the deposited Ru, a peak of oxidation of Ru appears on the curve at about 0.9 V, and the double-layer region broadens slightly.

It follows from the strong effect of the deposited Ru on the adsorption characteristics of platinized Pt that Ru must be in the adsorbed state. If the deposited Ru were mostly in the form of three-dimensional nuclei on the Pt surface, then curve 2 in Fig. 1 would be the sum of the voltammograms of the two metals, as experienced in the case of Pd deposition onto Pt also in hydrochloric acid media [4]. As a consequence, not a decrease but an increase should have been observed in the hydrogen adsorption.

This experiment was also carried out in 4 M HCl solution, but the cyclic voltammograms before and after the surface reaction were measured in 0.5 M HCl. The result was almost the same as that depicted in Fig. 1.

In contrast to the specific adsorption and complex-forming effect of Cl^- ions, the results of Ru deposition via ionization of hydrogen adsorbed on platinized Pt measured in hydrochloric acid media are very similar to those obtained in 0.5 M H_2SO_4 [1]. The apparent similarity can be verified by the ratio of the hydrogen capacity (Q_H^r) of Pt covered with Ru and the initial hydrogen capacity (Q_H^o) of the Pt electrode.

On the basis of the curves in Fig. 1, Q_H^r/Q_H^o was calculated to be equal to 0.66. When 4 M HCl was used as the supporting electrolyte, $Q_H^r/Q_H^o = 0.65$, and in the case of 0.5 M H_2SO_4 solution (data of Fig. 1 in ref. 1), $Q_H^r/Q_H^o = 0.62$.

The above data show that the Ru coverage formed via ionization of pre-adsorbed hydrogen hardly depends on the Cl^- ion activity.

Ruthenium deposition at different potentials and chloride ion activities

The final potential (0.85 V) of the spontaneous reaction of hydrogen adsorbed on platinized Pt and ruthenium ions is the evidence of oxidation–reduction processes at a rather high potential. These processes were investigated by cathodic polarization of a smooth Pt electrode in the presence of 5×10^{-4} M Ru ion in 0.5 M HCl solution (Fig. 2).

The curve was measured step by step with 0.05 V between the steps, and one point was measured until the polarization current became constant.

Apart from hydrogen deposition, two reduction processes may be considered probable. The first runs up to 0.45 V and the second one begins at this point. The first is $Ru^{4+} + e^- = Ru^{3+}$. The diffusion limiting current of this reaction can be seen between 0.65 and 0.45 V. The reduction of Ru^{3+} to Ru^{2+} starts at 0.45 V and with decreasing potential, the reduction proceeds to metallic ruthenium.

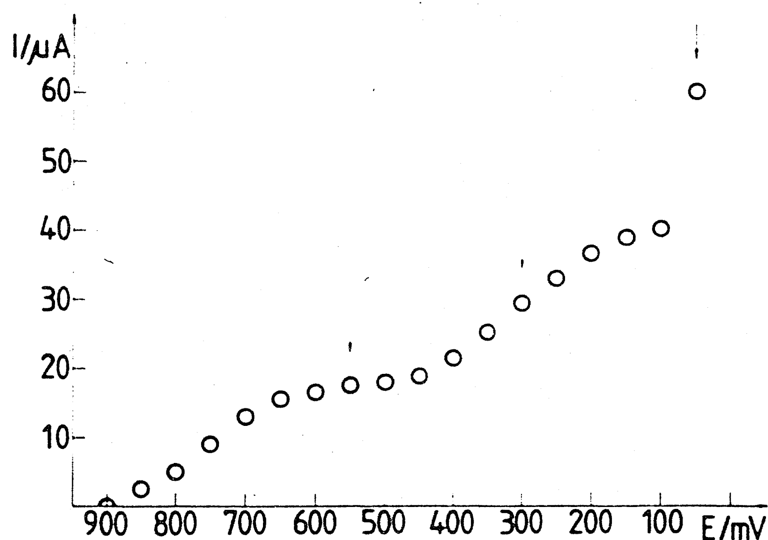

Fig. 2. Potentiostatic polarization curve of a smooth Pt electrode in 0.5 M HCl in the presence of 5×10^{-4} M ruthenium ion.

At the potentials denoted with arrows (Fig. 2), the Ru deposition was carried out potentiostatically onto a smooth Pt electrode, then the cell was rinsed with deoxygenated 0.5 M HCl, and the cyclic voltammogram of the electrode covered with Ru was recorded. The results are summarized in Fig. 3.

For Ru deposition 40 times as much charge was used as corresponds to the amount of hydrogen adsorbed on the Pt electrode free of Ru.

As can be seen from Fig. 3, the Ru coverage is strongly dependent on the potential of deposition and the Cl^- ion activity, since at 0.55 V a considerable Ru coverage could be measured in 0.5 M H_2SO_4 solution [1], but not in 0.5 M HCl.

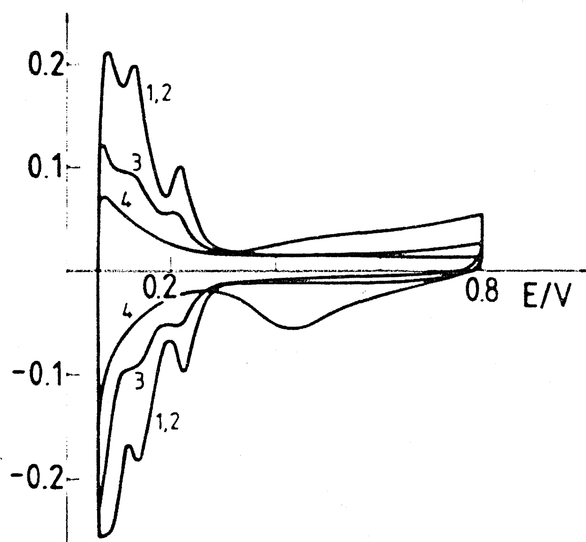

Fig. 3. (1) Voltammogram of a Pt electrode in 0.5 M HCl; voltammogram of a Pt electrode covered with Ru at 0.55 V (2), 0.3 V (3) and 0.05 V (4) in 0.5 M HCl free of Ru ions. Sweep rate: 40 mV/s.

The experiment illustrated in Fig. 3 was repeated using 2 M and 4 M HCl as the supporting electrolyte. As a result of these experiments, increasing chloride ion activity induces a negative shift in the potential of the beginning of Ru deposition.

From the above results it follows that the final potential (0.85 V) of the spontaneous reaction of hydrogen adsorbed on a platinized Pt electrode with Ru ions is so positive that all the adsorbed material should have been oxidized and desorbed because at this potential no Ru deposition could be observed in 0.5 M HCl.

Relationship between hydrogen adsorption on platinum and ruthenium

As can be seen from the cyclic voltammograms of a Pt electrode covered with Ru, Ru deposition decreases the amount of adsorbed hydrogen although Ru also adsorbs hydrogen. Consequently, the decrease of hydrogen adsorption must approach a limiting value which is the amount of hydrogen adsorbed only on Ru adsorbed on Pt.

If the surface roughness of the Pt electrode does not change due to Ru deposition, then the amount of hydrogen adsorbed at full coverage of Ru on a Pt electrode will be characteristic of hydrogen adsorption on a Ru surface with the same size as the initial Pt surface.

On the basis of the above concept, Ru was deposited onto a smooth Pt electrode and from time to time its cyclic voltammogram was measured in Ru ion-free 0.5 M HCl. This procedure was continued until a change could be observed in the hydrogen adsorption. The result is in accordance with curve 4 in Fig. 3.

On the basis of curves 1 and 4 in Fig. 3, it could be calculated that the amount of hydrogen adsorbed on a Pt electrode fully covered with adsorbed Ru (H_a^{Ru}) is only 15% of the hydrogen adsorbed on the same Pt surface (H_a^{Pt}) free of adsorbed Ru. This is in good agrement with earlier results [6].

Site requirement of an adsorbed Ru atom

Before calculation it must be assumed that all of the hydrogen adsorbed on platinized Pt is transformed into adsorbed Ru ($Q_H^o = Q_M$, where Q_M is the charge used for either metal deposition or oxidation of adsorbed metal). This can be assumed since Q_H^r/Q_H^o does not depend either on the Cl^- ion activity or on stirring when Ru deposition takes place via ionization of hydrogen adsorbed on platinized Pt.

Since the hydrogen coverage on the Ru surface can also be calculated, we have enough data to calculate the number of hydrogen adsorption sites (S) occupied by one adsorbed Ru atom [5]:

$$S = \frac{Q_H^o - Q_H^x}{\frac{Q_M}{z}} \qquad (1)$$

The hydrogen adsorbed on a Pt electrode covered with adsorbed Ru (Q_H^r)

consists of two kinds of adsorbed species. One is the hydrogen adsorbed on that part of the Pt surface free of adsorbed Ru (Q_H^x) and the other is the hydrogen adsorbed on the adsorbed Ru (Q_H^{Ru}).

The charge which would be required for the oxidation of the hydrogen adsorbed on the Pt surface covered with Ru before Ru adsorption is

$$Q_H = Q_H^o \theta_{Ru} = \frac{Q_H^o}{z} S \tag{2}$$

In the light of the relationship between the adsorbed hydrogen on Pt and Ru surfaces of the same area (preceding section), the charge required for the oxidation of the hydrogen adsorbed on that part of the surface covered with adsorbed Ru is

$$Q_H^{Ru} = 0.15 S \frac{Q_H^o}{z} \tag{3}$$

The charge required for the oxidation of hydrogen adsorbed on the surface area free of adsorbed Ru is given by

$$Q_H^x = Q_H^r - 0.15 S \frac{Q_H^o}{z} \tag{4}$$

Combination of eqns. (1) and (4) results in

$$S = \frac{z}{0.85}\left(1 - \frac{Q_H^r}{Q_H^o}\right) \tag{5}$$

If we take $z = 4$ [7] and $Q_H^r/Q_H^o \approx 0.64$, then $S \approx 1.7$. The above results were verified as follows. Ru deposition via ionization of hydrogen adsorbed on platinized Pt was carried out with the Ru solution reduced before Ru deposition. Reduction took place at 0.5 V in the first experiment and at 0.3 V in the second. (On the other hand, the experiments were carried out in the same way as described earlier.) In this case, $Q_H^r/Q_H^o \approx 0.44$, and thus $S \approx 2$ if it is assumed that $z = 3$.

The considerable difference between the site requirement data can be explained by the inaccuracy of the z values. It is very likely that z is lower than 3 in the experiments where the reduced Ru solution was used. The smaller z results in a smaller difference between the two site requirement values calculated by the above method.

Ruthenium deposition at 0.05 V

After determination of the cyclic voltammogram of the platinized Pt electrode (curve 1 in Fig. 4), the potential was scanned to 0.05 V. At this potential, 1 ml of the Ru solution was introduced into the main compartment of the cell and Ru deposition was continued until a quantity of electricity of Q^o was consumed (the amount of charge corresponding to the potential shift of the Pt electrode from 0.05 to 0.85 V is denoted by Q^o) (curve 2 in Fig. 4).

This experiment was repeated, but now the electrode was maintained at 0.05 V

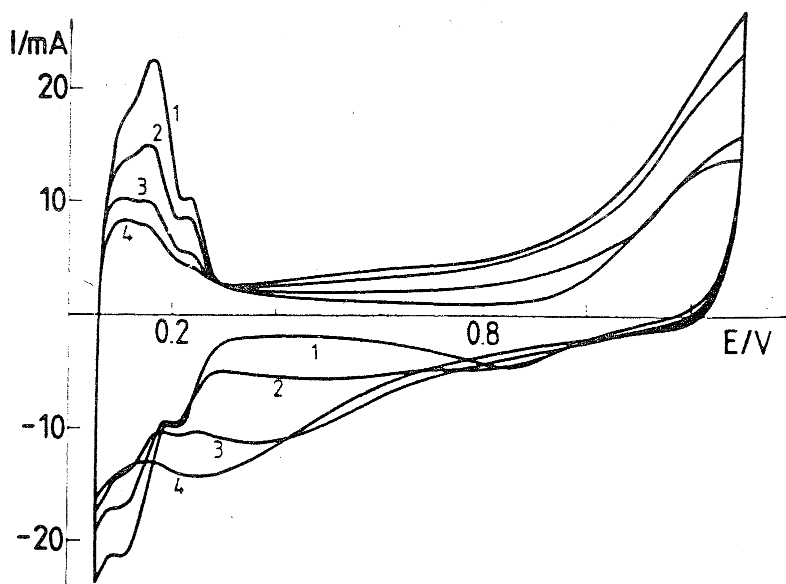

Fig. 4. (1) Voltammogram of a Pt electrode in 0.5 M HCl solution; voltammogram of a Pt electrode covered with Ru equivalent of Q° (2), $4Q^\circ$ (3) and $10Q^\circ$ (4) in 0.5 M HCl free of Ru ions.

until a charge of $4Q^\circ$ (curve 3 in Fig. 4) or of $10Q^\circ$ (curve 4 in Fig. 4) was consumed for reduction.

With the increasing amount of Ru on the surface, the hydrogen adsorption character of the Pt electrode approaches that of a fully covered electrode (curve 4 in Fig. 3), but when a charge of $10Q^\circ$ is used for the Ru deposition the surface is still not completely covered with Ru (curve 4 in Fig. 4). On the other hand, the anodic branches of the voltammograms also differ considerably from the results measured in 0.5 M H_2SO_4 [1].

An explanation for the discrepancies might be the increasing ratio of side reactions at higher Ru coverages. The results of side reactions are only reduced Ru ions in the supporting electrolyte.

Formation of three-dimensional nuclei has to be taken into account also in the interpretation of experimental results because the metal deposition at 0.05 V is carried out at a much more negative potential than the Nernst potential.

The value of Q_H^r/Q_H° has been determined in this case as well. By calculation on the basis of curves 1 and 2 in Fig. 4 it is 0.69. Calculated from curves 1 and 2 in Fig. 4 in our earlier paper [1], however, Q_H^r/Q_H° is equal to 0.7, which is practically the same as that measured in 0.5 M HCl.

It should be noted, however, that Q_H^r/Q_H° values measured in this way have always been higher than values measured by means of spontaneous reaction of adsorbed hydrogen with Ru ions.

On the mechanism of ruthenium adsorption via ionization of hydrogen adsorbed on platinized platinum

The mechanism published in our earlier paper proved to be correct and valid also in hydrochloric acid media. The very first step of the reaction is ionization of

adsorbed hydrogen with the simultaneous formation of an adsorbed Ru layer (reactions 1 and 3 in our earlier paper [1]). This process results in virtually the same Ru coverage irrespective of the medium.

Since Q^{r}_{H}/Q^{o}_{H} values are always lower in the case of Ru deposition via ionization of pre-adsorbed hydrogen than in the case of potentiostatic Ru deposition at 0.05 V, the spontaneous increase of the potential results in some rearrangement of the deposited material in both acids. As a result of this rearrangement, the Ru coverage increases somewhat, but the increase is quite small because the Q^{r}_{H}/Q^{o}_{H} values calculated on the basis of the data of Figs. 1 and 4 hardly differ from each other. It follows from this observation that the rearrangement reactions (reactions 2, 4, 5 and 6 in our earlier paper [1]) have minor importance and for this reason the increase of the Ru coverage has been ignored in the calculation of site requirement.

The role of bulk deposition in the mechanism of spontaneous formation of an adsorbed Ru layer on the Pt surface is less significant than in the processes of spontaneous adsorption of other noble metals on the Pt surface [3–5]. The different character of Ru can be explained by the assumption that the rate of charge transfer preceding the adsorption is low

$$Ru^{n+} + n\,e^- \rightarrow Ru \qquad (6)$$

related to transport processes and adsorption. For this reason a ruthenium ion has enough time to diffuse — without discharge — into the depth of the pores of the Pt black deposited on the Pt surface; hence, instead of bulk deposition mostly an adsorbed layer is formed.

From the above assumption it may be explained why the oxidation state of the adsorbed Ru layer depends on the potential of formation [1] and why the spontaneously formed Ru layer is not oxidized and desorbed at 0.85 V in hydrochloric acid media. Owning to the slow charge transfer, the Ru layer formed at a given potential can maintain its oxidation state for some time despite even a strong polarization.

Finally, this assumption can also serve as an explanation for the observation that the Ru coverage depends strongly on the Cl^- ion activity if the deposition is carried out at a rather positive potential, but it hardly depends on it if the metal deposition takes place close to the hydrogen potential.

Naturally, reaction (6) consists of different elementary reactions of various rates. However, the rate of desorption of the intermediates of reaction (6) must be very low when the Ru deposition takes place close to the hydrogen potential because the Q^{r}_{H}/Q^{o}_{H} data are independent of the medium. Therefore, it may be assumed that $Q^{o}_{H} = Q_{M}$, as has been proposed in the preceding section.

ACKNOWLEDGEMENT

The authors are indebted to the Hungarian Research Fund (No. OTKA: 1004) for financial support.

REFERENCES

1 S. Szabó and I. Bakos, J. Electroanal. Chem., 230 (1987) 233.
2 D.A.J. Rand and R. Woods, J. Electroanal. Chem., 44 (1973) 83.
3 S. Szabó and F. Nagy, J. Electroanal. Chem., 85 (1977) 339.
4 S. Szabó and F. Nagy, Isr. J. Chem., 18 (1979) 162.
5 S. Szabó and F. Nagy, J. Electroanal. Chem., 70 (1976) 357.
6 M.W. Breiter, J. Electroanal. Chem., 178 (1984) 53.
7 E.A. Seddon and K.R. Seddon, The Chemistry of Ruthenium, Elsevier, Amsterdam, 1984, p. 159.

J. Electroanal. Chem., 77 (1977) 193—203
© Elsevier Sequoia S.A., Lausanne — Printed in The Netherlands

INVESTIGATIONS OF COPPER, SILVER AND BISMUTH DEPOSITION ON PALLADIUM IN PERCHLORIC ACID MEDIA

S. SZABÓ

Central Research Institute for Chemistry, Hungarian Academy of Sciences, H-1525/17 Budapest (Hungary)

(Received 15th January 1976; in revised form 22nd April 1976)

ABSTRACT

Investigations have shown that copper and silver ions deposited at more positive potentials than the Nernst potential — similarly to bismuth ions — are not adsorbed but form alloys with palladium. Similarly, in the case of metal deposition via the ionization of sorbed hydrogen, the same alloys were formed as observed by the potentiostatic method.

With the exception of the work of Mikuni and Takamura [1,2], metal adsorption on palladium has not yet been investigated. This fact is well demonstrated by a summary of the mutual adsorption of various metals, in the paper of Kolb et al. [3]. The most interesting finding of Mikuni and Takamura is that bismuth, unlike the other metals deposited on palladium, is not adsorbed but dissolved in the base metal, forming various Pd/Bi alloys.

The purpose of the present work has been to determine in the case of copper and silver deposition whether alloy-forming or adsorption takes place, and to examine the properties of the resulting alloy or adsorbed metal layer. Metal deposition via the ionization of sorbed hydrogen has also been investigated. On account of the very good solubility of hydrogen in palladium, the latter case could be studied by introducing only a known amount of hydrogen into the metal. The amount of hydrogen introduced should not be considerably greater than it would be in the adsorption phase, otherwise the thickness of the metal coating formed on the surface would be a drawback to the evaluation of the results.

When choosing the supporting electrolyte, the dissolution of palladium in the following reaction:

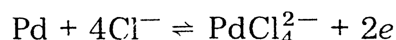

$$Pd + 4Cl^- \rightleftharpoons PdCl_4^{2-} + 2e$$

had to be taken into consideration. The dissolution takes place at a relatively low potential (E_0 = 0.62 V), thus confining the investigations to a rather narrow potential range in the presence of chloride ions. Consequently, only perchloric acid media could be used.

The properties of the resulting alloys or adsorbed metal layers have been studied by means of constant-current charging curves, as in our previous work [4]. In this case, however, the site demand of the adsorbed metal could not be determined from the charging curves, for the hydrogen adsorptive properties of palladium are very different from those of platinum [4].

EXPERIMENTAL

The apparatus was the same as described in our previous paper [4]. The electrolyte was 1 *M* $HClO_4$ in all cases.

In the investigation of metal deposition at a constant potential, the newly activated electrode was kept at some given potential by a potentiostat for a given time in the solution containing metal ions, then the charging curve was determined in the same solution.

When investigating metal deposition via the ionization of sorbed hydrogen, the electrode was polarized cathodically for a given time (measured from 0.5 V), and the charging curve of the electrode thus prepared was determined (curves 1 in the Figures). Then the treatment was repeated and metal ions were introduced into the solution. In most cases, the charging curve of the electrode was determined in the presence of the metal ions after the completion of the metal deposition. In some cases the deposition processes were frozen before completion by removing the solution containing metal ions. Then the cell was rinsed with deoxygenated distilled water and filled with deoxygenated base solution, and the charging curve was determined.

The electrode was a palladized platinum, with a geometrical surface of about 2 cm^2. It was palladized in a 2% $PdCl_2$ solution containing 0.1 *M* HCl, at 0° C and 25 mA for 15 min. (In our experience, palladization at 0° C gave a larger surface than at room temperature.)

Before each measurement the electrode was activated in a separate cell in 0.1 *M* $HClO_4$ solution by a short anodic polarization. Its potential was measured with respect to a hydrogen electrode in the same supporting electrolyte.

During the experiments the apparatus was continually rinsed with purified nitrogen, in order to deoxygenate and agitate the solution.

THE DEPOSITION OF COPPER

Copper deposition studies with the potentiostatic method

After the determination of the charging curve of the newly activated palladized platinum electrode from 0.65 V (curve 1 in Fig. 1), 0.02 g $Cu(ClO_4)_2 \cdot 6H_2O$ was added to the base solution, giving a copper ion concentration of $\sim 10^{-3}$ mol l^{-1}. The electrode was polarized in this solution at 0.65 V for 60 min by means of a potentiostat, then the charging curve of thus prepared electrode was determined (curve 2 in Fig. 1). The experiment was

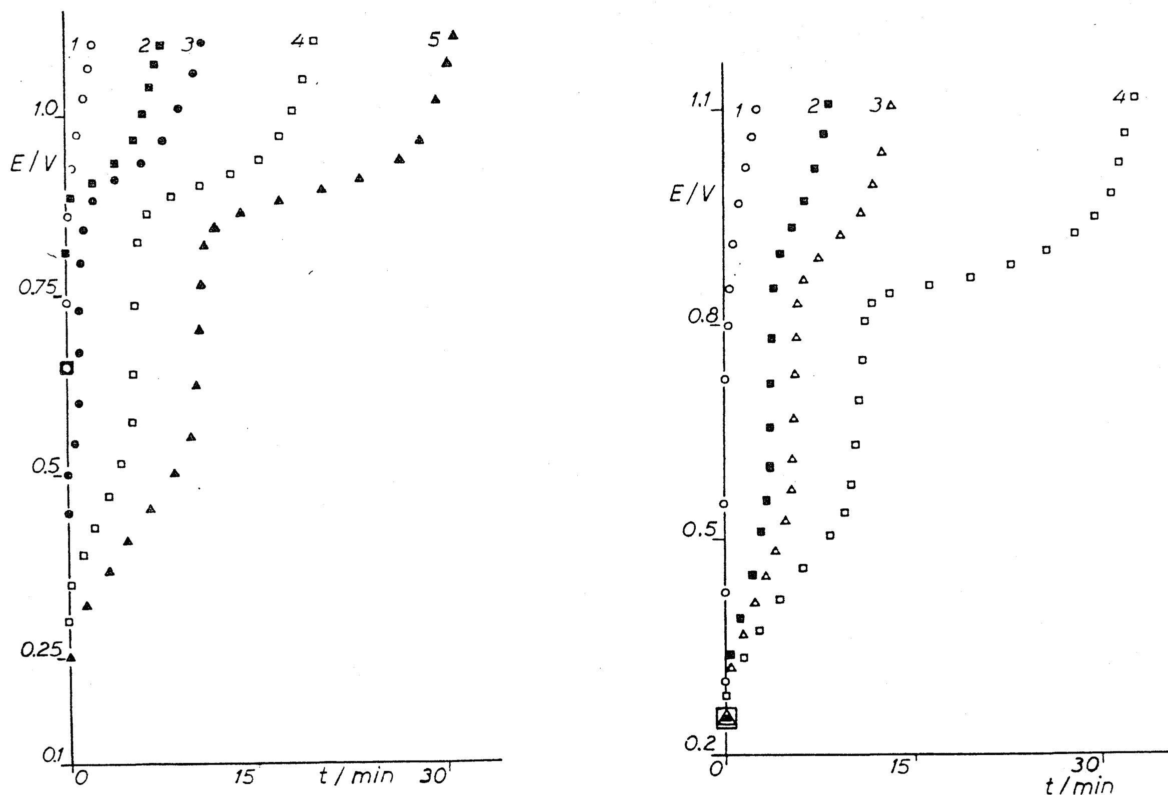

Fig. 1. Charging curve in 1 *M* $HClO_4$ solution from 0.65 V (1), and after polarization in a solution containing 10^{-3} mol l^{-1} copper ions for 60 min at 0.65 V (2), 0.45 V (3), 0.3 V (4) and 0.25 V (5). I = 0.25 mA.

Fig. 2. Charging curve in 1 *M* $HClO_4$ solution (1), and after polarization at 0.25 V for 5 (2), 20 (3) and 60 min (4) in a solution containing 10^{-3} mol l^{-1} copper ions. I = 0.25 mA.

repeated at 0.45 V, 0.3 V and 0.25 V, giving curves 3, 4 and 5, respectively. Since all potentials were more positive than the Nernst potential, bulk deposition was not possible. The Figure demonstrates the formation of two types of adsorbed copper. One of them is ionized at about 0.9 V and the other at about 0.45 V.

Having determined the undervoltage values, the next problem was the sequence of the formation of the adsorbed types. In order to determine this, the electrode was polarized at 0.25 V in the above mentioned conditions for 5, 20 and 60 min (curves 2, 3 and 4 in Fig. 2). The curves show that if the chosen potential is more negative than 0.45 V, both types are formed simultaneously.

The Figures, especially Fig. 2 show that the quantity of the adsorbed copper increases monotonically with increasing polarization times and does not approach a limit of total coverage. This leads to the conclusion that alloy formation has to be considered, as in the case of bismuth adsorption [2]. This was confirmed by the following experiment. A bright palladium disk

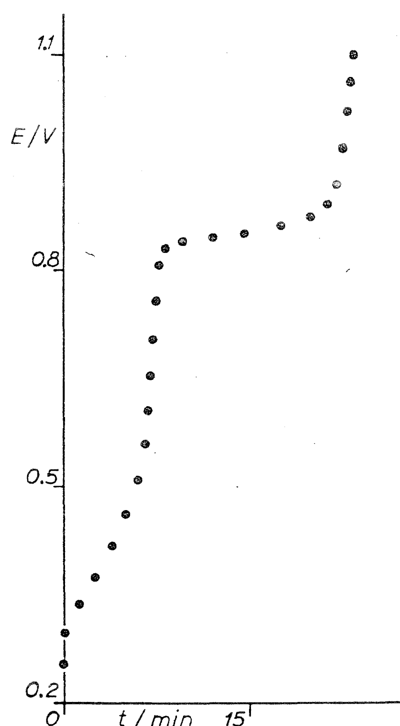

Fig. 3. Charging curve of a bright palladium electrode after polarization at 0.25 V for 60 min in a solution containing 10^{-3} mol l^{-1} copper ions. I = 0.1 mA.

(diameter 1.2 cm, thickness 35 μm) was heated red, rinsed with aqua regia, and polarized at 0.25 V for 60 min at the above mentioned copper ion concentration. The charging curve of the thus prepared electrode is shown in Fig. 3. Considering that, in the case of a bright palladium electrode, the adsorbed amount is small, the curve shown in Fig. 3 can be only the result of alloy formation. Alloy formation is also indicated by the fact that at the end of the 1-hour polarization the current of the potentiostat was still 50 μA, meaning that the quantity of the alloys would have continued to grow with further polarization.

From the experiment with the bright palladium electrode it can be concluded without doubt that the potentials formerly regarded as undervoltage values are in fact the decomposition potentials of the alloys. Consequently, the existence of two distinct types of palladium/copper alloy is indicated. According to metallographic investigations, there are two metal-metal compounds in the palladium/copper system, one of which is richer in copper ($PdCu_5$) than the other (Pd_3Cu_5) [5].

Studies of copper deposition via the ionization of sorbed hydrogen

In these experiments, the palladized platinum electrode was polarized cathodically in the supporting electrolyte with 1 mA for 4 min, then the po-

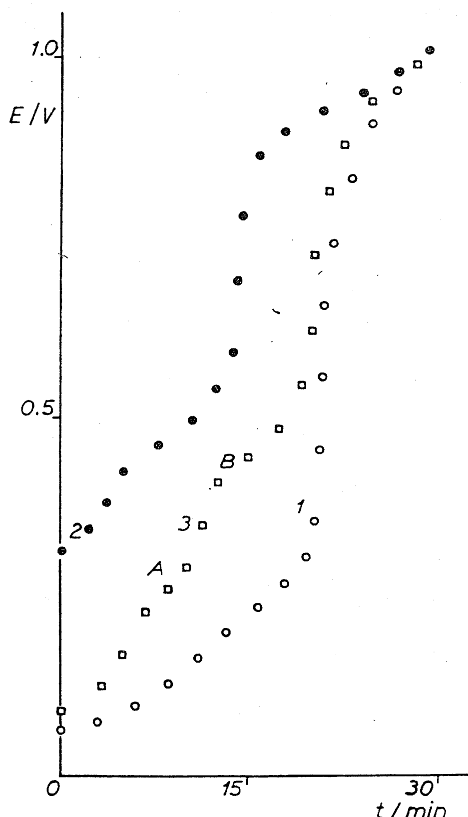

Fig. 4. Charging curve in 1 *M* $HClO_4$ solution after polarization cathodically with 1 mA for 4 min (1), and after copper deposition (2). Charging curve of the electrode in 1 *M* $HClO_4$ solution if the deposition processes were frozen (3). I = 0.2 mA.

larity was reversed and a charging curve was determined (curve 1 in Fig. 4). Then the electrode was polarized cathodically again and 0.02 g $Cu(ClO_4)_2 \cdot 6H_2O$ was introduced into the solution, as in the previous experiments. Then the electrode potential rose to 0.29 V in 20 min. The charging curve of the thus prepared electrode is curve 2 in Fig. 4. The character of the curve is the same as in the previous experiments indicating the formation of the same alloy types as in the case of deposition at constant potential.

The experiment was then repeated so that before the complete ionization of the sorbed hydrogen, the deposition processes were frozen by the removal of the solution containing copper ions. This resulted in charging curve 3 in the base solution, showing the presence of bulk copper on the surface at 0.25 V (region A) and the formation of only one alloy type, ionized at 0.45 V (region B). There is no sign of the other alloy, ionized at 0.9 V; thus it is formed only at the end of the bulk deposition, via the ionization of the remaining hydrogen or the transformation of the transitional metallic form.

Now, two ways offer themselves for the metallic form to be transformed into alloys. The copper crystals can dissolve into the base metal, or, similarly to the mechanism observed in the case of platinum, they can get ionized

while copper depositing at areas relatively deficient in copper forms alloys [4]. The fact that the bulk form could be stabilized by the removal of copper ions, indicates that this mechanism may play a part in the formation of the alloys.

From the formation sequence of the alloys it can be concluded that the alloy ionized at 0.45 V is the one richer in copper; for it would be difficult to imagine the formation of an alloy deficient in copper together with the initial deposition of copper crystals, probably at their points of adhesion. Accordingly, 0.9 V is the ionization potential of the alloy comparatively deficient in copper.

THE DEPOSITION OF SILVER

Silver deposition studies with the potentiostatic method

In this case, first the charging curve of the palladized platinum electrode was determined from 0.625 V. Then 0.01 g $AgClO_4 \cdot H_2O$ was introduced into the solution, resulting in a silver ion concentration of about 10^{-3} mol l^{-1}. Then the electrode was polarized first at 0.7 V, 0.65 V and 0.625 V for 15 min (curves 2, 3 and 4 in Fig. 5). Two undervoltage values could be determined from the curves: one at ~0.75 V and the other at ~0.95 V.

The determination of undervoltage values was followed by an investigation of the formation sequence of the adsorbed forms in this case, too. For this

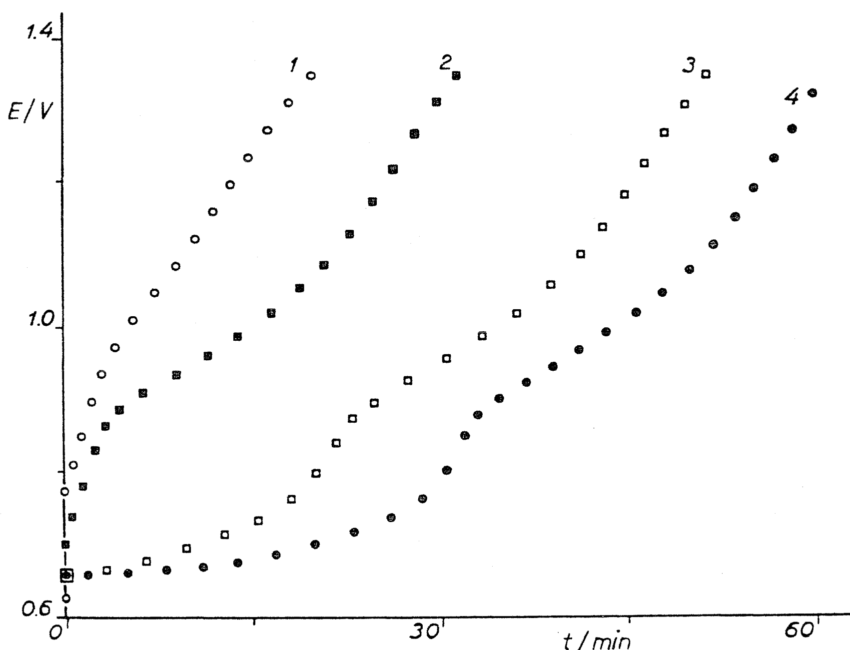

Fig. 5. Charging curve in 1 *M* $HClO_4$ solution from 0.65 V (1), and after polarization for 15 min at 0.7 V (2), 0.65 V (3) and 0.625 V (4) in a solution containing 10^{-3} mol l^{-1} silver ions. I = 0.25 mA.

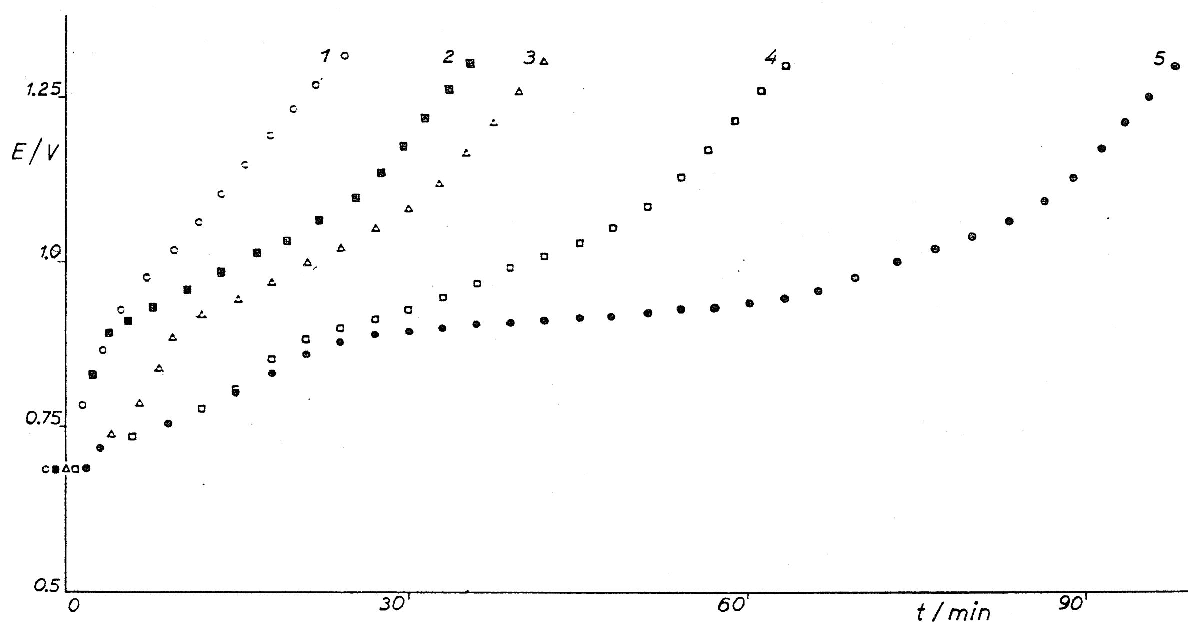

Fig. 6. Charging curve in 1 *M* $HClO_4$ solution from 0.65 V (1), and after polarization at 0.65 V for 5 (2), 15 (3), 200 (4) and 500 min (5) in a solution containing 10^{-3} mol l^{-1} silver ions. I = 0.25 mA.

purpose, the electrode was polarized at 0.65 V for 5, 15, 200 and 500 min, resulting in curves 2, 3, 4 and 5 in Fig. 6. Two fundamental conclusions can be drawn from the curves. First, the formation of the species ionized at 0.95 V precedes the formation of the other species, ionized at 0.75 V. Second, the adsorbed quantity, although very slowly, grows monotonously. This indicates in this case, too, that the process is not adsorption but alloy formation. This conclusion is supported by the observation that the polarization current was ~30 μA even after 500 min, meaning that the formation of the alloys would have continued with further polarization. From the foregoing it is clear that the measured undervoltage values are, in fact, the ionization potentials of the different alloys in this case, too.

No alloys could be observed on a bright palladium electrode. The reason may be that the diffusion of the silver atoms into the base metal (surface alloy) is much slower than that of the copper atoms; hence a very prolonged experiment would have been required to obtain an observable quantity of alloys.

In the silver/palladium system, too, metallographic investigations have found metal-metal compounds. The composition of the one richer in silver is AgPd and that of the other is Ag_2Pd_3 [5].

Studies of silver deposition via the ionization of sorbed hydrogen

First, the charging curve of the electrode was determined in the supporting electrolyte, then it was polarized cathodically again (1 mA for 4 min). After

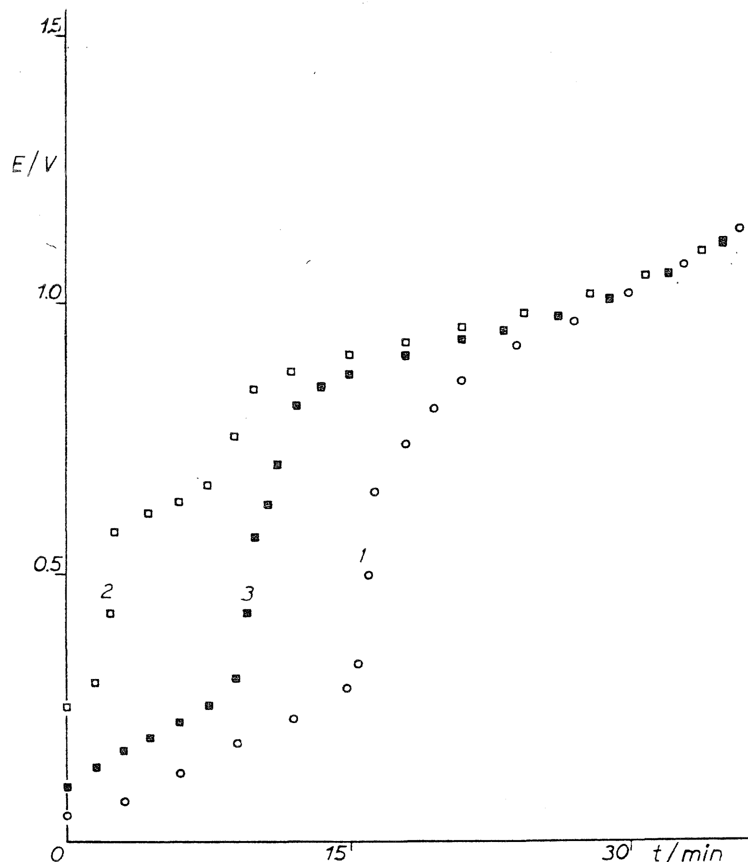

Fig. 7. Charging curve in 1 M $HClO_4$ solution after polarization cathodically with 1 mA for 4 min (1). Charging curve in 1 M $HClO_4$ solution after silver deposition if the deposition processes were frozen at 0.24 V (2) and 0.09 V (3). I = 0.25 mA.

the polarization 0.01 g $AgClO_4 \cdot H_2O$ was introduced into the solution. When visually observable silver appeared on the electrode (at 0.24 V), the deposition processes were frozen by the removal of the solution containing silver ions. Then the charging curve was determined in the supporting electrolyte, giving curve 2 in Fig. 7. Apart from the sorbed hydrogen that had not yet been ionized, the character of the curve is the same as that of curve 3 and 4 in Fig. 5, indicating the formation of the same alloys.

When the deposition processes were frozen at 0.09 V, curve 3 was obtained in the supporting electrolyte. This shows that the alloy ionized at 0.95 V is the first to be formed, and the alloy ionized at 0.75 V or bulk silver will not appear before the formation of a certain quantity of the alloy ionized at 0.95 V. Consequently, the initial formation rate of this alloy is very high, and the formation of the alloy ionized at 0.75 V or the bulk form becomes possible only when this rate becomes lower than that of the metal deposition. The only possible explanation for this slowing down is that the diffusion of the silver atoms through the previously formed alloy becomes extremely hindered. (The same conclusion can be reached on the basis of the experiments illustrated in Fig. 6.)

Since the electrode potential during the deposition was much more negative than the Nernst potential of the Ag^+/Ag system in both cases, the Ag/Pd alloys could be formed only by diffusion on the surface and in the lattice of the base metal.

Finally the question arises that which of the two alloys is richer in silver. According to Fig. 7, the formation of a certain quantity of the alloy ionized at 0.95 V is followed by the simultaneous appearance of the other alloy (ionized at a lower potential) and the metallic form. Since it is highly improbable that an alloy comparatively deficient in silver would be formed together with bulk silver, it can be presumed that the alloy ionized at 0.95 V is the one comparatively deficient in silver (Ag_2Pd_3) and that ionized at 0.75 V is the one richer in silver (AgPd).

THE DEPOSITION OF BISMUTH

First the published results [2] were reproduced. The charging curves of a palladized platinum electrode polarized at 0.2 V for different times in a solution containing $\sim 10^{-3}$ mol l^{-1} Bi^{3+} ions is shown in Fig. 8. (The bismuth ions were introduced by dissolving Bi_2O_3.) The ionization potentials of the different alloys can be identified and their formation is demonstrated. The different alloys are separated best on curve 7. Region A represents the ionization of bulk bismuth ($Bi \rightarrow Bi^{3+} + 3e$; $E_0 = 0.277$ V), and regions B, C and D represent the ionization of bismuth-palladium alloys. The ionization potentials are in agreement with those in the literature [2].

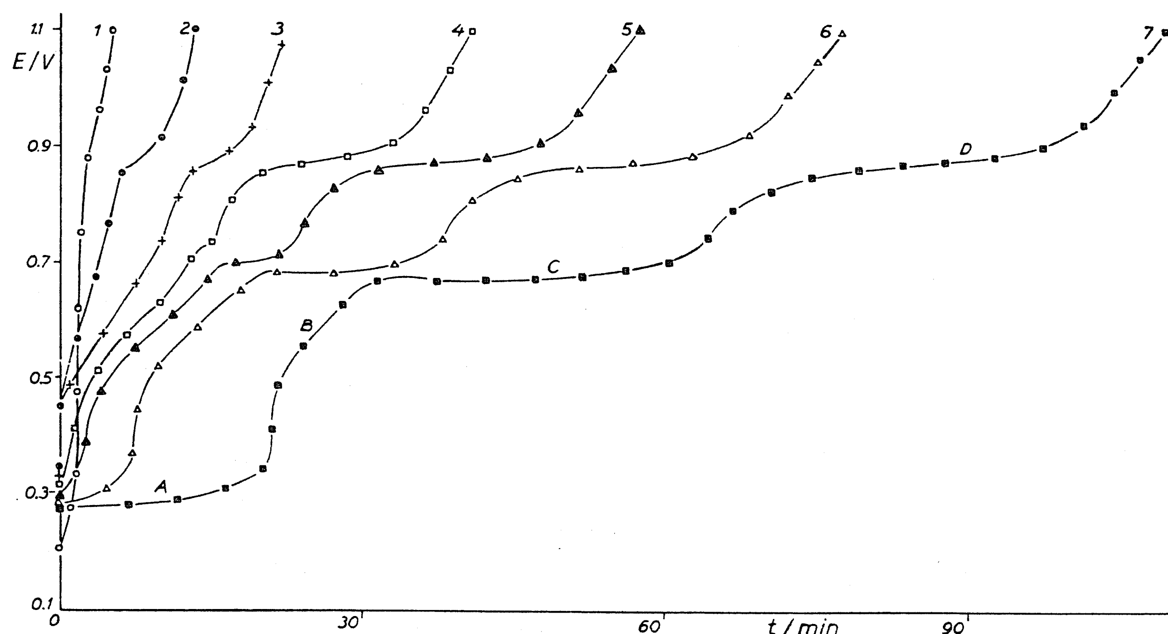

Fig. 8. Charging curve in 1 *M* $HClO_4$ solution from 0.2 V (1), and after polarization at 0.2 V for 5 (2), 15 (3), 30 (4), 45 (5), 60 (6) and 90 min (7) in a solution containing 10^{-3} mol l^{-1} bismuth ions. $I = 0.5$ mA.

The metallographic studies of the bismuth-palladium system have demonstrated the existence of Pd_3Bi, Pd_5Bi_3 (γ type), PdBi and $PdBi_2$ (α and β types) metal-metal compounds. According to the phase diagram of the system, Pd_5Bi_3 is probably not formed at room temperature at all [5]. From our results it has not been possible to establish a definite correspondence between the regions of the charging curve and the different alloy types. The formation sequence of the alloys (Fig. 8), however, leads to the conclusion that region D represents the alloy most deficient in bismuth, and as the quantity of deposited bismuth increases, the alloys formed are successively richer in bismuth, with bulk bismuth at the end, of course.

The reproduction of the published results was followed by an investigation of the formation of the alloys in the course of the deposition via the ionization of sorbed hydrogen. First the charging curve was determined, then the electrode was polarized cathodically at 4 mA for 6 min, and Bi^{3+} ions were introduced. When the deposition processes were frozen at 0.08 V by the removal of the solution containing Bi^{3+} ions, curve 2 in Fig. 9 was obtained in supporting electrolyte. When the Bi^{3+} ions were present for 60 min, curve 3 was obtained. The comparison of the two curves shows that a significant

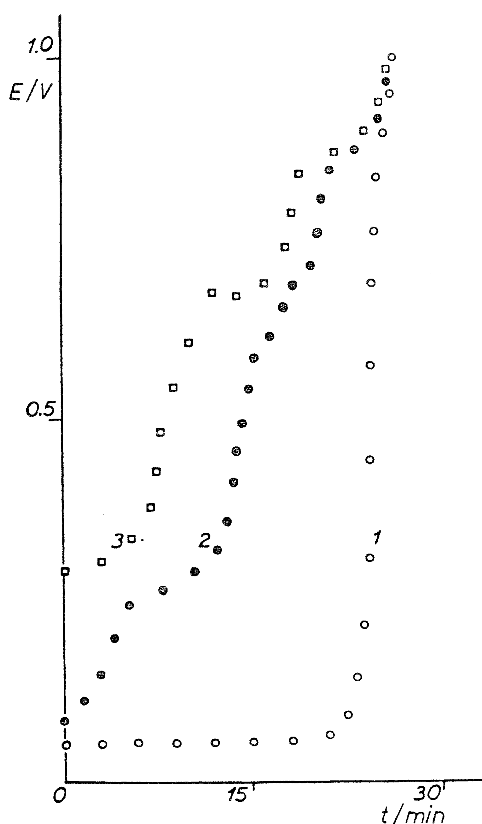

Fig. 9. Charging curve in 1 M $HClO_4$ solution after polarization cathodically with 4 mA for 6 min (1). Charging curve in 1 M $HClO_4$ solution after bismuth deposition if the deposition processes were frozen at 0.08 V (2). Charging curve after bismuth deposition (3). I = 1 mA.

quantity of bulk bismuth is formed in the course of the deposition, which is then transformed into alloys in 60 min, together with the hydrogen unionized yet. From Fig. 9 it can be concluded that the formation of the alloys is similar to that observed in the potentiostatic experiments, that is, the Pd/Bi alloys are formed mainly by means of the diffusion of bismuth in the palladium lattice. This is supported by the observation that the formation of the Pd/Bi alloys was already under way when the electrode potential was much more negative than the Nernst potential of the Bi^{3+}/Bi system (curve 2 in Fig. 9).

REFERENCES

1 F. Mikuni and T. Takamura, Denki Kagaku, 37 (1969) 852.
2 F. Mikuni and T. Takamura, Denki Kagaku, 38 (1971) 237.
3 D.M. Kolb, M. Przasnyski and H. Gerischer, J. Electroanal. Chem., 54 (1974) 25.
4 S. Szabó and F. Nagy, J. Electroanal. Chem., 70 (1976) 357.
5 E.M. Savicki, V.P. Polyakova and M.A. Tilkina, Palladium Alloys, Nauka, Moscow, 1967 (in Russian).

J. Electroanal. Chem., 160 (1984) 299–303
Elsevier Sequoia S.A., Lausanne – Printed in The Netherlands

12.

INVESTIGATION OF LEAD ADSORPTION VIA THE IONIZATION OF HYDROGEN ADSORBED ON PLATINIZED PLATINUM

S. SZABÓ and F. NAGY

Central Research Institut for Chemistry, Hungarian Academy of Sciences, H-1525 Budapest, P.O. Box 17 (Hungary)

(Received 28th November 1982; in revised form 11th February 1983)

ABSTRACT

In the case of lead adsorption via the ionization of hydrogen adsorbed on platinized platinum, adsorbed Pb^+ ions are also formed on, and partly desorbed from, the surface. The site requirement of an adsorbed lead atom is $S = 2.3$ and 1.9.

INTRODUCTION

Although no separate paper has been devoted to the investigation of lead adsorption on platinum, many details are known about it because this phenomenon has been dealt with in a number of paper [1–5]. The different values of site requirement [1,2] and underpotential values of site requirement [1,2] and underpotential [1,2,4,5] have shown that this phenomenon is not understood in detail.

Our paper aims at elucidating Pb adsorption via the ionization of hydrogen adsorbed on Pt. In the present work the constant current charging curve and the linear potential sweep techniques were utilized.

EXPERIMENTAL

The cell and method used were the same as described in our earlier paper [6]. The solution in the cell could be replaced with the exclusion of air. As supporting electrolytes, 1 *M* $HClO_4$ and 1 *M* HCl were used. The concentration of Pb^{2+} ions was 10^{-4} *M*. Lead ions were added to the solution in the form of $Pb(ClO_4)_2$ and $PbCl_2$. The apparent surface of the polycrystalline platinized platinum electrode was about 2 cm^2. The reference electrode was a hydrogen electrode in the same solution.

RESULTS AND DISCUSSION

Adsorption of lead from 1 M $HClO_4$

Before the experiments the electrode was activated in a separate cell in 1 *M* $HClO_4$ for a few seconds with strong anodic polarization and was then placed into

0022-0728/84/$03.00 © 1984 Elsevier Sequoia S.A.

the cell and saturated with hydrogen by strong cathodic polarization. After completion of the saturation, when—as a result of hydrogen desorption due to N_2 flowing through the cell—the electrode potential reached 0.06 V, the charging curve was measured and the electrode was again resaturated. At 0.06 V $Pb(ClO_4)_2$ was added to the solution at open-circuit conditions. It was followed by the spontaneous formation of an adsorbed lead layer. In 90 min the potential was increased to 0.18 V and then the charging curve was measured again (curve 2 in Fig. 1). This experiment was repeated in such a way that after 90 min the cell solution was changed to 1 *M* $HClO_4$ under oxygen-free conditions and then we obtained curve 3 in Fig. 1.

It follows from Fig. 1 that the hydrogen adsorbed on the platinized Pt electrode exchanged into adsorbed lead but only with some loss of charge, since curves 1–3 do not overlap after lead desorption. The loss could even be increased by changing the cell solution, as is clearly indicated by the discrepancy between curves 2 and 3.

In Fig. 1, curve 4 is the charging curve measured from 0.06 V in 1 *M* $HClO_4$ for the electrode covered with Pb_{ads}. Apparently, Pb_{ads} almost completely inhibits hydrogen adsorption and even the charge required for the oxidation of the sum of H_a and Pb_{ads} is smaller than the charge used for the oxidation of H_a adsorbed on the electrode free of Pb_{ads}.

For comparison with data published in the literature, the experiment characterized by curve 4 in Fig. 1 was repeated by the potential sweep method (Fig. 2). The result is different from the data published earlier [1–5]. Here, Pb_{ads} desorbs at 0.1 V more positive potential and covers the active sites where strongly adsorbed hydrogen has been adsorbed. It may be supposed that those differences are caused by a slow rearrangement of Pb_{ads}, which could take place under the 90 min exposure to electrolyte containing Pb^{2+} ions, and changing of the cell solutions to lead ion free supporting electrolyte.

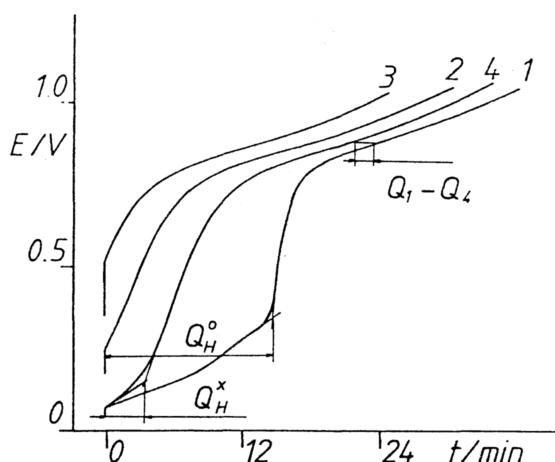

Fig. 1. (1) Charging curve in 1 *M* $HClO_4$ solution; (2) charging of the electrode covered with Pb_{ads} in the presence of Pb^{2+} ions; (3) in supporting electrolyte; (4) in supporting electrolyte after saturation with hydrogen. ($I = 0.1$ mA.)

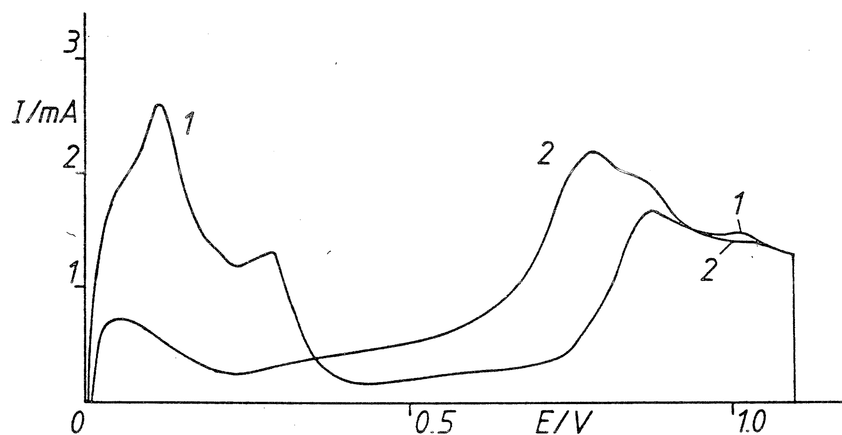

Fig. 2. (1) Potential sweep in 1 *M* $HClO_4$ solution; (2) potential sweep of the electrode covered with Pb_{ads}. (Sweep rate: 6.2 mV s^{-1}.)

Adsorption of lead from 1 M HCl

On the basis of Fig. 1, it cannot be decided whether the loss of charge was caused by the reduction of ClO_4^- ions or the formation of Pb_{ads}^+ ions desorbed from the surface. For these reasons the experiments depicted in Fig. 1 were repeated in 1 *M*

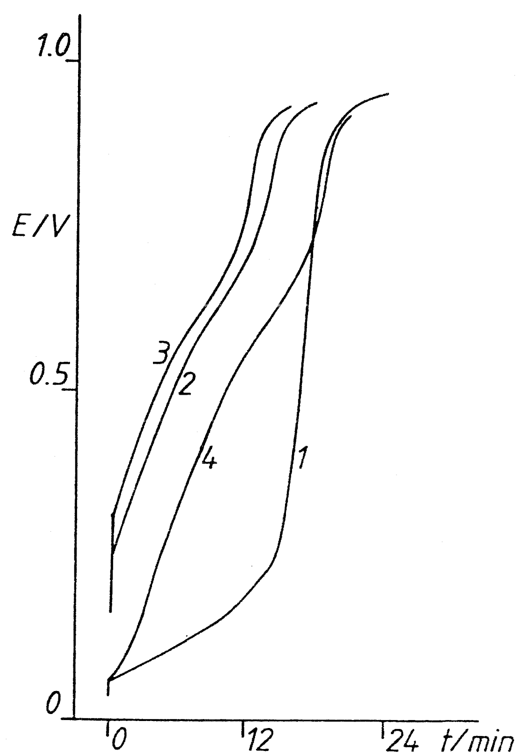

Fig. 3. (1) Charging curve in 1 *M* HCl solution; (2) charging curve of the electrode covered with Pb_{ads} in the presence of Pb^{2+} ions; (3) in supporting electrolyte; (4) in supporting electrolyte after saturation with hydrogen. ($I = 0.1$ mA.)

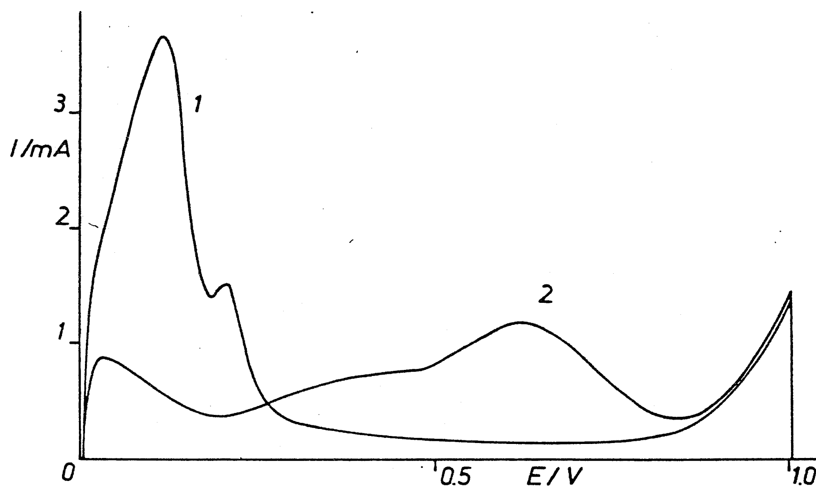

Fig. 4. (1) Potential sweep in 1 *M* HCl solution; (2) potential sweep of the electrode covered with Pb_{ads}. (Sweep rate: 5.85 mV s^{-1}.)

HCl solution. According to Fig. 3, there is also loss in this case, and it can only be explained by formation and desorption of Pb^{+}_{ads} ions.

Figure 4 shows the voltammetry curve of the Pt electrode covered with Pb_{ads}. On the basis of curve 2 it can be ascertained that lead adsorbs mostly on the sites of strongly adsorbed hydrogen and it desorbs at a more negative potential than it does in 1 *M* $HClO_4$ solution. The negative shift is caused by the complex-forming effect of chloride ions.

Mechanism of formation of adsorbed monolayer

Taking into consideration the above experimental results the following mechanism can be assumed:

$$H_a \rightleftharpoons H^+ + e \qquad (1)$$

$$Pb^{2+} + 2\,e \rightleftharpoons Pb_{ads} \qquad (2)$$

$$Pb^{2+} + e \rightleftharpoons Pb^{+}_{ads} \qquad (3)$$

$$Pb^{+}_{ads} + e \rightleftharpoons Pb_{ads} \qquad (4)$$

$$Pb^{+}_{ads} \rightleftharpoons Pb^{+}_{solution} \qquad (5)$$

The Pb^{+}_{ads} ions formed in reaction (3) can be reduced to Pb_{ads} (4), or on dissolving from the surface (5) in the form of Pb^{+} ions, they can cause the loss of charge.

Site requirement of an adsorbed lead atom

For calculation of this constant the amount of charge required for the oxidation of adsorbed lead must be determined. When determining this quantity, it must be

taken into consideration that at the desorption potential oxygen adsorption or, in HCl media, chlorine adsorption also takes place. Figures 2 and 4 show that the electrode surface after Pb desorption reaches the same state as before lead adsorption in the supporting electrolyte, because curves 1 and 2 converge. This fact makes possible the determination of the charge required for the oxidation of Pb_{ads}.

Charge of the lead-free surface:

$$Q_1 = Q_H^\circ + Q_{dl} + Q_O \tag{6}$$

where Q_H° is the charge required for the oxidation of adsorbed hydrogen, Q_{dl} the charge corresponding to the double layer and Q_O the charge required for oxygen adsorption.

Charge of the surface covered with lead:

$$Q_4 = Q_H^x + Q_{dl} + Q_O + Q_{Pb} \tag{7}$$

where Q_H^x is the charge required for the oxidation of the hydrogen adsorbed on the active sites free of lead, and Q_{Pb} the charge corresponding to the oxidation of Pb_{ads}.

From eqns. (6) and (7)

$$Q_{Pb} = Q_H^\circ - Q_H^x - (Q_1 - Q_4) \tag{8}$$

The Q_{Pb} calculated above is inserted into the equation reported earlier [6]:

$$S = \frac{Q_H^\circ - Q_H^x}{(Q_{Pb}/z)} = \frac{Q_H^\circ - Q_H^x}{(Q_H^\circ - Q_H^x - Q_1 + Q_4)/z} \tag{9}$$

Using eqn. (9) and supposing that $z = 2$, from the data of Figs. 1 and 3 the value of S for a lead adatom was calculated to be 2.3 and 1.9 respectively. Our results confirm the results of Furuya and Motoo [2].

The difference between the results measured in hydrochloric and perchloric acid might be explained by the specific adsorption of Cl^- ions. A similar difference, but with opposite sign, can be found between the site requirement of adsorbed Cu atoms measured in hydrochloric [7,8] and sulphuric [9] acid solutions.

REFERENCES

1 R.R. Adzic, M.D. Spasojevic and A.R. Despic, Electrochim. Acta, 24 (1979) 569.
2 N. Furuya and S. Motoo, J. Electroanal. Chem., 98 (1979) 195.
3 B. Beden, F. Kardigan, C. Lamy and J.M. Leger, J. Electroanal. Chem., 127 (1981) 75.
4 G. Kokkinidis and P.D. Jannakoudakis, J. Electroanal. Chem., 130 (1981) 153.
5 F. Kadirgan, B. Beden and C. Lamy, J. Electroanal. Chem., 136 (1982) 119.
6 S. Szabó and F. Nagy, J. Electroanal. Chem., 70 (1976) 357.
7 B.J. Bowles, Electrochim. Acta, 15 (1970) 589.
8 S. Szabó and F. Nagy, J. Electroanal. Chem., 84 (1977) 93.
9 N. Furuya and S. Motoo, J. Electroanal. Chem., 72 (1976) 165.

J. Electroanal. Chem., 172 (1984) 359–366
Elsevier Sequoia S.A., Lausanne – Printed in The Netherlands

13.

INVESTIGATION OF TIN ADSORPTION ON A PLATINIZED PLATINUM ELECTRODE IN HYDROCHLORIC ACID MEDIA

S. SZABÓ

Central Research Institute for Chemistry, Hungarian Academy of Sciences, H-1525 Budapest, P.O. Box 17, (Hungary)

(Received 2nd November 1983; in revised form 9th March 1984)

ABSTRACT

It is demonstrated that via the catalytic disproportionation of Sn^{2+} ions an adsorbed tin layer can be formed on the Pt surface. The characteristics of this monolayer are similar to those formed from $SnCl_4$ solution via the ionization of hydrogen adsorbed on Pt. It is proved that the desorbing tin, upon anodic polarization, dissolves in the form of Sn^{4+} ions. The site requirement of an adsorbed tin atom is $S = 2.2$ hydrogen adsorption sites and its electrosorption valency is $\gamma = 3.6$.

INTRODUCTION

Considerable interest has been devoted recently to the adsorption of tin on Pt and its effect on the electrocatalytic oxidation of organic substances at Pt electrodes modified with adsorbed tin [1–7]. The modified platinum electrodes were prepared in sulfuric acid supporting electrolytes in which either Sn^{4+} or Sn^{2+} ions were dissolved. It has been shown that Sn adsorbs so strongly on the Pt surface that in H_2SO_4 solution it does not desorb completely upon anodic polarization of the tin-covered Pt electrode [2,7]. Consequently, the data published about tin adsorption on Pt [2–7], most likely, can be applied to only such a Pt surface covered with irreversibly adsorbed tin.

With the objective of the preparation of a Pt electrode covered with adsorbed tin, a hydrogen-covered Pt electrode was immersed into an aqueous solution of $SnCl_4 \cdot 5\,H_2O$. This has been called the immersion method and is essentially metal adsorption via the ionization of hydrogen adsorbed on Pt [2].

In the present paper tin adsorption in hydrochloric acid media was investigated taking into account the differences between the deposition of Sn^{2+} and Sn^{4+} ions. Tin adsorption via the ionization of hydrogen adsorbed on Pt has also been dealt with. Finally, new evidence about the slow desorption of the tin adsorbed on Pt is presented.

In this work the linear potential sweep technique and the constant current charging curve method were used.

0022-0728/84/$03.00 © 1984 Elsevier Sequoia S.A.

EXPERIMENTAL

All measurements were carried out in the same three-compartment cell described earlier [8]. A characteristic of our cell is that the cell solutions can be replaced with the exclusion of air, which permits the study of the properties of a Pt electrode covered with adsorbed metal in the absence of adsorbing ions.

The solutions were prepared from Merck reagents with triply distilled water. Pure nitrogen was bubbled through the cell to deoxygenate the solutions.

The concentration of both Sn^{2+} and Sn^{4+} ions was 2 m*M*. The ions were added to the supporting electrolyte in the form of $SnCl_2$ and $SnCl_4$ dissolved in 1 *M* HCl.

The polycrystalline platinized platinum electrode was platinized as described previously [8], and its apparent surface was ca. 2 cm^2.

The potentials were measured against a hydrogen electrode in the same solution.

RESULTS AND DISCUSSION

Catalytic disproportionation of Sn^{2+} ions

First, the charging curve of the Pt electrode was determined in 1 *M* HCl (Fig. 1, curve 1) and then under open circuit conditions at a potential of 0.3 V, Sn^{2+} ions were added to the supporting electrolyte. At the moment of introducing Sn^{2+} ions into the main compartment of the cell, the potential of the electrode quickly rose to ca. 0.45 V and then decreased to ca. 0.2 V, as plotted in Fig. 2.

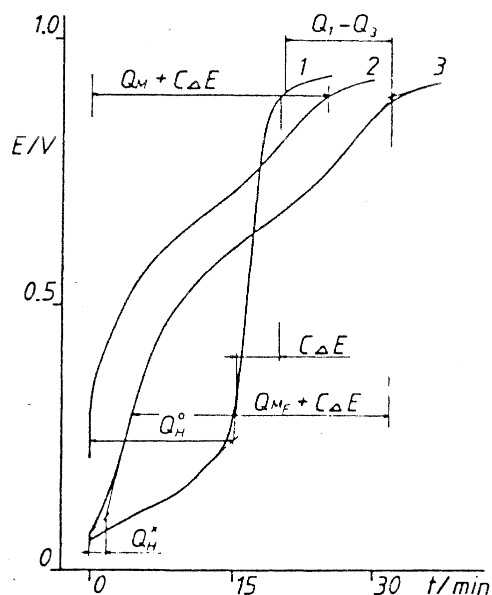

Fig. 1. (1) Charging curve in 1 *M* HCl solution; (2) charging curve in 1 *M* HCl solution of the electrode covered with adsorbed tin formed via disproportionation, without saturation with hydrogen; (3) as in (2) but after saturation with hydrogen $I = 0.25$mA.

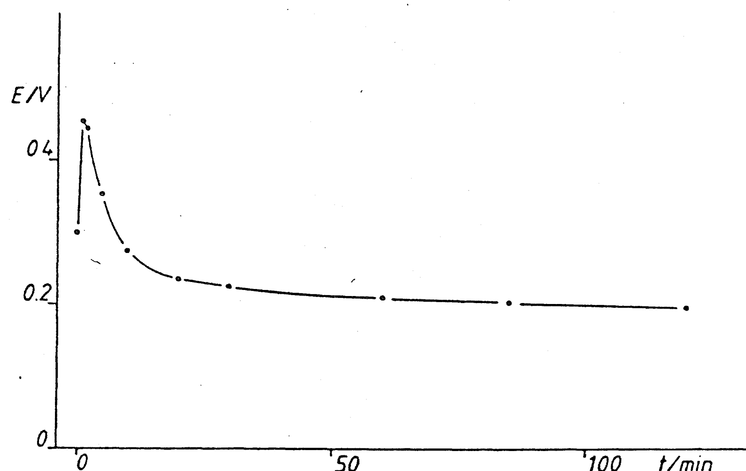

Fig. 2. Variation of the electrode potential during the formation of the adsorbed tin monolayer via disproportionation.

After equilibrium was reached, the charging curve of the electrode (curve 2 in Fig. 1) was determined in Sn^{2+} ion-free 1 *M* HCl solution, because the tin ions would have been oxidized during anodic polarization under these circumstances. This experiment was then repeated in the same way with the difference that the Pt electrode was saturated with hydrogen before determination of the charging curve (curve 3 in Fig. 1).

On the basis of Fig. 1, it can be stated that a monolayer of adsorbed tin was formed on the Pt surface and this monolayer almost completely inhibited the hydrogen adsorption. The question arises, however, what process is responsible for the unexpected tin adsorption.

In order to answer this question, the curve in Fig. 2 must be understood. No doubt, an electron-consuming process is responsible for the rising branch of the curve. The electron-consuming process can only be:

$$Sn^{2+} + 2\,e^{-} \rightarrow Sn_{ads} \quad (1)$$

Of course, for the decreasing branch an electron-producing process must be responsible, and it can only be catalytic oxidation of Sn^{2+} ions resulting in electrons and Sn^{4+} ions:

$$Sn^{2+} \rightarrow Sn^{4+} + 2\,e^{-} \quad (2)$$

The sum of reactions (1) and (2) is:

$$2\,Sn^{2+} \rightarrow Sn_{ads} + Sn^{4+} \quad (3)$$

which is a disproportionation. We call it catalytic disproportionation because it is a result of the catalytic feature of the platinum surface.

However, it is well known that Sn^{2+} ions do not disproportionate, because the

standard electrode potentials of the tin redox systems are:

$$Sn^{2+} + 2\,e^- \rightleftarrows Sn \qquad E^\circ = -0.136\,V \tag{4}$$

$$Sn^{4+} + 4\,e^- \rightleftarrows Sn \qquad E^\circ = 0.01\ V \tag{5}$$

$$Sn^{4+} + 2\,e^- \rightleftarrows Sn^{2+} \quad E^\circ = 0.15\ V \tag{6}$$

and their sequence is:

$$E^\circ_{Sn^{2+}/Sn} < E^\circ_{Sn^{4+}/Sn} < E^\circ_{Sn^{4+}/Sn^{2+}} \tag{7}$$

Standard electrode potentials, however, cannot be applied to underpotential deposition. Instead, the standard potentials (U_p) of the underpotential equilibria must be used because the equilibrium is established between adsorbed metal atoms and their ions in the solution [9]:

$$Sn^{2+} + 2\,e^- \rightleftarrows Sn_{ads} \qquad U_{p,Sn^{2+}/Sn_{ads}} \tag{8}$$

$$Sn^{4+} + 4\,e^- \rightleftarrows Sn_{ads} \qquad U_{p,Sn^{4+}/Sn_{ads}} \tag{9}$$

The surface does not affect the equilibrium of the Sn^{4+}/Sn^{2+} redox system, because this equilibrium exists in the homogeneous phase. For this reason, equilibrium (6) must be valid in the case of underpotential deposition, too. As a consequence, during underpotential depositon of tin, the following sequence of redox potentials must be valid:

$$U_{p,Sn^{2+}/Sn_{ads}} > U_{p,Sn^{4+}/Sn_{ads}} > E^\circ_{Sn^{4+}/Sn^{2+}} \tag{10}$$

which is the condition and so the explanation of disproportionation.

One of the most important problems in adsorption studies is the degree of charge transfer of the species undergoing adsorption. The degree of charge transfer of a layer of adatoms on the electrode is described by introducing the concept of electrosorption valency (γ) [10,11]. It follows that the charge required for the oxidation of adsorbed tin (Q_M, curve 2 in Fig. 1) is

$$Q_M = -\gamma F \Gamma_{ads} \tag{11}$$

where Γ_{ads} is the amount of adsorbed tin. (C is the double layer capacity in Fig. 1.)

As a consequence of the negative polarization (curve 3 in Fig. 1) for saturation with hydrogen, the adsorbed metal layer might be reduced to a zero valent layer; therefore, the charge Q_{M_F} required for its oxidation is

$$Q_{M_F} = -zF\Gamma_{ads} \tag{12}$$

Assuming that the experimental manipulations do not cause any loss of adsorbed tin, eqns. (11) and (12) can be used for the determination of electrosorption valency. It is calculated to be $\gamma = 3.6$.

The linear potential sweep of the electrode covered with adsorbed tin formed via disproportionation was also determined. Preparation of the electrode before the experiment was the same as in the case of curve 3 in Fig. 1. From the measurement it could be established that tin adsorption almost completely inhibited the hydrogen

adsorption and at 0.75 V there was a maximum which was 0.04 V more negative than the result published earlier [5]. This discrepancy can be explained by the complex-forming capacity of the chloride ions.

In this context it has to be mentioned that at the moment of introducing the required amount of the $SnCl_2$ salt solution to the main compartment of the cell the 1 *M* HCl supporting electrolyte became light yellow. This is very probably caused by the formation of $[Pt(SnCl_3)_2Cl_2]^{2-}$ complex ions [12].

Tin adsorption from the $SnCl_4$ solution via the ionization of hydrogen adsorbed on platinized platinum

After determining the charging curve from 0.06 V in 1 *M* HCl solution (curve 1 in Fig. 3), the platinized Pt electrode was resaturated with hydrogen by strong cathodic polarization. The surplus hydrogen was then flushed out of the cell with nitrogen and when the potential reached 0.06 V, $SnCl_4$ solution was introduced into the main compartment of the cell. As a consequence, the potential of the electrode rose to ca. 0.25 V, and its charging curve was curve 2 in Fig. 3. This experiment was then repeated in the same way but the charging curve of the tin-covered electrode was determined from 0.06 V in Sn^{4+} ions-free 1 *M* HCl supporting electrolyte (curve 3 in Fig. 3).

The convergence of curves 1 and 2 clearly indicates that adsorbed hydrogen has been replaced by tin adatoms without any loss. It follows that the mechanism of formation and desorption of the adsorbed tin layer is:

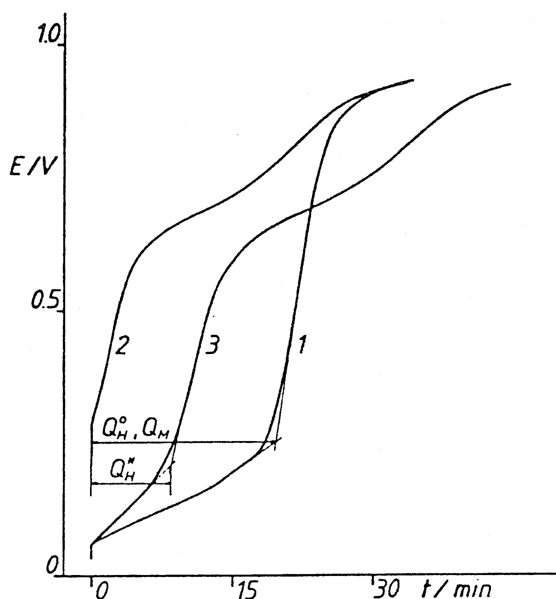

Fig. 3. (1) Charging curve in 1 *M* HCl solution; (2) charging curve of the electrode covered with adsorbed tin formed in $SnCl_4$ solution via the ionization of hydrogen adsorbed on platinized Pt in the presence of Sn^{4+} ions; (3) as in (2) but after saturation with hydrogen in the supporting electrolyte. I = 0.2 mA.

Formation:

$$Sn^{4+} + 4\,e^- \rightleftarrows Sn^{2+}_{ads} + 2\,e^- \rightleftarrows Sn_{ads} \quad (13)$$

$$H_{ads} \rightarrow H^+ + e^- \quad (14)$$

Desorption:

$$Sn_{ads} \rightleftarrows Sn^{2+}_{ads} + 2\,e^- \rightleftarrows Sn^{4+} + 4\,e^- \quad (15)$$

Since occasionally curves 1 and 2 in Fig. 3 did not overlap, during the formation of the adsorbed tin layer there was some loss of charge. For this reason the

$$Sn^{4+} + 2\,e^- \rightleftarrows Sn^{2+}_{ads} \rightleftarrows Sn^{2+}_{solution} \quad (16)$$

reaction must also be taken into consideration. This reaction, however, has always been of secondary importance because the loss never exceeded 10%.

By using the same method described in the preceding section, we also determined the electrosorption valency. From the data of Fig. 3 it is calculated to be $\gamma = 3.6$, which is the same value as that found in the case of disproportionation.

The linear potential sweep technique was also utilized to investigate this system. Pretreatment of the electrode before the experiment was the same as in the case of curve 3 in Fig. 3. As could be expected, the hydrogen adsorption was not completely inhibited and there was a maximum of tin desorption at 0.75 V.

Both the values of underpotential and electrosorption valency show that tin adsorption via disproportionation resulted in an adsorbed monolayer with the same character as tin adsorption via the ionization of hydrogen adsorbed on platinum.

Site requirement of an adsorbed tin atom

The number of hydrogen adsorption sites occupied by one adsorbed tin atom may be readily determined using the data of Figs. 1 and 3. In order to calculate this quantity, first the number of charges of the tin ions formed in the oxidation of adsorbed tin layer has to be determined.

As has been mentioned in the preceding section, from Fig. 3 it is immediately apparent that in the case of tin adsorption from $SnCl_4$ solution, via the ionization of adsorbed hydrogen the tin ions formed in the desorption are Sn^{4+} ions. Since the characteristics of the adsorbed tin layer formed via catalytic disproportionation are similar to an adsorbed tin layer formed via the ionization of adsorbed hydrogen, it may be supposed that the tin ions formed in the oxidation of adsorbed tin atoms are Sn^{4+} ions in the case of a tin layer formed via catalytic disproportionation, too.

In addition to the charge number of desorbing tin atoms, for the calculation of site requirement the amount of charge required for the oxidation of the adsorbed tin layer has to be determined. For adsorbed tin layers formed via disproportionation, the method and the equation:

$$S = \frac{Q^{\circ}_{\mathrm{H}} - Q^{x}_{\mathrm{H}}}{(Q^{\circ}_{\mathrm{H}} - Q^{x}_{\mathrm{H}} - Q_1 + Q_3)/z} \quad (17)$$

derived for the calculation of the site requirement of an adsorbed lead atom can be used to solve this problem [13]. From the data of Fig. 1 and using eqn. (17), the number S for an adsorbed tin atom was calculated to be 2.2 hydrogen adsorption sites.

From Fig. 3 it is apparent that the charge required for the oxidation of the adsorbed tin layer is equivalent to the charge needed for the oxidation of hydrogen adsorbed on the Pt surface free of adsorbed tin. Using the equation reported in our earlier paper [8]:

$$S = (Q_H^\circ - Q_H^x)/Q_M/z \qquad (18)$$

and taking into consideration that $Q_H^\circ = Q_M$, from the data of Fig. 3 the number of adsorption sites occupied by one adsorbed tin atom was calculated to be 2.2, which is the same number calculated for an adsorbed tin atom deposited via disproportionation. This is additional evidence of the similarity of the tin layers formed by these two methods.

4. On the slow desorption of adsorbed tin

Having decreased the HCl concentration in the supporting electrolyte, it became obvious that much tin remained on the Pt surface after anodic polarization. This observation is demonstrated in Fig. 4. In this experiment between the two positive-going sweeps (curves 2 and 3) the cell was rinsed with deoxygenated 0.2 *M* HCl solution in order to remove the desorbed tin ions. Despite this manipulation, tin could be detected on the surface (curve 3 in Fig. 4). It follows from this result that not only tin atoms but also tin ions adsorb so strongly on the Pt surface that only the complex-forming effect of chloride ions enables them to be desorbed. The desorption did not take place in perchloric acid media [7].

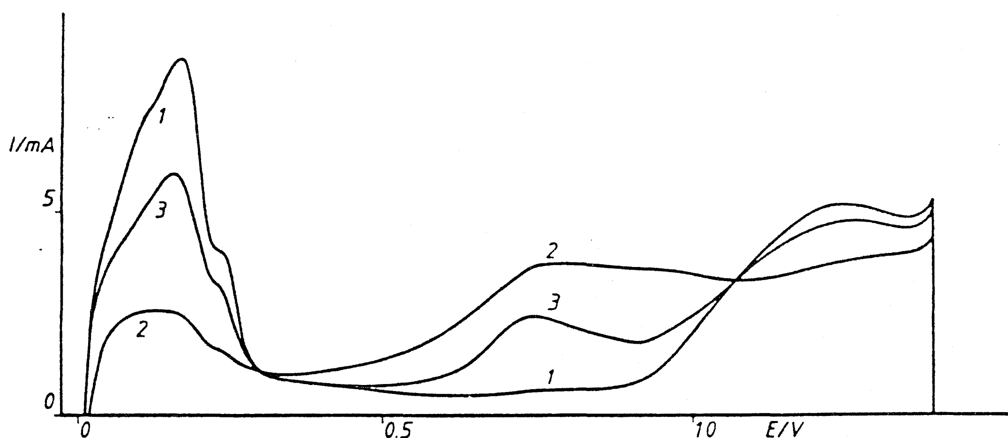

Fig. 4. (1) Potential sweep in 0.2 *M* HCl solution; (2) potential sweep of the electrode covered with adsorbed tin in 0.2 *M* HCl; (3) potential sweep of the electrode covered with adsorbed tin remaining on the surface after the preceding polarization. (Sweep rate = 7.7 mV/s.

Without strong adsorption of tin ions, the results shown in Fig. 3 could not have been obtained because the desorbing Sn^{2+} ions would have caused a loss of surface charge similar to that in copper or lead adsorption [11,13].

REFERENCES

1 B.J. Bowles and T.E. Cranshaw, Phys. Lett., 17 (1965) 258.
2 M.M.P. Janssen and J. Moolhuysen, Electrochim. Acta, 21 (1976) 861.
3 A.A. Mikhailova, N.V. Osetrova and Yu.B. Vassilyev, Elektrokhimiya, 13 (1977) 518.
4 Yu.B. Vassilyev, V.S. Bagotzky, N.V. Osetrova and A.A. Mikhailova, J. Electroanal. Chem., 97 (1979) 63.
5 N. Furuya and S. Motoo, J. Electroanal. Chem., 98 (1979) 195.
6 B. Beden, F. Kadirgan, C. Lamy and J.M. Leger, J. Electroanal. Chem., 127 (1981) 75.
7 V.A. Safonov, A.S. Lana, G.N. Mansurov and O.A. Petrii, Elektrokhimiya, 18 (1982) 1261.
8 S. Szabó and F. Nagy, J. Electroanal. Chem., 70 (1976) 357.
9 D.M. Kolb, M. Przasnyski and H. Gerischer, J. Electroanal. Chem., 54 (1974) 25.
10 J.W. Schultze and K.J. Vetter, J. Electroanal. Chem., 44 (1973) 63.
11 S. Szabó and F. Nagy, J. Electroanal. Chem., 84 (1977) 93.
12 Yu.A. Ryndin, private communication
13 S. Szabó and F. Nagy, J. Electroanal. Chem., 160 (1984) 299.

14.

J. Electroanal. Chem., 344 (1993) 303–311
Elsevier Sequoia S.A., Lausanne
JEC 02319

Study of electrochemical gold adsorption on polycrystalline platinum substrates

I. Bakos and S. Szabó *
Central Research Institute for Chemistry, Hungarian Academy of Sciences, PO Box 17, H-1525 Budapest (Hungary)

(Received 2 March 1992; in revised form 29 May 1992)

Abstract

The underpotential shift of adsorbed gold is about 0.06 V. Adatom deposition on a platinum surface may take place via ionization of the substrate metal. It may be assumed that during the oxidation of adsorbed gold, corrosion of the substrate metal catalysed by adsorbed gold also takes place. Contrary to earlier results, the number of hydrogen adsorption sites covered by one gold adatom is only about one.

INTRODUCTION

There are only a few papers in the electrochemical literature devoted to the study of gold adsorption on platinum substrates [1–6]. Although some of them have focused on the electrocatalytic effects of deposited gold atoms [3–5,7], our current knowledge concerning the processes of gold electrosorption on platinum surfaces is still rather limited.

As early as 1971, Cadle and Bruckenstein stated that gold does not deposit on platinum at underpotential and that deposited gold inhibits hydrogen adsorption [1]. Later, it was reported that bulk gold (Au_{bulk}) deposited via ionization of hydrogen adsorbed on platinized platinum spontaneously transformed into adsorbed gold (Au_{ads}) in the presence of $AuCl_4^-$ ions, but also without significant underpotential shift [2,8]. Although the study of gold electrodeposition on platinum surfaces revealed no underpotential shift, theoretical considerations suggest that the two phases (Au_{bulk}, Au_{ads}) existing on the surface must be different thermodynamically.

* To whom correspondence should be addressed.

0022-0728/93/$06.00 © 1993 – Elsevier Sequoia S.A. All rights reserved

It was also found that the number of hydrogen adsorption sites covered by one adsorbed gold atom depended on the gold coverage, and during oxidation of the adsorbed gold some other oxidation process was taking place in hydrochloric acid solution [2].

Continuing from our preliminary investigations [2], in this paper we seek to offer a deeper understanding of the phenomena occurring in the course of the electrodeposition of gold atoms on polycrystalline platinum surfaces.

EXPERIMENTAL

Experiments were carried out at room temperature in a three-compartment cell described earlier [9]. The most important feature of our cell is that cell solutions can be replaced with the exclusion of air; therefore a study of the substrate covered with foreign metal can be carried out in the absence of depositing ions or in different supporting electrolytes. This cell construction is excellent for the preparation of sandwich monolayer structures by the underpotential deposition of metals [10].

During the experiments purified nitrogen was bubbled through the main compartment of the cell to deoxygenate and agitate the solutions. The 0.2 M HCl and 0.5 M H_2SO_4 supporting electrolytes were prepared from Merck p.a. grade reagents with triply distilled water prepared as described elsewhere [9].

Smooth polycrystalline and platinized platinum electrodes were used as working electrodes; their apparent surface areas were 2 cm^2 and the roughness factors were about 1.9 and about 200 respectively. Platinization took place as described earlier [9].

One gram of $HAuCl_4$ was dissolved in 50 ml of 0.1 M HCl and in the course of gold deposition 0.5 ml of this solution was pipetted into the main compartment of the cell, which resulted in a 5×10^{-4} M gold ion concentration.

All potentials were referred to a hydrogen electrode immersed in the same supporting electrolyte in the main compartment of the cell.

RESULTS AND DISCUSSION

Determination of the underpotential shift of gold adsorption on platinum

Initially an attempt was made to reproduce our earlier results [2]. The method was the same as in our previous study of gold adsorption on platinized platinum electrodes. Exactly the same results were obtained, including the anomaly in the charging curve of the platinum electrode covered with Au_{ads} [2].

Next we attempted to determine the underpotential shift (defined by Kolb et al. [11]) of adsorbed gold. In this case the formation of an adsorbed monolayer also took place via ionization of hydrogen adsorbed on platinized platinum. The platinum electrode was first saturated with hydrogen, then, under open-circuit conditions (at 0.05 V), the gold ions were introduced into the main compartment

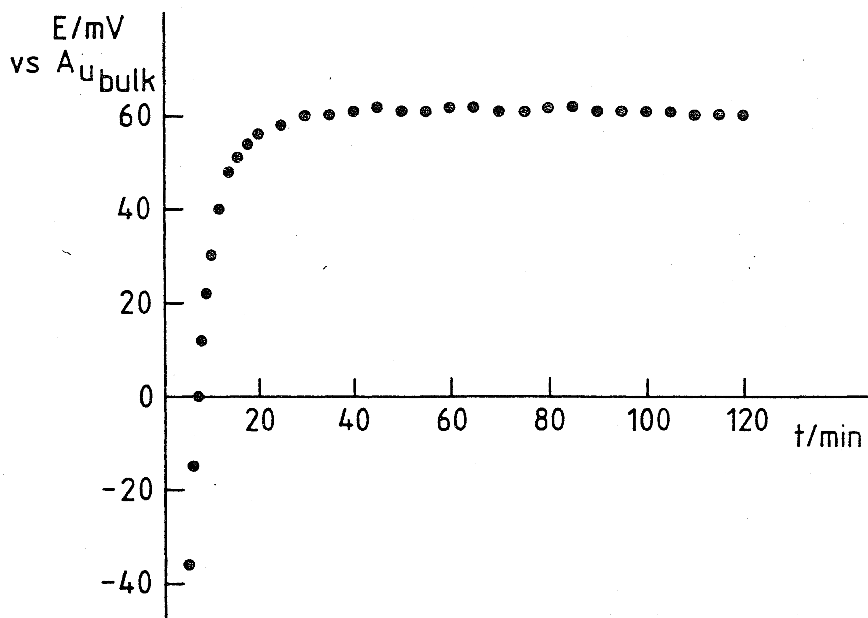

Fig. 1. The final section of potential variation during gold adsorption via ionization of hydrogen adsorbed on platinized platinum. (Reference electrode is bulk gold.)

of the cell [2]. This was followed by the transformation of adsorbed hydrogen into Au_{ads} with a simultaneous rise in potential towards the positive direction. The final section of the potential variation is illustrated in Fig. 1.

(Before the introduction of gold ions, a gold electrode in the form of a heavily gilded, smooth platinum needle was put in the main compartment of the cell and this gold electrode was used as a reference electrode during gold adsorption as illustrated in Fig. 1.)

As can be seen from Fig. 1, within 30 min the adsorbed hydrogen was ionized, the double layer was recharged and the potential rose to 0.06 V vs. the gold electrode, and then no further change was observed. ($Au_{bulk} \rightarrow Au_{ads}$ conversion took place rapidly in this case because the roughness factor of the electrode was small.) With respect to earlier observations [1,2] the 0.06 V underpotential (UPD) shift is quite significant.

At the end of this experiment the gold coverage was calculated from the decrease in hydrogen coverage. The result was $\theta \approx 0.75$, which is a much higher value than was attained in our previous investigations [2].

Since the measured potential shift is an equilibrium value (measured under open-circuit conditions) and the gold coverage is also known, an attempt can be made to calculate the standard UPD shift ($E^\circ_{Au^{3+}/Au_{ads}} - E^\circ_{Au^{3+}/Au} = \Delta U^\circ$) defined by Swathirajan and Bruckenstein [12]:

$$\Delta U = \Delta U^\circ + \frac{RT}{F}\left(\frac{1}{\gamma} - \frac{1}{z}\right) \ln(a_{Au^{3+}}) - \frac{RT}{\gamma F}\ln\left(\frac{\theta}{1-\theta}\right) \qquad (1)$$

When $\gamma \approx z$, which is usually the case with most UPD systems, and disregarding

the multiple-state character of the adsorbed species (assuming that $\theta \approx 0.75$ and $\Delta U \approx 0.06$ V),

$$\Delta U = \Delta U^\circ - \frac{RT}{3F}\ln\left(\frac{0.75}{0.25}\right) \tag{2}$$

The result of eqn. (2) shows that $\Delta U^\circ \approx 0.07$ V in the hypothetical absence of any interaction between adsorbed species and substrate metal (i.e. the Temkin and Frumkin parameters are equal to zero).

When HCl is used as the supporting electrolyte, mixed electrosorption can be expected because halide electrolytes do not behave indifferently during UPD processes [13]. The thermodynamic treatment of such an electrosorption reaction results in the definition of mixed electrosorption valency (γ_{mix}), which refers to the simultaneous adsorption or desorption of metal ions and halide ions [13]. The electrosorption valency (γ) in eqn. (1) is related to the mixed electrosorption valency by $\gamma_{mix_{Au}} = \gamma + \rho\gamma_{Cl^-}$, where ρ is the coupling factor.

Based on the change in oxidation state of Au_{ads} under more negative polarization of a gold-covered electrode, a rough estimation of $\gamma_{mix_{Au}}$ was made and resulted in $\gamma_{mix_{Au}} \approx 2.6$. Assuming $\gamma \approx 2.9$ and $\gamma_{Cl^-} \approx -1$ as in the case of silver electrodes [13], we obtain a value of $\rho \approx 0.3$. This result indicates a co-adsorption of gold and chloride and is in accordance with earlier experimental observations, i.e. anion adsorption is increased by metal adsorption [14].

The increased chloride adsorption brought about by gold adsorption may serve as an explanation for the corrosion of a platinum substrate being enhanced by adsorbed gold.

Spontaneous gold adsorption

The different gold coverage data measured by gold adsorption via ionization of pre-adsorbed hydrogen indicated that some other reaction must also take place on the surface which results in adatoms. The following experiment was carried out to verify this concept.

After determination of the cyclic voltammogram of the platinized platinum electrode in 0.5 M H_2SO_4 (curve 1 in Fig. 2), the cell solution was replaced by 0.2 M HCl and the potential was scanned to 0.9 V. Under open-circuit conditions at this potential 0.5 ml of gold solution was introduced into the main compartment of the cell. As a result the potential rose to 1.057 V within 30 min and then did not change. After 150 min the cell was washed free of chloride ions with deoxygenated, triply distilled water and refilled with deoxygenated 0.5 M H_2SO_4. The cyclic voltammogram of the platinum electrode after this procedure is shown as curve 2 in Fig. 2.

It is immediately evident from the figure that considerable gold coverage is formed on the platinum surface without any external intervention. The question arises as to what kind of a process is responsible for this unexpected gold adsorption.

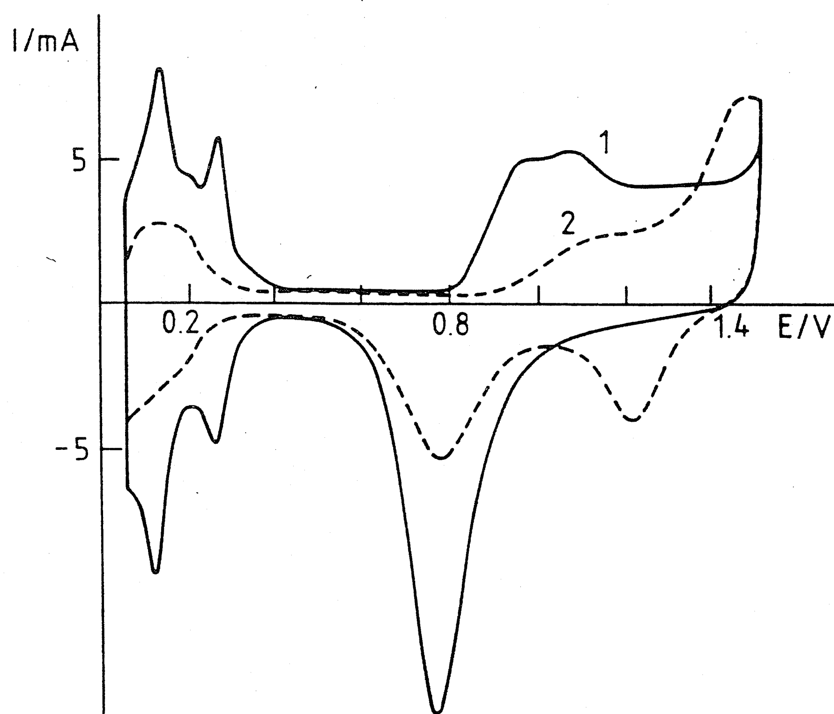

Fig. 2. Cyclic voltammogram of the platinized platinum electrode in 0.5 M H_2SO_4 (curve 1). Cyclic voltammogram of the same platinized platinum electrode (also in 0.5 M H_2SO_4) covered with adsorbed gold deposited spontaneously in 0.2 M HCl (curve 2). (Sweep rate 25 mV s^{-1}.)

One possible reaction is the disproportionation of Au^+ ion traces (similar to the disproportionation of Sn^{2+} ions [15]) resulting in adsorbed gold atoms. In order to verify the correctness of this assumption, we repeated the above-described experiment under the same conditions (open circuit, 0.9 V), but with the difference that the gold deposition was carried out in 0.5 M H_2SO_4 instead of 0.2 M HCl. In this case only about 20% gold coverage was formed on the platinum surface, whereas the gold coverage calculated from the decrease in hydrogen coverage using the data of Fig. 2 was found to be 66%. Very probably the exchange of the supporting electrolyte cannot cause such a great decrease in gold coverage if disproportionation plays an important role.

Another method to prove that disproportionation of Au^+ ions cannot be responsible for the spontaneous gold adsorption is to use a smooth platinum electrode. (The smaller real surface area makes it possible to develop a higher gold coverage in the same time interval, because the diffusion is proportional to the apparent surface area.) Although gold deposition took place also in 0.2 M HCl, only 20% gold coverage was formed, which proves that disproportionation cannot be the cause of the gold adsorption.

There is now only one reaction which can explain the spontaneous gold adsorption, namely metal adsorption via ionization of the substrate metal [8]:

$$Pt \rightarrow Pt^{4+} + 4e^- \tag{3}$$

$$Au^{3+} + 3e^- \rightarrow Au_{ads} \tag{4}$$

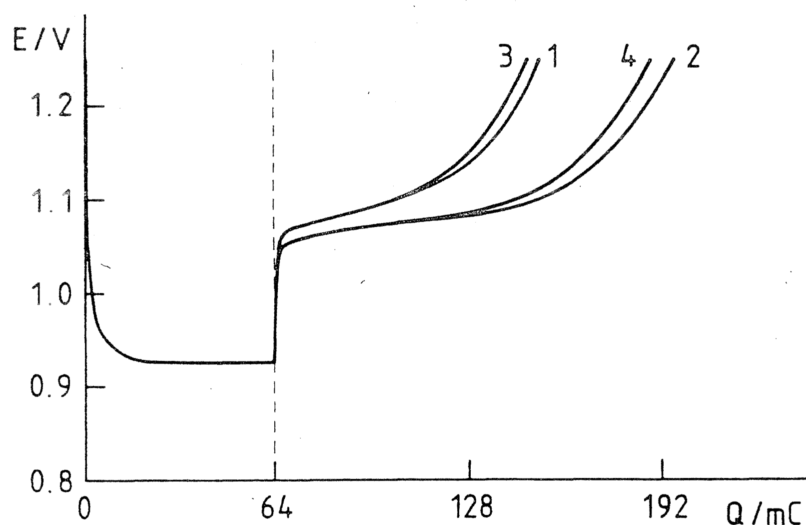

Fig. 3. Cathodic polarization of the platinized platinum electrode in 0.2 M HCl and 5×10^{-4} M $AuCl_3$ solution at 0.2 mA from 1.25 V to 64 mC. The current is then reversed and polarization is continued to 1.25 V (curve 1). The experiment is repeated, but with the difference that the reverse current is 0.04 mA (curve 2). (Curves 3 and 4 are the results of repetition.)

In other words, platinum is oxidized by Au^{3+} ions and as a result adsorbed gold is formed on the platinum surface. It can be assumed that Pt^{4+} ions are formed, because at the potential of gold deposition (about 1.06 V) the formation of such ions can be expected.

Dependence of the amount of charge used for oxidation of Au_{ads} on the current density

The gold coverage formed on platinum via ionization of pre-adsorbed hydrogen is always subject to error caused by uncontrolled gold adsorption via ionization of the substrate metal. For this reason, in the course of these experiments the adsorbed gold was deposited by cathodic polarization in 0.2 M HCl and 5×10^{-4} M $AuCl_3$ solution at 0.2 mA for 320 s, starting from 1.25 V. The direction of the current was then reversed and polarization was continued up to 1.25 V as well (curve 1 in Fig. 3). This experiment was repeated, but with the difference that the anodic branch of the curve was polarized at 0.04 mA (curve 2 in Fig. 3). (Curves 3 and 4 in the figure depict the results of the repeated experiments. The discrepancies between curves 1 and 2 as well as between curves 3 and 4 are due to aging caused by corrosion as a result of anodic polarization.)

As can be seen from the figure, the amount of charge required for the oxidation of adsorbed gold depended on both current density and surface activity. It follows from this that besides the oxidation of adsorbed gold, one or more other surface reactions were going on as a result of the catalytic effect of the gold-covered platinum surface, because destruction of the adsorbed gold layer by anodic polarization puts an end to the unknown reactions.

On the anomaly in the charging curve of the gold-covered platinum electrode

For the oxidation of adsorbed gold deposited via ionization of pre-adsorbed hydrogen, two or three times as much charge was required as for the oxidation of adsorbed hydrogen used for its deposition (including double-layer recharging) [2]. In our earlier paper the phenomenon was termed the "anomaly in the charging curve of the gold-covered platinum electrode" and was explained by chloride ion oxidation because the anomaly was experienced only in hydrochloric acid media [2].

As has been demonstrated earlier, gold adsorption may take place via ionization of the platinum substrate metal and naturally also results in a charge surplus during the oxidation of adsorbed gold. This surplus, however, is too small to explain the anomaly. (On the other hand, the amount of charge required for the oxidation of adsorbed gold cannot depend on the current density.)

According to Fig. 3, however, the amount of charge used for the oxidation of the same amount of adsorbed gold depends on the current density and surface activity; therefore the calalytic oxidation of chloride ions catalysed by gold-covered platinum cannot be excluded [2].

The existence of spontaneous gold adsorption and the formation of platinum ions, which are detectable (with $SnCl_2$ solution [16]) at the end of polarization of a gold-covered platinum electrode, indicate that besides the oxidation of Cl^- ions, the corrosion of substrate metal (reaction (3)) catalysed by gold adatoms must also be taken into consideration in the explanation of the anomaly.

The concept of corrosion of the platinum substrate is supported by an old observation, namely that if platinum is alloyed with gold and silver, it then becomes soluble in nitric acid [17].

Site requirement of an adsorbed gold atom

From the results of spontaneous gold adsorption it may be concluded that the number of hydrogen adsorption sites covered by one adsorbed gold atom (site requirement) is lower than was measured earlier [2], because spontaneous gold adsorption makes impossible the calculation of the gold coverage from the amount of charge used for its deposition. For the above reasons the differences in oxygen adsorption on platinum and gold can be utilized better for this purpose than the earlier method [2].

The above concept was verified in the following experiments. The smooth platinum electrode was kept at 1.5 V in 0.5 M H_2SO_4 solution for 100 s and then polarized to the onset of hydrogen adsorption (curve 1 in Fig. 4). After this polarization its charging curve (from 0.08 V) was also determined (curve 2 in Fig. 4) and the cell solution was exchanged for 0.2 M HCl. In the presence of a 5×10^{-4} M Au^{3+} ion concentration an adsorbed gold layer was formed on the platinum surface by polarization at 1.01 V for 10 min.

When the gold deposition was finished, the cell was washed free of Au^{3+} and Cl^- ions with deoxygenated, triply distilled water and filled with deoxygenated 0.5

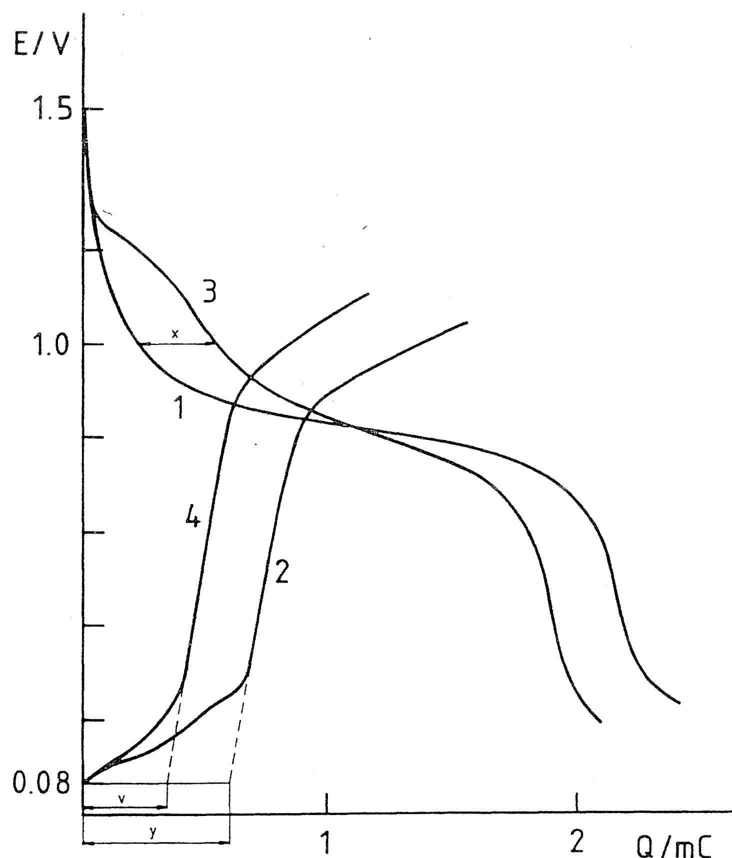

Fig. 4. Charging curve of the smooth platinum electrode in 0.5 M H_2SO_4 kept at 1.5 V for 100 s ($I = 0.02$ mA) (curve 1). Charging curve of the same electrode also in 0.5 M H_2SO_4 from 0.08 V with the same current (curve 2). Charging curves of the gold-covered electrode in the same electrolyte (curves 3 and 4).

M H_2SO_4; then the oxygen adsorption character (curve 3 in Fig. 4) and hydrogen adsorption character (curve 4 in Fig. 4) of the gold-covered electrode were determined. From Fig. 4 the data required for the calculation of the number of hydrogen adsorption sites covered by one adsorbed gold atom (S) can easily be determined.

The amount of charge required for the oxidation of hydrogen adsorbed on platinum free of gold is $Q_H^0 = y/0.8$ assuming that at 0.08 V the hydrogen coverage on the platinum surface is about 0.8 [18].

The amount of charge required for the oxidation of hydrogen adsorbed on gold-covered platinum is $Q_H^x = v/0.8$.

The amount of oxygen adsorbed on the gold-covered area of the platinum surface is $O_{ads}^{Au} = x/0.52$, because at 1.5 V, according to our measurements based on literature data, the oxygen coverage on gold is about 0.52 [18] and it is assumed that the oxygen adsorption character of the adsorbed gold is equal to that of pure gold.

Thus the site requirement is now [8,9]

$$S = \frac{Q_H^0 - Q_H^x}{Q_M/z} = \frac{Q_H^0 - Q_H^x}{O_{ads}^{Au}/2} \tag{5}$$

because instead of the oxidation of adatoms, in this case the oxygen adsorbed on adatoms is reduced and every oxygen atom requires two electrons. Calculated from the data of Fig. 4, $S = 1.06$, which is considerably lower than our earlier result [2]; therefore it may be concluded that spontaneous gold adsorption in fact plays an important role in adsorbed gold layer formation.

Considering the results of our other measurements, $S \approx 1$ and is not dependent on the coverage. The equilibrium coverage of absorbed gold on platinum, however, depends on the deposition potential. At 1.03 V it is $\theta \approx 0.3$, but at 1.01 V it is as high as $\theta \approx 0.9$.

ACKNOWLEDGMENT

The authors are indebted to the Hungarian Research Fund (No. OTKA: 1 777) for financial support.

REFERENCES

1 S.H. Cadle and S. Bruckenstein. Anal. Chem., 43 (1971) 1858.
2 S. Szabó and F. Nagy. J. Electroanal. Chem., 85 (1977) 339.
3 M. Watanabe and S. Motoo, J. Electroanal. Chem., 60 (1975) 259.
4 N. Furuya and S. Motoo. J. Electroanal. Chem., 88 (1978) 151.
5 G. Pierre, M. El Kordi and G. Cauquis, Electrochim. Acta, 30 (1985) 1219.
6 D.M. Kolb, in H. Gerischer and C.W. Tobias (Eds.), Advances in Electrochemistry and Electrochemical Engineering. Vol. 11. Wiley, New York, 1978, p. 125.
7 R.R. Adzic, in H. Gerischer and C.W. Tobias (Eds.), Advances in Electrochemistry and Electrochemical Engineering. Vol. 13, Wiley, New York, 1985, p. 159.
8 S. Szabó, Int. Rev. Phys. Chem., 10 (1991) 207.
9 S. Szabó and F. Nagy. J. Electroanal. Chem., 70 (1976) 357.
10 H.-J. Pauling and K. Jüttner, Abstr. ISE 42nd Meeting, Montreux, 1991, p. 3–17.
11 D.M. Kolb, M. Przasnyski and H. Gerischer, J. Electroanal. Chem., 54 (1974) 25.
12 S. Swathirajan and S. Bruckenstein, Electrochim. Acta, 28 (1983) 865.
13 J.W. Schultze and K.J. Vetter, Electrochim. Acta, 19 (1974) 45.
14 G. Horányi, J. Electroanal. Chem., 55 (1974) 45.
15 S. Szabó, J. Electroanal. Chem., 172 (1984) 359.
16 S. Szabó, I. Bakos, F. Nagy and T. Mallát, J. Electroanal. Chem., 263 (1989) 137.
17 I.E. Cottington, Platinum Met. Rev., 35 (1991) 141.
18 R. Woods, in A.J. Bard (Ed.), Electroanalytical Chemistry, Vol. 9, Marcel Dekker, New York/Basel, 1976, p. 1.

15.

т. XVIII, вып. 9 ЭЛЕКТРОХИМИЯ 1982

УДК 541.183

ИССЛЕДОВАНИЕ АДСОРБЦИИ РЕНИЯ НА ПЛАТИНИРОВАННОМ ПЛАТИНОВОМ ЭЛЕКТРОДЕ В РАСТВОРЕ ХЛОРНОЙ КИСЛОТЫ

Ифанди М., Сабо Ш., Надь Ф.

Изучена адсорбция рения на Pt/Pt-электроде по влиянию ее на ионизацию адсорбированного водорода с учетом реакций диспропорционирования. Определено количество адсорбционных мест S, занятых адатомами рения. Рассмотрено влияние рения на адсорбцию водорода и гидрогенизацию ацетона.

В настоящее время хорошо известно, что активность платиновых катализаторов при добавке других металлов может возрастать. С этой точки зрения особый интерес представляют катализаторы платина – рений [1]. Тем не менее процесс адсорбции рения на платине мало изучен [2], хотя изучение платиновых катализаторов, содержащих адсорбированный рений, может способствовать лучшему пониманию специфических особенностей системы Re — Pt.

Изучение адсорбции рения затруднено из-за большого числа степеней его окисления и протекания во время адсорбции различных редокс-реакций [3].

Цель настоящей работы — изучение адсорбции рения на платине и особенностей покрытого рением платинового электрода. Исследовали также влияние адсорбции рения на ионизацию водорода на Pt/Pt-электроде.

Экспериментальная часть

Опыты проводили в трехэлектродной ячейке, описанной в [4]. Вводимые в ячейку растворы предварительно освобождались от растворенного воздуха продувкой азота. Раствор фона 1 M $HClO_4$ готовили на тридистиллате из 60%-ной хлорной кислоты марки МЕРК. Раствор 0,2 M HCl+ +2,3 M $(NH_4)_2ReCl_6$ готовили из кристаллического $(NH_4)_2ReCl_6$ марки ICN.

Рабочим электродом служил платинированный платиновый электрод, приготовленный по методу, описанному в [4], с истинной поверхностью ~1 м². Опыты проводили при комнатной температуре. Потенциалы E измеряли относительно водородного электрода в 1 M $HClO_4$.

Для изучения адсорбции Re применяли методы кривых заряжения, потенциодинамический и адсорбционных потенциалов.

После снятия кривой заряжения в растворе фона Pt-электрод выдерживался в течение нескольких секунд при E=0, после чего анодным током убывающей силы потенциал электрода доводили до потенциала адсорбции. Раствор рения вводили при замкнутой цепи и следили за изменением потенциала во времени. По достижении постоянной величины потенциала раствор удалялся, ячейку промывали 2—3 раза раствором фона, предварительно продутым азотом, и снова снимали кривую заряжения.

Результаты и их обсуждение

Из кривых зависимости потенциала от времени, представленных на рис. 1, видно, что адсорбция на платине носит сложный характер и зависит от начального потенциала адсорбции. Следует также отметить, что при исходном потенциале в интервале 0,3÷0,7 В конечное значение потенциала лежит в промежутке 0,39÷0,42 В. Наблюдаемое поведение потенциала электрода можно объяснить с точки зрения термодинамической теории платинового водородного электрода [5], учитывая, что в нашем случае имеет место совместная адсорбция хлорид-иона, как присутствующего в рениевом растворе, так и входящего в состав гексахлороренит-иона, и катиона рения.

Исследование адсорбции рения на платине по влиянию ее на ионизацию водорода. Как видно из рис. 2, адсорбция Re при потенциалах водородной области приводит к образованию соединения по количеству, эквивалентному количеству адсорбированного водорода. Это подтверждает совпадение кривых *1* и *3*. Из потенциодинамических кривых, приведенных на рис. 3, следует, что образующееся соединение приводит к уменьшению адсорбции водорода обоих видов.

Поскольку задержка, соответствующая окислению рениевого соединения на кривых *2*, *3* рис. 2, одинакова, то, очевидно, что катодная поляри-

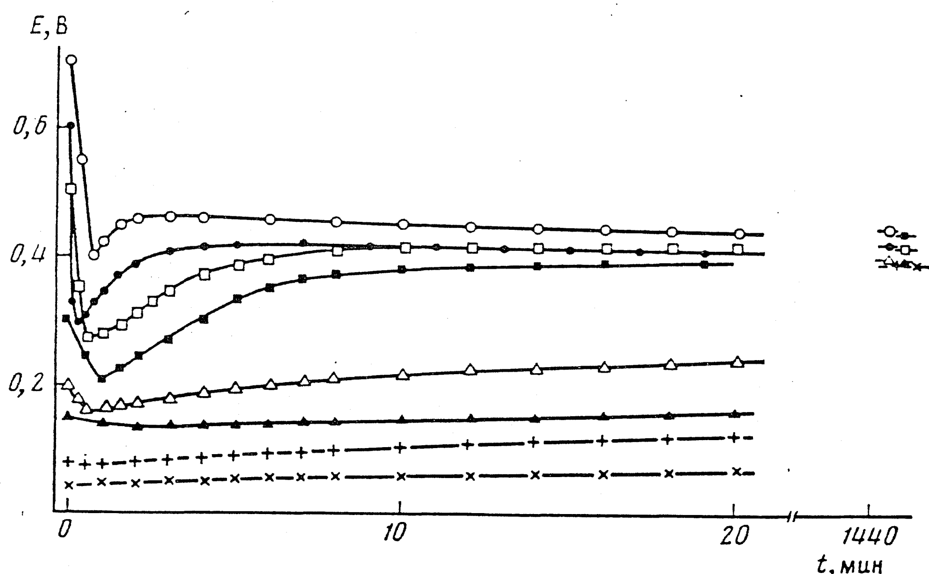

Рис. 1. Изменение потенциала во времени при введении 2,3 *М* $(NH_4)_2ReCl_6$+0,2 *М* HCl в раствор 1 *М* $HClO_4$ при различных исходных потенциалах

зация электрода не изменяет валентность адсорбированного вещества. На основании этих данных можно предположить наличие на поверхности платины адсорбированного рения, образующегося в ходе следующих процессов:

$$H_a \rightarrow H^+ + e, \quad (1)$$

$$ReCl_6^{2} \pm 4e \rightarrow Re_a + 6Cl^-. \quad (2)$$

Определение числа адсорбционных мест, занятых адсорбированными атомами рения. Исходя из предыдущих реакций и используя кривые *1*, *2* рис. 2, можно определить количество адсорбционных мест S (в расчете, что на каждое адсорбционное место адсорбируется один атом водорода), занятых одним адсорбированным атомом рения, как это описано в [4, 6].

$$S=\frac{Q_{\text{н}}^0-Q_{\text{н}}^x}{\frac{Q_{\text{м}}}{z}}=\frac{\Delta Q_{\text{н}}}{\frac{Q_{\text{м}}}{z}}\approx 2,3, \quad (3)$$

где $\Delta Q_{\text{н}}$ — изменение покрытия водородом, $Q_{\text{м}}$ — количество электричества, пошедшее на окисление адсорбированного вещества, z — изменение заряда иона рения в результате адсорбции.

Тот же самый результат следует и из рис. 4, где приведена зависимость величины $Q_{\text{м}}/\Delta Q_{\text{н}}$, определяющей количество электронов на единицу поверхности адсорбции, необходимых для окисления специфически адсорбированного рения, от потенциала адсорбции. Для потенциалов $E<0,3$ В эта величина равна ~2 и уменьшается до единицы для $E\geqslant 0,5$ В. Если предположить, что на поверхности платины протекает реакция (2), получим $S=2$.

Из рис. 4 следует, что при потенциалах $E>0,5$ В на поверхности электрода имеются Re_a^{2+}-ионы или ReO, так как число электронов, принимаю-

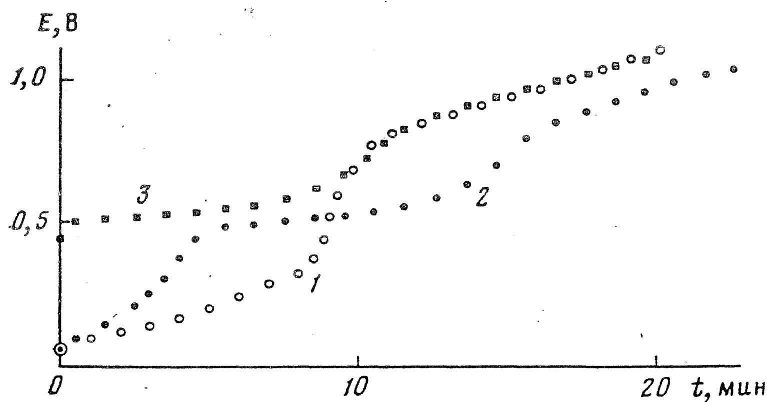

Рис. 2. Влияние адсорбции катионов рения на ход кривых заряжения: *1* – исходная кривая заряжения в 1 *М* $HClO_4$; *2*, *3* – кривые заряжения платинового электрода, покрытого адсорбированным рением, после насыщения электрода водородом (*2*) и без насыщения электрода водородом (*3*) в 1 *М* $HClO_4$ I=0,75 мА

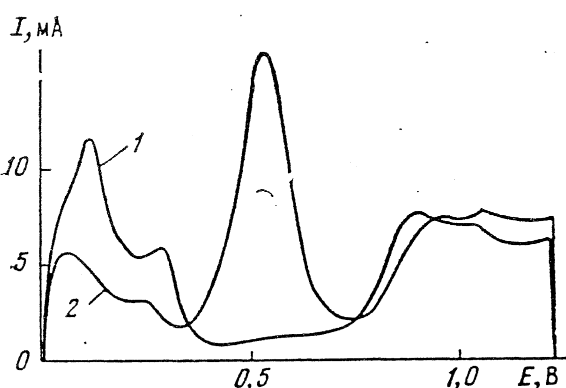

Рис. 3. Потенциодинамические кривые Pt/ /Pt-электрода в 1 *М* $HClO_4$: *1* – чистый электрод; *2* – электрод, покрытый адатомами рения. Скорость развертки потенциала 10,3 мВ/с

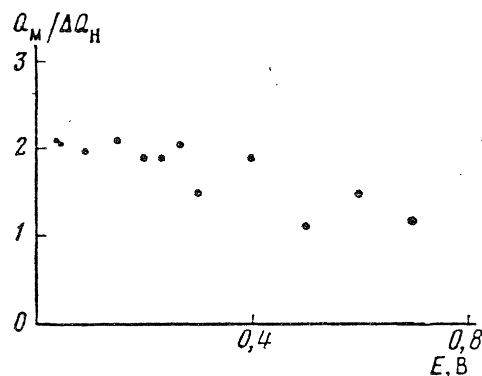

Рис. 4. Зависимость величины $Q_м/$ $/\Delta Q_н$ от потенциала в 1 *М* $HClO_4$

щих участие в реакции, равно 2, а не 4. Этот вывод справедлив, если величина S не изменяется при изменении степени покрытия поверхности рением.

Адсорбция рения при потенциалах двойнослойной области. В этой области потенциалов адсорбция рения протекает по другому механизму.

Общее количество адсорбированного соединения почти не изменяется, а потенциал его окисления лежит в той же области, что и для рения, образующегося за счет ионизации водорода, как это видно на рис. 5. Это говорит о том, что на поверхности платины и в этом случае имеется адсорбированный рений, образующийся, однако, за счет диспропорционирования $ReCl_6^{2-}$ по следующим реакциям [7]:

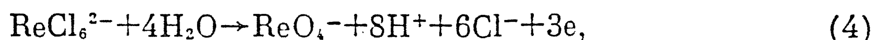

$$ReCl_6^{2-}+4H_2O \rightarrow ReO_4^-+8H^++6Cl^-+3e, \quad (4)$$

$$ReCl_6^{2-}+4e \rightarrow Re_a+6Cl^-. \quad (5)$$

Как было показано выше расчетом количества электронов, необходимых для окисления имеющегося на поверхности соединения, при этих потенциалах также можно предположить наличие Re_a^{2+}-ионов или ReO. Нормальный потенциал редокс-системы $ReCl_6^{2-}/Re^{2+}$, рассчитанный по правилу Лютера, составляет 0,45 В. В этом случае вместо реакции (5) имеем

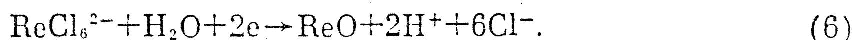

$$ReCl_6^{2-}+H_2O+2e \rightarrow ReO+2H^++6Cl^-. \quad (6)$$

Адсорбции оксида рения противоречит то, что адсорбированное вещество не растворяется даже в 4 *М* HCl. Из этого можно сделать вывод, что па-

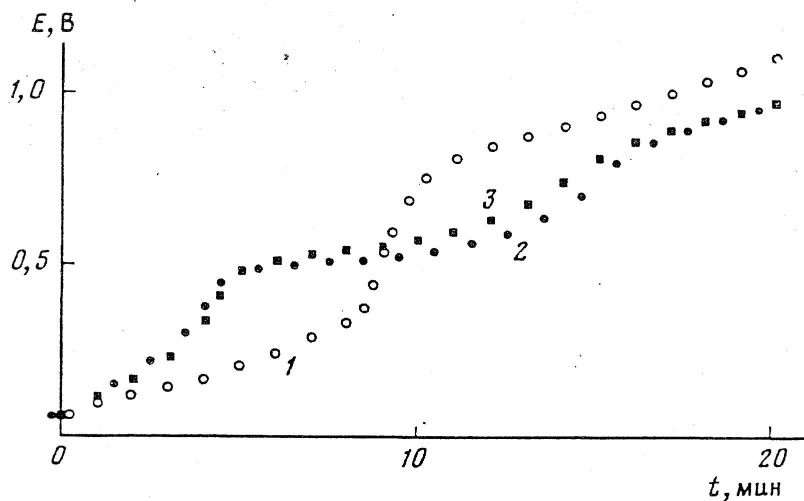

Рис. 5

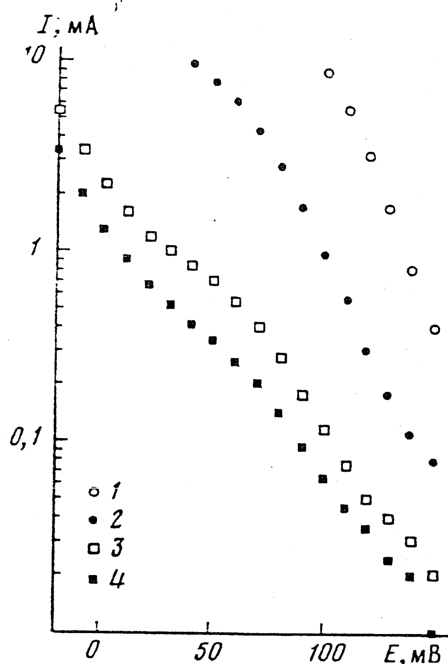

Рис. 6

Рис. 5. Исходная кривая заряжения Pt-электрода в 1 *М* $HClO_4$ (*1*) и кривые заряжения Pt-электрода, покрытого рением, адсорбированным при E=80 мВ (*2*) и 500 мВ (*3*) после насыщения электрода водородом. I=0,75 мА

Рис. 6. Зависимость поляризационных кривых Pt-электрода в растворе 0,14 *М* $CH_3-CO-CH_3$+1 *М* $HClO_4$ от степени покрытия платины адсорбированным рением. Значения θ_{Re}: *1* – 0,0; *2* – 0,41; *3* – 0,54; *4* – 0,60

дение величины $Q_м/\Delta Q_н$ до единицы (рис. 4) имеет место из-за изменения S, а реакция (6) не протекает.

Гидрогенизация ацетона на Pt/Pt-электроде, покрытом адсорбированным рением. Представлялось интересным изучить влияние адатомов рения на различные каталитические реакции. В качестве примера была выбрана реакция гидрогенизации ацетона [8].

На рис. 6 показано влияние адатомов рения на гидрогенизацию ацетона. Как видно, чем больше степень покрытия платины рением, тем с меньшей скоростью идет процесс. В дальнейшем интересно исследовать только область малых степеней покрытия.

ЛИТЕРАТУРА

1. *Ciapetta F. G., Wallace D. N.* Catalysis Reviews, 1971, v. 5, p. 67.
2. *Janssen M. M. P., Moolhuysen J.* Electrochim. Acta, 1976. v. 21, p. 869.
3. *Рипан Р., Четяну И.* Неорганическая химия, т. 2. М.: Мир, 1972, с. 440.
4. *Szabó S., Nagy F.* J. Electroanalyt. Chem., 1976, v. 70, p. 357.
5. *Frumkin A. N., Balashova N. A., Kazarinov V. E. J.* Electrochem. Soc., 1966, v. 113, p. 1011.
6. *Furuya N., Motoo S.* J. Electroanalyt. Chem., 1979, v. 98, p. 189.
7. *Busey R. H., Gayer K. H., Gilbert R. A., Bevan R. B.* J. Phys. Chem., 1966, v. 70, p. 2609.
8. *Horányi Gy., Sólt J., Szabó S., Nagy F.* Acta Chim. Acad. Sci. Hung., 1971, v. 68, p. 205.

Центральный исследовательский химический институт Академии наук Венгрии, Будапешт

Поступила в редакцию 8.VI.1981

16.

React. Kinet. Catal. Lett., Vol. 6, No. 1, 89–94 (1977)

TPD STUDIES OF HYDROGEN SORPTION ON PLATINUM POWDER CATALYSTS MODIFIED WITH ADSORBED GOLD

S. Szabó, D. Móger, M. Hegedűs and F. Nagy

Central Research Institute for Chemistry,
Hungarian Academy of Sciences,
1525 Budapest, P. O. Box 17

Received September 8, 1976
Accepted September 15, 1976

It has been shown that hydrogen determined from the TPD curves of platinum saturated with hydrogen sorbed above room temperature is chiefly absorbed and not adsorbed hydrogen; this absorbed hydrogen has no effect on the charging curve.

На основании измерений кривых термодесорбции сорбированного на платине водорода показано, что водород, главным образом, абсорбируется, а не адсорбируется; этот абсорбированный водород не оказывает влияния на ход кривых заряжения.

When interpreting the results of thermodesorption (TPD) studies on the platinum/hydrogen system, one encounters the problem of the source of desorbed hydrogen: does it come from the surface, or from "within" the catalyst, or from both? The solution is important theoretically and practically, because it helps both the interpretation of TPD curves and surface determination by means of hydrogen adsorption.

A way to separate adsorbed hydrogen from absorbed hydrogen is to cover the hydrogen adsorption sites of the platinum surface with an adsorbed substance that will not adsorb hydrogen and will withstand the thermal treatment during TPD. According to our investigations, gold adsorbed on platinum meets these requirements /2, 3/.

EXPERIMENTAL

The TPD apparatus and method, as well as the preparation and pretreament of the the catalyst used was the same as described in our previous papers /4-6/. The only difference was that the catalyst covered with adsorbed gold was heated only to 300°C in order to avoid the formation of an alloy, and then it was kept at this temperature for 10 min.

The gold-covered catalyst was prepared by means of metal adsorption via the ionization of hydrogen adsorbed on platinum, in a 0.2 M HCl solution /2/. Prior to use, Cl^- ions were removed from the catalyst by washing with deoxygenated, triply distilled water.

The preparation of the modified catalyst and the determination of the charging curves was performed in an electrochemical cell, the main compartment of which was bottomed with a polished platinum plate. The thermally treated platinum catalyst particles were placed on this plate and could be polarized through the plate in the same manner as a compact electrode.

In the modification of the catalyst and the determination of the charging curves, the potential was measured with respect to the 1 atm hydrogen electrode in a solution of the same pH.

RESULTS

1. Thermodesorption studies

Prior to the thermodesorption experiments, it was ascertained that a prolonged thermal treatment at 300°C did not change the catalytic properties of the platinum catalyst covered with adsorbed gold. This was followed by the TPD investigation of the gold-covered and of the clean catalyst, as described in our previous paper /4/.

3 g of the catalyst was placed in the reactor and heated to 300°C in nitrogen in 10 min, then evacuated to 10^{-3} Torr. The reactor was then filled with 1 atm hydrogen and kept at 300°C for 1 hr, then the system was cooled to room temperature in 3 hrs and the catalyst left under hydrogen for the next 18 hrs.

The TPD curves were recorded in a flow of N_2 (20 cm^3/min) at a heating rate of 15°C/min. The result is shown in Fig. 1. It can be seen that gold adsorption has

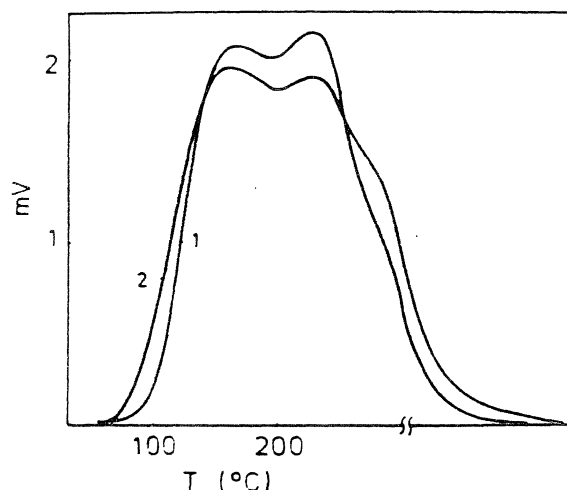

Fig. 1. TPD curves of the gold-free (1) and of the gold-covered catalyst (2)

practically no effect on the amount of adsorbed hydrogen, consequently, the hydrogen in the various sorption states, as observed by TPD above 20°C, does not occupy the same active sites as gold. In other words, the hydrogen is not directly on the surface.

Results obtained in studies of the interaction of platinum and hydrogen sorbed above room temperature /7/, and of the reaction of the hydrogen and oxygen thus sorbed /8/, support this conclusion.

2. Charging curve of the gold-covered catalyst after determination of the TPD curve

The charging curve of the gold-covered catalyst as well as that of the clean surface after removal of the gold layer were recorded after determination of the TPD

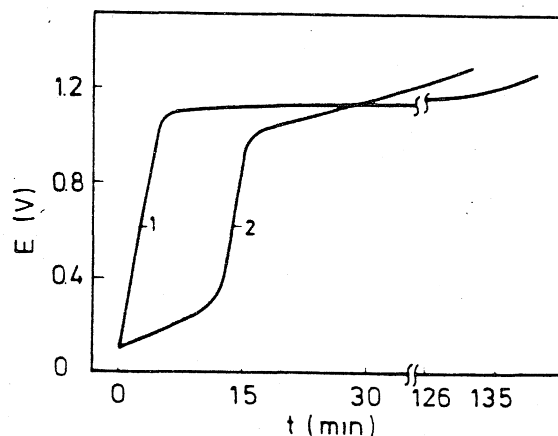

Fig. 2. Charging curves of the gold-covered catalyst in 0.2 M HCl solution after recording the TPD curve (1) and after removing the gold layer (2)

curve. The comparison of curves 1 and 2 in Fig. 2, respectively, shows that the surface was almost completely covered with gold; the hydrogen capacity is close to zero. Consequently, the hydrogen determined by TPD could not come from the adsorption sites where gold was adsorbed.

Supposing that hydrogen sorbed from both the gas phase and aqueous solutions occupies the same adsorption sites /9/, it can be concluded that the hydrogen determined by TPD is not adsorbed but absorbed.

The area under the TPD curves in Fig. 1 is equivalent to $\sim$700 μl gaseous hydrogen; the amount of hydrogen calculated from the hydrogen region of the charging curve of clean platinum (shown in Fig. 2) is $\sim$90 μl. These data also indicate that the hydrogen determined by TPD is chiefly absorbed hydrogen.

3. Charging curve of platinum saturated with hydrogen above room temperature

Investigations of the reaction of hydrogen and oxygen sorbed above room temperature have shown that platinum saturated with hydrogen remains stable in the presence of oxygen /8/. An electrochemical investigation of this was made in the following way. 3 g of the catalyst was saturated with hydrogen and the charging curve was determined (curve 1 in Fig. 3), then the catalyst was washed to remove Cl^- ions,

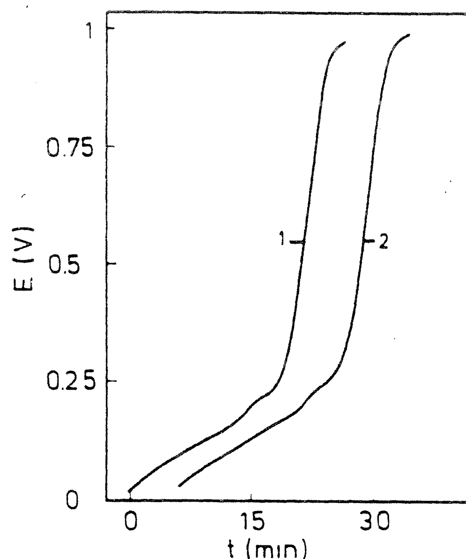

Fig. 3. Charging curve of the platinum catalyst saturated with hydrogen sorbed above room temperature in 0.2 M HCl (1). Charging curve after removal of the sorbed hydrogen (2) (curve 2 is shifted by 6 min)

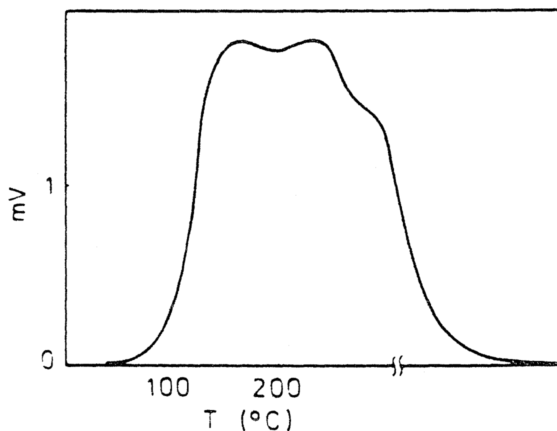

Fig. 4. TPD curve after the first charging curve of Fig. 3

placed back (wet) into the TPD reactor and evacuated to 10^{-3} Torr for 1 hr. The carrier gas was then started and the oxygen adsorbed in the course of the previous operations /8/ was reduced with 50 μl hydrogen pulses in the carrier gas. This was followed by the determination of the TPD curve of the catalyst (shown in Fig. 4). The curve demonstrates that operations needed to determine the charging had no effect on the amount of sorbed hydrogen.

After the determination of the TPD curve, the charging curve of the catalyst was determined again (curve 2 in Fig. 3). The comparison of the two charging curves shows that hydrogen sorbed above room temperature has no effect on the charging curve.

REFERENCES

1. S. Tsuchiya, Y. Amenomiya, R. J. Cvetanovič: J. Catal., 19, 245 (1970).
2. S. Szabó, F. Nagy: Magy. Kém. Foly. (to be published).
3. S. Szabó. D. Móger, F. Nagy: Acta Chim. (Budapest) (To be published).
4. D. Móger, G. Kovács: Magy. Kém. Foly., 81, 123 (1975).
5. D. Móger, G. Besenyei, F. Nagy: Magy. Kém. Foly., 81, 284 (1975).
6. D. Móger, G. Besenyei, F. Nagy: React. Kinet. Catal. Lett., 3, 231 (1975).
7. Z. Paál, S. J. Thomson: J. Catal., 30, 96 (1973).
8. D. Móger, M. Hegedüs, G. Besenyei, F. Nagy: React. Kinet. Catal. Lett., 5, 73 (1976)
9. J. Bett, K. Kinoshita, K. Routsis, P. Stonehart: J. Catal., 29, 160 (1973).

J. Electroanal. Chem., 263 (1989) 137–146
Elsevier Sequoia S.A., Lausanne – Printed in The Netherlands

Study of the underpotential deposition of copper onto polycrystalline palladium surfaces

S. Szabó, I. Bakos and F. Nagy

Central Research Institute for Chemistry, Hungarian Academy of Sciences, H-1525, Budapest, P.O. Box 17 (Hungary)

T. Mallát

Organic Chemical Technology Research Group, Hungarian Academy of Sciences, H-1521, Budapest, P.O. Box 91 (Hungary)

(Received 19 July 1988; in revised form 14 December 1988)

ABSTRACT

The underpotential deposition of copper onto a palladized Pt electrode has been studied. It has been shown that Cl^- ion traces and adsorbed Cu atoms form a catalyst on the Pd surface which accelerates Pd corrosion during the desorption of adsorbed Cu. The Pd^{2+} ions formed in this corrosion process may bring about Cu/Pd alloy deposition, suggesting alloy formation owing to copper absorption. The quantities of copper and oxygen adsorbed on the same palladium surface are roughly equal. A mechanism of copper deposition via ionization of presorbed hydrogen is proposed.

INTRODUCTION

Very few papers have been devoted to the study of the underpotential deposition of metals onto palladium surfaces and the results published in these papers are contradictory. In earlier papers it had been claimed that not only metal adsorption but also alloy formation occurred during underpotential deposition [1,2]. Later investigations, however, have not verified the earlier findings about metal absorption on palladium [3,4].

In this paper, investigations aimed at clarifying the contradictions of earlier results of Cu deposition onto palladium surfaces are reported.

EXPERIMENTAL

Experiments were carried out in the same three-compartment cell described in our earlier paper [5]. A characteristic feature of our cell is that cell solutions can be

0022-0728/89/$03.50 © 1989 Elsevier Sequoia S.A.

replaced with the exclusion of air. This allows the study of the properties of an electrode covered with adsorbed metal in the absence of depositing ions.

The volume of the main compartment of the cell was 50 ml. 1 *M* $HClO_4$ and 0.5 *M* H_2SO_4 supporting electrolytes were prepared from Merck p.a. grade reagents with triply distilled water.

Purified nitrogen was bubbled through the cell to deoxygenate the solutions.

The polycrystalline Pt electrode was first washed with aqua regia and then it was palladized in a 2% $PdCl_2$ solution containing 0.1 *M* HCl at 0 °C with 25 mA for 15 min. After palladization chloride ions were removed from the electrode as follows: when palladization was finished, the electrode was rinsed with triply distilled water and then anodized and cathodized alternately six times in 0.5 *M* H_2SO_4 solution with a strong current (0.5 A), beginning with cathodic and ending with anodic polarization. This procedure took place in a separate cell. After three polarizations, the cell solution was changed to remove the desorbed chloride ions.

The apparent surface area of the Pt electrode was ca. 2 cm^2.

Copper ions were added to the electrolyte as perchlorate or sulphate in a concentration of 2.5×10^{-3} *M* in the main compartment of the cell. Copper perchlorate was prepared by dissolving Merck p.a. grade CuO in 1 *M* $HClO_4$ in order to avoid surplus chloride contamination.

All potentials are referred to a hydrogen electrode immersed into the same supporting electrolyte which was in the main compartment of the cell.

All measurements were carried out at room temperature.

RESULTS AND DISCUSSION

Reproduction of the results published earlier

Initially, we attempted to reproduce the experiments performed earlier by Adzic et al. [3] and Chierchie and Mayer [4], showing Cu to adsorb on Pd.

A polycrystalline Pd wire (geometrical area ca. 0.5 cm^2) served as the working electrode when the measurement of Adzic et al. was reproduced. Before the experiments, the electrode was activated by a brief immersion into nitric acid [3] and then cyclic voltammograms were measured in 1 *M* $HClO_4$ in the presence of 5×10^{-4} *M* Cu^{2+} ions, with the same results as those published [3].

The reproduction of the measurements of Chierchie and Mayer [4] was carried out in 1 *M* $HClO_4$ instead of acidic $NaClO_4$ solution with a smooth polycrystalline Pd electrode. The concentration of Cu^{2+} ions was 2.5×10^{-3} *M*. In spite of the different supporting electrolyte, our results were very similar to those published earlier [4].

Finally, an attempt was made to reproduce our earlier results [2]. In this experiment, a freshly palladized Pt electrode was polarized cathodically in 1 *M* $HClO_4$ solution with 1 mA for 10 min from 0.3 V, then the polarity was reversed and a charging curve was determined with 0.3 mA (curve 1 in Fig. 1). The electrode was then polarized cathodically again under the same conditions. When the polari-

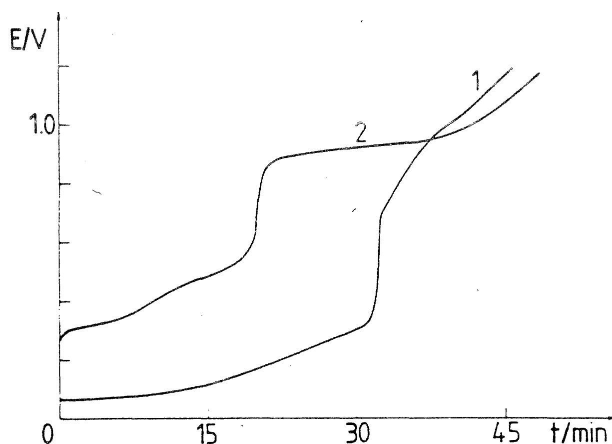

Fig. 1. Charging curve of a freshly palladized Pt electrode in 1 M $HClO_4$ (1) and after Cu deposition (2). $I = 0.3$ mA.

zation was finished, 0.01 g of CuO dissolved in 1 M $HClO_4$ was introduced into the main compartment of the cell. Via ionization of presorbed hydrogen under open-circuit conditions, spontaneous metal adsorption took place while the electrode potential rose to 0.303 V for 2 h.

After the above procedure, in the presence of the depositing Cu^{2+} ions the charging curve of the electrode is curve 2 in Fig. 1. This result is similar to those published in our earlier paper [2], but very different from the result obtained with cyclic voltammetry [3,4]. The marked difference is the reaction at ~ 0.9 V, which is discussed below.

The effect of chloride ion contamination

The experiment illustrated in Fig. 1 was repeated with the difference that the polarization currents were 1.0 and 0.15 mA. The charge values used for carrying out the reaction at ~ 0.9 V with different current densities are summarized in Table 1.

As can be seen from Table 1, the lower the current density, the higher the charge used for the oxidation. It follows from this that the materials taking part in the reaction are not exclusively in the adsorbed phase.

The experiment illustrated in Fig. 1 was repeated using a 0.5 M H_2SO_4 supporting electrolyte. The result was found to be quite different. The reaction at ~ 0.9 V

TABLE 1

Charge values for the reaction at 0.9 V at different current densities

Current/mA	Charge/C
1.0	0.18
0.3	0.35
0.15	1.77

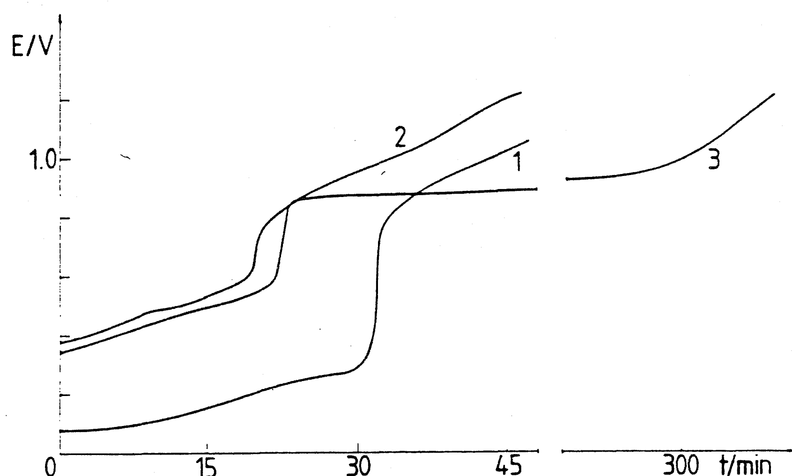

Fig. 2. Charging curve of a freshly palladized Pt electrode in 0.5 M H_2SO_4 (1) and after Cu deposition in Cl^- ion-free (2) and chloride-containing (10^{-5} M) supporting electrolyte (3). $I = 0.3$ mA.

did not take place (Fig. 2, curve 2). This experiment was repeated under identical conditions; there was, however, 10^{-5} M HCl in the supporting electrolyte, resulting in curve 3 in Fig. 2. After completion of the reaction described by curve 3 in Fig. 2, Pd^{2+} ions could be detected in the main compartment of the cell when a few ml of $SnCl_2$ solution (0.1 M $SnCl_2 \cdot 2\ H_2O$ in 1 M HCl) was added to the solution.

10^{-5} M HCl was added to the 0.5 M H_2SO_4 supporting electrolyte because in 1 M $HClO_4$ solution prepared from Merck p.a. grade concentrated $HClO_4$ the Cl^- ion contamination is about 10^{-5} M. On the other hand, in our experience this amount of Cl^- ions causes hardly any change in the course of the charging curve in a copper-free supporting electrolyte. After copper adsorption, however, a huge wave appears in the curve at ~ 0.9 V. On the basis of these results, it can be stated that Cl^- ions and adsorbed copper atoms form some kind of catalyst on the Pd surface which accelerates Pd corrosion. The quantity of catalyst is very small and so with the potential sweep method only a very low peak can be detected in the curve at ~ 0.9 V.

Although these results were observed in the course of Cu deposition via ionization of presorbed hydrogen, the same phenomena could also be detected with the application of potentiostatic polarization [2].

Addition of bromide ions resulted in similar phenomena.

The effect of palladium ion contamination

From the above results it follows that the rate of corrosion of palladium covered with adsorbed copper can be fairly high in the presence of traces of Cl^- ions. For instance, at the end of curve 3 in Fig. 2, 4.25 mg of $PdCl_2$ was formed. The question is: what is the effect of Pd^{2+} ions on Cu deposition onto the Pd surface? To study this effect the following experiments were carried out.

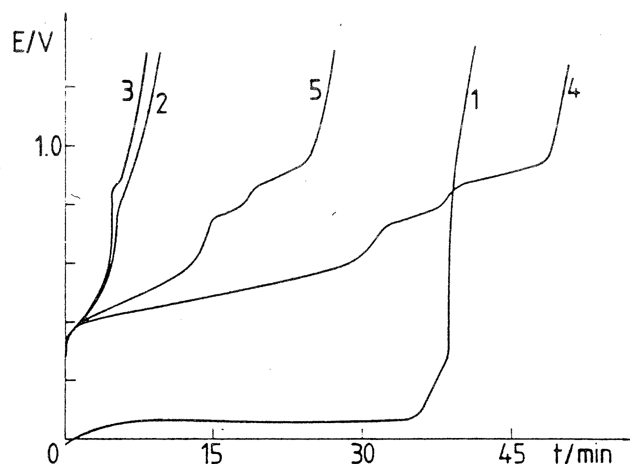

Fig. 3. Charging curve of a freshly palladized Pt electrode saturated with hydrogen in 0.5 M H_2SO_4 (1) and after Cu deposition at 0.275 V for 22 h in Cl^- ion-free (2) and chloride containing (3) (10^{-5} M HCl) supporting electrolyte. Charging curve of the electrode after Cu deposition at 0.275 V for 22 h in the presence of 1 mg of $PdCl_2$ (4) and 0.4 mg of $PdCl_2$ (5). $I = 2$ mA.

First the charging curve of the palladized Pt electrode was determined in 0.5 M H_2SO_4 supporting electrolyte (curve 1 in Fig. 3); then 20 mg of $CuSO_4$ was introduced into the main compartment of the cell and the electrode was polarized at 0.275 V for 22 h. The charging curve of the electrode prepared this way is curve 2 in Fig. 3. This experiment was repeated in the presence of 10^{-5} M HCl (curve 3 in Fig. 3).

Curves 2 and 3 are very similar. The only difference is the small wave in curve 3 at ~ 0.9 V caused by oxidation of the catalytic material mentioned in the previous section. In this case, a long corrosion process is prevented by the fairly high current density.

Before the next polarization, 0.05 ml (1 mg $PdCl_2$) of the solution used for palladization was introduced into the main compartment of our cell (on the other hand, this resulted in 10^{-4} M HCl in the supporting electrolyte) and then the electrode was polarized at 0.275 V for 22 h. The charging curve of the electrode is curve 4 in Fig. 3. After repalladization, this experiment was repeated in the presence of 0.02 ml (0.4 mg $PdCl_2$) of the solution of palladization (curve 5, Fig. 3).

It is evident from curves 4 and 5 (Fig. 3) that addition of Pd^{2+} ions results in alloy formation and its quantity depends on the amount of Pd^{2+} ions added. At the end of the charging curves there are two waves. The wave at more negative potential is caused by slow diffusion of Cu atoms to the Pd surface because on switching the polarizing current off the potential went back to ~ 0.55 V.

The other wave was, at least partly, caused by Pd corrosion. This can be verified as follows. After alloy formation the cell was rinsed with deoxygenated 0.5 M H_2SO_4 and the charging curve was determined in Cl^-- and Cu^{2+}-free supporting electrolyte. The result was very similar to curves 4 and 5 in Fig. 3. When the polarization was completed, 20 mg of $CuSO_4$ was added to the solution and the electrode was kept at 0.275 V for a long time. The result was also alloy formation,

indicating the fact that Pd^{2+} ions were formed during the previous polarization in a quantity much larger than the quantity of Pd^{2+} ions formed as a result of the charging curve measured in 0.5 *M* H_2SO_4.

Oxidation of a larger amount of corrosion catalyst mentioned in the previous section cannot be excluded unambiguously.

If the conditions of Cu diffusion were more unfavourable, only one wave would be observed at the end of the charging curve.

Copper deposition in Cl^- ion- and Pd^{2+} ion-free electrolytes

In the preceding sections it has been shown that traces of both Cl^- and Pd^{2+} ions bring about side reactions which have a considerable effect on copper deposition onto a polycrystalline Pd surface. It follows that the underpotential deposition of copper on palladium can be investigated only under strictly Cl^- ion- and Pd^{2+}-free conditions.

Taking into account the above considerations, we studied copper deposition at 0.275, 0.265 and 0.255 V, polarizing the electrode for 17 h in 0.5 *M* H_2SO_4 in the presence of 2.5×10^{-3} *M* $CuSO_4$ (Fig. 4). (After every voltammogram the cell was rinsed with deoxygenated 0.5 *M* H_2SO_4 to remove traces of Pd^{2+} ions and the deposition procedure was repeated.)

The results are somewhat different from those published earlier [3,4] indicating that the number of observable peaks depends on the experimental technique, preparation and history of the electrode. Adzic et al. reported a voltammetric curve of Cu desorption with two peaks [3]. However, there are six peaks on the voltammetric curve reported recently by Chierchie and Mayer [4].

There are four peaks on our curves in Fig. 4. The doublet at about ~ 0.5 V is the desorption of adsorbed Cu but the other doublet between 0.3 and 0.4 V is

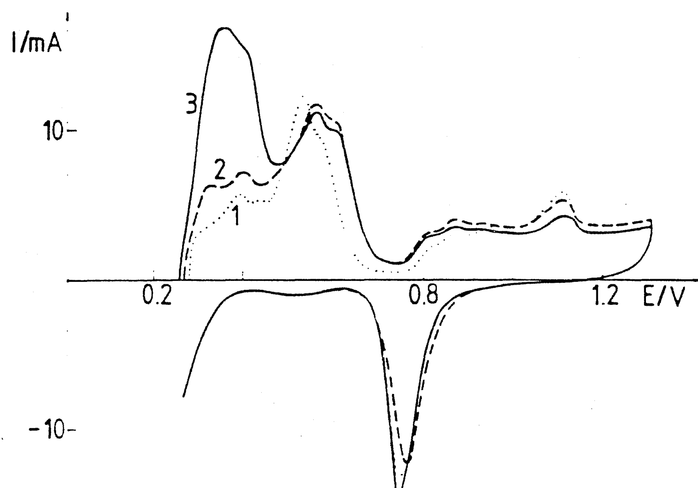

Fig. 4. Underpotential deposition of Cu^{2+} on a palladized Pt electrode at 0.275 V (1), 0.265 V (2) and 0.255 V (3), polarizing the electrode for 17 h in Cl^-- and Pd^{2+}-free 0.5 *M* H_2SO_4. Sweep rate = 0.02 V/s.

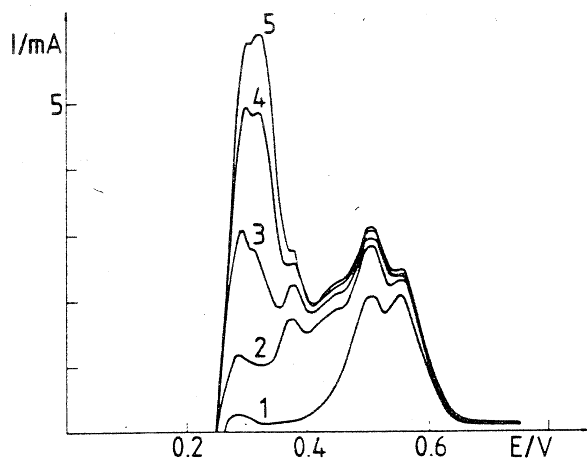

Fig. 5. Electrodeposition of Cu^{2+} on a palladized Pt electrode at 0.25 V for different times. (1) Anodic branch of continuous cycling between 0.25 and 0.75 V. Positive sweeps after 2 min (2), 5 min (3), 10 min (4) and 15 min (5) polarization at 0.25 V. Sweep rate = 0.005 V/s.

questionable. According to earlier results [4], there is an adsorption peak which is separated by only a few mV from bulk deposition and this phenomenon would result in a doublet. This seems to be a reasonable explanation but there is still an open question as to why the bulk peak does not increase indefinitely at the rather negative potential.

If the electrode is polarized at 0.25 V also in the presence of 2.5×10^{-3} *M* $CuSO_4$ (Fig. 5), the bulk peak, which is still a double peak, grows indefinitely, depending on the time of polarization. On the basis of these results, it can be supposed that the two peaks at ~ 0.3 V are very likely bulk peaks but with different thermodynamic character. Similar results have been observed in the study of electrodeposition of Ag and Pd onto a platinum subtrate [6,7].

Another explanation for the doublet between 0.3 and 0.4 V in Fig. 4 can be the decomposition of the Cu + Pd alloy formed at 0.255 V or more positive potentials, supposing that the beginning of bulk deposition is only at 0.25 V. When the electrode is polarized at 0.25 V, this alloy peak is visible as a shoulder at ~ 0.38 V on the large bulk peak, as shown in Fig. 5.

Disregarding the shoulder at ~ 0.38 V on the curves in Fig. 5, their shapes are almost the same as the shape of the curve published by Chierchie and Mayer [4], but they differ from the curves in Fig. 4.

Because of the long time of polarization the curves in Fig. 4 are characteristic of the deposited Cu which is in equilibrium with Cu^{2+} ions in the supporting electrolyte. In the case of the measurements illustrated in Fig. 5, however, this is not true; consequently, the difference between the curves of Figs. 4 and 5 can be explained by the different equilibrium conditions.

Relationship between oxygen and copper adsorption

Rand and Woods studied oxygen adsorption on Pd and found that the coverage increased linearly with the potential until it reached a distinct plateau at about

~ 1.5 V [8]. The plateau on the oxygen coverage vs. potential curve offers a better method for determining the real surface area of the palladium electrode than hydrogen adsorption between 0.09 and 0.28 V.

On the basis of curve 1 in Fig. 4, the charge consumed between 0.275 and 0.7 V was determined (0.105 C), and then the charge used for the formation of an oxygen monolayer on the same electrode was calculated (0.099 C) according to Rand and Woods [8]. The ratio of the two quantities of charge was very close to 1.

From this result it follows that copper adsorption may be used for the surface determination of Pd.

Mechanism of copper deposition on palladium via ionization of presorbed hydrogen

The following experiment was carried out with the aim of studying the mechanism of copper deposition onto Pd via ionization of presorbed hydrogen. The palladized Pt electrode was polarized cathodically in 0.5 M H_2SO_4 with 1 mA for 10 min from 0.3 V and then the polarity was reversed and the voltammogram of the electrode was determined (curve 1 in Fig. 6). The electrode was polarized cathodically again under the same conditions and when the polarization was finished under open-circuit conditions 0.008 g (10^{-3} M) of $CuSO_4$ was introduced into the main compartment of the cell.

When the potential reached 0.075 V as a result of the spontaneous reaction of Cu^{2+} ions with sorbed hydrogen, the reaction was interrupted by removing the copper-containing supporting electrolyte from the cell. The cell was then refilled with deoxygenated 0.5 M H_2SO_4 and the voltammogram of the palladized Pt electrode prepared in this manner was recorded (curve 2 in Fig. 6). This experiment

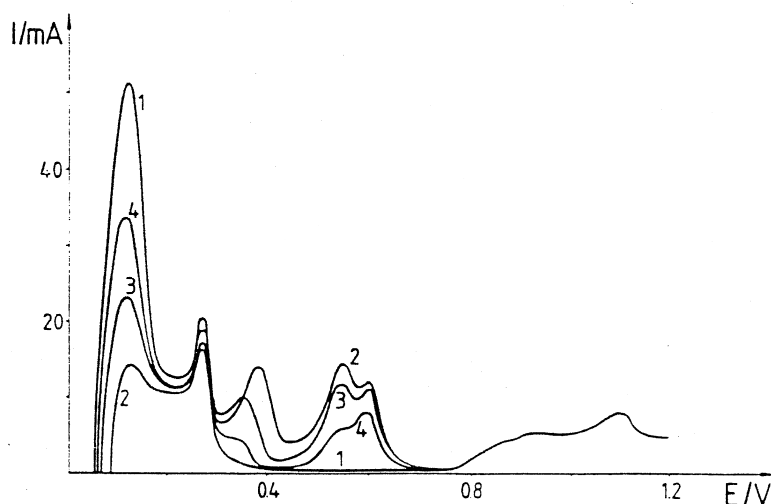

Fig. 6. Potential sweep of a Pd/Pt electrode polarized cathodically before a sweep from 0.3 V with 1 mA for 10 min in 0.5 M H_2SO_4 (1). Potential sweep of a Pd/Pt electrode in Cu^{2+} ion-free 0.5 M H_2SO_4 after Cu deposition when the deposition was interrupted at 0.075 V (2), 0.065 V (3) and 0.057 V (4). Sweep rate = 0.01 V/s.

was repeated twice more with the difference that interruption of the reaction took place at 0.065 V (curve 3) and 0.057 V (curve 4).

The curves in Fig. 6 can be divided into two parts. From about 0.05 to 0.3 V is the hydrogen region and further from ~ 0.65 V is the copper region. In the copper region between 0.3 and 0.4 V, the bulk copper is oxidized and then the two peaks of oxidation of adsorbed copper can be seen.

On the basis of curves in Fig. 6, it can be stated that bulk copper and adsorbed copper are deposited simultaneously while the sorbed hydrogen is ionized because the smaller the hydrogen peaks, the larger the copper peaks:

$$H_{sorbed} \rightarrow H^{+} + e^{-} \quad (1)$$

$$Cu^{2+} + 2\ e^{-} \rightarrow Cu_{ads} \quad (2)$$

$$Cu^{2+} + 2\ e^{-} \rightarrow Cu_{bulk} \quad (3)$$

From the discrepancy of curves 1 and 2 in Fig. 2, it follows that during a longer period some of the charge is lost and so there must be side reactions that result in soluble products. The only soluble product can be the Cu^{+} ion.

Formation of Cu^{+} ions can take place in two reactions. Firstly, the reduction of Cu^{2+} ions:

$$Cu^{2+} + e^{-} \rightarrow Cu^{+} \quad (4)$$

and secondly, the oxidation of Cu_{bulk} by Cu^{2+} as a result of the rising potential:

$$Cu_{bulk} + Cu^{2+} \rightarrow 2\ Cu^{+} \quad (5)$$

With rising potential, another reaction must be considered:

$$Cu_{bulk} \rightarrow Cu^{2+} + 2\ e^{-} \quad (6)$$

Electrons originating from this reaction are used up in reactions (2) and (4).

In the presence of traces of Cl^{-} ions, however, besides Cu_{bulk} and Cu_{ads} an adsorbed material is formed on the Pd surface which enhances the corrosion of the Pd substrate during Cu desorption (Figs. 1 and 2). This material can be either adsorbed CuCl or adsorbed $CuCl_2$. On the basis of our earlier results [2], it may be concluded that the catalytic material is formed in a reduction process because its quantity depends on the duration of polarization; consequently, it cannot be any other material but $CuCl_{ads}$.

$CuCl_{ads}$ can be formed on the Pd surface in two reactions:

$$Cu_{ads} + Cu^{2+} + 2\ Cl^{-} \rightarrow 2\ CuCl_{ads} \quad (7)$$

$$Cu^{2+} + e^{-} + Cl^{-} \rightarrow CuCl_{ads} \quad (8)$$

Further experimental proof of this assumption is that the catalytic material enhancing the Pd corrosion during Cu desorption is formed on polarizing the electrode at a more negative potential than 0.4 V. At this potential, however, the surface is already covered with adsorbed copper; consequently, reaction (7) plays the most important role in the formation of $CuCl_{ads}$.

Electrodissolution of Pd in $HClO_4$ and H_2SO_4 solutions has already been studied [9,10] and it is claimed that the rate-determining step depends on the kind of acid applied. In our experience, Cl^- ions in both acids formed the same adsorbed material that enhanced Pd corrosion during copper desorption. The question is: which step of the anodic dissolution is enhanced by the spontaneously formed catalyst? It is very probably the rate of formation of $PdCl_2^-$ [9]:

$$Pd + 2\,Cl^- \rightarrow PdCl_2^- + e^- \qquad (9)$$

On the basis of our results, it is concluded that in both acids the rate-determining step of Pd corrosion must be reaction (9) published by Genescá and Victori [9].

CONCLUSIONS

The experimental results published in earlier papers could be repeated [2–4]. However, their interpretation is not entirely correct. None of the authors realized that a corrosion process takes place in the presence of traces of Cl^- ion during the desorption of adsorbed copper. The Pd^{2+} ions formed in the corrosion process bring about Cu/Pd alloy deposition, suggesting fast alloy formation owing to copper absorption [2].

ACKNOWLEDGEMENT

The authors are indebted to the Hungarian Research Fund (No. OTKA : 1004) for financial support.

REFERENCES

1 F. Mikuni and T. Takamura, Denki Kagaku, 38 (1971) 237.
2 S. Szabó, J. Electroanal. Chem., 77 (1977) 193.
3 R.R. Adzic, M.D. Spasojevic and A.R. Despic, J. Electroanal. Chem., 92 (1978) 31.
4 T. Chierchie and C. Mayer, Electrochim. Acta, 33 (1988) 341.
5 S. Szabó and F. Nagy, J. Electroanal. Chem., 70 (1976) 357.
6 R.G. Barradas, S. Fletcher and S. Szabó, Can. J. Chem., 56 (1978) 2029.
7 S. Szabó and F. Nagy, Isr. J. Chem., 18 (1979) 162.
8 R. Woods in A.J. Bard (Ed.), Electroanalytical Chemistry, Vol. 9, Marcel Dekker, New York and Basel, 1976, p. 111.
9 J. Genescá and L. Victori, Platinum, Met. Rev., 30 (1986) 80.
10 J. Genescá and R. Durán, Electrochim. Acta, 32 (1987) 541.

React. Kinet. Catal. Lett., Vol. 35, Nos 1-2, 133-139 (1987)

MODIFICATION OF SUPPORTED METAL CATALYSTS BY ADSORBED METALS

F. Nagy and S. Szabó

Central Research Institute for Chemistry, Hungarian Academy of Sciences, H-1525 Budapest, P.O. Box 17, Hungary

Received February 26, 1987

INTRODUCTION

The bimetallic and multimetallic catalysts have great technological importance. They are scientifically very interesting because their catalytic characteristics differ from those of the components, therefore, the preparation of such type of catalysts has been widely studied.

The commonly accepted method is the coimpregnation or subsequent impregnation technique, followed by high temperature heat treatment in appropriate atmospheres. The advantage of this method is its simplicity, the easy variability of the ratio of the components. But it has a disadvantage, too, namely the metallic phase is not well defined.

In this paper a relatively new scientific method of preparation of bimetallic and multimetallic catalysts is described, which is based on the adsorption of metals on metals.

Adsorption of metals on metals

As early as in 1912, a deviation from Nernst's law was reported by Hevesy [1], when small amounts of radioactive metals were deposited onto Cu. Herzfeld [2] tried to give a formal explanation for this violation of Nernst's law. Later Haissinsky [3] and Nicholson [4] went on with the investigation of this phenomenon which is today called underpotential deposition (UPD). Instead of UPD, sometimes it is called electrochemical metal adsorption or electrosorption. This phenomenon has great significance not only in electrochemical surface science but also in

other fields of science and technology connected with metal surface chemical processes [5-7].

In an electrolyte solution, when metal ions discharge on a foreign metal surface, the following processes take place:

$$Me^{z+} + z\,e^- \longrightarrow (Me)_{bulk} \;;\; \Delta G_{b,i} \qquad (1.1)$$

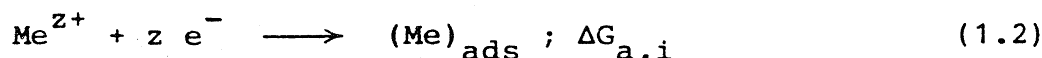

$$Me^{z+} + z\,e^- \longrightarrow (Me)_{ads} \;;\; \Delta G_{a,i} \qquad (1.2)$$

where Me^{z+} is the ion being deposited, the index "bulk" and "ads" refer to the bulk and adsorption phase. $\Delta G_{b,i}$ and $\Delta G_{a,i}$ are the free enthalpy changes of the given processes.

It can be seen that for a discharging ion there are two possibilities – disregarding the kinetics – when the coverage is smaller than unity. Process (1.1) affords metal crystallites, which have similar characteristics as the bulk phase. In the case of process (1.2) the discharged ions forms are converted to adsorbed metal. The probability at the two processes depend on the free enthalpy change (ΔG).

The expressions for ΔG's are

$$\Delta G_{b,i} = \Delta G^{o}(Me)_{bulk} - \Delta G^{o}(Me^{z+}) - RT\ \ln[Me^{z+}] \qquad (2.1)$$

$$\Delta G_{a,i} = \Delta G^{o}(Me)_{ads} - \Delta G^{o}(Me^{z+}) - RT\ \ln[Me^{z+}] \qquad (2.2)$$

The adsorbed form is stable, if

$$\Delta G_{a,i} < \Delta G_{b,i}$$

or from eqs. (2.1) and (2.2)

$$\Delta G^{o}(Me)_{ads} < \Delta G^{o}(Me)_{bulk} \qquad (3)$$

From electrochemistry it is well known that

$$\Delta G = -\ z\ F\ \Delta E \qquad (4)$$

where F is Faraday's constant and ΔE the electrode potential difference.

Equations (3) and (4) give the definition and the measuring possibility of the adsorption potential shift (ΔU^o) or of the standard free enthalpy change of adsorption (ΔG_a^o):

$$\Delta G_a^o = \Delta G^o(Me)_{ads} - \Delta G^o(Me)_{bulk} = - z F \Delta U^o \qquad (5.1)$$

$$E_a = E^o + \Delta U^o + \frac{RT}{zF} \ln[Me^{z+}] \qquad (5.2)$$

where E_a is the electrode potential of the adsorbed metal, E^o is the standard potential of the given redox reaction (in bulk form) and $[Me^{z+}]$ is the concentration of the metal ions in the solution.

It is clear that ΔU^o (and ΔG_a^o) depends on the other metal surface on which the adsorption of the given metal takes place.

For example in the Table are given the values of ΔG_a^o of different metals on platinum.

Table 1
Standard free enthalpy change of adsorption of some metals on Pt

Metal	ΔG_a^o kJ/mol	References
Cu	65 / 82	8
Ag	35 / 55	9
Pd	~50	10
Bi	~188	11
Sn	330	12,13
Pb	166 / 198	13
Re	~100	14
Cd	216	15
Au	~1.5	16

The above discussion can be regarded as a rough approach only. The electrochemical literature provides more exact discussion [17-19] of the phenomenon.

Formation of an adsorbed metal layer on foreign metal catalyst surfaces

According to eq. (1.2), the adsorbed metal layer can be formed as a result of the discharge of metal ions. The source of electrons may be different. In the case of massive metal catalysts it can be the electric current, from a system of electrochemical polarization. If the catalyst is a supported one, the first metal can be produced by the impregnation technique and then for deposition of the adsorbed metal atoms a redox system can be applied as a source of electrons. Such reducing agent may be

a) the hydrogen adsorbed on the base (first) metal

$$(H)_{ads} \longrightarrow H^{+} + e^{-} \qquad (6)$$

b) the metal ion itself (disproportionation reaction)

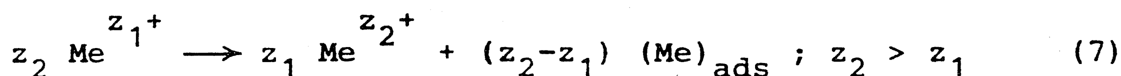

$$z_2\ Me^{z_1+} \longrightarrow z_1\ Me^{z_2+} + (z_2-z_1)\ (Me)_{ads}\ ;\ z_2 > z_1 \qquad (7)$$

In both cases it is very important that (i) charge transfer takes place not in the homogeneous phase, but on the surface of the base metal too and (ii) a true adsorbed metal layer is formed and not "bulk" metal on the surface. These processes are regulated by thermodynamic and kinetic factors.

In the case of adsorbed hydrogen the chemical process is the following:

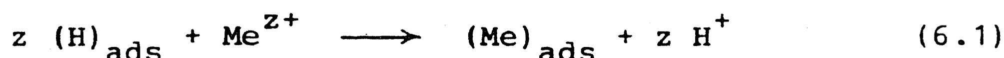

$$z\ (H)_{ads} + Me^{z+} \longrightarrow (Me)_{ads} + z\ H^{+} \qquad (6.1)$$

Its conditions are that the base metal contain adsorbed hydrogen and both metals have to be noble with respect to hydrogen. Electrochemically this means that the electrode potential of the metal (see eq. 5.2) is more positive than the electrode potential of hydrogen ($RT/F \ln[H+]/ pH_2$). The preparation technique has been elaborated by us [20-22].

The homogeneous reaction is not a problem in this case, because the adsorbed hydrogen is on the surface of the base metal. As has been mentioned, the thermodynamically stable form is $(Me)_{ads}$, but kinetically it may be more favorable than the formation of $(Me)_{bulk}$. In this case time is required for the $(Me)_{bulk}$ to transform to $(Me)_{ads}$. The amount of the adsorbed metal can be regulated by the amount of adsorbed hydrogen.

The first condition of using the disproportionation reaction is the existence of several valence states of the given metal (e.g., Sn^{2+}, Sn^{4+}). The second is a favorable equilibrium. For process [7] the following equilibrium constant can be written

$$Kd = [Me^{z_2+}]^{z_1}/[Me^{z_1+}]^{z_2} \qquad (7.1)$$

As is known from electrochemistry

$$\frac{RT}{F} \ln K_d = E_d^o \qquad (7.2)$$

where E_d^o is the standard potential of disproportionation

$$E_d^o = z_1(z_2-z_1)(E_{z_1}^o + \frac{1}{z_1} \Delta U^o - E_{z_2,z_1}^o) \qquad (7.3)$$

where $E_{z_1}^o$ is the standard electrode potential of the reaction

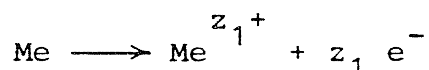

$$Me \longrightarrow Me^{z_1+} + z_1 e^-$$

and E_{z_2,z_1}^o the standard electrode potential of the process

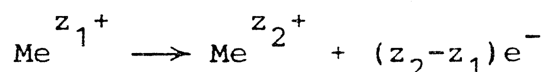

$$Me^{z_1+} \longrightarrow Me^{z_2+} + (z_2-z_1)e^-$$

(Both standard potentials are available from handbooks).

The material balance of process (7) is

$$- v \frac{[Me^{z_1+}]}{z_2} = v \frac{[Me^{z_2+}]}{z_1} = \frac{N(Me)_{ads}}{z_2-z_1} \qquad (7.4)$$

where $N(Me)_{ads}$ is the amount of adsorbed metal (in mol), is

the volume of the solution.

As can be seen from eq. (7.3), the disproportionation standard potential and, consequently, the equilibrium constant (7.2), depends very strongly on the value of adsorption potential ΔU^o.

As an example, we calculated the disproportionation standard potential and the equilibrium constant in the case of Sn^{2+} at various adsorption potentials.

Table 2

Dependence of E_d^o and of lg K_d on ΔU^o for the process

$$Sn^{2+} \longrightarrow Sn^{4+} + (Sn)_{ads}$$

ΔU^o, V	Ø	0.5	1.0	1.5	2.0	2.5	3.0
E_d^o, V	-1.16	-0.16	0.84	1.84	2.84	3.84	4.84
lg K_d	-19.66	-2,71	14.24	31.19	48.14	65.08	82.03

It may be seen from Table 2 that in the case of Sn^{2+} ion disproportionation can take place if ΔU^o is greater than 0.5 V. It follows that the homogeneous disproportionation need not be taken into consideration.

—

REFERENCES

1. G.V. Hevesy: Physik Z., 13, 715 (1912)
2. K.F. Herzfeld: Physik Z., 14, 29 (1913)
3. M. Haissinsky: J. Chim. Phys., 43, 21 (1946)
4. M.M. Nicholson: J. Am. Chem. Soc., 79, 7 (1957)
5. D.M. Kolb, M. Przasnycki, H. Gerischer: J. Electroanal. Chem., 54, 25 (1974)
6. R.R. Adzic, A.R. Despic: Z. Phys. Chem. N.F., 98, 95 (1975)
7. D.M. Kolb: In Advances in Electrochemistry and Electrochemical Engineering (Edited by H. Gerischer and C. Tobias), Vol. 11, p. 125. Wiley-Interscience, New York 1978.

8. N. Furuya, S. Motoo: J. Electroanal. Chem., 72, 165 (1976)
9. R.G. Barrades, S. Fletcher, S. Szabó: Can. J. Chem., 56, 2029 (1978)
10. S. Szabó, F. Nagy: Israel J. Chem., 18, 162 (1979)
11. S. Szabó, F. Nagy: J. Electroanal. Chem., 70, 307 (1971)
12. S. Szabó: J. Electroanal. Chem., 172, 359 (1984)
13. N. Furuya, S. Motoo: J. Electroanal. Chem., 98, 195 (1979)
14. M. Ifandi, S. Szabó, F. Nagy: Elektrokhimiya, 18, 1205 (1982)
15. F. Mikuni, T. Takamura: Denki Kagaku, 38, 113 (1970)
16. S. Szabó, F. Nagy: J. Electroanal. Chem., 85, 239 (1977)
17. K.J. Vetter, J.W. Schultze: J. Electroanal. Chem., 53, 67 (1974)
18. B.E. Conway, S. Marshall: Electrochim. Acta, 28, 1003 (1983)
19. A. Frumkin, B. Damaskin, O. Petrii: Elektrokhimiya, 12, 3 (1976)
20. S. Szabó, F. Nagy: J. Electroanal. Chem., 84, 93 (1977)
21. S. Szabó, F. Nagy: J. Electroanal. Chem., 88, 259 (1978)
22. S. Szabó, F. Nagy: J. Electroanal. Chem., 160, 299 (1984)

On the multiple states of gold deposited onto polycrystalline platinum substrates

I. Bakos and S. Szabó*

Central Reserach Institute for Chemistry, Hungarian Academy of Sciences, H-1525 Budapest, P.O. Box 17 (Hungary)

The most striking feature of many adsorbed monolayers is the multiple states of adsorption of the deposited species revealed by cyclic voltammetry [1-6]. This feature of adsorbed layers can already be observed below the limit of monolayer coverage. In spite of the multiple state character of the adsorbed species deposited on foreign metal surfaces, gold adsorption on platinum has not revealed the slightest hint of this feature [7-9].

Despite the above experimental observations the existence of multiple states of adsorbed gold has been studied (also with cyclic voltammetry) and in continuation of our earlier investigations [8,9] the results are published in this paper.

EXPERIMENTAL

The method and cell have been described elsewhere [8-10]. In the experiments a 0.2 M HCl supporting electrolyte prepared from Merck reagent was used. The smooth and platinized Pt electrodes (apparent surface is about 2 cm^2) were prepared as described earlier [8 - 10]. The Au^{3+} ion concentration during gold deposition was $5x10^{-4}$ M.

Continuous bubbling of purified nitrogen through the main compartment of our cell deoxygenated and agitated the so-

*To whom correspondence should be addressed.

lutions. The gas bubbling also removed the traces of hydrogen dissolved in the supporting electrolyte during the saturation of the working electrode with hydrogen.

The reference electrode was a Pt/H_2 electrode in the same supporting electrolyte the cell was filled up with.

RESULTS AND DISCUSSIONS

Effect of surface structure on the results of study of gold deposition on Pt surface

In order to study this question we performed gold deposition first on platinized Pt then on a smooth Pt electrode. Gold deposition in both cases also took place via ionization of hydrogen adsorbed on Pt before the metal deposition [8].

The platinized Pt electrode:

First the cyclic voltammogram of the platinized Pt electrode was determined in 0.2 M HCl (curve 1 in Fig.1) and then the electrode was saturated with hydrogen by scanning its potential to 0.05 V. At this potential, under open circuit circumstances gold ions were introduced into the main compartment of the cell. After 6 min the potential rose to 1.00 V, the adsorbed hydrogen was exchanged for mostly visible bulk gold coating and the sweep of the electrode measured from 1.00 V was curve 2 in Fig. 1. This experiment was repeated with the difference that we waited for 60 min. after introduction of gold ions (curve 3 in Fig. 1). During this period of time the potential rose to 1.058 V (this potential is in the UPD region), the visible gold coating disappeared, i.e., the total amount of gold deposited via ionization of hydrogen adsorbed on platinized Pt was transformed into adsorbed state [8].

According to our earlier studies, during anodic polarization of a gold covered Pt electrode three processes take place almost at the same potential [8, 9]. Oxidation of bulk gold, oxidation of adsorbed gold and a third one which

is presumably oxidation of platinum substrate metal catalysed by adsorbed gold only [9]. The result of this behaviour is that the potentials of peaks of gold oxidation are almost independent of the structure of the deposited gold, as can be seen in Fig. 1. From the figure it may also be seen that more charge is required for the oxidation of gold than required for the oxidation of hydrogen used for its deposition. (This difference is caused by the side reaction called "anomaly" in earlier papers [8,9].) The difference between the curves 2 and 3 is due to the inequality of the ratio of adsorbed and bulk gold in the gold layers and the gold adsorption via ionization of Pt substrate[9].

The smooth Pt electrode:

The cyclic voltammogram of the smooth Pt electrode is curve 1 in Fig. 2. After this measurement the electrode was polarized to 0.05 V and at this potential, also under open circuit circumstances, gold ions were introduced into the main compartment of the cell. In 30 seconds the potential rose to 1.00 V and from this potential the sweep of the electrode is curve 2 in Fig. 2.

The above experiment was repeated two times. First, after introducing the gold ions we waited for 5 min, the potential rose to 1.048 V and the sweep from this potential was curve 3. Then after 40 min, the potential rose to 1.061 V and the sweep from this potential was curve 4.

In contradiction to the results obtained with platinized Pt, in this case the different stages of spontaneous formation of an adsorbed gold layer deposited via ionization of hydrogen adsorbed on Pt before gold deposition, can be distinguished. The more negative peaks on curves 2 and 3 are the results of the dissolution of bulk gold.The more positive peaks are derived from the oxidation of adsorbed gold.

Another striking result of this experiment is that the "anomaly" discussed in our earlier paper can hardly be observed here [8,9], i.e., for the oxidation of adsorbed hydrogen and gold roughly the same amount of charge is required. This result supports the theory (developed for the explanation of the "anomaly") of corrosion of Pt substrate rather than Cl^- ion oxidation [9].

Finally, it may be stated that the potential difference between the peaks of oxidation of adsorbed and bulk gold (Fig. 2) is roughly the same (0.06 V) as published in our earlier paper [9].

Study of gold deposition in the underpotential region

In the earlier chapter it has been clearly shown that the only use of smooth Pt electrodes makes it possible to observe the multiple state character of gold adsorption on Pt. Another condition of reaching significant results in this question is to take into consideration the oxygen adsorption taking place in the same potential interval where the gold adsorption can be observed.

Before the experiments, the underpotential region had to be determined. For this purpuse, potential of gold electrode (gold ion concentration was also 5×10^{-4} M $AuCl_3$ in 0.2 M HCl) was measured with respect to a hydrogen electrode in the same 0.2 M HCl. It was about 1.00 V, therefore, the region more positive than one volt was regarded as UPD region.

For the above reasons smooth Pt electrode was used in the experiments and before gold deposition it was polarized in the 0.2 M HCl supporting electrolyte with 0.02 V/s from 1.35 V to 0.05 V and back to 1.01 V. At this potential

Au^{3+} ions were introduced into the main compartment of the cell and in the presence of gold ions the electrode was polarized for 10 min then its potential sweep was determined also with 0.02 V/s (curve 1 in Fig. 3). This experiment was repeated four times increasing the time of keeping the electrode at 1.01 V (curves 2-5 in Fig.3). In the last experiment, however, the electrode was polarized at 0.96 V (i.e. in the overvoltage region) for 4 min (curve 6 in Fig.3).

The most surprising result of this series of experiments (curves 1-5 in Fig. 3) is that the peak of oxidation of adsorbed gold is a doublet with ~0.04 V potential difference between the peaks.

Since the same electrode was used in this case than in the experiments depicted in Fig. 2, the results can easily be compared. According to our calculations (based on that $3H_a + Au^{3+} \rightarrow Au_{ads}$ (where H_a is the hydrogen adsorbed on Pt) and one gold adatom covers one hydrogen adsorption site [9]) curve 4 in Fig. 2 and curve 1 in Fig. 3 represent more or less the same gold coverage ($\theta_{Au} \approx 0.3$). By increasing the time of polarization to 40 min the gold coverage rose to about $\theta \approx 1$ (curve 5 in Fig.3). From this calculation it can be concluded that the second peak appears on the curve above $\theta_{Au} = 0.5$,and above this coverage the gold adsorbed on Pt surface is composed of weakly and strongly adsorbed gold.

If gold deposition was carried out at 0.96 V then a completely different sweep was obtained (curve 6 in Fig. 3). Two peaks and a shoulder can be seen on the curve. No doubt that the shoulder is the result of oxidation of adsorbed gold and the peak at ~1.16 V is the result of bulk deposits.(As can be seen from Fig. 3, the potential difference between the bulk gold and strongly adsorbed gold is also about 0.06 V which on the other hand verifies that the peak at ~1.16 V is result of bulk gold oxidation.)The only questionable peak is at

$\sim$1.09 V.

The nature of adsorbed species causing the peak at $\sim$1.09 V was studied as follows. When the polarization at 0.96 V was finished the cell was rinsed with deoxygenated triply distilled water and refilled with deoxygenated 0.2 M HCl. After this procedure the peak at $\sim$1.09 V disappeard from the curve, consequently, the adsorbed material oxidized at $\sim$1.09 V can be washed off the surface either with water or with the supporting electrolyte. The soluble gold compound deposited onto Pt surface at 0.96 V can only be adsorbed AuCl which is soluble in these media.

Gold deposition onto oxygen covered platinum surfaces

In the experiments described in the preceding chapter, oxygen coverage was tried to be kept as low as possible by reaching the potential of polarization from the negative direction. In the study of these phenomena, however, before gold deposition oxygen was deposited on the Pt surface in a reproducible manner.

In the case of the first experiment the smooth Pt electrode was taken out of the cell at 1.35 V, washed with distilled water and anodized in a separate cell for 10 s with 2.5 mA in 0.5 M H_2SO_4. After this pretreatment the electrode was washed again with water and placed back into the cell. Gold deposition was then carried out at 0.91 V for 40 s in 0.2 M HCl in the presence of 5×10^{-4} M $AuCl_3$. The sweep of the gold-covered electrode in the gold ion containing 0.2 M HCl with 0.02 V/s sweep rate is curve 1 in Fig. 4.

When the above experiment was finished the potential of the electrode was scanned to 0.05 V, then back to 1.35 V and finally to 0.91 V. It was maintained at this potential also for 40 s and then polarized with 0.02 V/s to 1.35 V (curve 2 in Fig. 4). This experiment was repeated under the same conditions with 120 s polarization at 0.91 V (curve 3).

The most apparent difference between the curvesin Fig. 4 is the peak at 1.09-1.15 V which is missing from curve 1. It follows from this that the material oxidized at this potential can only be deposited on a Pt surface free of adsorbed oxygen, therefore, it can be on the surface in adsorbed state only.

On the other hand, from the run of curve 1 (Fig.4) it can be concluded that mostly bulk gold can be deposited on an oxygen covered Pt surface because anodization of the electrode before gold deposition prevented the appearance of oxidation peaks of adsorbed gold. Another evidence of this behaviour is the experience that onto an anodized Pt surface at 1.010 V (UPD region) practically no gold deposition can be carried out(because there are no free adsorption sites on the Pt surface).

It follows from the above experimental facts that composition of the deposited gold strongly depends on the oxygen coverage and surface oxides of the Pt substrate.

ABSTRACT

The multiple state character of gold deposited onto a smooth Pt surface has been demonstrated but this phenomenon cannot be observed in the case of platinized Pt electrode. Two kinds of adsorbed species, bulk deposit and presumably adsorbed AuCl have been detected. Interaction between gold and oxygen adsorption has been observed.

REFERENCES

1. H. Angerstein-Kozlowska, B.E. Conway and W.B.A. Sharp, J. Electroanal. Chem., 43 (1973) 9.
2. B.E. Conway and H. Angerstein-Kozlowska, Acc. Chem. Res., 14 (1981) 49.
3. N. Furuya and S. Motoo, J. Electroanal. Chem., 72 (1976) 165.
4. R.G. Barradas, S. Fletcher and S. Szabó, Can. J. Chem., 56 (1978) 2029.
5. T. Chierchie and C. Mayer, Electrochim. Acta, 33 (1988) 341.
6. S. Szabó, I. Bakos, F. Nagy and T. Mallát, J. Electroanal. Chem., 263 (1989) 137.
7. S.H. Cadle and S. Bruckenstein, Anal. Chem., 43 (1971) 1858.
8. S. Szabó and F. Nagy, J. Electroanal. Chem., 85 (1977) 339.
9. I. Bakos and S. Szabó, J. Electroanal. Chem., 344 (1993) 303.
10. S. Szabó and F. Nagy, J. Electroanal. Chem., 70 (1976) 357.

Figure captions

Fig. 1

Cyclic voltammogram of the platinized Pt electrode in 0.2 M HCl (1). Potential sweeps of the same electrode covered mostly with bulk gold (2) and adsorbed gold (3) deposited via ionization of hydrogen adsorbed on platinized Pt before gold deposition. Sweep rate: 5×10^{-3} V/s.

Fig. 2

Cyclic voltammogram of the smooth Pt electrode in in 0.2 M HCl (1). Potential sweeps of the same electrode covered with gold deposited via ionization of the preadsorbed hydrogen when the lengths of time of reaction of Au^{3+} ions with hydrogen adsorbed on Pt were 0.5 min (2), 5 min (3) and 40 min (4). Sweep rate 0.02 V/s.

Fig. 3

Potential sweep in the 0.2 M HCl + 5×10^{-4} M $AuCl_3$ electrolyte of the smooth Pt electrode polarized at 1.01 V for 10 min (1), 15 min (2), 20 min (3), 30 min (4), 40 min (5) and at 0.96 V for 4 min (6). Sweep rate: 0.02 V/s.

Fig. 4

Potential sweep of the smooth Pt electrode (anodized for 10 s with 2.5 mA in 0.5 M H_2SO_4 before Au deposition) covered with gold by polarization in 0.2 M HCl+5×10^{-4} M $AuCl_3$ for 40 s at 0.91 V (1). The sweep of the same electrode covered partly with oxygen by polarization to 1.35 and then back to 0.91 V and then with gold by polarization in 0.2 M HCl + 5×10^{-4} M $AuCl_3$ at 0.91 V for 40 s (2) and 120 s (3).

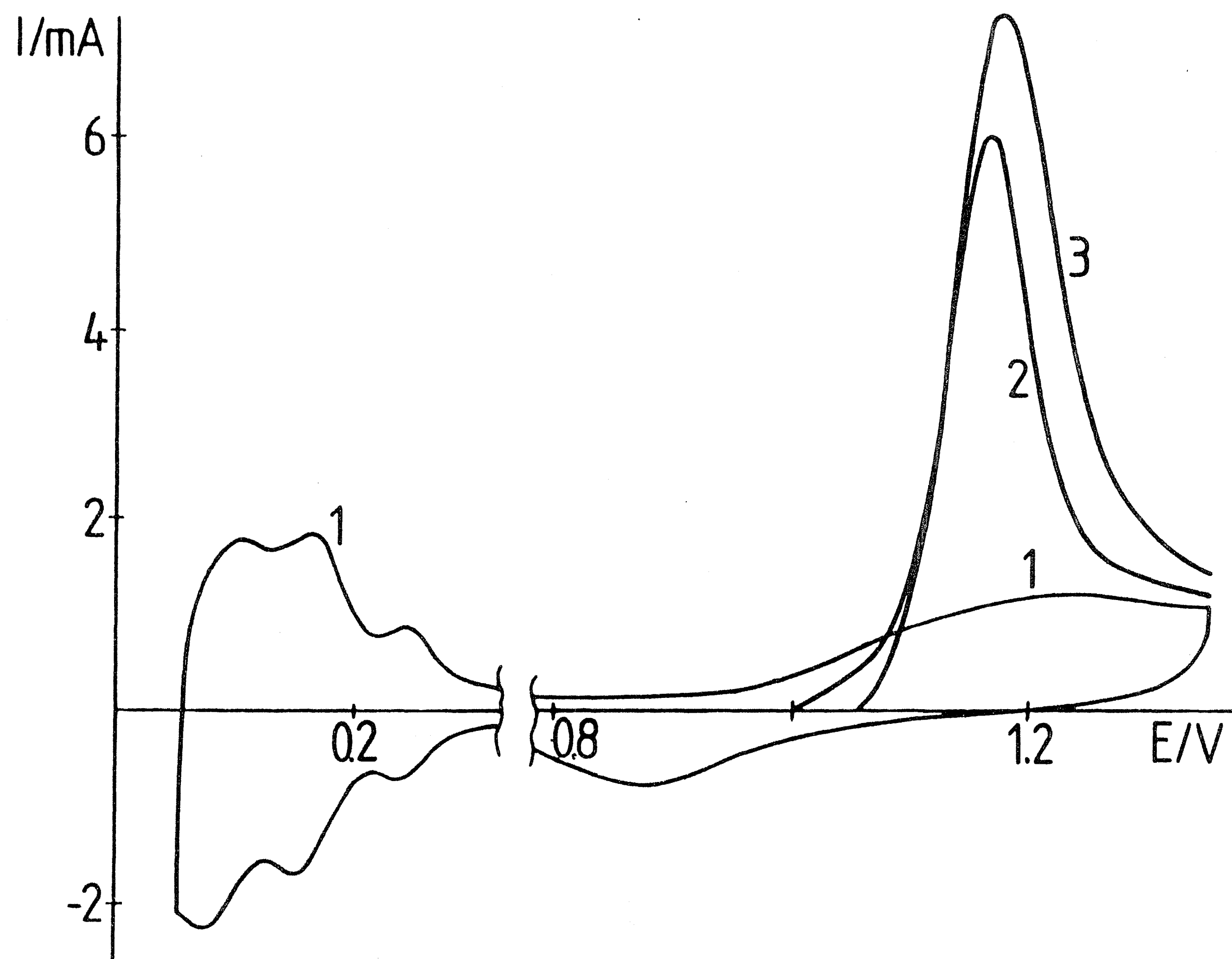
I/mA
6
4
2
-2
1
1
2
3
0.2
0.8
1.2
E/V

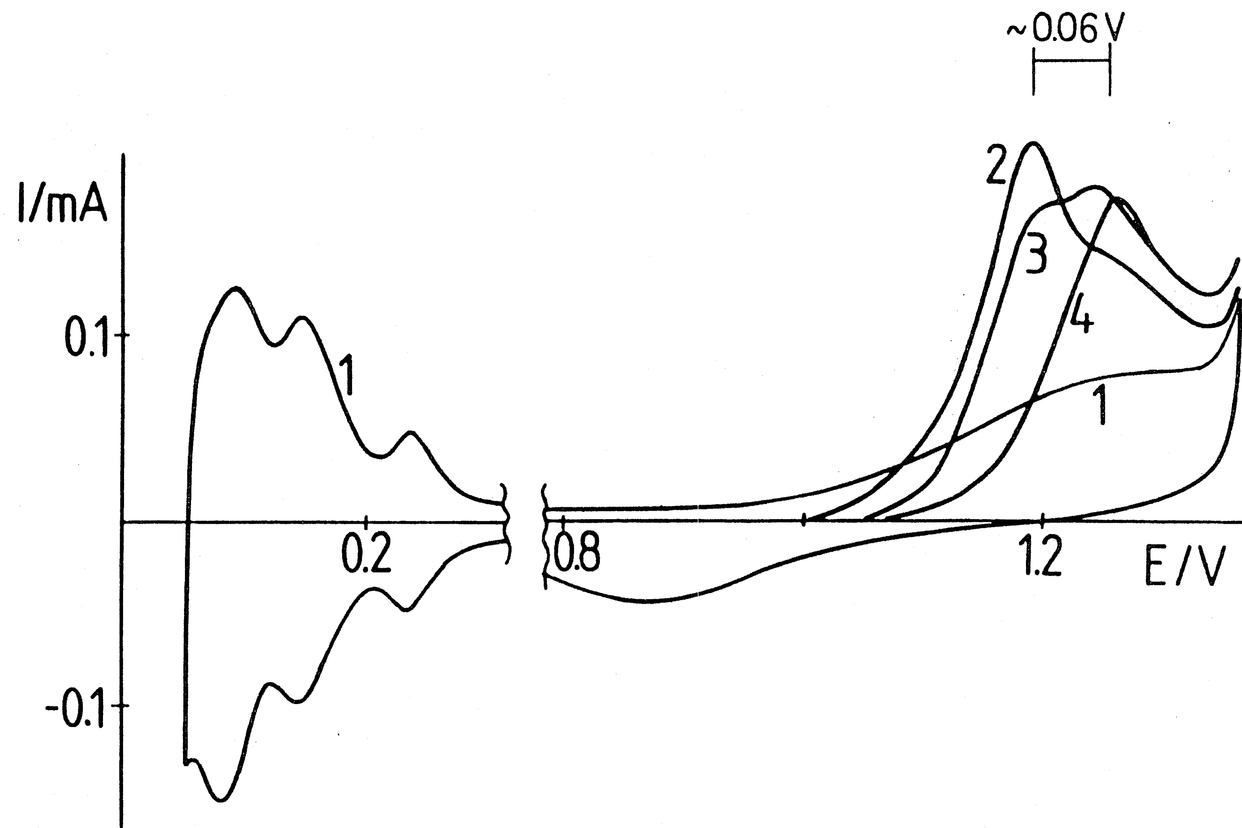
~0.06 V
I/mA
0.1
-0.1
0.2
0.8
1.2
E/V
1
2
3
4
1

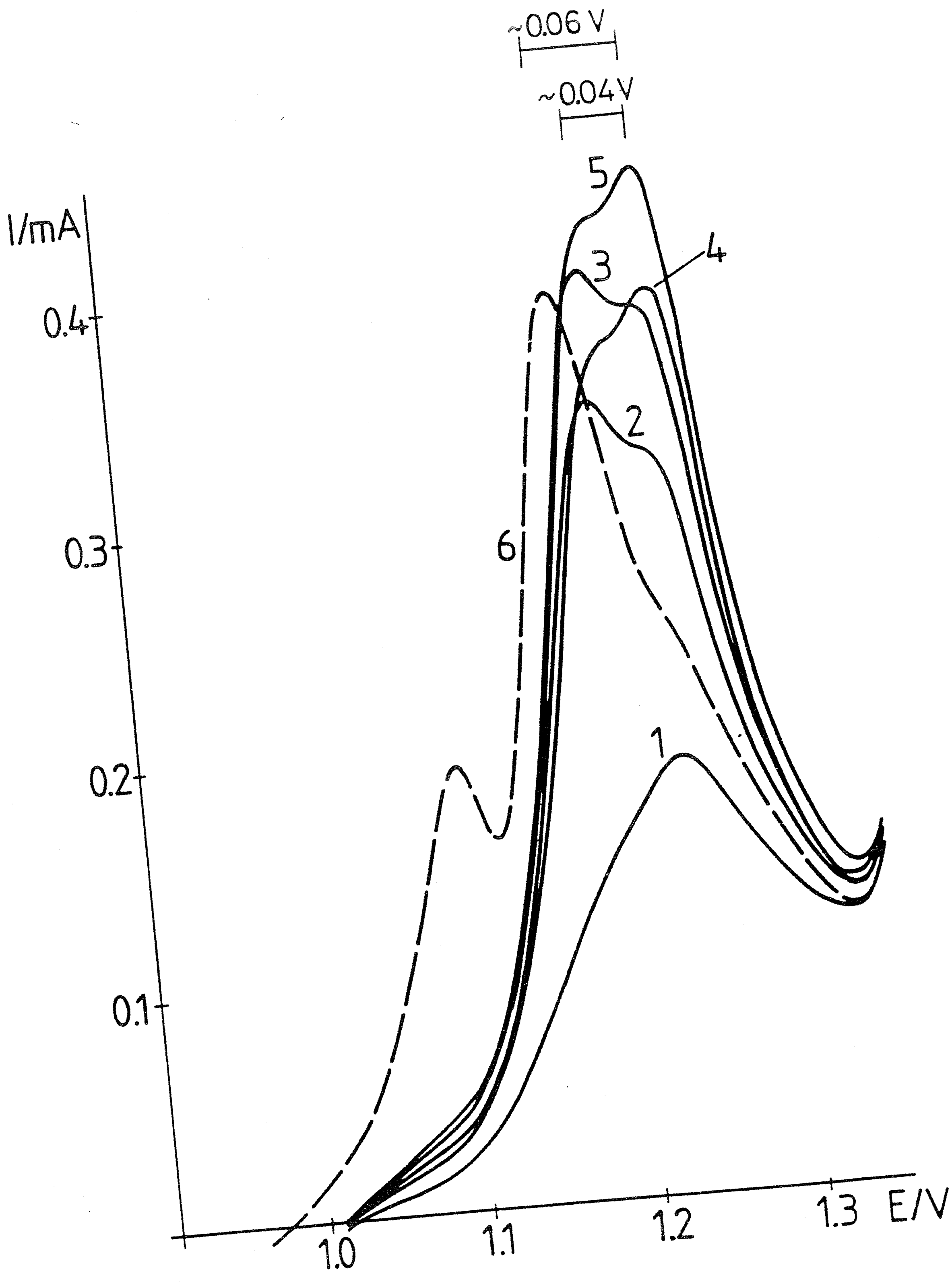
~0.06 V
~0.04V
I/mA
0.4
0.3
0.2
0.1
5
3
4
2
6
1
1.0
1.1
1.2
1.3
E/V

Fig. 4

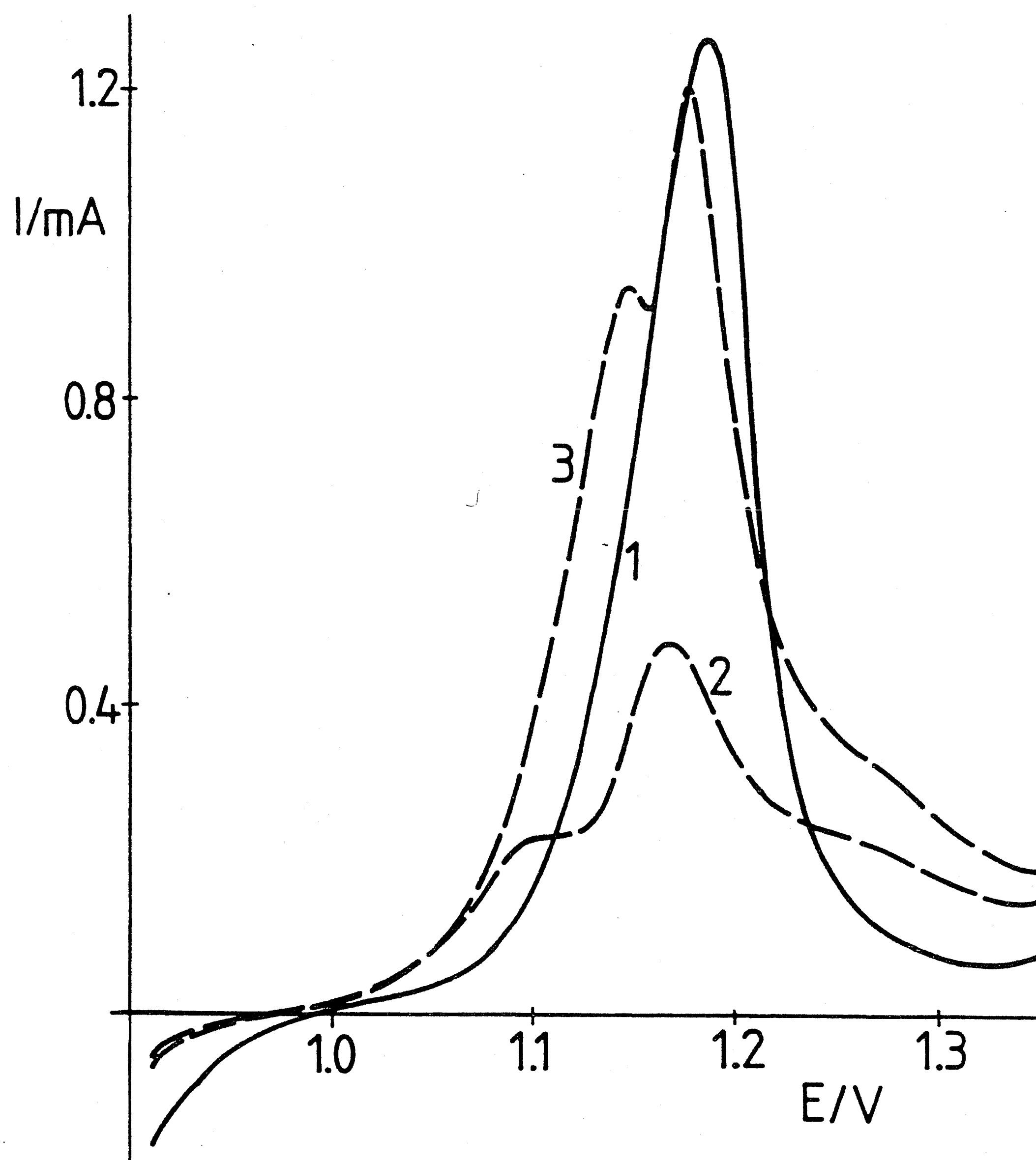

bontó hatással működő kén-tartalmú szerves nikkel-komplex (Ni-DBTC) stabilizátornál, amennyiben az oxigéntartalmú csoportok képződése még 200 Mlxh-s dózissal történő besugárzás után sem indult meg. (Nagyobb dózisoknál a folyamat nem volt követhető, mivel a minták minden esetben még a karbonil és a hidroperoxid csoportok képződésének megindulása előtt eltörtek.)

Tanulmányoztuk ezen adalék, és a fenti, más mechanizmussal működő stabilizátorok együttes adagolásának hatását a fotooxidáció folyamán. Azt találtuk, hogy csak az UV-abszorber hidroxi-benzofenon és a piperidin szebacát együttes adagolása esetén érhető el stabilitás javulás. A kétféle adalék hatása additívnak bizonyult, és a minták spontán törése csak igen nagy dózisú besugárzás után — mintegy 250 Mlxh — következett be.

Szerzők köszönetüket fejezik ki *Jókay Lászlónak* a laboratóriumban előállított adalékok szintetizálásában nyújtott segítségéért.

Effect of some stabilizers with different mode of action on polypropylene photooxidation. *G. Bálint, T. Kelen, F. Tüdős* and *Á. Rehák*

The photostabilizing effects of different stabilizers were studied during polypropylene photooxidation by following the formation of carbonyl and hydroperoxide groups as well as the change of stabilizer concentrations. The sterically hindered piperidine derivative — tetramethyl-piperidine sebacate (Tinuvin 770) — proved to be more effective than the UV-absorbers: hydroxy-benzophenone (Cyasorb UV 531), substituted benzotriazole (Tinuvin 326), and the hydroperoxide decomposer: an organic nickel complex containing sulphur (Ni-DBTC). In presence of the piperidine derivative no oxidation product formation was observed even after irradiation with 200 Mlxh dose. (The process could not be investigated after longer irradiation, because of the spontaneous rupture of the samples.)

The effect of the addition of hindered piperidine derivative together with other stabilizers working by different mechanisms has also been investigated. We have found that stability improvement can be achieved only by adding piperidine sebacate together with the UV absorber hydroxy-benzophenone. The effect of these two stabilizers proved to be additive, and the spontaneous rupture of the samples took place only after a long period of irradiation (~250 Mlxhs).

Budapest, MTA, Központi Kémiai Kutató Intézet
Érkezett: 1979. XI. 13.

Platinán végbemenő palládiumleválás vizsgálata sósavas közegben

SZABÓ SÁNDOR és NAGY FERENC

Platinafémek más platinafémeken végbemenő adszorpcióját viszonylag kevéssé tanulmányozták[1,2]. Korábbi közleményünkben beszámoltunk arról, hogy az adszorpció mind potenciosztatikus körülmények között mind pedig az adszorbeált hidrogén ionizációjának révén végbemehet[2]. Megállapítottuk az adszorbeált hdrogén ionizációjának révén végbemenő Pd-adszorpció mechanizmusát és az adszorbeált Pd-atom helyigényét.

Jelen közleményünk tárgya; újabb eredményeink a platinán végbemenő Pd-leválás és adszorpció területén. Ezen túlmenően foglalkozunk az adszorbeált palládiummal módosított Pt-katalizátor hőállandóságával H_2 és levegő atmoszférában. Végül bemutatjuk az adszorbeált palládium hatását az aceton hidrogénezésének kinetikájára.

Vizsgálataink során használt kísérleti módszerek a ciklikus voltammetria és az állandó erősségű árammal felvett töltésgörbék voltak.

Kísérleti rész

Az előző közleményünkben leírt módszert és cellát használtuk[3]. A potenciált az ugyanolyan pH-jú oldatba merülő hidrogén-elektródhoz képest mértük.

A mérések során PAR 170 és Radelkis műszereket használtunk, az oldatokat MERCK és ARISTAR vegyszerekből készítettük. Oxigénmentesítésre tisztított nitrogénáramot használtunk.

Az adszorbeált hidrogén ionizációjának révén végbemenő fémadszorpció vizsgálatánál $1{,}3\times10^{-1}$ mol/l $PdCl_2$ koncentrációt alkalmaztunk. Az aceton hidrogénezésének vizsgálatakor az acetonkoncentráció 0,27 mol/l volt.

Eredmények és értékelésük

A palládiumadszorpció vizsgálata

Az 1. ábrán mutatjuk be egy királyvízzel mosott sima Pt-elektród 5×10^{-4} mol/l $PdCl_2$ koncentráció mellett 1mólos HCl oldatban felvett ciklikus voltametriás görbéjét. A lineáris polarizáció sebessége 0,05 V/s volt 1.3 és 0,04 V potenciálhatárok mellett.

A görbét összehasonlítva a tiszta alapoldatban felvett görbével, több egymástól független folyamat különíthető el. A hidrogén adszorpciója és deszorpciója, valamint a levált Pd ionizációja. Az ezüstleválástól eltérően a Pd-adszorpció eseté-

[1] *D. A. Rand, R. Woods:* J. Electroanal. Chem.. *44.* 83. 1973.

[2] *Szabó S., Nagy F.:* Magy. Kém. Folyóirat, *81.* 365. 1975.

[3] *S. Szabó, F. Nagy:* J. Electronala. Chem., *70.* 357. 1976.

ben a kristálygócképződés és növekedés nem különíthető el a görbén[4].

Nem kétséges, hogy a görbe *B* szakasza az adszorbeált Pd ionizációjától származik. A szakasz két csúcs átlapolásának tűnik, azonban ezt más kísérleteink nem erősítették meg. Figyelembe véve

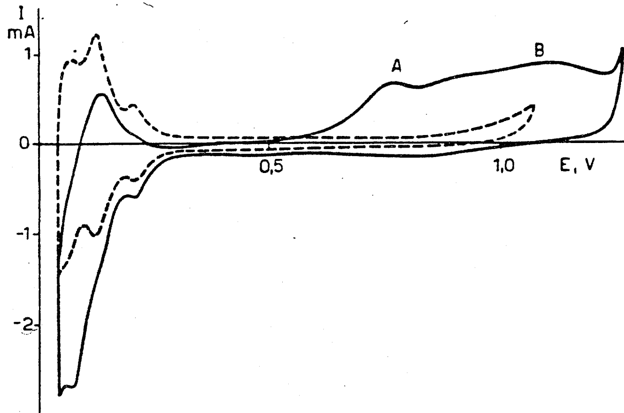

1. ábra

Egy sima platina elektród ciklikus voltamogramja 5×10^{-2} mol/l $PdCl_2$ jelenlétében. A polarizáció sebessége 0.05 V/s; a szaggatott vonal a voltamogram 1 mólos HCl oldatban

a nagyobb Pd koncentráció mellett kapott eredményeinket is (2. ábra), az *A* csúcs a tömb Pd ionizációjától származhat. Ennek az a tény mond ellent, hogy az *A* csúcsnak megfelelő potenciál pozitívabb, mint ami a $PdCl_4^{2-} + 2\,e \rightleftharpoons Pd + 4\,Cl^-$ egyensúly alapján várható lenne. Ez azzal magyarázható, hogy az ionizáció bizonyos „előfeszültség" (undervoltage) mellett megy végbe, ami azt jelenti, hogy az egyatomnyi vastag adszorbeált rétegre leváló Pd szintén pozitívabb potenciálon ionizálódik mint a Nernst potenciál. Ebből következik, hogy a tömb és az adszorbeált fázis között egy átmeneti fázisnak kell lennie.

A palládiumleválás vizsgálata

Az előző fejezetben leírt kísérletet $1{,}2\times10^{-2}$ mol/l $PdCl_2$ mellett, 1,34 és 0,00 V potenciálhatárnál, 0,1 V/s polarizációsebeséggel ismételtük meg. Az eredményt a 2. ábrán mutatjuk be. Az ábra tanúsága szerint az adszorbeált Pd mennyisége

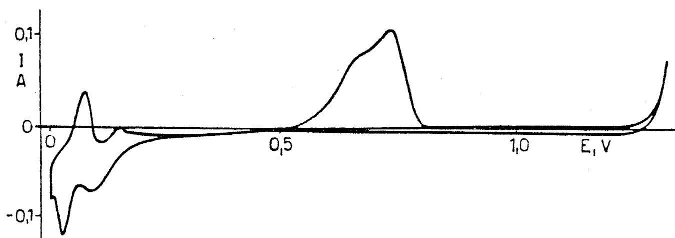

2. ábra

Egy sima platina elektród ciklikus voltamogramja 1.2×10^{-2} mol/l $PdCl_2$ jelenlétében. A polarizáció sebessége 0,1 V/s

[4] *R. G. Barradas, S. Fletcher, S. Szabó:* Can. Journal of Chem., *56.* 2029. 1978.

elhanyagolható a tömb Pd-hez képest. A koncentrációváltozás legmeglepőbb eredménye az, hogy a tömb fém ionizálódása nem egy, hanem két csúcsot eredményezett. Az eredmény az ezüstleválásnál kapott eredménnyel együtt azt az elképzelést erősíti meg, hogy két csúcs megjelenésének okát a Pt felületén kell keresni[4]. A kettő és nem több csúcs arra mutat, hogy az adszorpció és leválás a Pt két kristálysíkján, valószínűleg a 111 és 100 síkon megy végbe, két csúcsot eredményezve[5, 6, 7], ha ezt más folyamatok nem zavarják meg[6, 8].

A másik meglepő eredmény a kristálygócképződés és növekedés miatt várható csúcs hiánya, amelyet ~0,5 V-nál kellett volna kapni, amikor a potenciál negatív irányba változott. Ez a folyamat hasonló körülmények mellett egy határozott csúcs eredményezett az ezüstleválás esetén, tehát a diffúzió nem lehet a különbség oka[4].

Igen fontos azt megjegyezni, hogy 1,34 és 0,3 V között végzett ciklusok nem vezettek észrevehető fémleváláshoz, pedig ez termodinamikailag lehetséges lett volna.

Az előzőekben ismertetett eredmények arra mutatnak, hogy a fémleválás főleg a 0,3—0,0 V potenciáltartományban megy végbe, ahol a $H^+ + e \rightarrow H_a$ folyamat szintén végbemegy, következésképpen az adszorbeált hidrogén-atomoknak is részt kell venniük a redukcióban, tehát a fémleválás folyamatai:

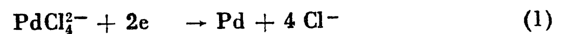

$$PdCl_4^{2-} + 2e \rightarrow Pd + 4\,Cl^- \qquad (1)$$

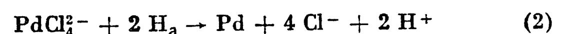

$$PdCl_4^{2-} + 2\,H_a \rightarrow Pd + 4\,Cl^- + 2\,H^+ \qquad (2)$$

Az előzőekben ismertetett kísérleti eredmények alapján az is megállapítható, hogy a (2) folyamat sebessége a nagyobb.

A platinán adszorbeált hidrogén ionizációjának révén végbemenő palládiumadszorpció vizsgálata

A kapott eredményeket a 3. ábrán mutatjuk be. melynek eredményei teljesen megegyeznek az előző közleményünkben publikált eredményekkel[2]. Ennek ellenére a kísérletet érdemes közölni, mivel világosan mutatja, hogy a képződő adszorbeált fémréteg első lépése tömb Pd (3. görbe *B* szakasza) leválása. Még a palládiumból deszorbeálódó hidrogén által okozott α—β fázisátmenetnek megfelelő 0,06 V potenciál is felismerhető a görbén (3. görbe *A* szakasza).

Tapasztalataink szerint a tömb leválást mindig figyelembe kell venni, ha az termodinamikailag lehetséges[3, 9]. Mivel a vélemények megoszlanak erről a kérdésről[3, 10, 11, 12], ezért szeretnénk bemutat-

[5] *A. T. Hubbard, R. N. Ishikawa, J. Katekaru:* J. Electroanal. Chem., *86.* 271. 1978.

[6] *P. N. Ross, Jr.:* J. Electrochem. Sos., *126.* 67. 1979.

[7] *K. Yamamoto, D. M. Kolb, R. Kötz, G. Lehmpfuhl:* J. Electroanal. Chem., *96.* 233. 1979.

[8] *M. Nakamura, H. Kita:* J. Electroanal. Chem., *68.* 49. 1976.

[9] *S. Szabó, F. Nagy:* J. Electroanal. Chem., *85.* 339. 1977.

[10] *S. Stucki:* J. Electroanal. Chem., *80.* 375. 1977.

ni azokat a kinetikai okokat, amelyek szükségszerűen tömb leválást eredményeznek.

Ha egy Pt-elektród potenciálja negatívabb mint a Me^{n+}/Me rendszer Nernst potenciálja, akkor a következő folyamatok mennek végbe:

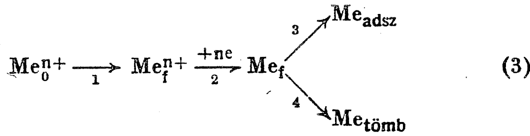

$$Me_0^{n+} \xrightarrow{1} Me_f^{n+} \xrightarrow[2]{+ne} Me_f \begin{cases} \xrightarrow{3} Me_{adsz} \\ \xrightarrow{4} Me_{tömb} \end{cases} \quad (3)$$

ahol az 1 folyamat a fémion diffúziója a felülethez, a 2 folyamat a töltéstátlépés, a 3 folyamat a fém-

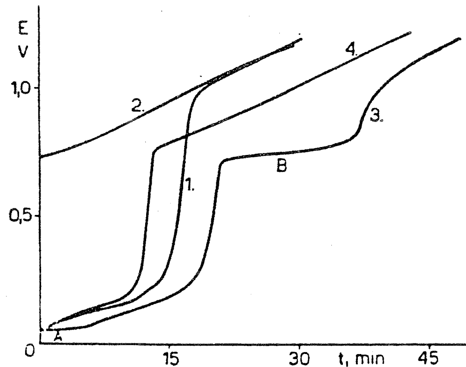

3. ábra (I = 0,5 mA)

1: töltésgörbe 0,2 mólos HCl oldatban; 2: a palládiummal borított elektród töltésgörbéje; 3: a tömb palládiummal borított elektród töltésgörbéje; 4: az adszorbeált palládiummal borított elektród töltésgörbéje

adszorpció és a 4 folyamat a tömb leválás. Feltételezve, hogy a töltésátlépés sebessége a legnagyobb, a sebességmeghatározó folyamat lehet a diffúzió vagy az adszorpció és a tömb leválás, azaz

$$r_1 = r_3 + r_4$$

A kísérleti tapasztalatoknak megfelelően a tömb leválást mindig megelőzte az adszorpció[11, 12], tehát kezdetben $r_3 > r_4$. Az adszorpció sebessége azonban a borítottságtól is függ, tehát a tömb leválának akkor meg kell kezdődnie, ha $r_1 \geq r_3$. Természetesen az r_3 és r_4 aránya erősen függ a felület durvaságától[3, 10, 11].

Egy adszorbeált Pd-atom helyigénye

Előző közleményünkben[2] közöltük a helyigény meghatározását, jelen közleményünkben pedig szeretnénk bemutatni, hogy a hidrogén adszorpciójának a Pd adszorpciója által okozott csökkenése hogyan használható fel a helyigény meghatározására. Ebből a célból a következő jelölések bevezetése szükséges:

S: egy adszorbeált Pd-atom által elfoglalt hidrogén adszorpciós helyek száma;

Q_H^0: a platinán adszorbeált hidrogén oxidációjához szükséges töltés mennyisége;

Q_H: a palládiummal borított platinán adszorbeálódó hidrogén oxidációjához szükséges töltés mennyisége;

$Q_{H_{Pd}}$: a palládium-atomokon adszorbeált hidrogén oxidációjához szükséges töltés mennyisége, feltéve hogy: $H_a/P_{adsz} \approx 1$;

Q_{Pd}: az adszorbeált Pd-atomok oxidációjához szükséges töltés mennyisége;

$Q_{H_{Pt}}$: a palládiummal nem borított Pt-felületen adszorbeálódó hidrogén oxidációjához szükséges töltés mennyisége.

Pd-adszorpció után a felületen adszorbeálódó hidrogén mennyiségének megfelelő töltés:

$$Q_H = Q_{H_{Pd}} + Q_{H_{Pt}} \quad (5)$$

Mivel

$$Q_{H_{Pd}} = 0{,}5 Q_{Pd} \quad (6)$$

és

$$Q_{H_{Pt}} = Q_H^0 - 0{,}5\, Q_{Pd}\, S \quad (7)$$

A (6) és (7) egyenletekből megkapható, hogy:

$$S = 1 + \frac{2\,\Delta Q_H}{Q_{Pd}} \quad (8)$$

ahol $\Delta Q_H = Q_H^0 - Q_H$.

A 3. ábra adatainak alapján $S = 1{,}5$, ami jó egyezést mutat az előző közleményünkben publikált[2] $S = 1{,}6$ értékkel. Az eltérés oka az lehet, hogy a felület nem volt teljesen borítva palládiummal amikor mi úgy tekintettük, és ez természetesen pozitív változást okozott a helyigény nagyságában.

Mivel a helyigény más fémek esetében függ a borítottságtól[9, 13], ezért ezt a kérdést is megvizsgáltuk. A 4. ábrán a helyigényt ábrázoltuk a borítottság függvényében, Q_H^0 ionizációjának révén

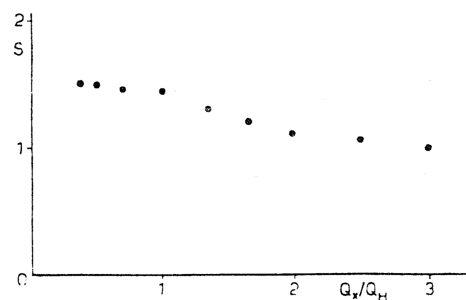

4. ábra

A helyigény függése a borítottságtól

lérejövő Pd-borítottságot egységnek tekintve. Nyilvánvaló, hogy a helyigény csökken a borítottság növekedésével, azonban olyan éles változás mint az arany és a bizmut adszorpciója esetében, itt nem figyelhető meg[9, 13].

[11] *N. Furuya, S. Motoo:* J. Electroanal. Chem., *72.* 165. 1976.

[12] *N. Furuya, S. Motoo:* J. Electroanal. Chem., *78.* 243. 1977.

[13] *S. Szabó, F. Nagy:* J. Electroanal. Chem.. *88.* 259. 1978.

Az adszorbeált Pd réteg elektroszorpciós vegyértéke

Az előző közleményünkben közölt meggondolások alapján meghatároztuk az adszorbeált fémréteg elektroszorpciós vegyértékét[14]. Ebből a célból felvettük a Pt elektród töltésgörbéjét 0.2 mólos HCl oldatban (5. ábra 1 görbe) és ezután az adszorbeált hidrogén ionizációja révén adszorbeált Pd-réteget hoztunk létre rajta. Az adszorbeált Pd oxidációjához szükséges töltés (q_m) meghatározása céljából ismét felvettük a töltésgörbét (5. ábra 2 görbe). A kísérletet ezután úgy ismételtük meg, hogy a töltésgörbe felvétele előtt a Pd-mal borított elektródot hidrogénnel is telítettük, meghatározván a redukált adszorbeált fémréteg oxidációjához szükséges töltés mennyiségét (q_{m_F}). Az egyszerűség kedvéért a görbe hidrogénszakaszát elhagytuk (5. ábra 3 görbe).

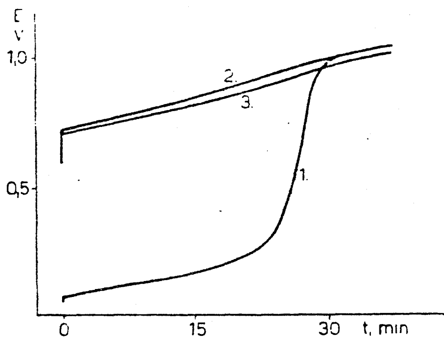

5. ábra (I = 0,075 mA)
1: töltésgörbe 0,2 mólos HCl oldatban; 2: adszorbeált Pd-mal borított elektród töltésgörbéje 0.2 mólos HCl oldatban; 3: adszorbeált palládiummal borított elektród töltésgörbéje 0.2 mólos HCl oldatban hidrogénnel való telítés után

Az elektroszorpciós vegyérték kiszámítható az előző közleményünkben publikált egyenlet segítségével[14]:

$$dq_m/dq_{m_F} = \gamma/z \qquad (9)$$

Több mérésünk átlaga: $\gamma = 1,8$.

Az oxigénadszorpció hatása a palládiummal borított platina sajátságaira

Adszorbeált fémekkel módosított katalizátorok használatakor igen fontos tudni azt, hogy az oxigén adszorpciója hogyan befolyásolja a katalizátor sajátságait.

Az ábrák szerint az adszorbeált palládiummal borított platina ~0,72 V-ig állandó. tehát levegő atmoszférában nem. Kérdés mi a helyzet kloridionok távollétében? A kérdés vizsgálatára vonatkozó kísérlet eredményét a 6. ábrán mutatjuk be. Először a Pt-elektród töltésgörbéjét vettük fel 0.2 M HCl oldatban. Ezután az adszorbeált hidrogén ionizációjának révén adszorbeált Pd-réteget hoztunk létre a felületen és tiszta alapoldatban ismét felvettük az elektród töltésgörbéjét (6. ábra 2. görbe). A kísérletet úgy ismételtük meg. hogy az adszorbeált fémréteg kialakulása után a cellát kloridionmentesre mostuk és 0,2 mólos $HClO_4$ oldatban határoztuk meg az elektród töltésgörbéjét. A töltésgörbe után katódos polarizációval redukáltuk az adszorbeált oxigént és ismét meghatároztuk az elektród töltésgörbéjét 0.2 mólos HCl oldatban.

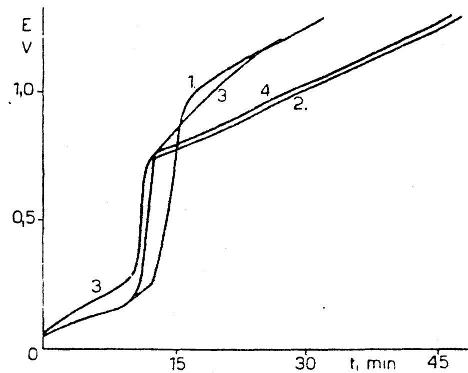

6. ábra (I = 0,5 mA)
1: töltésgörbe 0.2 mólos HCl oldatban; 2: adszorbeált Pd-mal borított elektród töltésgörbéje 0.2 mólos HCl oldatban; 3: adszorbeált Pd-mal borított elektród töltésgörbéje 0,2 mólos $HClO_4$ oldatban; 4: töltésgörbe 0.2 mólos HCl oldatban az előző töltésgörbe után

A 2 és 4 görbe összehasonlítása azt mutatja, hogy az oxigénadszorpció nem okozott változást az adszorbeált Pd szerkezetében, tehát felhasználható a cellán kívül, illetve anódosan aktiválható elektrokatalitikus vizsgálatokban.

A Pd-adszorpció hatása a platinán végbemenő hidrogénadszorpcióra

A konstans árammal felvett töltésgörbék jól mutatják, hogy a Pd-adszorpció csökkenti a platinán végbemenő hidrogénadszorpciót, azonban arra vonatkozóan, hogy milyen fajtájú hidrogén adszorpcióját csökkenti, nem adnak felvilágosítást A kérdés vizsgálatakor először a Pt-elektród lineá-

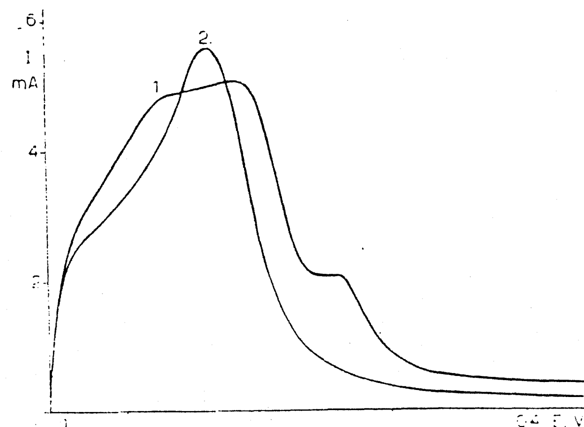

7. ábra
1: egy Pt-elektród lineáris voltamogramja 0.2 mólos HCl oldatban; 2: adszorbeált Pd-mal borított elektród lineáris voltamogramja 0.2 mólos HCl oldatban: a polarizáció sebessége 2.7×10^{-1} V/s

[14] A. Szabó, F. Nagy: J. Electroanal. Chem.. 84. 93. 1977.

ris voltamogramját vettük fel $2,7 \times 10^{-3}$ V/s polarizációsebességgel. Ezután az adszorbeált hidrogén ionizációjának révén végbemenő fémadszorpció útján adszorbeált Pd-mal borítottuk a felületet és ismét meghatároztuk a lineáris voltamogramot. A 7. ábrán az 1 és 2 görbe összevetése mutatja azt az alapvető változást, ami a Pd okozott a hidrogén adszorpcióban, különösen az erősen adszorbeált hidrogén mennyiségében.

Az aceton hidrogénezése Pd-mal borított platinán

A 8. ábrán mutatjuk be egy Pd-mal borított és Pd-mentes elektród polarizációs görbéjét 1 mólos $HClO_4$ oldatban 0,27 mol/l acetonkoncentráció mellett. A Pd-borítottság 0,75 volt. Az 1 görbe tanúsága szerint ilyen jelentős Pd-borítottság mellett az aceton hidrogénezése gyakorlatilag megszűnik, a mért áram csupán a hidrogénleválásból adódik. Bár a Pd adszorpciója csökkenti a hidrogén adszorpcióját, a sebesség lecsökkenésének okát nem lehet csupán a hidrogén adszorpciójában bekövetkezett változásban keresni, mivel ez ~20%. A Pd adszorpciója elsősorban az acetonadszorpcióban bekövetkező változáson keresztül akadályozhatja meg a hidrogénezést. Ez megnyilvánulhat az aceton-borítottság csökkenésében és az adszorpció módjában. A kísérlet magyarázatul szolgál arra a kísérleti tényre, hogy Pd-katalizátoron miért nem lehet megvalósítani a ketonok hidrogénezését.

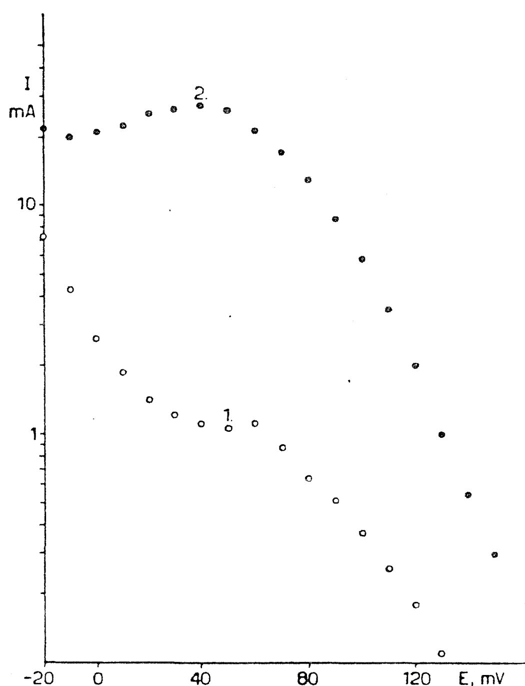

8. ábra
1: adszorbeált Pd-mal borított platina elektród polarizációs görbéje 1 mólos $HClO_4$ oldatban 0.27 mol/l aceton mellett; 2: a Pd-mentes elektród polarizációs görbéje

[15] S. Szabó, F. Nagy, D. Móger: Acta Chim. Acad. Sci. Hung., 93, 33, 1977.

A hőkezelés hatása a palládiummal borított platina sajátságaira

a) Hidrogén atmoszféra

A hőkezelés hatását az előző közleményünkben leírt módon, előzetesen 500 °C-on hőkezelt Pt-lemez katalizátor segítségével vizsgáltuk meg[15]. Először adszorbeált Pd-réteget hoztuk létre a felületen, utána meghatároztuk az elektród töltésgörbéjét. A Pd-adszorpciót megismételve, a cellát Cl^--mentesre mostuk és elvégeztük a hőkezelést.

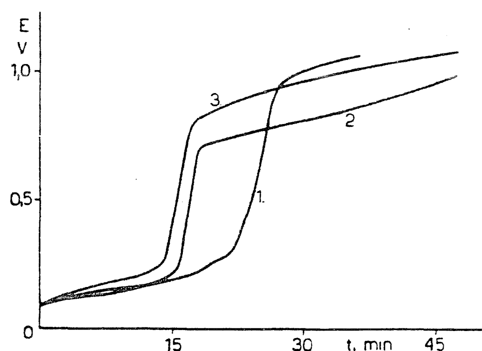

9. ábra (I = 0,02 mA)
1: töltésgörbe 0,2 mólos HCl oldatban; 2: adszorbeált Pd-mal borított elektród töltésgörbéje; 3: adszorbeált Pd-mal borított elektród töltésgörbéje 250 °C-on végzett hőkezelés után

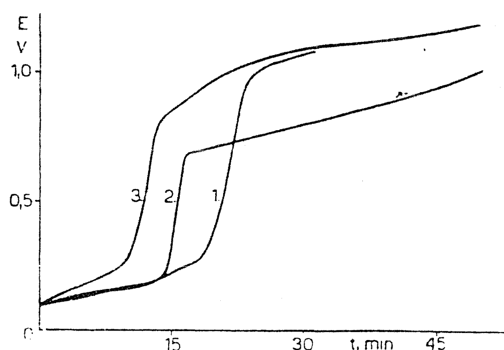

10. ábra (I = 0,02 mA)
1: töltésgörbe 0,2 mólos HCl oldatban; 2: adszorbeált Pd-mal borított elektród töltésgörbéje; 3: adszorbeált Pd-mal borított elektród töltésgörbéje 350 °C-on végzett hőkezelés után

A mintát 20 percig tartottuk az adott hőfokon hidrogéngáz atmoszférában, és utána a cellába visszahelyezve a katalizátort, ismét meghatároztuk a töltésgörbét. A két görbe összevetése jól mutatja a hőkezelés okozta változásokat.

A vizsgálatot 150 °C-nál kezdtük és 50 fokonként emeltük a hőmérsékletet. A 9. és 10. ábrán a 250 °C-on és 350 °C-on végzett mérések eredményét mutatjuk be. Az ábrán alapján megállapítható, hogy az adszorbeált palládiummal módosított platina katalizátor legfeljebb ~250 °C-ig használható eredeti szerkezetének megőrzése mellett.

b) Levegő atmoszféra

A hidrogén atmoszférában végzett vizsgálatot levegőben is megismételtük. Az eredményt a 11. ábrán mutatjuk be. Az ábra tanúsága szerint az

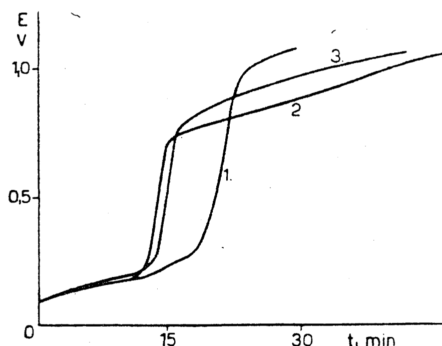

11. ábra (I = 0,02 mA)

1: töltésgörbe 0,2 mólos HCl oldatban; 2: adszorbeált Pd-mal borított elektród töltésgörbéje; 3: adszorbeált Pd-mal borított elektród töltésgörbéje 300 °C-on levegőben végzett hőkezelés után

adszorbeált palládiummal borított platina katalizátor levegőn ~300 °C-ig aktiválható a szerkezet megőrzése mellett.

Összefoglalás

A platinán adszorbeálódó palládium csökkenti a hidrogénadszorpciót, mert a Pd helyigénye 1,5. Az adszorbeált Pd-mal borított platinára leváló tömb Pd kristályszerkezete függ attól, hogy a platina melyik kristálysíkjára válik le. Az adszorbeált hidrogén ionizációjának révén végbemenő fémadszorpció két lépésben megy végbe. Az első lépés tömb leválást eredményez, és ennek ionizálódásával jön létre az adszorbeált fémréteg. Az ily módon létrehozott adszorbeált fémréteg elektroszorpciós vegyértéke ~1,8. Az adszorbeált Pd kloridmentes közegben nem deszorbeálódik. Az adszorbeált Pd gátolja az aceton platinán végbemenő hidrogénezését. Az adszorbeált palládiummal borított platina katalizátor hidrogénatmoszférában ~250 °C-ig, levegőn pedig ~300 °C-ig őrzi meg eredeti szerkezetét.

Investigation of palladium deposition on platinum in hydrochloric acid media. *S. Szabó* and *F. Nagy*

Palladium adsorbed on Pt decreases the hydrogen adsorption because the site requirement of an adsorbed Pt atom is 1.5. The crystal structure of bulk Pd deposited on Pt covered by adsorbed Pd depends on which crystal plane the Pd deposits. Pd adsorption via the ionization of adsorbed hydrogen takes place in two steps. The first step is the bulk deposition then the adsorbed monolayer is formed via the ionization of bulk Pd. The electrosorption valency of the adsorbed Pd is ~1.8. The adsorbed Pd does not desorb in Cl^--free media. The adsorbed Pd retards the hydrogenation of acetone at platinized platinum electrodes. It has been shown that a platinum catalyst covered by adsorbed Pd preserves its specific features up to 250 °C in hydrogen atmosphere and up to 300 °C in air.

Budapest, MTA Központi Kémiai Kutató Intézet
Érkezett: 1979. XI. 1.

Izociánsav adszorpciójának infravörös spektroszkópiai vizsgálata*

(Rövid közlemény)

SOLYMOSI FRIGYES és BÁNSÁGI TAMÁS

Míg a nemesfémet tartalmazó fém-oxidok felületén a NO + CO katalitikus reakcióban felületi izocianát könnyen képződik[1], nemesfém távollétében az oxidokon hasonló körülmények között izocianát-képződést nem észleltek. Ennek ellenére a legújabb kísérleti eredmények és megfontolások alapján arra lehet következtetni, hogy a fémen kialakult izocianát a hordozóra vándorol, amely döntően befolyásolja további reakcióit[2−4]. Mivel a feltételezések szerint a felületi izocianát kialakulása okozza a robbanómotorok kipufogó gázainak katalitikus átalakításakor fellépő nemkívánatos ammónia és hidrogén-cianid képződését[1, 5−7], az izocianát szerepének megítélése szempontjából szükségessé vált tulajdonságainak alaposabb megismerése az oxidok felületén. Mivel fém-oxidokon

* A dolgozat angol nyelven megjelent: J. Phys. Chem., *83*, 552, 1979.

[1] *M. L. Unland:* J. Phys. Chem., *77*, 1952, 1973.

[2] *R. A. Dalla Betta, M. Shelef:* J. Mol. Catal., *1*, 431, 1976.

[3] *F. Solymosi, J. Kiss, J. Sárkány:* „Proceedings of the 3rd International Conference on Solid Surfaces". R. Dobrozemsky, Vienna, 1977, 819. o.

[4] *F. Solymosi, L. Völgyesi, J. Sárkány:* J. Catal., *54*, 336, 1978.

[5] *R. J. H. Voorhoeve, C. K. N. Patel, L. E. Trimble, R. J. Kerl, P. K. Gallagher:* J. Catal., *45*, 297, 1976.

[6] *R. J. H. Voorhoeve, L. E. Trimble:* J. Catal., *38*, 80, 1975.

[7] *F. Solymosi, J. Raskó:* J. Catal., *49*, 240, 1977.

27.

Adszorbeált fémekkel módosított katalizátorok előállítása

SZABÓ SÁNDOR*
NAGY FERENC*

Bevezetés

Az elmúlt évtizedben az elektrokémikusok között általánossá vált az a felismerés, hogy a fémek más fémeken végbemenő adszorpciója a fémek között általános jelenség. Annak ellenére, hogy az első megfigyeléseket nem az elektrokémia területén végezték [1], mégis az elektrokémiai módszerek bizonyultak a legalkalmasabbaknak a jelenség részleteinek a felderítésére. Ennek oka az, hogy az adszorbeált forma elektrokémiai módszerekkel különíthető el legegyszerűbben a tömb formától.

Az alkalmazott vizsgálati módszerek következtében a jelenség leírásában az elektrokémiai terminológia dominál, azt az érzetet keltve, mintha tipikusan elektrokémiai jelenséggel lenne dolgunk, pedig adszorbeált fémrétegek nem csupán elektrokémiai módszerekkel hozhatók létre és nem is csupán így vizsgálhatók.

Ilyen alapvető felismerés, mint a fémek fémeken végbemenő adszorpciója, természetesen a tudomány, a technika és a technológia számtalan és látszólag igen távolinak tűnő területén módosítja az eddigi elképzeléseket. Ezek között az egyik legfontosabb a katalízis. A fémadszorpció adta lehetőségek a katalízisben felhasználhatók fémkatalizátorok felületének módosítására és a különféle adszorpciós jelenségek vizsgálatára, beleértve a katalizátorok mérgezésének és öregedésének folyamatait is.

Mielőtt azonban rátérnénk az adszorbeált fémekkel módosított katalizátorok előállításának részleteire, célszerűnek látszik összefoglalni a fémek fémeken végbemenő adszorpciójának vizsgálatában elért legfontosabb eredményeket.

A fémek adszorpciójáról

Fémek más fémeken végbemenő adszorpciója az adszorbeálódó fém reverzibilis Nernst potenciáljánál pozitívabb potenciálon megy végbe. A Nerst potenciál és az adszorpció potenciálja közötti különbséget „undervoltage"-nak vagy „előfeszültség"-nek nevezik. Ez a potenciálkülönbség annak a szabadentalpia-különbségnek a mértéke, amennyivel kedvezőbb termodinamikai állapotban van az adszorbeált fématom az idegen fém felületén mint a saját kristályrácsában.

Ez a szabadentalpia-különbség néhány tized joule-tól —200 kjoule-ig változik [2, 3, 4, 5].

Megállapították, hogy a fémek a platinán ugyanazokon az aktív helyeken adszorbeálódnak, mint a hidrogén. Meghatározták egy adszorbeált fématom által elfoglalt hidrogén adszorpciós helyek számát is. Ezt helyigénynek nevezik és 0,75-től 4-ig változik [6, 7].

* MTA Központi Kémiai Kutató Intézete, Budapest

Mivel a kutatások céljául szolgáló adszorbeált fémréteget általában vizes oldatban katódos polarizációval hozták létre, ezért az adszorpciót megelőzte a fémionok redukciója. Sikerült kimutatni, hogy az ily módon létrehozott adszorbeált fémrétegek nem csupa kisült fématomból állnak, vannak közöttük adszorbeált fémionok is [8, 9, 10, 11]. Ennek következtében természetesen az anionok felületi koncentrációja is megváltozik [12]. Megfelelő körülmények között ez a nem csupán teljesen kisült fémionokból létrejött adszorbeált fémréteg tovább redukálható [13]. Az adszorbeált fémréteg oxidációs fokát az elektroszorpciós vegyérték fogalmának bevezetésével írják le [8, 9, 10, 11, 12, 13]. Ez azt fejezi ki, hogy az adszorbeált fématomok átlaga mennyire van redukálva. Teljes redukció esetén az elektroszorpciós vegyérték megegyezik az iontöltéssel.

A leggyakrabban alkalmazott vizsgálati módszerek a konstans árammal és a potenciodinamikus módszerrel felvett töltésgörbék. Az előbbiek elsősorban mennyiségi vizsgálatokra, az utóbbiak pedig a különféle kristálysíkokon adszorbeálódó fématomok elkülönítésére és előfeszültség értékeinek pontos meghatározására alkalmasak. A jelenségek vizsgálatában gyakran használták az izotópos nyomjelzés módszerét is [12].

Az adszorbeált hidrogén ionizációjának révén végbemenő fémadszorpcióról

Az elektrokémiai módszerek nem alkalmasak finomeloszlású fémek (fémkatalizátorok) illetve hordozós katalizátorok felületén adszorbeált fémrétegek kialakítására, mivel nem építhető elektromos kontaktus minden fémszemcséhez. Megállapították azonban, hogy azokon a fémeken, amelyeken a hidrogén jól adszorbeálódik, az adszorbeált hidrogén ionizációjának révén ugyanolyan sajátságú adszorbeált fémréteg hozható létre mint elektrokémiai módszerrel [5, 13, 14, 15, 16]. Ez lehetővé teszi adszorbeált fémréteg kialakítását finomeloszlású fémeken, sőt hordozós katalizátorokon is, csak a megfelelő kísérleti módszert kell kidolgozni.

Az adszorbeált hidrogén ionizációjának révén végbemenő fémadszorpció olyan fémek esetén, amelyek Nernst potenciálja pozitívabb mint a hidrogénpotenciál, tömb leválással kezdődik, amely második reakciólépésben ionizálódva eredményezi az adszorbeált fémréteget [5, 13, 15]. Ha a második lépés sebessége igen kicsi, akkor a módszer csupán tömb és nem adszorbeált fémréteget eredményezhet. Hordozós katalizátorok esetében ez azt jelenti, hogy az alapfémen az adszorbeált hidrogénnel ekvivalens nagyságú idegen fémkristály keletkezik, de az alapfém felülete gyakorlatilag mentes az adszorbeált fémtől. Legfeljebb az idegen fémkristály környezetében lehet némi adszorbeált fém.

Az adszorbeált fémekkel módosított katalizátorok előállításának és felhasználásának néhány kérdése

Akár elektrokémiai módszerrel, akár az adszorbeált hidrogén ionizációjának révén végbemenő fémadszorpció útján állítjuk elő az adszorbeált fémmel borított katalizátort, mindig felmerül az a kérdés, hogyan vigyük át egy reaktorba a kész katalizátort. Az oxigén és víz együttes jelenléte esetén ugyanis az adszorbeált fém ismét ionizálódik és elmozdul a felülethez tapadó folyadékfilmben. A nedves katalizátor tehát a levegővel érintkezve elveszti eredeti szerkezetét. Ebből következik, hogy a katalizátort csak úgy vihetjük át a reaktorba, ha a víz és az oxigén együttes jelenlétét elkerüljük. Mivel az oxigénmentes körülmény technikailag nehezen oldható meg, ezért célszerű a víz kizárásának útját választani [18]. Ezt úgy lehet megoldani, hogy a kész katalizátort az atmoszférával való érintkezés előtt oxigénmentes körülmények között megszárítjuk. Néhány esetben azonban elegendő a Cl ionmentesre való mosás is [13, 15].

Az adszorbeált fémekkel módosított katalizátorok felhasználhatósága szempontjából igen fontos annak ismerete, hogy a katalizátorok milyen magas hőmérsékletig őrzik meg eredeti szerkezetüket. Ezt minden egyes adszorbens adszorptivum párosra meg kell határozni. A feladat megoldására hőkezeléssel kombinált elektrokémiai módszert dolgoztak ki [17], amelynek segítségével a következő rendszerek hőstabilitásának határát mérték meg hidrogén-atmoszférában: Cu/Pt $\approx$ $\approx$ 150 °C; Au/Pt $\approx$ 350 °C; Bi/Pt = 300 °C és Pd/Pt $\approx$ 250 °C.

Az ily módon meghatározott hőmérsékleti maximum felett a katalizátor kezdi elveszteni eredeti szerkezetét, általában ötvözetképződés következtében. Egyes esetekben azonban az adszorptivum egyedi sajátosságai a szerkezet más úton való megváltozását is lehetővé teszik [18].

Természetesen az adszorbeált fémekkel módosított katalizátorok mint ötvözetkatalizátorok is felhasználhatók. Az ötvöző fém eloszlása az alapfémben azonban valószínűleg más mint az együttes lecsapással készített katalizátorok esetében, mennyisége pedig az adszorbeált hidrogénnel ekvivalens. Kivételt képeznek a változó vegyértékű fémek (Cu, Re stb.), amelyeknél mellékfolyamatok okozhatnak eltéréseket.

Az előállítás technikai feltételei

Az adszorbeált fémekkel módosított katalizátorok előállításakor az egyik legfontosabb követelmény a tökéletesen oxigén és szervesanyagmentes nitrogén és hidrogén. A másik alapvető követelmény az olyan reaktor, amelyben a különféle kémiai műveletek és a módosított katalizátor szárítása levegő kizárásával végezhető el. Az erre a célra épített reaktorunkat az 1. ábrán mutatjuk be. A reaktor három fő részből áll. Az *A* reaktorteret felülről a *B* csiszolatos dugó zárja le, amelyhez a *C* oxigénmentesítő tér csatlakozik. A reaktort szorítórugók tartják össze, amelyeket a rajzon nem ábrázoltunk. Használat közben az *1, 2, 3, 4* csap igényel zsírozást. Más csiszolatok és az *5* csap zsírozása felesleges.

A készülék alkalmas a szükséges műveletek oxigénmentes körülmények között történő elvégzésére, megfelelő tisztaságú H_2 és inert gáz biztosítása mellett.

Az adszorbeált fémekkel módosított hordozós katalizátorok előállításakor olyan alapkatalizátort kell felhasználni, amelyekben a fém már redukált állapotban van,

Mivel az adszorbeált fémréteg kialakítása csak vizes oldatban mehet végbe, ezért az első művelet a katalizátor bevitele a megfelelő elektrolitba. Tekintettel arra, hogy a hordozós katalizátorokat általában a nemesfémek kloridjaiból állítják elő, elektrolitként célszerű sósavoldatot használni. A katalizátor azonban még oxigénmentesített sósav oldatba sem önthető bele megfelelő előkészítés nélkül, mert a katalizátoron adszorbeált oxigén oxidáló hatása miatt számítani kell az aktív helyek egy részének a megsemmisülésére. Ezt úgy tudjuk elkerülni, hogy az adszorbeált oxigént száraz hidrogénnel redukáljuk a még száraz katalizátoron és utána a hidrogénnel telített sósavat adunk a rendszerhez. A hidrogénnel való telítést addig folytatjuk amíg a katalizátor felülete hidrogénnel nem telítődött.

Ha a hidrogénnel való telítés befejeződött, akkor inert gázzal eltávolítjuk az oldatban oldott

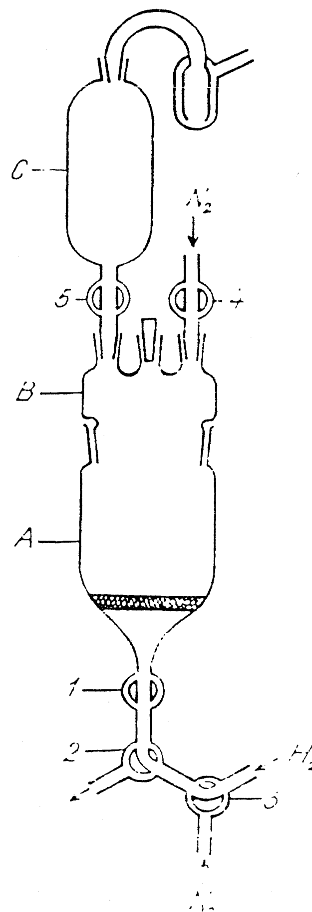

1. ábra

hidrogént és az adszorbeálódó fém kloridját adjuk a rendszerhez.

A fémadszorpció folyamatainak befejeződése után a katalizátort először oxigénmentesített elektrolittal, utána desztillált vízzel fémionmentesre mossuk és oxigénmentes körülmények között szárítjuk. A légszáraz katalizátor megőrzi eredeti szerkezetét még levegőn is tehát, átvihető a megfelelő katalitikus reaktorba [17].

A kézirat beérkezett: 1980. dec. 19.

IRODALOM

[1] *Haissinsky, M.:* Électrochimie des Substances Radioactives et des Solutions Extremement Diluées, Hermann Paris, 1946.
[2] *Breiter, M. W.:* Trans. Faraday Soc., *65.* 2197. 1969.
[3] *Kolb, D. M.—Przasnyski, M.—Gerischer, H.:* J. Electroanal. Chem., *54.* 25. 1974.
[4] *Rand, D. A. J.—Woods, R.:* J. Electroanal. Chem., *44,* 83. 1973.
[5] *Szabó S.—Nagy F.:* J. Electroanal. Chem., *70,* 357. 1976.
[6] *Taylor, A. H.—Kirkland, S.—Brummer, S. B.* Trans. Faraday Soc., *67,* 819. 1971.
[7] *Szabó S.:* Nem publikált eredmény.
[8] *Schultze, J. W.:* Ber. Bunsenges. Phys. Chem., *74,* 705. 1970.
[9] *Schultze, J. W.—Vetter, K. J.:* J. Electroanal. Chem., *44,* 63. 1973.
[10] *Vetter, K. J.—Schultze, J. W.:* J. Electroanal. Chem., *53,* 67. 1974.
[11] *Frumkin, A.—Damaskin, B.—Petrii, O.:* J. Electroanal. Chem., *53,* 57. 1974.
[12] *Horányi, G.—Vértes, G.:* J. Electroanal. Chem., *45,* 295. 1973.
[13] *Szabó, S.—Nagy, F.:* Israel. Journal of Chem. *18,* 162. 1979.
[14] *Szabó S.—Nagy, F.:* J. Electroanal. Chem., *84,* 93. 1977.
[15] *Szabó S.—Nagy F.:* J. Electroanal. Chem., *85,* 339. 1977.
[16] *Szabó S.—Nagy F.:* J. Electroanal. Chem., *88,* 259. 1978.
[17] *Szabó S.—Nagy F.—Móger D.:* Acta Chim. Acad. Sci. Hung. *93,* 33. 1977.
[18] *Szabó S.—Nagy F.:* Magy Kém. Folyóirat, *83,* 204. 1977.

РЕЗЮМЕ

Адсорбция металлов по металлам дает возможность для получения таких катализаторов платиновых металлов, на которых по местам адсорбции водорода частично адсорбированы другие металлы. Формирование адсорбционного слоя металла происходит за счет ионизации предварительно адсорбированного водорода и последующей адсорбции металла в условиях без доступа кислорода. Приготовленный таким образом катализатор промывается водой до отсутствия ионов металла и высушивается в условиях без доступа кислорода, и после этого переносится в соответствующий каталитический реактор.

SUMMARY

Adsorption of metals on metals makes possible the preparation of such platinum metals catalyts on which some part of hydrogen adsorption sites is covered by foreign metal atoms. The adsorbed metal monolayer can be formed via the ionization of adsorbed hydrogen, but only among oxygen free conditions. The finished catalyst among oxygen free conditions should be washed to metal ion free state and dried.

Applied Catalysis, 16 (1985) 209–214
Elsevier Science Publishers B.V., Amsterdam – Printed in The Netherlands

TITRATION OF HYDROGEN CHEMISORBED ON SUPPORTED PLATINUM CATALYSTS BY FERRIC CHLORIDE SOLUTION

S. SZABÓ and F. NAGY
Central Research Institute for Chemistry, Hungarian Academy of Sciences, H-1525, Budapest, P.O. Box 17, Hungary.

(Received 1 November 1984, accepted 2 January 1985)

ABSTRACT

It has been shown that titration of hydrogen chemisorbed on supported Pt catalyst by 0.1 M $FeCl_3$ solution in 1 M HCl electrolyte under oxygen free conditions can be used for surface determination. There is no hydrogen spillover in HCl solution.

INTRODUCTION

Measurement of hydrogen chemisorbed on supported platinum catalysts has almost routinely been used for determination of platinum dispersity in different catalysts.

According to data published earlier [1-3], electrochemical measurements and gas-phase methods for surface determination gave the same dispersity results. It follows that a simple titration of chemisorbed hydrogen by an oxidizing agent in a suitable electrolyte might be used for determination of Pt dispersity in a supported Pt catalyst. This possibility is already recognized, but there is still no suitable experimental method to measure hydrogen adsorbed on a supported Pt catalyst in water solution [4-5]. Deficiency of the method published earlier has been the use of organic oxidizing agents because these compounds may undergo self-oxidation which falsifies the results of the titration.

It follows that only inorganic oxidizing agents can be used for titration but their redox potential cannot be so high that the chloride content of a supported Pt catalyst would also be oxidized, thereby falsifying the results. On the other hand, the Pt content of a catalyst itself can be oxidized in the presence of chloride ions if the redox potential of the oxidizing agent is higher than the potential of the $PtCl_4^{2-}$/Pt system.

Taking into consideration the above discussed conditions, an $FeCl_3$ solution in hydrochloric acid medium seemed suitable for this purpose because ferric ions can oxidize neither the Pt nor the chloride ions and they do not decompose as organic oxidants often do. Of course, such a titration can only be made under oxygen-free conditions because the oxygen disolved in different electrolytes used in the titration would cause discrepancies in the final dispersity results.

0166-9834/85/$03.30 © 1985 Elsevier Science Publishers B.V.

EXPERIMENTAL METHODS

A three-compartment platinum bottomed electrochemical cell was used in the investigation of the similarity of electrochemical charging curve and the charging curve measured by titration of hydrogen adsorbed on a platinum powder catalyst with $FeCl_3$ solution. During the titrations or the measurement of the charging curves both the main compartment of the cell and the $FeCl_3$ titrating solution have been continuously deoxygenated in order to avoid errors due to dissolved oxygen. Deoxygenation (and purging of traces of hydrogen after saturation the catalysts with hydrogen) was effected by purified nitrogen gas.

Titration of hydrogen adsorbed on supported Pt catalyst was made in the same cell as described in our earlier paper [6].

The reference electrode was a platinized Pt hydrogen electrode in the same 1 M HCl electrolyte in which the titrations were performed. A platinized Pt needle electrode was used as an indicator electrode to indicate the actual redox potential of the electrolyte in the main compartment of the cells.

0.1 M $FeCl_3$ titrating solution was prepared by dissolving the measured quantity of reagent grade $FeCl_3.6H_2O$ in 0.1 M HCl solution.

Platinum powder catalyst was deposited from the solution of H_2PtCl_6 containing 0.5 g Pt/ml . 4.5 ml 40% CH_2O solution was added to every ml of H_2PtCl_6 solution and the reduction was completed at 3-5°C with 50% KOH solution. The catalyst was then washed free of electrolytes with triply distilled water and finally dried in vacuum. Supported Pt/Al_2O_3 catalyst was prepared as described earlier [7].

The titrations were performed with a type OP-930 RADELKIS Automatic Burette.

<u>Introduction of a Pt catalyst into an electrolyte solution containing chloride ions</u>

When studying platinum catalysts in electrolyte solutions it should first be decided how to place the Pt catalyst into an electrolyte solution containing chloride ions without destroying its original structure or activity. Since in atmospheric conditions the surface of platinum catalysts becomes saturated with oxygen chemisorbed from the air, in the presence of chloride ions some Pt may be dissolved from the catalyst even if a deoxygenated electrolyte is used, according to the following reaction:

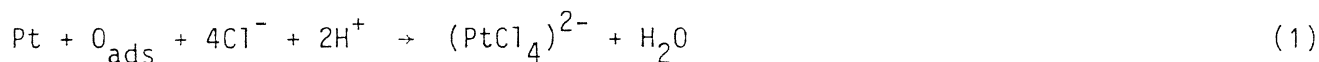

$$Pt + O_{ads} + 4Cl^- + 2H^+ \rightarrow (PtCl_4)^{2-} + H_2O \qquad (1)$$

$(PtCl_4)^{2-}$ ions can dissolve and deposit once more changing thereby the activity of the catalyst.

In accordance with our earlier experience [8], O_{ads} must be reduced with H_2 in the gas-phase and the catalyst, without any contact with air, can be introduced into a deoxygenated electrolyte.

For the above reasons, in our experiments the catalyst sample was poured into

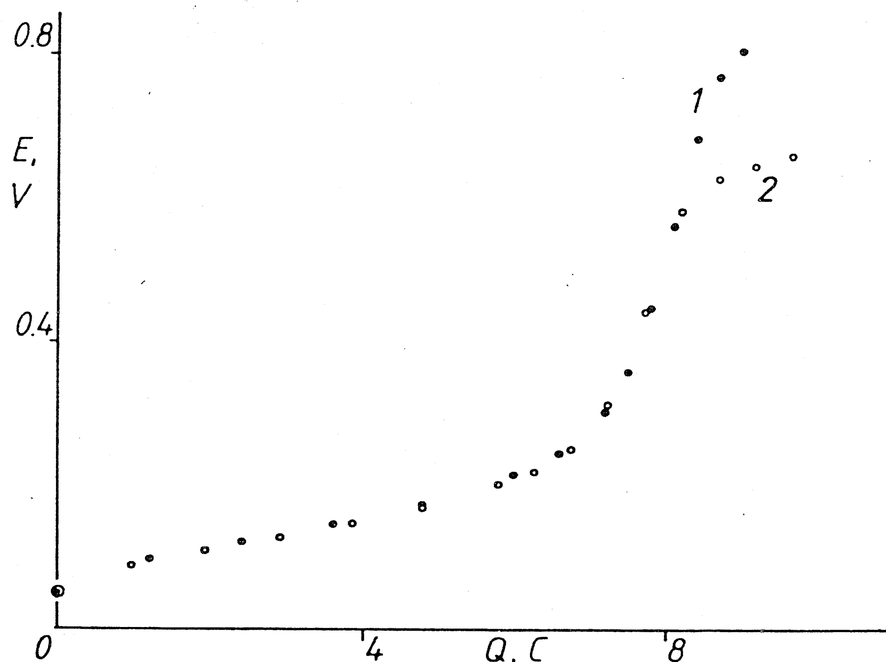

FIGURE 1 1, Charging curve of 0.3 g Pt powder (I = 5 mA). 2, Charging curve of the same Pt powder measured by titration with 0.1 M $FeCl_3$ solution.

the dry cell and then air was purged out from the cell by nitrogen. When this was finished, we switched to hydrogen and finally 1 M HCl supporting electrolyte deoxygenated with hydrogen was added to the cell and bubbling of hydrogen was continued up to the saturation of the catalyst sample by hydrogen.

Having finished saturation, the surplus hydrogen was flushed out of the cell by purified nitrogen and finally we had a catalyst sample whose surface was saturated with hydrogen in 1 M HCl solution.

In the case of massive platinum catalysts, saturation with hydrogen was occasionally carried out by strong cathodic polarization.

Titration of hydrogen chemisorbed on massive Pt catalysts by $FeCl_3$ solution

Before the titration of hydrogen adsorbed on supported Pt catalysts it had to be verified that the result of our titration was the same as the results of other methods of surface determination in water solution.

For this purpose, in the Pt-bottomed cell we determined the charging curve of 0.3 g Pt powder at first by electric current (curve 1 in Figure 1) and then by titration with 0.1 M $FeCl_3$ solution (curve 2 in Figure 1). Since the two curves converge, it can be stated that the two methods have given the same surface area. Taking into consideration the results of other measurements, the discrepancy between the two curves never exceeded 5%, therefore, the hydrogen adsorbed on Pt catalysts can be determined by titration with 0.1 M $FeCl_3$ solution.

In practice, however, it is not enough to satisfy this condition because the electrode potential of a supported Pt catalyst cannot be measured if the support does not conduct electricity. In theory, during titration the catalyst potential

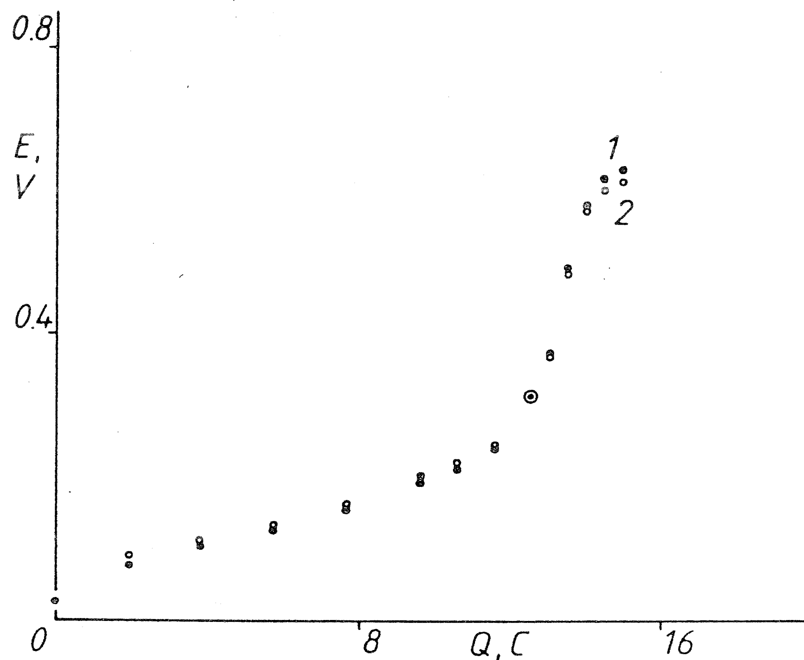

FIGURE 2 1, Titrated charging curve of 0.5 g Pt powder. 2, Potential of the platinized Pt needle indicator electrode as a function of the volume of titrating solution (in coulombs).

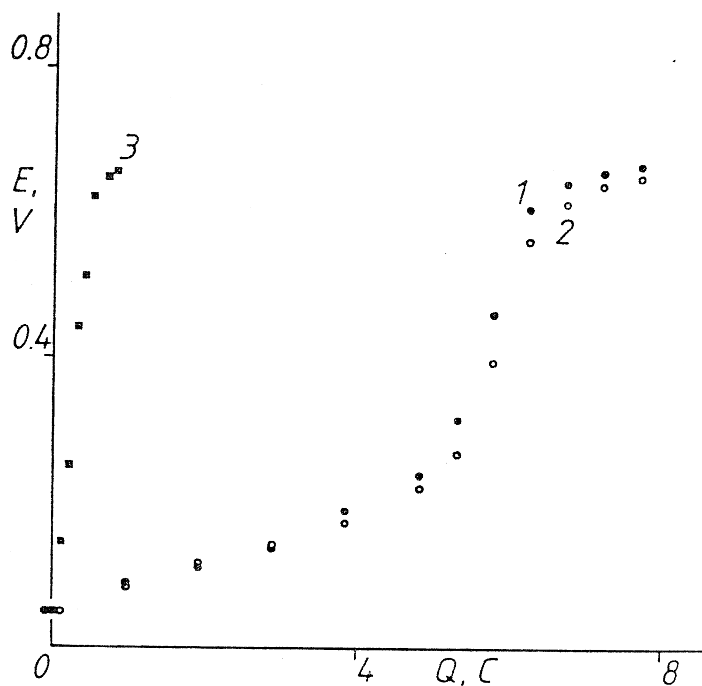

FIGURE 3 1, Titrated charging curve of 0.2 g Pt powder. 2, Titrated charging curve of 0.2 g Pt powder and 2 g alumina. 3, Titrated charging curve of 2 g alumina.

and the redox potential of the electrolyte must be the same, therefore, the potential of a supported Pt catalyst may be measured via the electrolyte by a small (platinized Pt needle) electrode. This concept has been tested with a massive Pt

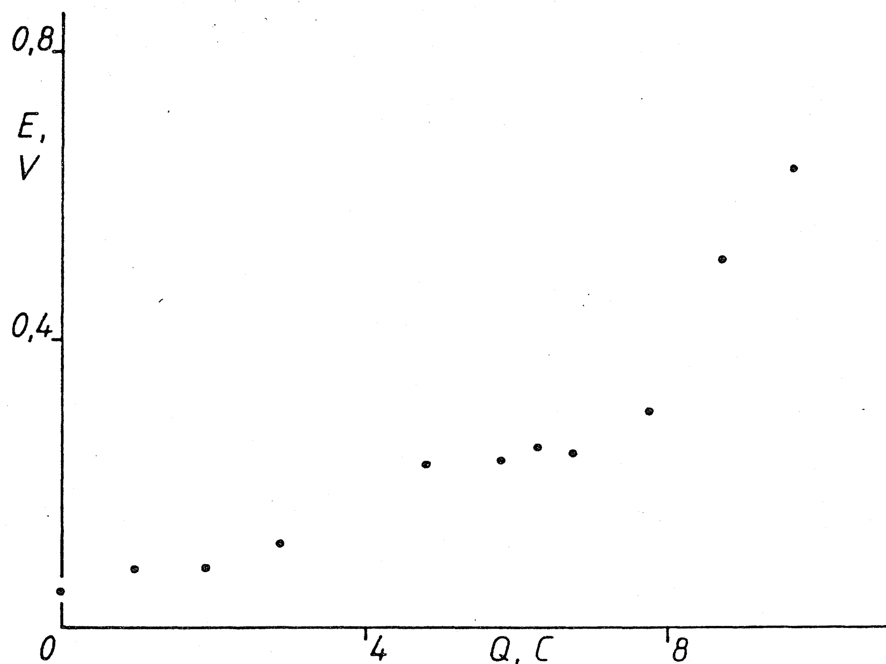

FIGURE 4 Titrated charging curve of 5 g Pt/Al_2O_3 catalyst.

catalyst because, in this case, the potential of both the catalyst sample and the Pt needle electrode could be measured.

According to Figure 2, the Pt needle electrode indicated the same potential as did the catalyst sample; consequently, this method can be used for the determination of the surface of a supported Pt catalyst.

Titration of hydrogen chemisorbed on supported platinum catalysts by $FeCl_3$ solution

Before testing a real supported Pt catalyst, a mixture of massive Pt catalyst and Al_2O_3 powder was examined in order to find out what differences would arise in the titration due to the presence of the support. On the other hand, this experiment might give information about hydrogen spillover in an aqueous phase.

On the basis of Figure 3 it can be asserted that the presence of alumina does not change the amount of hydrogen measured by titration. It follows that there is no spillover under such experimental conditions.

The titration of hydrogen chemisorbed on a Pt/Al_2O_3 catalyst is illustrated in Figure 4. In this experiment we used the same catalyst as in our earlier paper [9]. The H/Pt ratio measured by pulse adsorption was 0.105 and by TPD of hydrogen 1.36 [9].

On the basis of Figure 4, the H/Pt ratio and the surface of the catalyst sample can also be calculated. From the figure and charge required for the oxidation of adsorbed hydrogen is 7.5 C. Since 210 μC is required for the oxidation of hydrogen adsorbed on 1 cm^2 surface [2], the surface of 1 g catalyst is:

$$A = \frac{7.5 \times 10^{-4}}{5 \times 210 \times 10^{-6}} = 0.7\ m^2/g \qquad (2)$$

Not only the surface of a supported Pt catalyst but also the H/Pt ratio of the given catalyst can be determined by the titration illustrated in Figure 4. Taking into consideration that the Pt content of our catalyst is about 0.5% and 5 g was used in the titration:

$$H/Pt = (7.5/96500)/(5 \times 0.5 \times 10^{-2}/195) = 0.6 \qquad (3)$$

which is between the results measured by other methods [9]. It is very probable that pulse adsorption measurements give a smaller, whereas the TPD method a greater surface area than the real value, as has been shown in our earlier papers [10,11].

Finally it must be mentioned that two periods could be distinguished during the titration. Reaction of the first 20% of the titrating solution was very fast and then it slowed down, in our opinion, due to slow diffusion in the pores of the catalyst. It is interesting that the result of the fast part of our titration is about the same as the result of pulse adsorption.

REFERENCES

1 L. Spenadel and M. Boudart, J. Phys. Chem., 64 (1960) 204.
2 A.N. Frumkin, Advances in Electrochemistry and Electrochemical Engineering, Vol. 3, p.315, Interscience, New York (1963).
3 J. Bett, K. Kinoshita, K. Routsis and P. Stonehart, J. Catal., 29 (1973) 160.
4 L. Freidlin and K.G. Rudneva, Izvest. Acad. Nauk USSR, Otdel. Khim. Nauk, (1954) 491.
5 D.V. Sokolskii, Hydrogenation in Solutions (in Russian), p.172, Alma-Ata (1962).
6 S. Szabó and F. Nagy, J. Electroanal. Chem., 70 (1976) 357.
7 J. Margitfalvi, S. Szabó, F. Nagy, S. Göbölös and M. Hegedüs, Preparation of Catalysts III, p.473, Elsevier, Amsterdam (1983).
8 S. Szabó, F. Nagy and D. Móger, Acta Chim. Acad. Sci. Hung., 93 (1977) 33.
9 J. Margitfalvi, M. Hegedüs, S. Göbölös, E. Kern-Tálas, P. Szedlacsek, S. Szabó and F. Nagy, Proc. 8th International Congress on Catalysis IV - 903 Verlag Chemie 1984.
10 S. Szabó, D. Móger, M. Hegedüs and F. Nagy, React. Kinet. Catal. Lett., 6 (1977) 89.
11 F. Nagy, D. Móger, M. Hegedüs, Gy. Mink and S. Szabó, Acta. Chim. Acad. Sci. Hung., 100 (1979) 211.

2

) BUNDESREPUBLIK DEUTSCHLAND

DEUTSCHES PATENTAMT

⑫ **Patentschrift**

⑪ **DE 32 47 830 C2**

⑤① Int. Cl. 3:
B 23 K 1/04
B 23 K 1/19
B 23 K 35/34

DE 32 47 830 C2

②① Aktenzeichen: P 32 47 830.5-24
②② Anmeldetag: 23. 12. 82
④③ Offenlegungstag: 7. 7. 83
④⑤ Veröffentlichungstag der Patenterteilung: 8. 12. 83

ıerhalb von 3 Monaten nach Veröffentlichung der Erteilung kann Einspruch erhoben werden

) Unionspriorität: ③② ③③ ③①
23.12.81 HU 3921-81

) Patentinhaber:
.ITA Központi Kémiai Kutató Intézet; Fegyver és Gázkészülékgyár, Budapest, HU

Vertreter:
Beszédes, S., Dipl.-Chem. Dr.rer.nat., Pat.-Anw., 8060 Dachau

⑦② Erfinder:
Szabó, Sándor, 1025 Budapest, HU; Szentgyörgyi, Alfonz, 1202 Budapest, HU; Szabó, Péter, 1011 Budapest, HU; Nagy, Ferenc, 1145 Budapest, HU

⑤⑥ Im Prüfungsverfahren entgegengehaltene Druckschriften nach § 44 PatG:
NICHTS-ERMITTELT

Verfahren zum Hartlöten von Kupfer an Kupfer oder an Stahllegierungen

Patentansprüche:

1. Verfahren zum Hartlöten von Kupfer an Kupfer oder an Stahllegierungen durch Auftragen eines legierungsbildenden Metalles als Hartlötmaterial auf mindestens eine der Kupferflächen beziehungsweise die Kupferfläche, Aneinanderdrücken der zu verlötenden Flächen und Bringen des Werkstückes in gereinigtem Schutzgas oder unter Vakuum von einem Druck von höchstens 1 Pa auf Temperaturen von 850 bis 1080°C bis zum Entstehen der oberflächlichen Legierung, wobei man im Falle des Hartlötens von Kupfer an Stahllegierungen diese Temperatur 10 bis 200 Minuten lang hält, dadurch gekennzeichnet, daß man als legierungsbildendes Metall Zinn, Indium oder Mangan verwendet.

2. Verfahren nach Anspruch 1, dadurch gekennzeichnet, daß man vor dem Auftragen des legierungsbildenden Metalles einen Grundüberzug aus Nickel, Kobalt, Indium und/oder Silber in einer Stärke von höchstens 30 μm aufträgt.

3. Verfahren nach Anspruch 1 oder 2, dadurch gekennzeichnet, daß man das Auftragen des legierungsbildenden Metalles und/oder des Grundüberzuges aus Elektrolytlösungen vornimmt.

4. Verfahren nach Anspruch 1 bis 3, dadurch gekennzeichnet, daß man das Abscheiden des legierungsbildenden Metalles und/oder des Grundüberzuges in einer Stärke von 1 bis 30 μm vornimmt.

Die Erfindung betrifft ein Verfahren zum Hartlöten von Kupfer an Kupfer oder an Stahllegierungen, insbesondere an rostfreie Stähle.

Es ist bekannt, daß das Hartlöten von legierten Stählen an andere Metalle im allgemeinen schwierig ist, weil die Legierungsmetalle, welche weniger edel als Eisen sind, wie Chrom, Molybdän, Mangan, Titan und Vanadium, auch unter Bedingungen, unter welchen die Oberfläche der Kohlenstoffstähle noch rein bleibt, bereits schwer zersetzbare Oxydschichten bilden. Diese Oxydschicht verhindert die Benetzung des rostfreien Stahles mit dem Lot (Hartlot) und auf diese Weise das Entstehen einer festen Lötstelle. Besonders schwierig ist die Situation bei den ohne Flußmittel in Schutzgas oder unter Vakuum durchgeführten Lötarbeiten, weil in diesem Falle die im Schutzgas oder der Restluft vorhandenen Sauerstoff- und/oder Wasserdampfspuren die Oxydschicht auf der Oberfläche während der gesamten Dauer des Lötvorganges verstärken, was manchmal das Löten einfach unmöglich macht.

Die Verfahren zum Löten von rostfreien Stählen in Schutzgas oder unter Vakuum bedingen, daß zunächst Lötmaterial vor der Wärmebehandlung zum Schutz der Oberfläche des Stahls auf diese aufgebracht werden muß (ein bloßes Anordnen ohne Bedecken der Oberfläche genügt nicht) und in manchen Fällen sogar noch gasförmige Flußmittel eingesetzt werden müssen, damit die obenerwähnten Schwierigkeiten beseitigt werden können (N. Lashko und S. Lashko: Brazing and Soldering of Metals [MIR Publishers, Moscow]). Auch in den japanischen Patentschriften 77 76 254 und 79 85 158 wird ein Auftragen von Lot zum Oberflächenschutz vor der Wärmebehandlung empfohlen.

In den bekannten Verfahren zum Hartlöten von

rostfreien Stählen an andere Metalle muß also entweder mit Flußmitteln gearbeitet werden oder die aneinanderzulötenden Oberflächen müssen durch eine Vorbehandlung geschützt werden oder beide Maßnahmen sind erforderlich.

Das Hartlöten von Kupfer an Kupfer oder an andere Metalle als legierte Stähle ist im allgemeinen mit keinen besonderen technischen Schwierigkeiten verbunden, wenn das für den gewünschten Zweck geeignete Lot und das geeignete Verfahren gewählt werden. Der Schmelzpunkt des Lotes muß unter dem des Kupfers liegen und das Lot darf bei der Temperatur des Lötens mit dem Kupfer keine Legierung bilden, weil sonst eine Erosion des Grundmateriales eintreten würde. Manchmal sind jedoch das Anbringen und Befestigen des Lotes in der Nähe der zu lötenden Fläche kompliziert und erfordern eine aus vielen Schritten bestehende Verfahrenstechnik. Zum Beispiel bei der Herstellung von aus Kupferrohren und Kupferblechen bestehenden Wärmeaustauschern muß das Lot in in die wärmeableitenden Kupferplatten geschnittene Löcher eingebracht werden. Danach wird der zusammenmontierte Wärmeaustauscher in Schutzgas oder unter Vakuum wärmebehandelt. Ein modernes Beispiel für die Anwendung dieses Prinzips ist das in der britischen Patentschrift 15 58 264 beschriebene Verfahren.

Es ist auch aus Römpp, CHEMIE LEXIKON, 5. Auflage, 1962, Spalte 2078 das Hartlöten von Schwermetallen und Eisenwerkstoffen mit Silberloten bekannt. Ferner ist aus demselben Werk, Spalten 2998 bis 2999 das Hartlöten von Eisen und Kupfer mit Kupferlot bekannt. Die mit diesen bekannten Hartloten erzielten Lötungen lassen aber noch zu wünschen übrig.

Der Erfindung liegt die Aufgabe zugrunde, unter Verbesserung der bekannten Verfahren ein einfaches Verfahren zum Hartlöten, durch welches Stahllegierungen, insbesondere rostfreier Stahl, ohne Verwendung von Flußmitteln und ohne Vorbehandlung zum Schutz der Oberfläche mit besserem Ergebnis an Kupfer gelötet werden können, sowie auch das Hartlöten von Kupfer an Kupfer mit einer gegenüber dem Stand der Technik stark vereinfachten Verfahrenstechnik, insbesondere unter Fortfallen der das Vorbereiten der aneinanderzulötenden Flächen betreffenden Arbeitsgänge auch im Falle von solchen von komplexer Form und Ausführung, sowie der das Anbringen und Befestigen des Lotes betreffenden Maßnahmen, nach Belieben durchgeführt werden kann, zu schaffen.

Die Erfindung beruht auf der überraschenden Feststellung, daß in entsprechend reinem Schutzgas oder unter genügend geringem Druck und mit einer über eine ausreichend lange Zeit vorgenommenen Wärmebehandlung die meisten Stahllegierungen, wie rostfreien Stähle, auch ohne vorherigen Schutz der Oberfläche und ohne Flußmittel an Kupfer hartgelötet werden können, wenn als Hartlot bestimmte ausgewählte Reinmetalle verwendet werden. Das schmelzende Lot benetzt dann die Oberfläche der an das Kupfer zu lötenden Stahllegierung optimal. Dabei erfolgt dies nicht innerhalb eines Augenblickes, sondern die Benetzung ist ein langsamer Vorgang, weil das geschmolzene Metall zum Zersetzen und Verdrängen der Oberflächenoxyde eine bestimmte Zeitspanne braucht. Die erforderliche Lötdauer hängt von der Reinheit des Schutzgases beziehungsweise von der Menge des nach dem Evakuieren zurückbleibenden Restsauerstoffes und/oder Restwasserdampfes ab.

Ferner beruht die Erfindung auf der überraschenden

Feststellung, daß bei Verwendung von bestimmten ausgewählten Reinmetallen als Hartlot auch die sich während der Wärmebehandlung aus dem Grundmetall Kupfer und den auf dessen Oberfläche aufgebrachten anderen Reinmetallen »in situ« bildende oberflächliche Legierung, bei der es sich nicht notwendigerweise um eine solche, welche das Kupfer benetzt, handeln muß, als Lot unter Bildung einer überlegenen Lötung beim Hartlöten dienen kann, ohne daß eine Erosion des Grundmetalles erfolgt. Die zwischen den ausgewählten Reinmetallen und dem zu lötenden Kupfer in situ gebildete flüssige oberflächliche Legierung führt zu einer optimalen Benetzung der Oberfläche der an das Kupfer zu lötenden Stahllegierung und damit zu einer optimalen Lötung, wobei es andererseits wie bereits erwähnt keine Notwendigkeit ist, daß die oberflächliche Legierung auch das Kupfer benetzt.

Gegenstand der Erfindung ist daher ein Verfahren zum Hartlöten von Kupfer an Kupfer oder an Stahllegierungen durch Auftragen eines legierungsbildenden Metalles als Hartlot auf mindestens eine der Kupferflächen beziehungsweise die Kupferfläche, Aneinanderdrücken der zu verlötenden Flächen und Erhitzen des Werkstückes in gereinigtem Schutzgas oder unter Vakuum von einem Druck von höchstens 1 Pa auf Temperaturen von 850 bis 1080°C bis zum Entstehen der oberflächlichen Legierung, wobei im Falle des Hartlötens von Kupfer an Stahllegierungen diese Temperatur 10 bis 200 Minuten lang gehalten wird, welches dadurch gekennzeichnet ist, daß als legierungsbildendes Metall Zinn, Indium oder Mangan verwendet wird.

Nach einer vorteilhaften Ausführungsform des erfindungsgemäßen Verfahrens wird vor dem Auftragen des legierungsbildenden Metalles ein Grundüberzug aus Nickel, Kobalt, Indium und/oder Silber in einer Stärke von höchstens 30 µm aufgetragen.

Vorzugsweise wird das Auftragen des legierungsbildenden Metalles und/oder des Grundüberzuges aus Elektrolytlösungen vorgenommen.

Vorzugsweise wird das Abscheiden des legierungsbildenden Metalles und/oder des Grundüberzuges in einer Stärke von 1 bis 30 µm vorgenommen.

Auch beim Hartlöten von Kupfer an Kupfer kann eine Wärmebehandlung durch Halten der Temperatur von 850 bis 1080°C durchgeführt werden, sie ist aber nicht zwingend.

Das erfindungsgemäße Verfahren bringt gegenüber den Verfahren des Standes der Technik den Vorteil mit sich, daß durch es die Bildung einer festeren Legierungsverbindung zwischen dem Lot und der beziehungsweise den Kupferoberfläche(n) und eine bessere Benetzung der Oberfläche der an das Kupfer anzulötenden Stahllegierung durch die Legierung aus Lot und Kupfer und damit eine bessere Lötung erzielt werden kann. Dabei ist eine Vorbehandlung zum vorherigen Schutz der Oberfläche und die Verwendung eines Flußmittels in Argon oder unter Vakuum auch im Falle von an Kupfer zu lötenden Stahllegierungen entbehrlich. Ferner ist das erfindungsgemäße Verfahren einfacher.

Durch das erfindungsgemäße Verfahren werden Lötstellen von ausgezeichneter Qualität erhalten.

Das erfindungsgemäße Verfahren eignet sich besonders gut zum Hartlöten von rostfreien Stählen, vor allem solchen Stahllegierungen, welche Silber, Zinn, Indium, Mangan, Gallium und/oder Nickel oder Zinnbronze als Legierungsmetall(e) beziehungsweise Legierungsmetallegierung enthalten, an Kupfer. Eine vorteilhafte Anwendung des erfindungsgemäßen Verfahrens ist die bei der Herstellung von aus Kupfer oder aus Kupfer und rostfreien Stähle beziehungsweise anderen Stahllegierungen bestehenden Wärmeaustauschern und Maschinenteilen.

Die Erfindung wird an Hand der folgenden Beispiele näher erläutert. Die zur Durchführung der Beispiele verwendeten Rohröfen wurden evakuiert oder mit Argon, welches vorher an Kupferkatalysatoren und Molekülsieben gereinigt worden ist, durchgespült. Als rostfreie Stähle wurden die folgenden gemäß der Norm DIN 17 007 verwendet.

1.4113,
1.4122,
1.4301,
1.4306,
1.4541 und
1.4571

Die Beispiele gliedern sich in 3 Gruppen: Hartlöten von rostfreien Stählen an Kupfer, Hartlöten von Kupfer an Kupfer und schließlich die Zusammenfassung von weiteren Beispielen nach dem erfindungsgemäßen Verfahren.

A) Hartlöten von rostfreiem Stahl an Kupfer

Beispiel 1

Es wurde aus einer Elektrolytlösung auf einer Kupferfläche eine etwa 5 µm starke Zinnschicht abgeschieden. Die so überzogene Kupferfläche wurde an eine Oberfläche von rostfreiem Stahl angedrückt und das Ganze wurde in einer Schutzgasatmosphäre aus gereinigtem Argon 90 Minuten lang bei etwa 1000°C wärmebehandelt. Es wurde eine ausgezeichnete Lötverbindung erhalten.

Beispiel 2

Es wurde auf einer Kupferfläche elektrolytisch eine 1 µm starke Nickelschicht abgeschieden und auf die so vernickelte Kupferfläche wurde noch eine 7 µm starke Zinnschicht aufgebracht. Die so überzogene Fläche wurde auf die im Beispiel 1 beschriebene Weise mit rostfreiem Stahl verlötet. Es wurde eine ausgezeichnete Lötverbindung erhalten.

Beispiel 3

Es wurde die im Beispiel 1 beschriebene Verfahrensweise mit dem Unterschied wiederholt, daß an Stelle des Zinnes Indium auf der Kupferfläche abgeschieden wurde. Es wurde ebenfalls eine ausgezeichnete Lötverbindung erhalten.

B) Hartlöten von Kupfer an Kupfer

Beispiel 4

Es wurde die im Beispiel 1 beschriebene Verfahrensweise mit dem Unterschied wiederholt, daß an die verzinnte Kupferfläche statt der Fläche des rostfreien Stahles eine Kupferfläche angedrückt wurde und die Wärmebehandlung 15 Minuten lang durchgeführt wurde. Es wurde eine ausgezeichnete Lötverbindung erhalten.

Beispiel 5

Es wurde auf einer Kupferfläche zunächst eine 1 µm

ırke Nickelschicht und anschließend noch eine 8 µm ırke Indiumschicht abgeschieden. An die so überzoge- Fläche wurde eine Kupferfläche angedrückt und das Ganze wurde in einem Schutzgas auf etwa 1000°C erwärmt. Es wurde eine hervorragende Lötverbindung erhalten.

Beispiel 6

Es wurde wie im Beispiel 5 beschrieben gearbeitet, doch mit dem Unterschied, daß an Stelle des ckelüberzuges ein Kobaltüberzug abgeschieden wurde. Es wurde ebenfalls eine ausgezeichnete Lötverbindung erhalten.

C) Zusammenfassung von weiteren Beispielen nach dem erfindungsgemäßen Verfahren

Beispiele 7 bis 18

Zur Veranschaulichung des Hartlötens von rostfreiem ahl an Kupfer sind in der folgenden Tabelle weitere ɛispiele unter Angabe der Lötparameter zusammen- stellt. Die Versuche wurden unter Vakuum oder in ner Schutzgasatmosphäre aus gereinigtem Argon ıter einem Druck von 1 bar durchgeführt. Die zur ldung der oberflächlichen Legierung erforderlichen Lötmaterialmetalle wurden elektrolytisch aus Elektrolytlösungen auf der Kupferfläche abgeschieden. In den meisten Beispielen wurde ebenfalls elektrolytisch auch ein Grundüberzug auf dem Kupfer erzeugt und die legierungsbildende Metallschicht wurde auf diesen Grundüberzug abgeschieden.

.belle

ispiel Nr.	Legierungsbildendes Lot		Grundüberzug		Wärmebehandlung	
	Legierungs-bildendes Metall	Stärke [µm]	Metall	Stärke [µm]	Temperatur [°C]	Zeit [min]
	Indium	7,5	–	–	1000	20
	Indium	7,5	Nickel	0,5	1000	30
	Indium	10	Kobalt	1	1050	60
	Indium	2	Silber	7,5	1000	45
	Zinn	10	–	–	975	90
	Zinn	8	Nickel	1	975	90
	Zinn	7	Kobalt	0,5	975	90
	Zinn	4	Indium	4	1000	90
	Zinn	7	Silber	3	1000	75
	Mangan	10	–	–	975	90
	Mangan	10	Nickel	1	975	90
	Mangan	10	Kobalt	1	975	90

jedem Falle wurde eine ausgezeichnete Lötverbindung erhalten.

Beispiel 19

Die in den Beispielen 7 bis 18 für das Hartlöten von stfreiem Stahl an Kupfer beschriebenen Beispiele ch dem erfindungsgemäßen Verfahren konnten ohne änderung auch zum Hartlöten von Kupfer an Kupfer verwendet werden. In diesem Falle war es ausreichend, das Werkstück auf die notwendige Temperatur zu erwärmen, eine Wärmebehandlung durch Halten dieser Temperatur war praktisch nicht erforderlich.

MAGYAR
NÉPKÖZTÁRSASÁG

ORSZÁGOS
TALÁLMÁNYI
HIVATAL

Szabadalmi okirat

Az Országos Találmányi Hivatal az okirathoz fűzött leirás alapján

188 730

lajstromszámon szabadalmat adott.

A szabadalmi bejelentés napja és az oltalmi idő kezdete:

1981.12.23.

Feltalálók:

SZABÓ Sándor 40%,
SZENTGYÖRGYI Alfonz 35%,
SZABÓ Péter 15%,
NAGY Ferenc 10%,
Budapest

Szabadalmas:

MTA Központi Kémiai Kutató Intézete, Budapest,
Fegyver- és Gázkészülékgyár Budapest

A szabadalom címe:

Eljárás réznek rézhez vagy rozsdamentes acélhoz, illetve rozsdamentes acéloknak egymáshoz történő keményforrasztására

Budapest, 1988.10.10.

elnök

(19) HU

AGYAR
ZTÁRSASÁG

SZABADALMI LEÍRÁS

SZOLGÁLATI TALÁLMÁNY

(11) 188 730

B

Nemzetközi osztályjelzet:
(51) NSZO$_4$
B 23 K 1/19

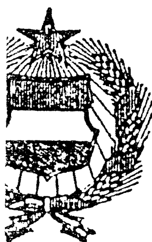

A bejelentés napja: (22) 81. 12. 23.

(21) (3921/81)

BZÁGOS
ÁLMÁNYI
VATAL

A közzététel napja: (41) (42) 83. 09. 28.

Megjelent: (45) 88. 07. 20.

(k): (72)
ndor, 40 %, Szentgyörgyi Alfonz, 35 %, Szabó Péter,
gy Ferenc, 10 %, Budapest

Szabadalmas: (73)
MTA Központi Kémiai Kutató Intézete, Budapest,
Fegyver- és Gázkészülékgyár, Budapest

ELJÁRÁS RÉZNEK RÉZHEZ VAGY ROZSDAMENTES ACÉLHOZ, ILLETVE ROZSDAMENTES ACÉLOKNAK EGYMÁSHOZ TÖRTÉNŐ KEMÉNYFORRASZTÁSÁRA

(57) KIVONAT

A találmány szerinti eljárás lényege, hogy alkalnazásával hőcserélők és más gépalkatrészek előillítására a rozsdamentes acélok nagy többsége védőgázban, vagy ezzel egyenértékű vákuumban rézzel felületi előkezelés és folyatóanyag nélkül is 850 °C – 1250 °C közötti hőmérsékleten 10 – 200 percig hőkezelve egymáshoz forrasztható. Rozsdamentes acélok hasonló feltételek mellett, de legfeljebb 1080 °C-on hőkezelve rézzel is összeforraszthatók a réz felületére felvitt ón- és/vagy indium- és/vagy mangánrétegből képzett felületi ötvözet útján.

A találmány tárgya eljárás réznek rézhez vagy rozsdamentes acélhoz történő keményforrasztására, rézből, rozsdamentes acélból vagy más acélötvözetekből készülő hőcserélők és más gépalkatrészek előállítására.

Ismeretes, hogy ötvözött acélok egymáshoz vagy más fémekhez történő keményforrasztása általában nehéz feladat, mert a vasnál kevésbé nemes ötvözők, mint a króm, a molibdén, a mangán, a titán, a vanádium stb. olyan körülmények között is nehezen megbontható oxidréteget hoznak létre a felületen, amikor a szénacélok felülete még tiszta marad. Ez az oxidréteg akadályozza a rozsdamentes acélnak a nedvesítését a forrasztóanyaggal, és ezáltal a megfelelő forrasztás kialakulását. Különösen nehéz a helyzet a folyatóanyag nélküli, védőgázas és vákuum forrasztások megvalósítása esetén. Ebben az esetben ugyanis a védőgázban vagy maradék nyomásban lévő oxigén- és/vagy vízgőzszennyezés a forrasztás egész időtartama alatt növeli a felületi oxidréteget, ami a forrasztás meghiúsulását is eredményezheti.

Rozsdamentes acélok védőgázas és vákuum forrasztásánál alkalmazott ismert eljárások legnagyobb hiányossága az, hogy a forrasztóanyagot a hőkezelés előtt kell felvinni az acél felületére és az azon kialakuló tömör és könnyen újraképződő oxidréteg miatt soklépcsős, bonyolult technológiával lehet csak felvinni, és esetenként még gázalakú folyatóanyagot is alkalmazni kell, hogy a keményforrasztás megvalósítható legyen, amint erre több helyen is található utalás N. Lashko és S. Lashko: Brazing and Soldering of Metals (MIR Publishers, Moscow) c. munkájában.

Ugyancsak a forrasztóanyagnak a hőkezelés előtti felvitelét írja elő a felület megvédése céljából a 77 76,254 és a 79 85,158 lajstromszámú japán szabadalmi leírásban és a 28 08,106 sz. NSZK nyilvánosságrahozatali iratban ismertetett eljárás.

Meg kell azonban jegyezni, hogy az NSZK nyilvánosságrahozatali iratban ismertetett diffúziós forrasztás a forrasztások egy olyan speciális esete, amely sok tekintetben közelebb áll a hegesztéshez, mint a forrasztáshoz, mert az összeforrasztandó felületek között a kötést létrehozó fémréteg összetétele azonos vagy közel azonos, mint az alapfém összetétele. A forrasztáshoz felhasznált diffúziós forraszanyagok tulajdonképpen diffúziós hegesztést megkönnyítő segédanyagok. Maga az eljárás körülményes és hosszadalmas, fémtömegcikkek előállítására alkalmatlan.

A réznek sem a rézhez, sem pedig más fémekhez történő keményforrasztása általában nem jár különösebb technikai nehézségekkel, csupán a kívánt célra alkalmas forrasztóanyagot és eljárást kell kiválasztani. A forrasztóanyag olvadáspontjának alacsonyabbnak kell lennie, mint a réz olvadáspontja, és a forrasztás hőmérsékletén nem szabad a réz alapfém erózióját okoznia.

A fenti alapelveken nyugvó eljárások hiányossága, hogy esetenként a forrasztóanyagnak a forrasztandó felület közelében való elhelyezése bonyolult, sok műveletből álló technológiát eredményez, amire példaként az egyébként korszerűnek tekinthető 1 558 264 lajstromszámú angol szabadalmi leírás szerinti eljárás szolgálhat.

Hőkezelés közben a forrasztás hőmérsékletén az arany megolvadása nélkül a forrasztandó rézfelületen képződő aranyban dús arany–réz-eutektikumnak forrasztóanyagként való felhasználásán alapszik az igen korszerűnek tekinthető 26 28 345 lajstromszámú NSZK nyilvánosságrahozatali iratban leírt eljárás, amelynek a legfőbb hiányossága az, hogy az eljárás csak színarany forrasztóanyag alkalmazása esetén használható, és ez széleskörű felhasználását nem teszi lehetővé.

Találmányunkkal az a célunk, hogy rozsdamentes acélból és/vagy rézből védőgázas vagy vákuumforrasztással előállítandó fémipari tömegcikkek előállítására alkalmas és olyan egyszerű eljárást dolgozzunk ki, amely kiküszöböli az előzőekben ismertetett eljárások hiányosságait.

A találmány alapja az a felismerés, hogy megfelelően tiszta védőgázban vagy elég kis nyomáson és elég hosszú ideig végzett hőkezelés mellett a rozsdamentes acélok többsége a felület előzetes védelme nélkül is keményforrasztható, ha van a forraszanyagnak a rozsdamentes acél felületén olyan jól adszorbeálódó komponense, ami a hőkezelés körülményei között képes leszorítani a rozsdamentes acélok felületén képződő oxidokat, és ezáltal előidézni a forrasztandó rozsdamentes acél felületnek a forraszanyaggal való nedvesítését, tehát a forrasztás megvalósulását.

A találmány alapja réznek rézhez vagy más fémekhez történő keményforrasztásánál, továbbá az a felismerés, hogy a réz alapfémből és a rézfelületre a forrasztás előtt felvitt ötvözetképző forraszanyagból, valamint az alapfém erózióját megszüntető alapbevonatból a hőkezelés során a helyszínen kialakuló felületi ötvözet is szolgálhat forraszanyagként, tekintet nélkül arra, hogy az ötvözetképző forraszanyagnak mi az olvadáspontja és milyen eróziót okozna a réz alapfémen.

Találmányunk értelmében az előzőekben ismertetett felismerések alapján réznek rézhez vagy rozsdamentes acélhoz való keményforrasztásánál az ismert megoldások hiányosságait úgy küszöböljük ki, hogy a rézfelületre ötvözetképző forrasztóanyagot viszünk fel. Az összeforrasztandó felületeket egymáshoz szorítjuk. A munkadarabot a keményforrasztás bekövetkeztéig tisztított védőgázba vagy 850–1080 °C hőmérsékletű, legfeljebb 1 Pa nyomású vákuumba helyezzük. A réznek a rozsdamentes acélhoz történő keményforrasztását 10–200 percig végezzük. Adott esetben az ötvözetképző forrasztóanyag alá legfeljebb 30 mikron vastagságú nikkel, kobalt, indium és/vagy ezüst alapbevonatot viszünk fel, és ötvözetképző forrasztóanyagként ónt, ónbronzot, indiumot és/vagy mangánt használunk.

Mind az ötvözetképző forrasztóanyagot, mind pedig az alapbevonatot célszerű elektrolitoldatból leválasztani 1–30 mikron vastagságban.

A találmányt részletesen példák alapján ismertetjük, amelyek a találmány szerinti keményforrasztá-

sok foganatosításának lehetséges módjai. Ezek elkészítéséhez rézkatalizátoron és molekulaszitán tisztított argon védőgázzal öblített, vagy evakuált és elektromos fűtéssel ellátott csőkemencét használtunk.

A példák, amelyeket eredményeink ismertetésére kívánunk bemutatni, három csoportra oszthatók. Először foglalkozunk a rozsdamentes acélok rézhez való forrasztásával, majd a réznek rézhez való forrasztásával, és végül összefoglaljuk a találmány szerinti eljárás foganatosításának általunk vizsgált változatait.

I. Példák rozsdamentes acélok rézhez való forrasztására

1. példa. Rézfelületre elektrolitoldatból kb. öt mikron vastag ónréteget választottunk le. Az ily módon előkészített rézfelületet rozsdamentes acél felületéhez szorítottuk, és tisztított argon védőgázban körülbelül 1000 °C hőmérsékleten 90 percig hőkezeltük. Kiváló forrasztást kaptunk.

2. példa. Rézfelületre elektrolitikusan húsz mikron vastag ónbronz réteget választottunk le, és az ily módon előkészített felülethez az 1. példában leírt módon rozsdamentes acélt forrasztottunk. Kiváló forrasztást kaptunk.

3. példa. Rézfelületre elektrolitikusan egy mikron vastag nikkel réteget választottunk le. A nikkelezett felületre még hét mikron vastag ónréteget is felvittünk. Az így előkészített felülethez az 1. példában leírt eljárás szerint rozsdamentes acélt forrasztottunk. Kiváló forrasztást kaptunk.

4. példa. Az 1. példában ismertetett kísérletet megismételtük úgy, hogy az ón helyett indiumot választottunk le a réz felületére. Szintén kiváló forrasztást kaptunk.

II. Példák réznek rézhez történő forrasztására

5. példa. Az 1. példában ismertetett kísérletet megismételtük oly módon, hogy az ónbevonattal ellátott rézfelületet rozsdamentes acél helyett rézfelülethez szorítottuk, és csupán egynegyed óráig folytattuk a hőkezelést. Kiváló forrasztást kaptunk.

6. példa. Rézfelületre egy mikron vastag nikkel réteget választottunk le, és erre még nyolc mikron vastag indium réteget is leválasztottunk. Az így előkészített felülethez rezet szorítva és védőgázban kb. 1000 °C hőmérsékletig hevítve igen kiváló forrasztást kaptunk.

7. példa. A 6. példában leírt kísérletet megismételtük azzal a különbséggel, hogy nikkel bevonat helyett kobalt bevonatot alkalmaztunk. Szintén kiváló forrasztást kaptunk.

III. További példák összefoglalása

A rozsdamentes acélok rézhez forrasztásának ismertetése végett leírt példák után táblázatban foglaljuk össze mindazokat a változatokat, amelyeket a találmány szerinti eljárás foganatosításának során kipróbáltunk, és keményforrasztásra alkalmasnak találtunk. A kísérleteket egy bar nyomású tisztított argon védőgázban vagy vákuumban végeztük. A réz felületére a felületi ötvözet képzéséhez szükséges fémeket elektrolitoldatból elektrolitikusan választottuk le. A felületi ötvözetet képező fémek eróziós hajlamának csökkentése végett más fémekből alapbevonatot is választottunk le, ugyancsak elektrolitikusan, és erre választottuk le az ötvözetképző fémet.

	Ötvözetképző fém és vastagsága (μm)		Alapbevonat fém és vastagsága (μm)		Hőkezelés hőmérs. (°C)	Hőkezelés időtartama (perc)
8.	indium	7,5	–	–	1000	20
9.	indium	7,5	nikkel	0,5	1000	30
10.	indium	10	kobalt	1	1050	60
11.	indium	2	ezüst	7,5	1000	45
12.	ón	10	–	–	975	90
13.	ón	8	nikkel	1	975	90
14.	ón	7	kobalt	0,5	975	90
15.	ónbronz	13	–	–	1000	90
16.	ónbronz	13	nikkel	1	975	90
17.	ón	4	indium	4	1000	90
18.	ón	7	ezüst	3	1000	75
19.	mangán	10	–	–	975	90
20.	mangán	10	nikkel	1	975	90
21.	mangán	10	kobalt	1	975	90

Minden esetben kiváló forrasztást kaptunk.

Példa. A találmány szerinti eljárás foganatosításának a rozsdamentes acélok rézhez forrasztásánál alkalmazott és a táblázatban összefoglalóan ismertetett módjai változtatás nélkül alkalmazhatók rézfelületek egymáshoz forrasztására is. Ebben az esetben azonban gyakorlatilag nincs szükség hőntartásra, csupán a munkadarabot kell felmelegíteni a szükséges hőmérsékletre.

Szabadalmi igénypontok

1. Eljárás réznek rézhez vagy rozsdamentes acélhoz történő keményforrasztására, ötvözetképző forrasztóanyagnak rézfelületre való felvitelével, az összeforrasztandó felületek egymáshoz szorításával és a munkadarabnak a keményforrasztás bekövetkeztéig tisztított védőgázba vagy 850–1080 °C hőmérsékletű, legfeljebb 1 Pa nyomású vákuumba 5 helyezésével, amikor is a réznek a rozsdamentes acélhoz történő keményforrasztását 10–200 percig végezzük, *azzal jellemezve*, hogy – adott esetben az ötvözetképző forrasztóanyag alá legfeljebb 30 mikron vastagságú nikkel, kobalt, indium és/vagy ezüst 10 alapbevonatot viszünk fel és – ötvözetképző forrasztó anyagként ónt és/vagy ónbronzot és/vagy indiumot és/vagy mangánt használunk.

2. Az 1. igénypont szerinti eljárás *azzal jellemezve*, hogy az ötvözetképző forrasztóanyagot és/vagy 15 az alapbevonatot elektrolitoldatból választjuk le 1–30 mikron vastagságban.

Ábra nélkül

Kiadja az Országos Találmányi Hivatal
A kiadásért felel: Himer Zoltán osztályvezető
Megjelent a Műszaki Könyvkiadó gondozásában

COPYLUX Nyomdaipari és Sokszorosító Kisszövetkezet

INSTITUT NATIONAL

DE LA PROPRIÉTÉ INDUSTRIELLE

25

EXEMPLAIRE
CERTIFIÉ CONFORME
3e alinéa de l'article 9 du décret 79/822 du 19/9/1979

(11) N° de publication : **2 518 440**
(à n'utiliser que pour les commandes de reproduction)

(21) N° d'enregistrement national : **82 21534**

(51) Int Cl³ : B 23 K 1/20, 1/04.

(12) **BREVET D'INVENTION** B1

(54) PROCEDE DE BRASAGE DE CUIVRE SUR DU CUIVRE OU SUR DES ALLIAGES D'ACIER

(22) Date de dépôt : 22.12.82.

(30) Priorité : 23.12.81 HU 392181.

(43) Date de la mise à disposition du public de la demande : 24.06.83 Bulletin 83/25.

(45) Date de la mise à disposition du public du brevet d'invention : 10.11.89 Bulletin 89/45.

(56) Liste des documents cités dans le rapport de recherche :

Se reporter à la fin du présent fascicule

(60) Références à d'autres documents nationaux apparentés :

(71) Demandeur(s) : MTA KOZPONTI KEMIAI KUTATO INTEZET et FEGYVER ES GAZKESZULEKGYAR -HU.

(72) Inventeur(s) : SANDOR SZABO, ALFONZ SZENTGYORGYI, PETER SZABO ET FERENC NAGY

(73) Titulaire(s) :

(74) Mandataire(s) : CABINET ORES

FR 2 518 440 - B1

L'invention concerne un procédé pour braser du cuivre sur du cuivre ou sur des alliages d'acier, en particulier sur des aciers inoxydables.

Il est connu que la brasure de métaux alliés sur d'autres métaux est en général difficile car les métaux d'alliage, qui sont moins nobles que le fer, comme le chrome, le molybdène, le manganèse, le titane et le vanadium, forment, même dans les conditions où les surfaces des aciers au carbone reste encore propre, des couches d'oxydes difficiles à détruire. Cette couche d'oxyde empêche l'imprégnation de l'acier inoxydable par le matériau de brasage et ainsi la formation d'une brasure résistante. La situation est particulièrement difficile dans les travaux de brasage exécutés sous gaz protecteur ou sous vide sans fondant, car dans ce cas les traces d'oxygène et/ou de vapeur d'eau présentes dans le gaz protecteur ou dans l'air résiduel renforcent la couche d'oxyde sur la surface pendant toute la durée du processus de soudage, ce qui rend parfois le soudage impossible.

Les procédés de soudure d'aciers inoxydables sous gaz protecteur ou sous vide ont pour inconvénient essentiel que le matériau de soudure doit tout d'abord être déposé sur la surface de l'acier avant le traitement thermique pour protéger cette surface (une simple disposition sans recouvrement de la surface ne suffit pas) et qu'il faut maintes fois même utiliser des fondants gazeux pour pouvoir éliminer les difficultés mentionnées ci-dessus [I. Lashko et S. Lashko:Brazing and soldering of metals (MIR éditeurs, Moscou)]. Dans les brevets japonais 77 76 254 et 79 85 158 il est également recommandé de déposer du matériau de soudure pour la protection des surfaces préalablement au traitement thermique.

Dans les procédés connus de brasure d'aciers inoxydables sur d'autres métaux il faut donc soit travailler avec des agents fondants, soit protéger par un traitement préalable les surfaces à braser l'une avec l'autre, soit

les deux sont nécessaires.

La brasure de cuivre sur du cuivre ou sur d'autres métaux que des aciers alliés ne présente en général pas de difficultés techniques particulières, si on choisit le matériau de soudure adapté au but poursuivi et le procédé adapté. Le point de fusion du matériau de soudure doit se trouver au-dessous de celui du cuivre et le matériau de soudure ne doit former aucun alliage avec le cuivre à la température de soudure, sinon il se produirait une érosion du matériau de base. Parfois cependant l'apport et la fixation du matériau de soudure au voisinage de la surface à souder sont compliqués et exigent une technique de procédé ou une technologie comprenant de nombreuses étapes. Par exemple pour la fabrication d'échangeurs de chaleur formés de tubes de cuivre et de tôles de cuivre, le matériau de soudure doit être amené dans des trous découpés dans les plaques de cuivre évacuant la chaleur, et ensuite on fait subir un traitement thermique à l'échangeur de chaleur monté, dans une atmosphère de gaz protecteur ou sous vide. Un exemple moderne pour l'application de ce principe se trouve dans le procédé décrit dans le brevet britannique 1 558 264.

On connait également par Römpp, CHEMIE LEXIKON, 5. édition, 1962, colonne 2078, la brasure de métaux lourds et de produits en fer par brasage à l'argent. On connait en outre par le même ouvrage, colonnes 2 998 à 2 999, la brasure de fer et de cuivre par brasage au cuivre. Les soudures obtenues avec ces brasures connues laissent cependant encore à désirer.

La présente invention a pour but de pourvoir, en remédiant aux imperfections des procédés connus, à un procédé simple de brasure grâce auquel on peut souder avec un meilleur résultat des alliages d'acier, en particulier de l'acier inoxydable, avec du cuivre sans utilisation de fondants et sans pré-traitement de protection des surfaces, et on peut réaliser à volonté la brasure de cuivre sur de

cuivre avec une technique de procédé ou une technologie
très simplifiée par rapport à l'état de la technique, en
particulier par suppression des opérations concernant la
préparation des surfaces à souder ensemble même dans le
5 cas de surfaces de forme et de réalisation complexes, ainsi
si que les mesures concernant l'apport et la fixation du
matériau de soudure.

L'invention repose sur la constatation étonnante
que la plupart des alliages d'acier, tels que les aciers
10 inoxydables, peuvent être brasés sur du cuivre même sans
protection préalable de la surface et sans fondant, dans
une atmosphère de gaz protecteur pur approprié ou sous une
pression suffisamment faible et avec un traitement thermi-
que d'une durée suffisante, si on utilise comme matériau
15 de brasure certains métaux purs sélectionnés. Le matériau
de soudure fondant imprègne alors de façon optimale la
surface de l'alliage d'acier à souder au cuivre. Ceci ne
se produit pas en un instant, mais l'imprégnation est un
processus lent car le métal fondu nécessite un certain
20 temps pour décomposer et supprimer les oxydes superfi-
ciels. La durée de soudage nécessaire dépend de la pureté
du gaz protecteur ou de la quantité d'oxygène résiduel
et/ou de vapeur d'eau résiduelle après réalisation du vide.

L'invention repose en outre sur la constatation
25 étonnante que lors de l'utilisation de certains métaux purs
sélectionnés comme matériau de brasure, l'alliage superfi-
ciel qui se forme "in situ" durant le traitement thermique
à partir du métal de base de cuivre et des métaux purs dépo-
sés sur sa surface, qui n'est pas nécessairement un alliage
30 qui imprègne le cuivre, peut servir de matériau de soudure
par formation d'une soudure superposée lors de la brasure,
sans qu'il se produise une érosion du métal de base. L'al-
liage fluide superficiel formé "in situ" entre les métaux
purs sélectionnés et le cuivre à souder conduit à une impré-
35 gnation optimale de la surface de l'alliage d'acier à sou-
der au cuivre et ainsi à une soudure optimale, où il n'y a

pas de nécessité, comme on l'a déjà indiqué, que l'alliage superficiel imprégne aussi le cuivre.

La présente invention a en conséquence pour objet un procédé pour la brasure de cuivre sur du cuivre
5 ou sur des alliages d'acier par dépôt d'un métal formant un alliage comme matériau de brasure sur au moins une des surfaces de cuivre ou sur la surface de cuivre, par compression des surfaces à souder et par traitement thermique de 10 à 200 minutes de la pièce dans un gaz protecteur purifié ou
10 sous vide à une pression d'au plus 1 Pa à des températures de 850 à 1080°C jusqu'à l'apparition de l'alliage superficiel, lequel procédé est caractérisé en ce qu'on utilise comme métal formant alliage, de l'étain, de l'indium ou du manganèse.

15 Selon un mode de réalisation avantageux du procédé selon l'invention, on dépose un revêtement de base en nickel, cobalt, indium et/ou argent d'une épaisseur d'au plus 30 μ avant le dépôt du métal formant alliage.

On procède de préférence au dépôt du métal formant alliage et/ou du revêtement de base à partir de solu-
20 tions électrolytiques.

On procède de préférence au dépôt du métal formant alliage et/ou du revêtement de base suivant une épaisseur de 1 à 30 μ.

25 Le procédé selon l'invention présente l'avantage par rapport aux procédés de l'état de la technique de permettre d'obtenir la formation d'une liaison d'alliage plus résistante entre le matériau de soudure et la ou les surface(s) de cuivre et une meilleure imprégnation de la sur-
30 face de l'alliage d'acier à souder au cuivre par l'alliage formé par le matériau de soudure et le cuivre, et ainsi une meilleure soudure. Il est alors superflu, même dans le cas d'alliages d'acier à souder au cuivre, de réaliser un traitement préalable pour assurer la protection préalable
35 de la surface et d'utiliser un fondant dans de l'argon ou sous vide.

On obtient des soudures de qualité remarquable par le procédé selon l'invention.

En ce qui concerne la brasure d'alliages d'acier sur du cuivre, le procédé selon l'invention est particulièrement approprié pourla brasure sur cuivre d'aciers inoxydables, avant tout des alliages d'acier qui contiennent de l'argent, de l'étain, de l'indium, du manganèse, du gallium et/ou du nickel ou du bronze d'étain comme métal ou métaux d'alliage ou comme alliage de métal d'alliage. Une application avantageuse du procédé selon l'invention concerne la fabrication d'échangeurs de chaleur et de pièces de machines en cuivre ou en cuivre et en aciers inoxydables ou en d'autres alliages d'acier.

L'invention est explicitée plus en détail à l'aide des exemples qui vont suivre. Les fours tubulaires utilisés pour la réalisation des exemples ont été mis sous vide ou balayés par de l'argon qui a été préalablement purifié sur des catalyseurs au cuivre et des filtres moléculaires. On a utilisé comme aciers inoxydables les suivants, conformément à la norme DIN 17007:

1.4113,
1.4122,
1.4301,
1.4306,
1.4541 et
1.4571

Les exemples s'organisent en 3 groupes : brasure d'aciers inoxydables sur du cuivre, brasure de cuivre sur du cuivre et enfin le regroupement d'autres exemples selon le procédé de l'inventon.

Il doit être bien entendu, toutefois, que ces exemples de mise en oeuvre sont donnés uniquement à titre d'illustration de l'objet de l'invention, dont ils ne constituent en aucune manière une limitation.

A) Brasure d'acier inoxydable sur du cuivre.

Exemple 1

On a déposé une couche d'étain d'environ 5 µ sur une surface de cuivre, à partir d'une solution électro-
5 lytique. La surface de cuivre ainsi recouverte a été comprimée contre une surface d'acier inoxydable et l'ensemble a été soumis à un traitement thermique à environ 1000°C pendant 90 minutes sous atmosphère de protection d'argon purifié. On a obtenu une liaison de soudure remarquable.

10 Exemple 2

On a déposé électrolytiquement une couche de nickel de 1 µ d'épaisseur sur une surface de cuivre et on a déposé sur la surface de cuivre ainsi nickelée une couche d'étain de 7 µ d'épaisseur. La surface ainsi recouverte
15 a été soudée avec de l'acier inoxydable de la façon décrite dans l'exemple 1. On a obtenu une liaison de soudure remarquable.

Exemple 3

On a repris le mode opératoire décrit dans l'e-
20 xemple 1 avec la différence qu'on a déposé de l'indium à la place de l'étain sur la surface de cuivre. On a également obtenu une liaison de soudure remarquable.

B) Brasure de cuivre sur du cuivre.

Exemple 4

25 On a repris le mode opératoire décrit dans l'exemple 1 avec la différence qu'on a appliqué sous pression une surface de cuivre sur la surface de cuivre étamée, au lieu de la surface de l'acier inoxydable et que le procédé thermique a duré 15 minutes. On a obtenu une liaison de
30 soudure remarquable.

Exemple 5

On a déposé sur une surface de cuivre tout d'abord une couche de nickel de 1 µ d'épaisseur et ensuite encore une couche d'indium de 8 µ d'épaisseur. On a pressé
35 une surface de cuivre contre la surface ainsi revêtue et

on a chauffé le tout à environ 1000 °C dans un gaz protecteur. On a obtenu une liaison de soudure excellente.

Exemple 6

On a opéré comme dans l'exemple 5 avec cependant
5 la différence qu'on a déposé un revêtement de cobalt à la place du revêtement de nickel. On a également obtenu une liaison de soudure remarquable.

C) Résumé d'autres exemples selon le procédé de l'invention.

10 Exemples 7 à 10

Pour illustrer la brasure d'acier inoxydable sur du cuivre, on a regroupé dans le tableau ci-après d'autres exemples avec indication des paramètres de soudure. Les expériences ont été effectuées sour vide ou dans une
15 atmosphère de gaz protecteur d'argon purifié, sous une pression de 1 bar. On a déposé électrolytiquement à partir de solutions électrolytiques, les métaux formant le matériau de soudure nécessaires pour réaliser l'alliage superficiel, sur la surface de cuivre. Dans la plupart des exem-
20 ples, on a réalisé également électrolytiquement un revêtement de base sur le cuivre et la couche métallique formant l'alliage a été déposée sur cette couche de base.

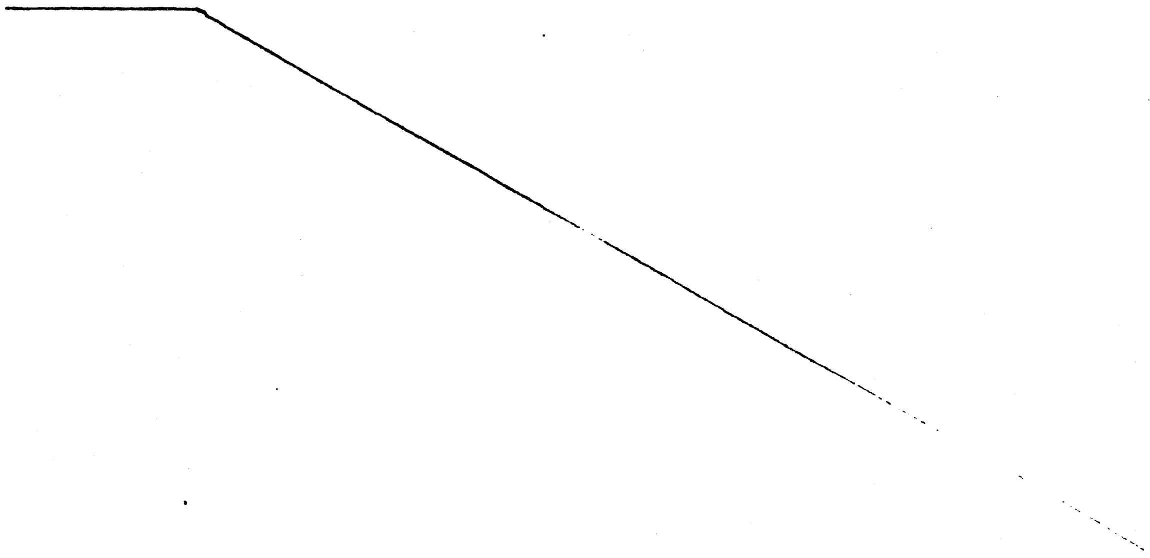

TABLEAU

Exemple	Matériau de soudure formant alliage		Revêtement de base		Traitement thermique	
	Métal formant alliage	Epaisseur en u	Métal	Epaisseur en u	Température en °C	Temps en minutes
7	Indium	7,5	–	–	1 000	20
8	Indium	7,5	nickel	0,5	1 000	30
9	Indium	10	cobalt	1	1 050	60
10	Indium	2	argent	7,5	1 000	45
11	Etain	10	-	-	975	90
12	Etain	8	nickel	1	975	90
13	Etain	7	cobalt	0,5	975	90
14	Etain	4	indium	4	1 000	90
15	Etain	7	argent	3	1 000	75
16	Manganèse	10	-	-	975	90
17	Manganèse	10	nickel	1	975	90
18	Manganèse	10	cobalt	1	975	90

Dans chaque cas, on a obtenu une liaison de soudure remarquable.

5 10 15 20 25 30 35

Exemple 19

Les exemples selon le procédé conforme à l'invention, décrits dans les exemples 7 à 18 pour la brasure d'acier inoxydable sur du cuivre, ont aussi pu être utilisés sans modification, pour la brasure de cuivre sur du cuivre. Dans ce cas, il a été suffisant de chauffer la pièce à la température nécessaire, un traitement thermique plus long n'étant pratiquement pas nécessaire à cette température.

Ainsi que cela ressort de ce qui précède, l'invention ne se limite nullement à ceux de ses modes de mise en oeuvre, de réalisation et d'application qui viennent d'être décrits de façon plus explicite ; elle en embrasse, au contraire, toutes les variantes qui peuvent venir à l'esprit du technicien en la matière, sans s'écarter du cadre, ni de la portée de la présente invention.

Revendications

1. Procédé de brasure de cuivre sur du cuivre ou sur des alliages d'acier, par dépôt d'un métal formant alliage comme matériau de brasure sur au moins une des surfaces de cuivre ou sur la surface de cuivre, par compression des
5 surfaces à souder ensemble et par traitement thermique de 10 à 200 minutes de la pièce dans une atmosphère de gaz protecteur purifié ou sous vide, sous une pression d'au plus 1 Pa, à des températures de 850° à 1080°C jusqu'à la formation de l'alliage superficiel, lequel procédé est ca-
10 ractérisé en ce qu'on utilise de l'étain, de l'indium ou du manganèse comme métal formant alliage.

2. Procédé selon la revendication 1, caractérisé en ce qu'on dépose un revêtement de base en nickel, cobalt, indium et/ou argent d'une épaisseur d'au plus 30 µ avant
15 le dépôt du métal formant alliage.

3. Procédé selon la revendication 1 ou 2, caractérisé en ce qu'on procède au dépôt du métal formant alliage et/ ou du revêtement de base à partir de solutions électrolytiques.

20 4. Procédé selon l'une quelconque des revendications 1 à 3, caractérisé en ce qu'on procède au dépôt du métal et/ou du revêtement de base suivant une épaisseur de 1 à 30 µ.

82. 21 534

N°

Etabli par

B. SCHMIDT

Ingénieur examinateur à l'Institut national de la propriété industrielle (Division Technique des Brevets)

AVIS DOCUMENTAIRE

(art. 19 de la loi n°68-1 modifiée du 2 janvier 1968 ; art. 40 à 53 du décret n° 79-822 du 19 septembre 1979)

OBJET DE L'AVIS DOCUMENTAIRE

■ Conférant à son titulaire le droit exclusif d'exploiter l'invention, le brevet constitue pour les tiers une **importante exception à la liberté d'entreprendre.**
C'est la raison pour laquelle la loi prévoit qu'un brevet n'est valable que si, entre autres conditions, l'invention :
• est "nouvelle", c'est-à-dire na pas été rendue publique en quelque lieu que ce soit avant la date de dépôt
• implique une "activité inventive, c'est-à-dire dépasse le cadre de ce qui aurait été évident pour un homme du métier

■ L'Institut n'est pas habilité, sauf absence manifeste de nouveauté, à refuser un brevet pour une invention ne répondant pas aux conditions ci dessus.
C'est aux tribunaux qu'il appartient d'en prononcer la nullité à la demande de toute personne intéressée, par exemple à l'occasion d'une action en contrefaçon.
L'Institut est toutefois chargé d'annexer à chaque brevet un "AVIS DOCUMENTAIRE" destiné à éclairer **le public et les tribunaux sur les antériorités susceptibles de s'opposer à la validité du brevet.**

CONDITIONS D'ETABLISSEMENT DU PRESENT AVIS

■ Il a été établi sur la base des "revendications" dont la fonction est de définir les points sur lesquels l'inventeur estime avoir fait œuvre inventive et entend en conséquence être protégé.

■ Il a été établi à l'issue d'une procédure contradictoire (1) au cours de laquelle :

☒ le résultat d'une recherche d'antériorités effectuée parmi les brevets et autres publications a été notifié au demandeur et rendu public.

☐ les tiers ont présenté des observations visant à compléter le résultat de la recherche

☐ le demandeur a modifié les revendications pour tenir compte du résultat de cette recherche

☐ le demandeur a modifié la description pour en éliminer les éléments qui n'étaient plus en concordance avec les nouvelles revendications

☒ le demandeur a présenté des observations pour justifier sa position

EXAMEN DES ANTERIORITES

☐ Les brevets et autres publications (1) ci-après, cités en cours de procédure, n'ont pas été examinés car pour pour être efficace, cet examen suppose au préalable une vérification des priorités (2)

☒ Les brevets et autres publications (1) ci-après, cités en cours de procédure, n'ont pas été retenus (3)

GB-A- 568 659 ; FR-A-1 052 958 ; US-A-3 675 310 ; GB-A- 578 003

☒ Les brevets et autres publications (1) ci-après, cités en cours de procédure, ont été retenus comme antériorités (voir page suivante)

(1) Les pièces du dossier, ainsi que les brevets et autres publications citées, peuvent être consultés à l'INPI ou délivrés en copie
(2) Tout renseignement peut être obtenu de l'INPI : demander l'aide mémoire "Intercalaires et interférences"
(3) Du fait que leur contenu est éloigné de l'invention ou qu'un document encore plus proche de celle-ci a été retenu

82. 21 534

N°

ANTERIORITES RETENUES

Brevets et autres publications retenus comme antériorités	Revendications du brevet objet du présent avis, concernées par les antériorités
I – WELDING PRODUCTION, vol. 24, n° 4, avril 1977, pages 19-21, Cambridge, GB ; I.A.FROLOV : "Examination of the contact melting of manganese in the brazing of copper to steel" *En entier*	1,4

COMPARAISON ENTRE LES ANTERIORITES RETENUES ET LES REVENDICATIONS CONCERNEES

Rev. 1 : L'antériorité I décrit un procédé de brasage de cuivre sur des aciers qui présente de nombreuses similitudes avec le procédé de brasage revendiqué.

Certes, le procédé revendiqué se distingue de celui de l'antériorité I en ce qu'il est précisé qu'il s'agit de brasage de cuivre sur du cuivre ou sur des aciers alliés et que la durée du traitement thermique est de 10 à 200 minutes, alors que dans l'antériorité I il est question de manière générale du brasage du cuivre sur les aciers, la durée du traitement thermique citée en exemple étant de 5 minutes.

La question se pose cependant de savoir si, compte tenu de la pratique courante, l'objet de la revendication ne découle pas de manière évidente, pour l'homme du métier, de cette antériorité.

Rev. 4 : Une observation analogue peut être faite en ce qui concerne la revendication dépendante ci-après. En effet :

Dans l'antériorité, on procède au dépôt d'une couche de manganèse de 15 à 20 micron d'épaisseur.

Rev. 2 à 3 – Aucune antériorité n'a été retenue.

MAGYAR
NÉPKÖZTÁRSASÁG

ORSZÁGOS
TALÁLMÁNYI
HIVATAL

26.

Szabadalmi okirat

Az Országos Találmányi Hivatal az okirathoz fűzött leirás alapján

188 340

lajstromszámon szabadalmat adott.

A szabadalmi bejelentés napja és az oltalmi idő kezdete:

1982.12.29.

Szabadalmasok:

MTA Központi Kémiai Kutató Intézete, Budapest,
Posta Kisérleti Intézet, Budapest

Feltalálók:

Szabó Sándor, okl.vegyészmérnök, 40%
Kovács Gizella, okl.vegyész, 30%
Szabó Péter, vegyésztechnikus, 20%
Kwaysser Endre, okl.vegyészmérnök, 10%
Budapest

A szabadalom cime:

Réz-acél vagy bronz-acél kötőelem és
eljárás annak előállitására

Budapest, 1988.08.08.

elnök

A találmány tárgya réz-acél vagy bronz-acél kötőelem eljárás annak előállítására tartós, karbantartást nem ıylő, korrózióálló és megbízható földelőkötések létese céljából.

.smeretes, hogy elektromos szerelvények érintésvédelıek és elektromos vezetékek árnyékolásának alapja ıegfelelő földelés. Ez látszólag igen egyszerű követelıy esetenként, – különösen tartósan –, igen nehezen osítható. Ennek az oka az, hogy az acélból készített lelőlemezek acél kivezetésein, a földelőnyársakon, a lelővezetékeken, illetve az elektromos készülékek vázán kialakított acél-réz földelési pontokon már kistékű korrózió esetén is az átmeneti ellenállások jelenmegnövekedésével kell számolni. Mivel az acél felü. – különösen légköri viszonyok között, vagy erősen rozív környezetben – könnyen korrodeál, az ilyen lelőkötések nem megbízhatóak.

llyen megoldásokat ismertet például a 2,028,155 sz. ol szabadalmi leírás, amely szerint a földelést réz vagy ötvözetű belső magból és azt borító acélköpenyből földelőnyárssal biztosítják, ahol is az acélköpeny tallurgikusan van a rézhez rögzítve, és az acélköpeny. levő rézrudat – magot – 350–500 °C-on megijtják.

Ugyancsak földelőnyársat ismertet az 1,467,723 sz. ol szabadalmi leírás is, amely szerint hegyben végő és felső végén hatlapú menetes anyával vagy anyákellátott rézbevonatú acélrúdhoz lehet a földelőkábelt zíteni.

Hasonló megoldású az 581,912 sz. svájci szabadalmi ásban ismertetett villamos földelőelem is, amelynek míniumból készült rúdját koaxiálisan kettős cső, ıtvözetlen vascső és azt borító rozsdamentes acélcső – zi körül.

A felsorolt szabadalmi leírásokkal ismertetett megások kivétel nélkül földelések létrehozására vonatkoz., de nem tartalmaznak semmilyen útmutatást a földelem és a földelőkábel közötti megbízható, korrónak ellenálló, tartós, karbantartást nem igénylő és korlatilag átmeneti ellenállás nélküli kötés létrehozá-ı.

Az ismertetett megoldások hiányosságait esetenként acélra felforrasztott réz, bronz vagy sárgaréz földelési ıtok kialakításával próbálták kiküszöbölni, amihez ható földelő kötések esetén különböző fémekből zített csavarokat és alátéteket használtak. Tekintettel elyszínen kialakított forrasztások és keményforraszok nehézkességére és csökkent megbízhatóságára, ábbá a többféle fém összeépítéséből kialakuló kontkorróziós problémák megoldhatatlanságára, ez a kérezzel a módszerrel sem oldható meg tökéletesen.

A találmánnyal az a célunk, hogy az előzőekben isrtetett hiányosságokat olyan kötőelemmel küszöbölki, amely az acél földelőelemek kivezetéseire, a földőnyársakra, készülékvázakra vagy más földelőlétesítnyekre felhegesztve tökéletes földelési pont kialakıt és földelőkábel rögzítését teszi lehetővé.

A találmány alapja az a felismerés, hogy egy acéliba keményforrasztott és az acélrúddal egyenértékű etőképességű réz- vagy bronzrúdból álló kötőelem l végét a földelő létesítményekhez vagy az adott ktromos berendezés acélvázához hegesztve olyan réz y bronz földelési pont jön létre, amely a korróziónak ellenáll.

A találmány értelmében földelőelemek és földelőkábelek között olyan réz-acél vagy bronz-acél kötőelemmel biztosítjuk a fémes kapcsolatot, amelynek réz- vagy bronzrúdja az acélrúd tengelyével azonos irányú furatban az acélrúdhoz keményforrasztással van rögzítve.

A találmány szerinti kötőelemet úgy állítjuk elő, hogy a beforrasztásra kerülő réz- vagy bronzrúddal megegyező vagy annál nagyobb vezetőképességű acélrúd végébe annak hossztengelyével azonos irányú és a réz- vagy bronzrúd átmérője felénél nagyobb átmérőjű lyukat fúrunk, és a lyukba, annak felületének minden négyzetcentiméterére számítva 4/1000–120/1000 g forrasztóanyagot helyezünk el, majd a lyukba helyezzük a réz- vagy bronzrúd egyik végét, és az így összeállított szerkezetet 10–100 percig 800–1080 °C közötti hőmérsékleten vákuumban vagy védőgázban hőkezeljük. Forrasztóanyagként előnyösen használható ón, ónbronz, indium, indiumbronz, ezüst és/vagy ezüst-réz ötvözet. A kötőelemmel elérhető biztonság és a korrózióvédelem úgy fokozható előnyösen, hogy az acélrúdba beforrasztott réz- vagy bronzrudat 1–100 mikrométer vastag nikkel-, króm-, ólom-, ón-, kadmium-, cink-, ezüst-, arany- és/vagy indiumbevonattal látjuk el. Az ily módon előállított kötőelem acél végét a földelőlétesítményhez vagy a készülékvázhoz kötve, célszerűen hegesztve, olyan réz vagy bronz földelési pont jön létre, amelyhez hideg kötéssel, oldható kötéssel vagy lágyforrasztással köthetünk földelő vezetékeket.

A találmányt részletesen rajz alapján ismertetjük. A rajzon a találmány szerinti földelőelem azonos részei azonos hivatkozási számokkal vannak jelölve. A rajz 1., 2., 3. és 4. ábrája a találmány szerinti kötőelem egy-egy lehetséges példakénti kiviteli alakját mutatja. A rajzon az 1 acélrúdhoz a 2 vagy a 3 vagy a 4 vagy az 5 réz- vagy bronzrúd van keményforrasztással rögzítve. Az 1. ábrán a hidegkötésre vagy utólagos megmunkálásra alkalmas változat van ábrázolva. A 2. és a 3. ábrán az oldható kötésre alkalmas változatok vannak ábrázolva. Az oldható kötést a 6 bronz szorítócsavarokkal és a 7 sarukkal lehet megvalósítani. A 3. ábrán ábrázolt földelőelem esetében az 1 acélrúdhoz nemcsak a 4 réz- vagy bronzrúd, hanem a 8 réz vagy bronz alátét is hozzá van forrasztva. A 4. ábrán van ábrázolva a lágyforrasztásra alkalmas változat, ahol az 5 réz- vagy bronzrúdon lyukak vannak kialakítva.

A 2, 3, 4 és az 5 réz- vagy bronzrudat a keményforrasztás után a korrózióállóság növelése céljából nikkel-, ón-, kadmium-, cink-, ólom-, ezüst-, arany- és/vagy indiumbevonattal láthatjuk el.

A példa szerinti kiviteli alakokkal a következőképpen hozható létre földelőkötés: A rajzon ábrázolt változatokból az adott célra legalkalmasabbat kiválasztjuk, és az elektromos készülék vagy földelőlétesítmény összeszereléskor a földelőlétesítményre vagy a készülékvázra ezt is felhegesztjük, vagy szegecseljük. Szereléskor a kötőelemhez hidegkötéssel, saruval vagy lágyforrasztással köthetünk földelővezetékeket, attól függően, hogy melyik változat felhasználása mellett döntöttünk. Természetesen egy készüléken egyszerre több kötőelem is elhelyezhető, felhegeszthető.

A találmány szerinti kötőelemek előállításánál alkalmazott eljárást részletesen példák alapján ismertetjük. A példák a találmány szerinti kötőelemek előállításakor alkalmazott keményforrasztások foganatosításának lehetséges módjai. Ezek előállításakor rézkatalizátoron

és molekulaszitán tisztított, argon védőgázzal öblített vagy evakuált és elektromos fűtéssel ellátott csőkemencét használtunk.

1. példa

14 mm átmérőjű acélrúd végébe, a rúd tengelyének irányába, 7 mm átmérőjű fúróval 14 mm mély lyukat fúrtunk, a furat aljára 100/1000 g ónt helyeztünk, majd a furatba 7 mm átmérőjű vörösréz rudat illesztettünk, és az így kapott darabot függőleges helyzetben 1 bar nyomású tisztított argon gázban 950 °C hőmérsékleten 30 percig hőkezeltük. Kiváló forrasztást kaptunk. A forraszanyag a rézrúd és az acélrúdba fúrt lyuk fala közötti rést teljesen kitöltötte.

2. példa

Az 1. példában leírt kísérletet megismételtük oly módon, hogy ón helyett 110/1000 g indiumot használtunk, és a hőkezelést 1000 °C hőmérsékleten végeztük. Szintén kiváló forrasztást kaptunk.

3. példa

Az 1. példában leírt kísérletet megismételtük oly módon, hogy ón helyett ugyanannyi lágyforraszanyagot használtunk és a hőkezelést 900 °C hőmérsékleten végeztük. Ismét kiváló forrasztást kaptunk.

4. példa

Az 1. példában leírt kísérletet megismételtük oly módon, hogy ón helyett színezüstöt használtunk, és a hőkezelést 900 °C hőmérsékleten végeztük. Kiváló forrasztást kaptunk.

5. példa

Az 1., 2., 3. és 4. példákban leírt kísérleteket megismételtük oly módon, hogy réz helyett bronzrudat alkalmaztunk. Minden esetben kiváló forrasztást kaptunk.

Az eddigi példák után összefoglaljuk mindazokat a változatokat, amelyeket a találmány szerinti eljárás foganatosítása során kipróbáltunk, és a kívánt célra alkalmasnak találtunk. A kísérleteket az 1. példában leírt körülmények között végeztük, az eltéréseket a táblázat tartalmazza.

Ötvözetképző forraszanyag név	Mennyiség (g)	Hőmérséklet (°C)
ón	100/1000	950
ónbronz	150/1000	1000
indium	110/1000	1000
indiumbronz	150/1000	1000
lágyforrasz	100/1000	900
ezüst	100/1000	900
ezüst-réz ötvözet	200/1000	1000

A példákban leírt forrasztások nagy szakítószilárdságú, résmentes keményforrasztást eredményeztek, amelyek elektromos ellenállása, — a mérőkészülék hozzávezetéseinek ellenállását is beleszámítva —, csupán milliohmokban mérhető.

Szabadalmi igénypontok

1. Réz-acél vagy bronz-acél kötőelem, földelőelem és földelőkábel közötti villamos érintkezés biztosítására, a földelőelemhez rögzíthető acélrúddal és a földelőkábelhez rögzíthető réz- vagy bronzrúddal, *azzal jellemezve,* hogy a réz- vagy bronzrúd (2, 3, 4, 5) az acélrúd (1) tengelyével azonos irányú furatban az acélrúdhoz (1) keményforrasztással van rögzítve.

2. Eljárás az 1. igénypont szerinti kötőelem foganatosítására, *azzal jellemezve,* hogy az acélrúd (1) végébe, annak tengelyével azonos irányú és a réz- vagy bronzrúd (2, 3, 4, 5) átmérője felénél nagyobb átmérőjű lyukat fúrunk, a lyukba, annak felületének minden négyzetcentiméterére számítva 4/1000–120/1000 g forrasztóanyagot helyezünk el, majd a lyukba helyezzük a réz- vagy bronzrúd (2, 3, 4, 5) egyik végét, és az így összeállított szerkezetet 10–100 percig 800–1080 °C közötti hőmérsékleten vákuumban vagy védőgázban hőkezeljük.

3. A 2. igénypont szerinti eljárás foganatosítási módja, *azzal jellemezve,* hogy a forrasztóanyagnak ónt, ónbronzot, indiumot, indiumbronzot, ezüstöt és/vagy ezüst-réz ötvözetet használunk.

4. A 2. vagy a 3. igénypont szerinti eljárás foganatosítási módja, *azzal jellemezve,* hogy az acélrúdba (1) beforrasztott réz- vagy bronzrudat (2, 3, 4, 5) 1–100 mikrométer vastag korrózióvédő nikkel-, króm-, ón-, ólom-, kadmium-, cink-, ezüst-, arany- és/vagy indiumbevonattal látjuk el.

4 db ábra

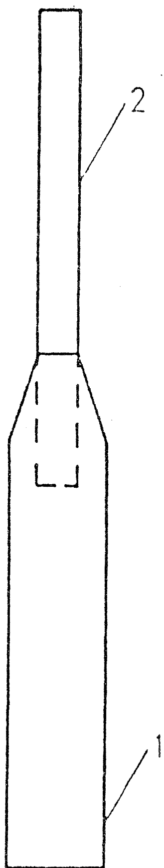

1. ábra

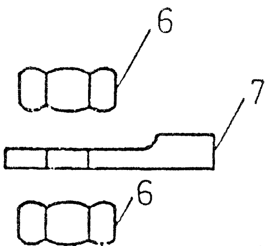

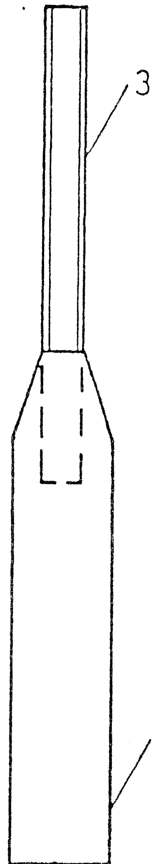

2. ábra

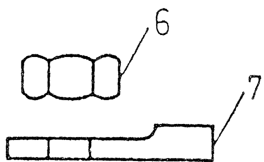

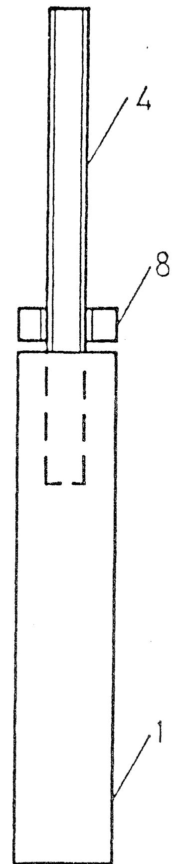

3. ábra

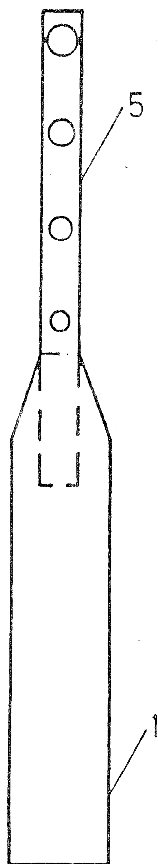

4. ábra

Kiadja az Országos Találmányi Hivatal
A kiadásért felel: Himer Zoltán osztályvezető
Megjelent a Műszaki Könyvkiadó gondozásában
COPYLUX Nyomdaipari és Sokszorosító Kisszövetkezet

(19) HU

MAGYAR
ÖZTÁRSASÁG

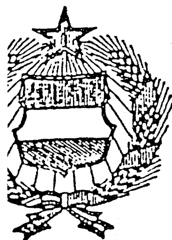

ORSZÁGOS
TALÁLMÁNYI
HIVATAL

SZABADALMI LEÍRÁS

SZOLGÁLATI TALÁLMÁNY

A

(11) 188 340

Nemzetközi osztályjelzet:
(51) $NSZO_4$

H 01 R 4/66;
H 02 B 1/16

A bejelentés napja: (22) 82. 12. 29.
25849

(21) 4216/82

Megjelent: (45) 88. 04. 20.

...ó(k): (72)
...ándor, okl. vegyészmérnök, 40 %, Kovács Gizella, okl.
... 30 %, Szabó Péter, vegyésztechnikus, 20 %, Kwaysser
...okl. vegyészmérnök, 10 %, Budapest

Szabadalmas: (73)
MTA Központi Kémiai Kutató Intézete, Budapest, Posta Kísérleti Intézet, Budapest

RÉZ-ACÉL VAGY BRONZ-ACÉL KÖTŐELEM ÉS ELJÁRÁS ANNAK ELŐÁLLÍTÁSÁRA

(57) KIVONAT

A találmány szerinti kötőelem lényege, hogy egy acélrúd végébe, annak tengelyével egyirányba réz- vagy bronzrúd van keményforrasztva. A földelőelem acél vége a földelőlétesítményhez vagy készülékvázhoz van kötve.

A találmány szerinti kötőelemet úgy állítjuk elő, hogy az acélrúd végébe, annak tengelyével azonos irányú és a réz- vagy bronzrúd átmérője felénél nagyobb átmérőjű lyukat fúrunk, a lyukba, annak felületének minden négyzetcentiméterére számítva 4/1000–120/1000 g forrasztóanyagot (ónt, ónbronzot, indiumot, ezüstöt stb.) helyezünk el, majd a lyukba helyezzük a réz- vagy bronzrúd egyik végét, és az így összeállított szerkezetet 10–100 percig 800–1080 °C közötti hőmérsékleten vákuumban vagy védőgázban hőkezeljük.